

**DRINKING WATER TREATMENT BY BIOLOGICAL PROCESS
FOR SIMULTANEOUS REMOVAL OF ARSENIC, NITRATE
AND IRON IN PRESENCE OF SULPHATE**

*Thesis submitted to the Indian Institute of Technology Guwahati, India,
for the award of the degree of*

DOCTOR OF PHILOSOPHY

by

ARVIND KUMAR SHAKYA



**DEPARTMENT OF CIVIL ENGINEERING
INDIAN INSTITUTE OF TECHNOLOGY GUWAHATI
GUWAHATI (INDIA)**

August, 2017





*Dedicated
to
My Country*





DEPARTMENT OF CIVIL ENGINEERING
INDIAN INSTITUTE OF TECHNOLOGY
GUWAHATI

STATEMENT

I hereby declare that the matter embodied in this thesis entitled “**Drinking Water Treatment by Biological Process for Simultaneous Removal of Arsenic, Nitrate and Iron in Presence of Sulphate**” is the result of investigations carried out by me at Department of Civil Engineering, Indian Institute of Technology Guwahati, Assam, India under the supervision of **Dr. Pranab Kumar Ghosh**. In keeping with the general practice of reporting scientific observations, due acknowledgements have been made wherever the work of other investigators are referred.

Dated

Arvind Kumar Shakya
Roll No. 10610404
Department of Civil Engineering
IIT Guwahati
Assam, India





DEPARTMENT OF CIVIL ENGINEERING
INDIAN INSTITUTE OF TECHNOLOGY
GUWAHATI

CERTIFICATE

This is to certify that the work presented in this thesis entitled “**Drinking Water Treatment by Biological Process for Simultaneous Removal of Arsenic, Nitrate and Iron in Presence of Sulphate**” submitted by **Mr. Arvind Kumar Shakya** (Roll No. 10610404) to the Indian Institute of Technology Guwahati, for the award of the degree of Doctor of Philosophy in Civil Engineering is a record of bonafide research work carried out by him under my supervision and guidance. The thesis work, in my opinion, has reached the requisite standard fulfilling the requirement for the degree of Doctor of Philosophy.

The results contained in this thesis have not been submitted in part or full to any other University or Institute for award of any degree or diploma.

IIT Guwahati
August, 2017

(Prof. Pranab Kumar Ghosh)
Department of Civil Engineering
IIT Guwahati
Guwahati-781039
Assam, India.



ACKNOWLEDGEMENT

Could I have done this Ph.D. by myself? of course not.

Starting from the very first moment I join my PhD till its completion, it seems as if I have been on a journey throughout. I have interacted with a variety of people at different juncture who have left both bad as well as good experience for a lifetime. All throughout these years, I have grown both academically as well as personally and I am thankful to each and everyone for all these experiences which have been instrumental in molding me for what I am today.

First and foremost I am grateful to my supervisor, **Professor Pranab Kumar Ghosh**, for introducing me in to the world of environmental engineering. I would also like to express my sincere thanks to him for his guidance, his invaluable suggestions, help, encouragement and support academically and emotionally through the rough road to finish this thesis work. I am also gratified with the personal as well as professional freedom provided to me throughout my research work. I would also like to take this opportunity to thank my Doctoral Committee members, **Prof. Chandan Mahanta, Prof. Kannan Pakshirajan** and **Dr. Ajay Kalamdhad** for their guidance and valuable suggestions through all these years which have been very helpful in shaping my thesis. Thanks also to **Prof. Mohammad Jawed, Prof. Saswati Chakraborty, Prof. Sharad Gokhale** and **Dr. Sri Harsha Kota** for optimally coordinating and stimulating me during my research work.

I am thankful to Department of Civil Engineering and Indian Institute of Technology Guwahati, India for providing me the facilities to carry out my research work. I am also thankful to Indian Institute of Technology Guwahati for the research fellowship.

I am grateful to the successive Heads of Department Civil Engineering, **Prof. S.K. Deb, Prof. A.K. Sharma** and **Prof. Subashisa Dutta** for providing me the departmental facilities to carry out my research work. Sincere thanks also pass through **Ms. Jonali saikia, Ms. Juri, Mr. C.R. Medhi** and **Mr. P. Pathak**, who were always helpful. I am also thankful to the staff members and technical officers of the other departments, **Dr. Sidananda Sarma, Mr. Nurul Islam, Mr. Niranjan Barah** and **Mr. Narayan Kalita** for extending all possible support. I deeply want to thank **Dr. Parasmani Rajput** for her support at RRCAT, Indore and her help with the XAS experiments as well. Furthermore, I would like to thank the office staff of the department for their support in administrative works. I gratefully acknowledge the unstinted help provided by PHED staff Bongaigaon, especially **Mr. L. Rahman** and **Mr. A. Das** during the collection of real groundwater for my research work. Thanks also to **Mr. Intajul Ali, Mr Bipul Chandra** and **Mr. Mridul Das** for their help during collection of sewage sludge. I thank **Mr. Tapan, Mr. Nayan, Mr. Kushal** and **Mr. Rantu Das** for their excellent assistance in the lab during experimental work.

Furthermore, I am thankful to Central Instruments Facility, Indian Institute of Technology Guwahati for the instrumentation facilities. I am also grateful to Ministry of Drinking Water and Sanitation (MDWS), India, for partial support to purchase minor equipments, consumables and scholarship for certain duration of my Ph.D. work through the sanctioned project [Project No. W-11017/44/2011-WQ].

I also want to thank all ex-lab members of Environmental Engineering Laboratory especially **Dr. Jiwan Singh, Dr. K. Dhamodharan, Dr. V. S. Varma, Dr. Susant Kumar Padhi** and **Dhananjaya**, as well as present lab mates **Rakhee, Subrat, Veluchamy C., Raghvendra, Sandip Sathe, Rajhans, Girish** and **Saurabh** for the help and good times I had shared in the Lab which have been my second home for the past six and half years. In addition to the academic work, the time I spent with all of you especially in organizing a Conference, Saraswati Puja and Vishwakarma Puja will be cherished throughout. Thank you people once again for the wonderful experience and environment. A special thanks to **Sachin, Damo, Ramkishore, Perla** and **Hari** for looking after my reactor whenever I am out of station.

I am thankful to my group members, **Dr. Atreyi Ghosh, Dr. Bharti, Vinay, Ramkishore, Hari, Pratik, Perla Harish, Ranjeeta, Rajashekhar, Himanshu** and everyone else I worked with for the moral support, and cooperation. I would like to thank my friends **Sachin, Nitin, Ruchira, Dr. Sambhavi, Saumya** and **Rajneesh** for all the good times and entertainment along with the serious discussions which I had shared with you. I would also like to thank my hostel mates **Dr. Ravikant, Ravishankar, Madhusudan, Mrityunjay, Abhipsit, Satyendra** and **Abhijeet** for the fun and frolic times we spent especially our dinner time. A special thanks to **Dr. Ramesh Ghosh, Dr. Indrajeet, Dr. Debanjan, Kiran C Babu, Mahak, Ananya, Gopi, Ashish, Laveti N.V. Satish, Pradeep, Reshmi** and **Deep** for their help.

I would never have been able to finish my dissertation without the help and support from my family and well-wishers, who were constant source of inspiration and encouragement to me. I would like to thank all of you for your love, affection, and helping me during my Ph.D. Special thanks go to my father, whose exemplary dedication in helping to uplift the downtrodden rural people has been an inspiration to me. I am equally indebted to my mother. Your dedicated caring, sincere love, and magnanimous guidance have carved me into the individual I am today. I would also like to thank my sister, and my brother for their love and moral support which have help me survive through the ups and downs throughout my research. Amrita, you are my soulmate and there is no limit to express my thanks to you. As my life partner and the closest confidante, you have accompanied me every moment of my life over the last 3 years, through times of trouble and enjoyment. Without you, nothing would have been possible.

Very importantly my heartfelt thanks go out to special persons Papa ji, Mummy ji, Ayushi and Anurag for their motivation, care and encouragement. You were my biggest support during this Ph.D.

Above all, I owe it all to Almighty God for granting me the wisdom, health and strength to undertake this research task and enabling me to its completion.

Arvind Kumar Shakya

Table of Contents

Table of Contents	v
List of Figures	ix
List of Tables	xvii
Abbreviations/Annotations	xix
ABSTRACT	xxiii
CHAPTER 1	1
INTRODUCTION	1
CHAPTER 2	7
LITERATURE REVIEW	7
2.1. Introduction, Source and Environmental Impact/ Health Effects of Contaminants	7
2.1.1 Arsenic	7
2.1.1.1 Sources and Occurrence in Water Environment	9
2.1.1.2 Environmental Impact	10
2.1.2 Nitrate	11
2.1.2.1 Sources and Occurrence in Water Environment	11
2.1.2.2 Environmental Impact	12
2.1.3 Iron	13
2.1.3.1 Sources and Occurrence in Water Environment	13
2.1.3.2 Environmental Impact	14
2.1.4 Fluoride	15
2.1.4.1 Sources and Occurrence in Water Environment	15
2.1.4.2 Environmental Impact	16
2.2 Simultaneous Co-occurrence of Multiple Pollutants in Groundwater	17
2.2.1 Co-occurrence due to Various Industrial Activities	17
2.2.2 Co-occurrence due to Geogenic Sources	18
2.2.3 Co-existence of Multiple Contaminants	20

2.2.4 Environmental Impact of Co-occurrence of Multiple Contaminants	20
2.3 Review of Removal Techniques	21
2.3.1 Oxidation	22
2.3.2 Coagulation-Flocculation	23
2.3.3 Ion Exchange	23
2.3.4 Membrane Technology	24
2.3.5 Adsorption Processes	25
2.3.6 Small Scale/Household Technologies	28
2.4 Biological Processes	29
2.4.1 Aerobic Respiration	30
2.4.2 Biological Denitrification	31
2.4.3 Biological Iron Removal	34
2.4.4 Microbial/Biological Arsenic Removal Mechanisms	36
2.4.4.1 Microbial Arsenic Oxidation	36
2.4.4.2 Microbial Arsenic Reduction	37
2.4.4.3 Arsenic Biomethylation	39
2.4.4.4 Microbially Mediated Adsorption/Co-precipitation on Biogenic Oxides	40
2.4.4.5 Microbial Arsenic Precipitation, Co-precipitation and/or Adsorption onto Biogenic Sulphides	42
2.5 Arsenic Containing Solids Treatment and Management	48
CHAPTER 3	51
AIM AND SCOPES OF THE STUDY	51
CHAPTER 4	53
MATERIALS AND METHODS	53
4.1 Materials	53
4.2 Waste Activated Carbon (WAC)	54
4.2.1 Microscopic Analysis of WAC	55
4.2.2 Bulk Density of WAC	55
4.2.3 Evaluation of WAC Adsorption Capacity on Arsenic Removal	56

4.3 Analysis of Liquid Samples	56
4.4 Experimental Methodologies	57
4.4.1 Seed sludge and Its Acclimatization in Reactor BR-0	57
4.4.2 Experimental Set-up and Bio-reactors	58
4.4.3 Batch Studies	59
4.4.3.1 Adsorption Studies in Batch Shake Flasks	59
4.4.3.2 Bio-removal Studies in Batch Shake Flasks	59
4.4.4 Semi-Batch Reactors (SmBR-1 & SmBR-2)	61
4.4.5 Flow through Reactors (AGR-1 and AGR-2)	66
4.4.5.1 Reactor Configuration and Experimental Set-up	66
4.5.2 Operation of AGR-1	72
4.5.2.1 Inoculation and Start-up of AGR-1	72
4.5.2.2 Phase-1: Effects of EBCT and Backwash Frequency	73
4.5.2.3 Phase-2: Effects of Influent Arsenic Concentration	73
4.5.2.4 Phase-3: Effects of Influent Nitrate Concentration	73
4.5.2.5 Phase-4: Effects of Influent pH	76
4.5.2.6 Phase-5: Effects of Operating Temperature	76
4.5.2.7 Phase-6: Effects of Influent Fluoride Concentration	76
4.5.2.8 Phase-7: Performance at Low EBCT	76
4.5.2.9 Phase-8: Performance After Shut down	76
4.5.3 Operation of AGR-2	77
4.5.3.1 Inoculation and Start-up of AGR-2	77
4.5.3.2 Phase-1: Effects of Influent Iron Concentration	77
4.5.3.3 Phase-2: Effects of Influent Arsenic Concentration	80
4.5.3.4 Phase-3: Effects of Influent Nitrate Concentration	80
4.5.3.5 Phase-4: Effects of Influent pH	80
4.5.3.6 Phase-5: Effects of Operating Temperature	80
4.5.3.7 Phase-6: Operation with Real Groundwater	81
4.5.3.8 Phase-7: Performance at Low EBCT	81

4.5.3.9 Phase-8: Performance after Shut down	81
4.6 AGR-2 operation with Real Groundwater	81
4.7 Microbial Population Identification and Diversity Analyses	83
4.7.1 Biofilm formation on WAC	83
4.7.2 T-RFLP analysis	83
4.7.3 Metagenomic analysis	84
4.8 Whole Effluent Toxicity (WET) Test of Treated Water	84
4.9. MPN test of Treated Water	85
4.10 Characterization of Biosolids	86
4.10.1. Collection and Preservation of Biosolids	86
4.10.2 X-ray Fluorescence (XRF)	87
4.10.3 Microscopic Methods	87
4.10.4 X-Ray Diffraction (XRD)	88
4.10.5 X-ray Absorption Spectroscopy (XAS)	88
4.11 Stability Check of Biosolids	89
4.11.1 Batch Ageing Test of Backwash Suspension	89
4.11.2 Toxicity Characteristics Leaching Procedure (TCLP) test	90
4.11.3 Long term Aerobic Leaching Test	92
4.12 Fluoride Removal by Water Treatment Residues (WTR)	93
4.12.1 Water Treatment Residues (WTR)	93
4.12.2 WTR Characterization	93
4.12.3 Batch Adsorption Experiments	94
4.12.4 Adsorption Equilibrium Study	95
CHAPTER 5	99
RESULTS AND DISCUSSION	99
5.1 Seed Sludge Collection and Acclimatization	100
5.2 Performance Evaluation of Batch Shakes Flasks	100
5.2.1. Adsorption Studies in Batch Shake Flasks	101
5.2.2 Adsorption of Arsenic by WAC	102

5.2.3 Bioremoval Studies in Batch Shake Flasks	103
5.2.3.1 Batch Studies in Absence of Iron	103
5.2.3.2 Batch Studies in Presence of Iron	107
5.3 Performance Evaluation of Semi-batch Bioreactor SmBR-1 in Absence of Iron	114
5.3.1 SmBR-1 Phase-1: Effect of HRT	114
5.3.2 SmBR-1 Phase-2: Effect of Initial Arsenic Concentration	115
5.3.3 SmBR-1 Phase-3: Effect of Initial Nitrate Concentration	116
5.3.4 SmBR-1 Phase-4: Effect of Different Carbon Sources	117
5.4 Performance Evaluation of Semi-batch Bioreactor SmBR-2 in Presence of Iron	118
5.4.1 SmBR-2 Phase-1: Effect of HRT	119
5.4.2 SmBR-2 Phase-2: Effect of Initial Arsenic Concentration	120
5.4.3 SmBR-2 Phase-3: Effect of Initial Nitrate Concentration	120
5.4.4 SmBR-2 Phase-4: Effect of Different Carbon Sources	121
5.5 Performance Evaluation of the Flow through Attached Growth Reactor, AGR-1	122
5.5.1. AGR-1 Start-up	122
5.5.2 AGR-1 Phase-1: Effects of EBCT and Backwash Frequency	123
5.5.3 AGR-1 Phase 2: Effect of Influent Arsenic Concentration	126
5.5.4 AGR-1 Phase 3: Effect of Influent Nitrate Concentration	129
5.5.5 AGR-1 Phase 4: Effect of pH	133
5.5.6 AGR-1 Phase 5: Effect of operating Temperature	135
5.5.7 AGR-1 Phase 6: Removal and Effects of Fluoride	137
5.5.8 AGR-1 Phase 7: Performance at Lower EBCT	137
5.5.9 AGR-1 Phase 8: Performance after Shutdown	138
5.6 Performance Evaluation of the Flow through Attached Growth Reactor, AGR-2	139
5.6.1 AGR-2 Start-up	140
5.6.2 AGR-2 Phase-1: Effects of Influent Iron Concentration	142

5.6.3 AGR-2 Phase 2: Effects of Arsenic	147
5.6.4 AGR-2 Phase 3: Effects of Influent Nitrate	149
5.6.5 AGR-2 Phase 4: Effect of Initial pH	153
5.6.6 AGR-2 Phase 5: Effect of operating Temperature	155
5.6.7 AGR-2 Phase 6: Treatment of Real Groundwater	157
5.6.8 AGR-2 Phase 7: Performance at Lower EBCT	157
5.6.9 AGR-2 Phase 8: Performance after Shutdown	158
5.7 AGR-2 Operation with Real Groundwater	159
5.8 Characterization of Bioreactor Treated Water	160
5.8.1 MPN Test	160
5.8.2 Whole Effluent Toxicity (WET) Test Results	160
5.9 Fluoride Removal using Water Treatment Plant Residues	163
5.9.1 Effect of WTR Dose	163
5.9.2 Effect of Contact Time	164
5.9.3 Effect of Agitation Speed	164
5.9.4 Effect of Initial Fluoride Concentration	165
5.9.5 Effect of Initial Temperature	166
5.9.6 Effect of Initial pH	167
5.9.7 Adsorption Isotherm	168
5.9.8 Characterization of WTR	171
5.10 Microbial Population Identification and Diversity Analyses	174
5.10.1 Microbial Biofilm on WAC	174
5.10.2 T-RFLP Analysis	174
5.10.3 Metagenomic Analysis	176
5.10.3.2 Prevalence of Sulphate Reducing Microorganisms	180
5.10.3.3 Prevalence of Nitrate-Reducing Microorganisms	180
5.10.3.4 Prevalence of Other Metabolically Important Microorganisms	181
5.11 Biosolids Characterization	183
5.11.1 Biosolids Characterization of Batch Shake Flasks in Absence of Iron	183

5.11.2 Biosolids Characterization of Batch Shake Flasks in Presence of Iron	184
5.11.3 Biosolids Characterization of Semi-batch Bioreactors	186
5.11.3.1 SmBR-1	186
5.11.3.2 SmBR-2	187
5.11.4 Biosolids Characterization of Flow-through Reactors	191
5.11.4.1 AGR-1	191
5.11.4.2 AGR-2	199
5.12 Stability Tests on Biosolids	207
5.12.1 Aging Tests Results of Biosolids of AGR-1 and AGR-2	207
5.12.2 TCLP Test Results	210
5.12.3 Long-term Aerobic Leaching Tests	217
CHAPTER 6	223
CONCLUSION AND SCOPE OF FUTURE STUDIES	223
VISIBLE RESEARCH OUTPUT	227
REFERENCES	229
APPENDIX	256



List of Figures

Figure 2.1 Eh–pH diagram for arsenic at 25 °C and 101.3 kPa.	8
Figure 4.1 Schematic diagram of semi-batch reactor set-up.....	61
Figure 4.2 Photographs of a screen (a) and deflector beam (b) used in the reactor.....	68
Figure 4.3 (a) Schematic diagram and (b) actual photograph of an attached growth reactor (AGR).	70
Figure 4.4 Lab scale schematic diagram of flow through reactors set-up AGR-1 (a) and AGR-2 (b).	71
Figure 4.5 Photographs of the lab scale reactor set-up of flow through reactors AGR-1 and AGR-2.....	72
Figure 4.6 Schematic diagram of container used for collecting backwash suspension.	86
Figure 5.1 Enrichment of mixed microbial consortium.....	100
Figure 5.2 Time series profile of average residual arsenic, nitrate and COD concentration after adsorption by 100 mg/L of inoculum (MLVSS).	102
Figure 5.3 Arsenic adsorption on to WAC.	102
Figure 5.4 Performance of batch shake flasks in absence of iron at initial arsenic = 250 µg/L, nitrate = 50 mg/L and sulphate = 25 mg/L.	103
Figure 5.5 Performance of batch shake flasks in absence of iron at initial arsenic = 350 µg/L, nitrate = 50 mg/L and sulphate = 25 mg/L.	104
Figure 5.6 Performance of batch shake flasks in absence of iron at initial arsenic = 450 µg/L, nitrate = 50 mg/L and sulphate = 25 mg/L.	104
Figure 5.7 Performance of batch shake flasks in absence of iron at initial arsenic of = 550 µg/L, nitrate = 50 mg/L and sulphate = 25 mg/L.	105
Figure 5.8 Performance of batch shake flasks in absence of iron at initial arsenic = 550 µg/L, nitrate = 100 mg/L and sulphate = 25 mg/L.	106
Figure 5.9 Performance of batch shake flasks in absence of iron at initial arsenic = 550 µg/L, nitrate = 150 mg/L and sulphate = 25 mg/L.	106
Figure 5.10 Performance of batch shake flasks in presence of iron at initial iron = 1.0 mg/L, arsenic = 500 µg/L, nitrate = 50 mg/L and sulphate = 25 mg/L.	108
Figure 5.11 Performance of batch shake flasks in presence of iron at initial iron = 2.0 mg/L, arsenic = 500 µg/L, nitrate = 50 mg/L and sulphate = 25 mg/L.	108
Figure 5.12 Performance of batch shake flasks in presence of iron at initial iron = 3.0 mg/L, arsenic = 500 µg/L, nitrate = 50 mg/L and sulphate = 25 mg/L.	109
Figure 5.13 Performance of batch shake flasks in presence of iron at initial iron = 4.0 mg/L, arsenic = 500 µg/L, nitrate = 50 mg/L and sulphate = 25 mg/L.	109

Figure 5.14 Performance of batch shake flasks in presence of iron at initial iron = 5.0 mg/L, arsenic = 500 µg/L, nitrate = 50 mg/L and sulphate = 25 mg/L.	110
Figure 5.15 Performance of batch shake flasks in presence of iron at initial iron = 5.0 mg/L, arsenic = 500 µg/L, nitrate = 50 mg/L and sulphate = 50 mg/L.	110
Figure 5.16 Performance of batch shake flasks in presence of iron at initial iron = 3.0 mg/L, arsenic = 600 µg/L, nitrate = 50 mg/L and sulphate = 25 mg/L.	111
Figure 5.17 Performance of batch shake flasks in presence of iron at initial iron = 3.0 mg/L, arsenic = 750 µg/L, nitrate = 50 mg/L and sulphate = 25 mg/L.	111
Figure 5.18 Performance of batch shake flasks in presence of iron at initial iron = 3.0 mg/L, arsenic = 1000 µg/L, nitrate = 50 mg/L and sulphate = 25 mg/L.	112
Figure 5.19 Performance of batch shake flasks in presence of iron at initial iron = 3.0 mg/L, arsenic = 1000 µg/L, nitrate = 100 mg/L and sulphate = 25 mg/L. ...	113
Figure 5.20 Performance of batch shake flasks in presence of iron at initial iron = 3.0 mg/L, arsenic = 1000 µg/L, nitrate = 150 mg/L and sulphate = 25 mg/L. ...	113
Figure 5.21 Performance evaluation of SmBR-1 in phase-1 at initial arsenic = 200 µg/L, nitrate = 50 mg/L and sulphate = 25 mg/L.	114
Figure 5.22 Performance evaluation of SmBR-1 in phase-2 at initial arsenic = 200-800 µg/L, nitrate = 50 mg/L and sulphate = 25 mg/L.	115
Figure 5.23 Performance evaluation of SmBR-1 in phase-3 at initial nitrate = 50-250 mg/L, arsenic = 600 µg/L and sulphate = 25 mg/L.	116
Figure 5.24 Performance evaluation of SmBR-1 in phase-4 at initial nitrate = 200 mg/L, arsenic = 600 µg/L and sulphate = 25 mg/L.	117
Figure 5.25 Performance evaluation of SmBR-2 in phase-1 at initial nitrate = 100 mg/L, arsenic = 250 µg/L, iron = 2 mg/L and sulphate = 25 mg/L.	119
Figure 5.26 Performance evaluation of SmBR-2 in phase-2 at initial nitrate = 100 mg/L, arsenic = 250-1000 µg/L, iron = 2 mg/L and sulphate = 25 mg/L.	120
Figure 5.27 Performance evaluation of SmBR-2 in phase-3 at initial nitrate = 100-250 mg/L, arsenic = 1000 µg/L, iron = 2 mg/L and sulphate = 25 mg/L.	121
Figure 5.28 Performance evaluation of SmBR-2 in phase-4 at initial nitrate = 250 mg/L, arsenic = 1000 µg/L, iron = 2 mg/L and sulphate = 25 mg/L.	122
Figure 5.29 Performance evaluation of AGR-1 in start up and phase-1 at initial nitrate = 50 mg/L, arsenic = 250 µg/L, and sulphate = 25 mg/L.	125
Figure 5.30 Sampling profile of the AGR-1 on day 228 (arsenic = 250 µg/L, nitrate = 50 mg/L, sulphate = 25 mg/L and EBCT 45 Min.).....	126
Figure 5.31 Performance evaluation of AGR-1 in phase-2 at initial nitrate = 50 mg/L, arsenic = 200-750 µg/L, and sulphate = 25 mg/L.	126
Figure 5.32 Sampling profile of the AGR-1 on day 398 (arsenic = 750 µg/L, nitrate = 50 mg/L, sulphate = 25 mg/L and EBCT 45 Min.).....	128
Figure 5.33 Sampling profile of the AGR-1 on day 457 (arsenic = 750 µg/L, nitrate = 50 mg/L, sulphate = 50 mg/L and EBCT 60 Min.).....	128

Figure 5.34 Performance evaluation of AGR-1 in phase-3 at initial nitrate = 50-200 mg/L, arsenic = 500 µg/L, and sulphate = 25 mg/L.	130
Figure 5.35 Sampling profile of the AGR-1 on day 480 (arsenic = 500 µg/L, nitrate = 50 mg/L, sulphate = 25 mg/L and EBCT 45 Min.).	130
Figure 5.36 Sampling profile of the AGR-1 on day 508 (arsenic = 500 µg/L, nitrate = 100 mg/L, sulphate = 25 mg/L and EBCT 45 Min.).	131
Figure 5.37 Sampling profile of the AGR-1 on day 540 (arsenic = 500 µg/L, nitrate = 150 mg/L, sulphate = 25 mg/L and EBCT 45 Min.).	131
Figure 5.38 Sampling profile of the AGR-1 on day 570 (arsenic = 500 µg/L, nitrate = 200 mg/L, sulphate = 25 mg/L and EBCT 45 Min.).	132
Figure 5.39 Sampling profile of the AGR-1 on day 603 (arsenic = 500 µg/L, nitrate = 200 mg/L, sulphate = 25 mg/L and EBCT 60 Min.).	132
Figure 5.40 Performance evaluation of AGR-1 in phase-4 at initial nitrate = 50 mg/L, arsenic = 500 µg/L and sulphate = 25 mg/L.	134
Figure 5.41 Performance evaluation of AGR-1 in phase-5 at initial nitrate = 50 mg/L, arsenic = 500 µg/L and sulphate = 25 mg/L.	136
Figure 5.42 Performance evaluation of AGR-1 in phase-6 at initial nitrate = 50 mg/L, arsenic = 500 µg/L, sulphate = 25 mg/L and fluoride = 5 mg/L.	137
Figure 5.43 Performance evaluation of AGR-1 in phase-7 at initial nitrate = 50 mg/L, arsenic = 500 µg/L and sulphate = 25 mg/L.	138
Figure 5.44 Performance evaluation of AGR-1 in phase-8 at initial nitrate = 50 mg/L, arsenic = 500 µg/L and sulphate = 25 mg/L.	139
Figure 5.45 Performance evaluation of AGR-2 in start up phase at initial arsenic = 250 µg/L, iron = 2.0 mg/L, nitrate = 50 mg/L and sulphate = 25 mg/L.	141
Figure 5.46 Sampling profile of the AGR-2 on day 102 (arsenic = 500 µg/L, iron = 2.0 mg/L, nitrate = 50 mg/L, sulphate = 25 mg/L and EBCT 45 Min.).	142
Figure 5.47 Performance evaluation of AGR-2 in phase-1 at initial arsenic = 500 µg/L, iron = 2.0 -10 mg/L, nitrate = 50 mg/L and sulphate = 25-75 mg/L.	143
Figure 5.48 Sampling profile of the AGR-2 on day 181 (Iron = 5.0 mg/L, arsenic = 500 µg/L, nitrate = 50 mg/L, sulphate = 25 mg/L and EBCT 45 Min.).	144
Figure 5.49 Sampling profile of the AGR-2 on day 208 (sulphate = 50 mg/L, iron 5.0 = mg/L, arsenic = 500 µg/L, nitrate = 50 mg/L and EBCT 45 Min.).	144
Figure 5.50 Sampling profile of the AGR-2 on day 264 (sulphate = 75 mg/L, iron = 7.5 mg/L, arsenic = 500 µg/L, nitrate = 50 mg/L and EBCT 60 Min.).	145
Figure 5.51 Sampling profile of the AGR-2 on day 326 (sulphate = 75 mg/L, iron = 10.0 mg/L, arsenic = 500 µg/L, nitrate = 50 mg/L and EBCT 90 Min.).	146
Figure 5.52 Performance evaluation of AGR-2 in phase-2 at initial arsenic = 500-1500 µg/L, iron = 10.0 mg/L, nitrate = 50 mg/L and sulphate = 75 mg/L.	147
Figure 5.53 Sampling profile of the AGR-2 on day 382 (arsenic = 1000 µg/L, sulphate = 75 mg/L, iron = 10.0 mg/L, nitrate = 50 mg/L and EBCT 90 Min.).	148

Figure 5.54 Sampling profile of the AGR-2 on day 444 (arsenic = 1500 µg/L, sulphate = 75 mg/L, iron = 10.0 mg/L, nitrate = 50 mg/L, and EBCT 90 Min.).	148
Figure 5.55 Performance evaluation of AGR-2 in phase-3 at initial arsenic = 1500 µg/L, iron = 10 mg/L, nitrate = 50-200 mg/L and sulphate = 75 mg/L.	149
Figure 5.56 Sampling profile of the AGR-2 on day 474 (nitrate = 100 mg/L, arsenic = 1500 µg/L, sulphate = 75 mg/L, iron = 10.0 mg/L and EBCT 90 Min.).	151
Figure 5.57 Sampling profile of the AGR-2 on day 505 (nitrate = 150 mg/L, arsenic = 1500 µg/L, sulphate = 75 mg/L, iron = 10.0 mg/L, nitrate = 150 mg/L and EBCT 90 Min.).	151
Figure 5.58 Sampling profile of the AGR-2 on day 533 (nitrate = 200 mg/L, arsenic = 1500 µg/L, sulphate = 75 mg/L, iron = 10.0 mg/L and EBCT 90 Min.).	152
Figure 5.59 Sampling profile of the AGR-2 on day 561 (nitrate = 200 mg/L, arsenic = 1500 µg/L, sulphate = 75 mg/L, iron = 10.0 mg/L, and EBCT 120 Min.).	152
Figure 5.60 Performance evaluation of AGR-2 in phase-4 at initial arsenic = 500 µg/L, iron = 3.0 mg/L, nitrate = 50 mg/L and sulphate = 25 mg/L.	154
Figure 5.61 Performance evaluation of AGR-2 in phase-5 at initial arsenic = 500 µg/L, iron = 3.0 mg/L, nitrate = 50 mg/L and sulphate = 25 mg/L.	156
Figure 5.62 Performance evaluation of AGR-2 in phase-7 at initial arsenic = 500 µg/L, iron = 3.0 mg/L, nitrate = 50 mg/L and sulphate = 25 mg/L.	158
Figure 5.63 Performance evaluation of AGR-2 in phase-8 at initial arsenic = 500 µg/L, iron = 3.0 mg/L, nitrate = 50 mg/L and sulphate = 25 mg/L.	159
Figure 5.64 Performance of AGR-2 with real groundwater.	160
Figure 5.65 Effects of WTR dose on fluoride removal (Ini. fluoride concentration = 5.0 mg/L, contact time = 120 min., agitation speed = 100 rpm, temperature = 30°C and pH = 6.9-7.4).	163
Figure 5.66 Effects of contact time on fluoride removal (Ini. fluoride concentration = 5.0 mg/L, WTR dose = 16 g/L, agitation speed = 100 rpm, temperature = 30°C and pH = 6.9-7.4).	164
Figure 5.67 Effects of agitation speed on fluoride removal (Ini. fluoride concentration = 5.0 mg/L, WTR dose = 16 g/L, contact time = 120 min, temperature = 30°C and pH = 6.9-7.4).	165
Figure 5.68 Effects of initial fluoride on fluoride removal (WTR dose = 16 g/L, contact time = 120 min., agitation speed = 200 rpm, temperature = 30°C and pH = 6.9-7.4).	166
Figure 5.69 Effect of initial temperature on fluoride removal (Ini. Fluoride = 5.0 mg/L, WTR dose = 16 g/L, contact time = 120 min., agitation speed = 200 rpm, and pH = 6.9-7.4).	167
Figure 5.70 Effect of initial pH on fluoride removal (Ini. Fluoride = 5.0 mg/L, WTR dose = 16 g/L, contact time = 120 min., agitation speed = 200 rpm, and temperature = 30°C).	168

Figure 5.71 Linearized Langmuir isotherm for fluoride ion adsorption by WTR (Ini. fluoride concentration = 5.0 mg/L, equilibrium contact time = 120 min., pH 7.0, and temperature = 30 °C).....	169
Figure 5.72 Linearized Freundlich isotherm for fluoride ion adsorption by WTR (Ini. fluoride concentration = 5.0 mg/L, equilibrium contact time = 120 min., pH 7.0, and temperature = 30 °C).....	170
Figure 5.73 Linearized Temkin isotherm for fluoride ion adsorption by WTR (Ini. fluoride concentration = 5.0 mg/L, equilibrium contact time = 120 min., pH 7.0, and temperature = 30 °C).	170
Figure 5.74 FESEM image (a) and EDX pattern (b) of WTR before fluoride adsorption.	171
Figure 5.75 FESEM image (a) and EDX pattern (b) of WTR after fluoride adsorption.	171
Figure 5.76 FT-IR patterns of WTR before and after adsorption.	172
Figure 5.77 X-ray powder diffraction patterns of WTR before and after adsorption.	173
Figure 5.78 FESEM image of WAC granules from AGR-1 (a) before and (b) after biofilm growth on WAC granules.	174
Figure 5.79 T-RFLP profile of microbial community present in AGR-1 collected after 250 days of operation.....	175
Figure 5.80 Taxonomic hits distribution at phylum level of (a) AGR-1 and (b) AGR-2.	178
Figure 5.81 Taxonomic hits distribution at class level of (a) AGR-1 and (b) AGR-2.	179
Figure 5.82 (a) FESEM micrograph and (b) EDX spectra of biosolids of batch shake flasks in absence of iron.	183
Figure 5.83 FESEM micrograph and X-ray elemental mapping of biosolids of batch shake flasks in absence of iron: (a) FESEM micrograph, (b,c) X-ray mapping of elements arsenic and sulphur.	184
Figure 5.84 (a) FESEM micrograph and (b) EDX spectra of biosolids of batch shake flasks in presence of iron.	185
Figure 5.85 FESEM micrograph and X-ray elemental mapping of biosolids of batch shake flasks in presence of iron: (a) FESEM micrograph, (b,c,d) X-ray mapping of elements sulphur, iron and arsenic.....	185
Figure 5.86 XRF spectra of biosolids of SmBR-1 showing presence of arsenic (a) and sulphur (b).....	186
Figure 5.87 TEM images (a,c,e) and their representative EDX spectra (b,d,f) of biosolids of SmBR-1.	188
Figure 5.88 XRF spectra of biosolids of SmBR-2 showing presence of arsenic (a) sulphur (b) and iron (c).	189
Figure 5.89 TEM images (a,b) and their representative EDX spectra (c) of biosolids of SmBR-2.	190
Figure 5.90 (a) HRTEM image and (b) SAED pattern of biosolids formed in SmBR-2.	191

Figure 5.91 (a) FESEM micrograph and (b) EDX spectra of AGR-1 biosolids collected on day 183 of reactor run.	192
Figure 5.92 FESEM micrograph and X-ray elemental mapping of the biosolids formed in AGR-1: (a) FESEM micrograph (b) X-ray mapping of element arsenic (c) X-ray mapping of element sulphur.	192
Figure 5.93 (a, b) X-ray Diffraction diagram of the precipitates formed in AGR-1 after 430 and 630 day of operation.....	193
Figure 5.94 (a,b) TEM images, (c) SAED pattern, (d) EDX spectra of the biosolids collected from backwash suspension of AGR-1, when backwash frequency was 7 days or shorter.....	194
Figure 5.95 (a,b) TEM images, (c) SAED pattern, (d) HRTEM image, (e) FFT, and (f) IFFT of biosolids of AGR-1.	196
Figure 5.96 (a) Normalized XANES data at As K-edge for biosolids of AGR-1 with As ³⁺ and As ⁵⁺ standards, (b) 1 st derivative data plot comparison of biosolids of AGR-1 and As ³⁺ standard.	198
Figure 5.97 Fourier transform of k^2 -weighted of As K-edge for biosolids of AGR-1. The symbol shows experimental data and solid lines are the best fit.	198
Figure 5.98 (a,b) Cross sectional FESEM-backscattered electron (BSE) images and (c,d) point EDS analyses of the biosolids precipitated in AGR-2.....	199
Figure 5.99 (a,b) Cross sectional FESEM-BSE images and (c,d) point EDS analyses of the precipitates formed in AGR-2.....	200
Figure 5.100 FESEM micrograph and X-ray elemental mapping of the biosolids formed in AGR-2: FESEM micrograph (a,b), X-ray mapping of element sulphur (c), X-ray mapping of element iron (d) and X-ray mapping of element arsenic (e).	201
Figure 5.101 (a, b) X-ray Diffraction diagram of the precipitates formed in AGR-2 after 310 and 430 days of operation.	202
Figure 5.102 (a, b) TEM images, (c) SAED pattern, (d) HRTEM image, (e) FFT and (f) IFFT of biosolids of AGR-2.	204
Figure 5.103 Normalized XANES data at As K-edge for biosolids of AGR-2 with As ³⁺ and As ⁵⁺ standards.	205
Figure 5.104 (a) Normalized XANES data at Fe K-edge for biosolids of AGR-2 with FeS (Fe ²⁺) and Fe foil, (b) 1 st derivative data plot comparison of biosolids of AGR-2 and FeS standard.	206
Figure 5.105 Fourier transform of k^2 -weighted of Fe K-edge for biosolids of AGR-2. The symbol shows experimental data and solid lines are the best fit.	206
Figure 5.106 Release of arsenic during anoxic and oxic aging of backwash solids of AGR-1.....	209
Figure 5.107 Release of arsenic and iron during anoxic and oxic aging of backwash solids AGR-2.....	209
Figure 5.108 Arsenic leaching profile during kinetic TCLP leaching tests on biosolids of AGR-1.....	212

Figure 5.109 Arsenic and iron leaching profile during kinetic TCLP leaching tests on biosolids of AGR-2.....	212
Figure 5.110 Leaching of arsenic and iron as estimated through extended TCLP test on biosolids of AGR-1 and AGR-2 at constant V_g/V_L ratio of 0.5.....	213
Figure 5.111 Effects of V_{air}/V_L ratios on leachability of arsenic from the biosolids of AGR-1 during extended TCLP tests.....	216
Figure 5.112 Effects of V_{air}/V_L ratios on leachability of arsenic from the biosolids of AGR-2 during extended TCLP tests.....	216
Figure 5.113 Effects of V_{air}/V_L ratios on leachability of iron from the biosolids of AGR-2 during extended TCLP tests.....	217
Figure 5.114 Arsenic leaching as observed during long-term leaching test on biosolids of AGR-1.....	218
Figure 5.115 Arsenic leaching as observed during long-term leaching test on biosolids of AGR-2.....	219
Figure 5.116 Iron leaching as observed during long-term leaching test on biosolids of AGR-2.....	219
Figure 5.117 (a) Normalized XANES data at Fe K-edge for long term leaching test in AGR-2 TCLP samples with FeS (Fe^{2+}), Fe_2O_3 (Fe^{3+}) standards and Fe foil, (b) 1 st derivative data plot comparison of AGR-2 TCLP sample and Fe_2O_3 standard.....	221
Figure 5.118 (a) Normalized XANES data at As K-edge for long term leaching test in AGR-2 TCLP samples with As(III), As (V) standards and sample, (b) 1 st derivative data plot comparison of AGR-2 TCLP sample and As (V) standard.	222
Figure 5.119 Fourier transform of k^2 -weighted of Fe K-edge for AGR-2 TCLP sample. The symbol shows experimental data and solid lines are the best fit.	222
Figure A1 Calibration curve for nitrate determination.	256
Figure A2 Calibration curve for sulphate determination.	256
Figure A3 Calibration curve for fluoride determination.....	257
Figure A4 Calibration curve for iron determination.....	257
Figure A5 Collection of sewage sludge from IIT Guwahati sewage treatment plant.....	258
Figure A6 Location of Bongaigaon district in India.	258
Figure A7 Location map of real groundwater sampling site.	259
Figure A8 (a) Collection of real ground water (b) onsite determination of water quality parameters and arsenic.....	259







List of Tables

Table 4.1 Instruments and equipment used in the present investigation.	54
Table 4.2 Composition of feed of synthetic groundwater and trace mineral solution.	58
Table 4.3 The operational schedule of semi batch reactor (SmBR-1) operated in absence of iron.....	64
Table 4.4 The operational schedule of semi batch reactor (SmBR-2) operated in presence of iron.....	65
Table 4.5 Specifications of AGRs.	66
Table 4.6 Operational schedule of AGR-1.	74
Table 4.7 Operational schedule AGR-2.....	78
Table 4.8 Characteristics of raw groundwater.	82
Table 5.1 Whole Effluent Toxicity test results of AGR treated water at $30\pm 2^{\circ}\text{C}$	162
Table 5.2 Isotherm parameters for the removal of fluoride by untreated adsorbent (Ini. fluoride concentration = 5.0 mg/L, equilibrium contact time = 120 min., pH 7.0 ± 0.1 , and temperature = $30\pm 2^{\circ}\text{C}$).	169
Table 5.3 Total number of OTUs read in AGR-1 and AGR-2	176
Table 5.4 The best fit values of the parameters for AGR-1 sample.	197
Table 5.5 The best fit values of the parameters for biosolids of AGR-2 sample.....	206
Table 5.6 Characteristics of AGR-1 and AGR-2 backwash solids.....	210
Table 5.7 Leachability of arsenic by the TCLP at different $V_{\text{air}}/V_{\text{L}}$ ratios in AGR-1.....	215
Table 5.8 Leachability of arsenic and iron by the TCLP at different $V_{\text{air}}/V_{\text{L}}$ ratios in AGR-2.	215
Table 5.9 The best fit values of the parameters for AGR-2 sample.	221







Abbreviations/Annotations

AAS	Atomic absorption spectroscopy
AGR	Attached growth reactor
AMD	Acid mine drainage
AOM	Arsenic oxidizing microbes
ASCR	Arsenic containing solid residuals
BR	Batch reactor
BSE	Back-scattered electron
CGWB	Central ground water board
COD	Chemical oxygen demand
DARP	Dissimilatory arsenic reducing prokaryotes
DI	Deionized
DIRB	Dissimilatory iron reducing bacteria
EBCT	Empty bed contact time
EC	European Commission
EDX	Energy dispersive X-ray spectroscopy
EU	European union
EXAFS	Extended X-ray absorption fine structure
FESEM	Field emission scanning electron microscopy
FFT	Fast fourier transform
FT-IR	Fourier transform infrared spectroscopy
HRT	Hydraulic retention time
HRTEM	High resolution transmission electron microscopy
IFFT	Inverse fast fourier transform
IOB	Iron oxidizing bacteria
IS	Indian standards
MCL	Maximum contaminant level
MPN	Most probable number
MLSS	Mixed liquor suspended solids
NF	Nano filtration
OTU	Operational taxonomic units

PCR	Polymerase chain reaction
ppm	Parts per million
RNA	Ribose nucleic acid
rpm	Revolutions per minute
RO	Reverse osmosis
SAED	Selected area electron diffraction
SmBR	Semi batch reactor
SRB	Sulphate reducing bacteria
SRP	Sulphate reducing prokaryotes
TCLP	Toxicity characteristics leaching procedure
TEAP	Terminal electron accepting process
TEM	Transmission electron microscopy
T-RFLP	Terminal restriction fragment length polymorphism
TSS	Total suspended solids
UF	Ultra filtration
USEPA	United states environmental protection agency
VSS	Volatile suspended solids
WAC	Waste activated carbon
WET	Whole effluent toxicity
WHO	World health organization
WTR	Water treatment residuals
XANES	X-ray absorption near edge structure
XAS	X-ray absorption spectroscopy
XRD	X-ray powder diffraction
XRF	X-ray fluorescence

Å	Angstrom
As	Arsenic
cm	Centimeter
eV	Electron volt
F ⁻	Fluoride
Fe	Iron
ft	Feet
gm	Gram
h	Hour
L	Litre
M	Molar
mA	Milliampere
mg	Miligram
min.	Minute
ml	Milliliter
mM	Milimolar
mm	Millimeter
nm	Nanometer
NO ₃ ⁻	Nitrate
SO ₄ ²⁻	Sulphate
v/v	Volume/volume
w/v	Weight/volume
µg	Microgram
µm	Micrometer



ABSTRACT

Arsenic is one among many oxyanions present in sources of drinking water as a potential contaminant. There are several reports on health effects of arsenic as well as technologies for its removal from contaminated drinking water. Although several methods of arsenic removal as sole contaminant from contaminated water are successful, simultaneous removal of co-pollutants along with arsenic is still a challenging job to the environmental engineers. Most of the highly efficient physicochemical processes are silent on simultaneous removal of multipollutants such as arsenic, nitrate, iron, sulphate, fluoride etc. Furthermore, the efficient treatment processes generate high volume of arsenic bearing unstable solids, which become a source of arsenic contamination of nearby drinking water sources. Based on thorough literature survey but limited information, reveals that biological process has a high potential on simultaneous removal of multiple number of contaminants of groundwater leaving low volume stable arsenic bearing waste which may disposed of safely in a landfill along with comingled municipal solid waste. The main objective of this research work is to develop a biological reactor for simultaneous removal of arsenic, nitrate and iron in presence of sulphate from simulated as well as real contaminated groundwater.

In this study, mixed microbial culture was collected from a wastewater treatment plant, mixed with small amount of (<5%) of bio-sludge collected from two nos. laboratory scale bioreactors treating perchlorate and nitrate, and sulphate, respectively. The mixed bacterial biomass thus prepared was acclimatized in presence of arsenic, nitrate and sulphate. The acclimatized sludge was used to evaluate its performance on simultaneous removal of target pollutants, arsenic, nitrate, iron and fluoride as well as effects of one pollutant on the others in batch, semi-batch and flow through reactor systems. The reactors were operated in absence as well as in presence of iron. Batch studies were carried out in shake flasks whereas studies in semi batch mode were conducted in 1 L bottles, operated in suspended growth mode. Reactors operated in continuous mode were of attached growth reactors (AGR), where waste activated carbon (WAC) was used as supporting material for bacterial growth. Adsorption characteristics of the WAC were evaluated before being used in AGRs. Besides performance evaluation of mixed bacterial culture on simultaneous removal of target pollutants from groundwater,

microbial population dynamics in AGRs, post treatment of AGR treated water and mechanisms of arsenic removal were also investigated through their characterization. Collection, preparation, characterization and performance evaluation of an adsorbent from water treatment plant residues (WTR) on fluoride removal from AGR treated water was performed to evaluate its potential as a post treatment unit. In addition to this, stability of the biosolids as well as the spent WAC were checked under aerobic as well as anoxic conditions through “Ageing test”, “Toxicity Characteristics Leaching Procedure (TCLP) test” and “Long Term Leaching test”.

Experimental results show that, in absence of iron, the mixed microbial culture could reduce arsenic to below permissible limit in drinking water, from an initial of 600 $\mu\text{g/L}$ in suspended growth mode. However, in attached growth mode, AGR-1 could reduce arsenic to below 10 $\mu\text{g/L}$, from an initial of up to 750 $\mu\text{g/L}$ in simulated groundwater. In presence of iron, arsenic was reduced to below 10 $\mu\text{g/L}$, from an initial of up to 1000 $\mu\text{g/L}$ and 1500 $\mu\text{g/L}$ in suspended growth (SmBR-2) and attached growth (AGR-2) systems, respectively. From an initial of up to 250 mg/L, complete removal of nitrate in all the reactor systems was noticed within 24 hours of operation. No presence of nitrite in the treated water suggests complete denitrification. From an initial of 13.2 mg/L, the AGR-2 could reduce iron to below 0.3 mg/L from real groundwater at appropriate feeding and operating conditions. At varying temperature, performance of either AGR did not get affected except for first few initial days at 20°C and 50°C. The T-RFLP and metagenomic analysis of microbial community confirmed the presence of arsenic, nitrate and sulphate reducers in AGRs. The adsorbent prepared from WTR could remove fluoride from an initial of 5 mg/L to 0.55 mg/L. FESEM/EDX, XRD, TEM and XAS analysis of biosolids in AGR-1 confirmed the presence of As(III) as orpiment and realgar in amorphous and nanocrystalline forms. Biosolids in AGR-2 contains As(III) and Fe(II) as pyrrhotite, and pyrite in addition to as orpiment and realgar in crystalline form. The results suggest that precipitation of arsenosulphide is the main mechanism of arsenic removal in AGR-1, whereas, in AGR-2 precipitation as arsenosulphide and/or co-precipitation of arsenic with biogenic iron sulphides are the main arsenic removal mechanisms. After 90 days of experiment in anoxic and oxic environment, ageing test results have shown that arsenic leaching from biosolids of either AGRs was less than or equal to 0.6%, whereas maximum iron leaching of 0.48% was noticed from AGR-2 biosolids. TCLP and long term leaching test results show that the concentration of arsenic

in the leaching solution does not exceed either the maximum Australian or USEPA leachate values of 300 and 5000 $\mu\text{g/L}$, respectively. Thus the biosolids in the AGRs, including the spent WAC, would not be classified as hazardous waste material.

In summary, the AGR systems developed in this project could remove arsenic and its co-pollutants such as nitrate and iron from simulated as well as real groundwater at wide range of temperature to meet the drinking water standards, leaving a non hazardous and stable biosolids as well as spent WAC, which can be dumped in sanitary landfill safely. However, fluoride needs to be treated separately in an additional treatment unit. A waste product, WTR, proved to be efficient for fluoride removal to meet the drinking water standards.





CHAPTER 1

INTRODUCTION

Safe drinking water is one of the most fundamental necessities for human population. Groundwater serves as the sole drinking water source in many rural and urban areas of the world. (WHO, 2006). Due to rapid technological developments and population increase, water resources such as groundwater are in danger of severe pollution in the world. Groundwater contamination may be due to either natural or anthropogenic sources. Major sources of natural groundwater pollution include geogenic factors, seawater intrusion, and geothermal fluid(s). Important anthropogenic sources include agricultural activities, mining activity, industrial waste and onsite septic tank systems etc. Some of the inorganic anions impose long-term serious health effects which affects sustainability of communities. Trace levels presence of toxic inorganic anions do not cause organoleptic changes in drinking water therefore some of them remain undetected hence increases health risks. A wide number of inorganic anions have been found potentially toxic and harmful to humans and animals at very low concentrations (ppb) in drinking water (Velizarov et al., 2004). Arsenic is one of such contaminant that affects groundwater quality worldwide. More than 100 million people of the world is at risk of arsenic contamination as per WHO provisional guideline for drinking water of 10 $\mu\text{g/L}$ arsenic, out of this more than 45 million people of developing countries from Asia are at risk of being exposed to more than 50 $\mu\text{g/L}$ of arsenic, which is the maximum concentration limit in drinking water in most of the Asian countries (Sharma et al., 2014a). Highly ferruginous groundwater is often found in many parts of the world which is unfit for domestic use and also forming slimy coatings in water pipes due to bacterial growth (Demlie et al., 2014). Excess consumption of highly ferruginous water by humans, may be linked to diseases such as diabetes, heart disease, cancer and kidney problems as a result of iron stores (high serum ferritin) in the body (Pourmoghaddas et al., 2014).

Nitrate (NO_3^-) is also a major groundwater contaminant in the most parts of the world due to its high water solubility (Mohseni-Bandpi et al., 2013). High NO_3^- contamination can be linked to increased risks of “Blue-baby syndrome”, various type of cancers, formation of carcinogenic nitrosamines, reproductive disorders, and other adverse health effects on humans (Horing & Chapman, 2004; WHO, 2004b). High nitrate concentration also causes acute poisoning in cattle. Environmental impact of high nitrate includes eutrophication of surface waters due to excess nutrients (Bhatnagar & Sillanpaa, 2011; Calderer et al., 2010). Due to severity of the health problems associated with excess nitrate in potable water, the European Union, WHO and Bureau of Indian Standard set the drinking standard for nitrate at 50 mg- NO_3^- /L and 45 mg- NO_3^- /L respectively (BIS:10500, 2012; EC, 1998; WHO, 2004b). In addition to arsenic, nitrate and iron, fluoride is also one of the most abundant anions present in groundwater worldwide and creates a major problem in safe drinking water supply. It is classified as one of the water contaminants by the World Health Organization (WHO), which cause adverse health effects on humans and animals (Jagtap et al., 2012; WHO, 2006).

The co-existence of multiple contaminants has been reported in many areas because of special geochemical conditions or industrial activities, (Velizarov et al., 2005). The co-existence of multiple contaminants is adding complexity to the problem of groundwater contamination. There are several reports on co-occurrence of arsenic and iron in groundwater. Along with arsenic and iron, the co-occurrence of nitrate and fluoride in groundwater is also reported from many locations of the world (Rezaie-Boroon et al., 2014; Smedley et al., 2008). The presence of one or a combination of these contaminants in drinking water sources often needs an expensive, multi-step treatment or abandonment of wells and other water bodies (Mazumder et al., 2010; Rosen et al., 2004).

Simultaneous removal of multiple number of contaminants from drinking water have been tried by adsorption, coagulation-flocculation, ion exchange, membrane separation, precipitation and cementation (Liu et al., 2012; Matos et al., 2006; Velizarov et al., 2004). However, these methods suffers from drawbacks in terms of application, high operational, maintenance costs and effectiveness as it usually results in the production of unstable sludge, which leads to a greater disposal expense.

In recent years, biological processes have gained increasing interest in drinking water treatment, mainly due to the conversion of many organic and inorganic contaminants to innocuous by-products. In addition, biological treatment achieves multiple contaminant removal in a single system in lesser contact times, potentially minimizing costs and suitable for large community scale operations, while avoiding the need for regeneration of solid phase sorbents or treatment of the generated wastes (Brown, 2008).

In groundwater systems, under anoxic conditions the ecological succession of terminal electron-accepting processes is O_2 followed by NO_3^{2-} , Mn(IV), Fe(III), SO_4^{2-} and finally CO_2 . Other oxyanions, including arsenate, selenate, chlorate and chromate, may also be used as terminal electron acceptors during microbial respiration depending on their availabilities in an aquatic system (Narasingarao & Haggblom, 2007). Thus in a biologically active aquatic environment where arsenic, iron and nitrate are present along with sulphate, the nitrate reducers reduces nitrate to nitrogen gas and sulphate-reducing bacteria (SRB) produces biogenic sulphides, which in turn lead to the precipitation of arsenic and iron sulphides. Hence, arsenic is removed from the water simultaneously as precipitates of arsenosulphides (orpiment and realgar) as well as adsorption/co-precipitation with iron sulphides (Altun et al., 2014; Battaglia-Brunet et al., 2012).

Recently, development of several bioreactor configurations either of attached or suspended growth types operated in up-flow or down-flow modes have led to effective removal of arsenic from mine waters (Altun et al., 2014; Battaglia-Brunet et al., 2012; Rodriguez-Freire et al., 2014). However, report on sulphidogenic arsenic removal and multi contaminant removal from drinking water/groundwater sources is scanty. In the scientific literature, so far, only a few efforts have been made to study the arsenic removal in sulphidogenic bioreactor from drinking water sources. Even the most relevant report on biological treatment of groundwater for simultaneous removal of multi-pollutants available so far is the outcome of the experiments carried out on simulated groundwater spiked with a fixed arsenic (200 $\mu\text{g/L}$), iron (2 mg/L), nitrate (50 mg/L) and sulphate (22 mg/L) concentration operated at a fixed EBCT (30 min) at 22°C (Upadhyaya et al., 2010). However, occurrences of such contaminants in real groundwater even at higher concentrations have been reported. There are no reports available so far, on simultaneous removal of multi-contaminant in a single bioreactor at varying arsenic, nitrate, iron and

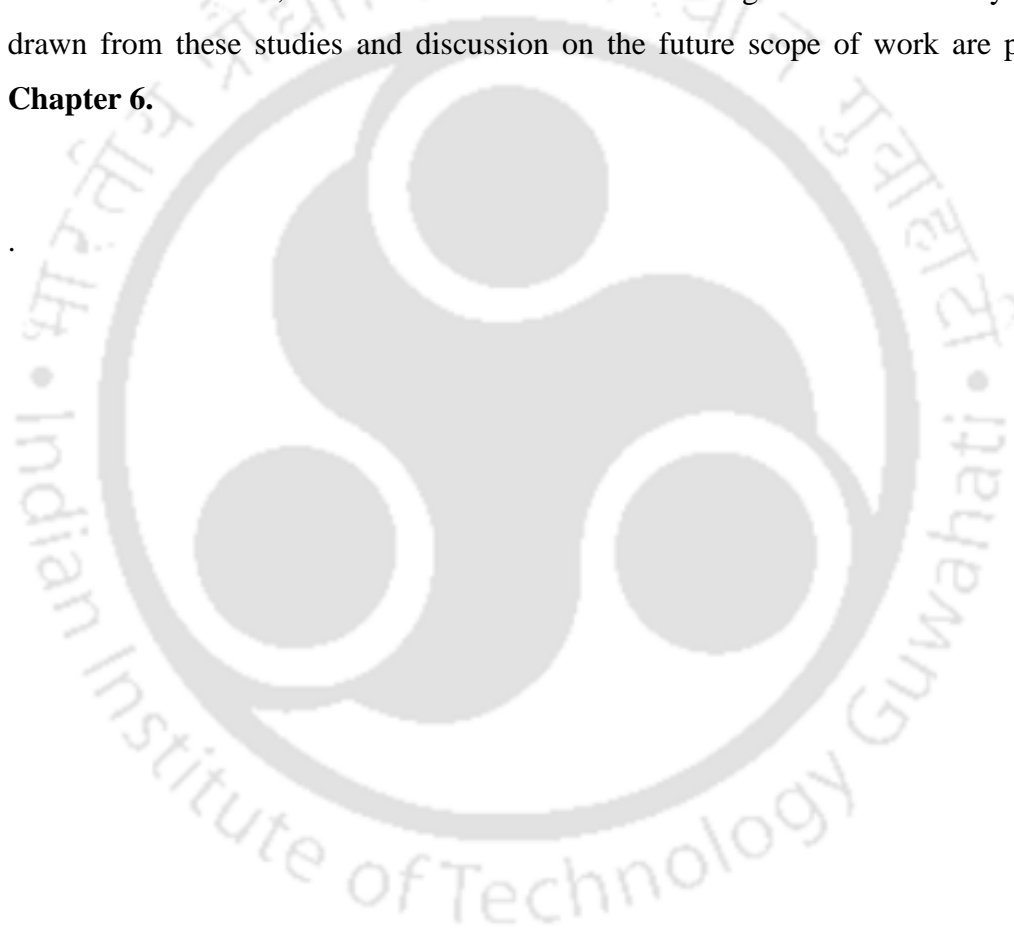
sulphate concentrations; effects of EBCT, pH and temperature. Also, there is no study reported so far on arsenic removal from real groundwater. With this background, the purpose of this research was to develop sulphidogenic anaerobic bioreactor systems for simultaneous removal of arsenic, iron and nitrate from simulated and real groundwater at varying feeding and operating conditions.

In this study, mixed microbial culture was collected from a wastewater treatment plant and acclimatized in presence of arsenic, nitrate and sulphate. The acclimatized sludge was used to evaluate its performance on simultaneous removal of target pollutants, arsenic, nitrate, iron and fluoride as well as effects of one pollutant on the others in batch, semi-batch and flow through reactor systems. The reactors were operated in absence as well as in presence of iron.

Firstly, the simultaneous removal of multipollutants was assessed in batch shake flasks and semi-batch reactors. The effect of arsenic, nitrate and/or iron concentration on the arsenic removal was investigated in batch as well as semi batch reactors. The experiments were also carried out with different carbon sources in semi-batch reactors in order to study effect of carbon sources on multipollutants removal. Furthermore, biological arsenic and nitrate-removing processes were performed in presence and absence of iron in anaerobic flow-through attached growth reactors (AGRs). Therefore, two sulphidogenic AGRs enriched with mixed bacterial culture, where waste activated carbon (WAC) was used as supporting material for bacterial growth were operated. In particular, the AGRs operation was directed to: 1) evaluate the arsenic removal efficiencies under different arsenic, nitrate and sulphate concentrations in absence and presence of iron from synthetic as well as real contaminated groundwater; 2) evaluating the bioreactor performance for simultaneous removal of pollutants in diverse range of temperature; 3) test the reactor performance under pH variations in the feed solution; 4) check the acute toxicity of the treated water; 5) collection, preparation, characterization and performance evaluation of an adsorbent from water treatment plant residues (WTR) on fluoride removal from AGR treated water; 6) identification of microbial population dynamics; 7) characterization of biosolids formed in AGRs; and finally, the experimentation for stability check of biosolids, carried out both in batch and continuous mode, aimed to study the leachability of arsenic from biosolids.

Organization of the Thesis

The thesis has been organized into six chapters. The current **Chapter 1** presents the general introduction to the present work while the literature that supports the present study is presented in **Chapter 2**. The primary objective and the scopes of the study are given in **Chapter 3**. Details of the materials and methods adopted in the present study along with the reactor configurations and operating conditions are discussed in details in **Chapter 4**. **Chapter 5** presents the results and discussions of sequential studies carried out on batch reactors, semi-batch reactors and flow through reactors. The key conclusions drawn from these studies and discussion on the future scope of work are presented in **Chapter 6**.





CHAPTER 2

LITERATURE REVIEW

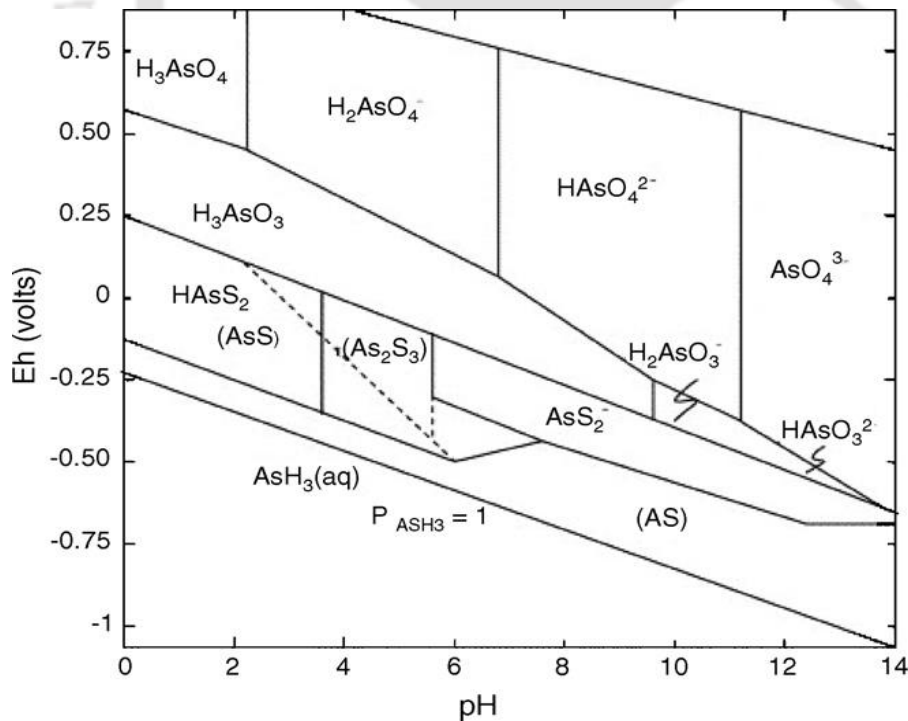
The drinking water contamination is a serious health and environmental threat in many parts of the India and the world. Millions of rural and urban population in the developing countries relies on groundwater, mostly through shallow dug wells. According to some estimates, groundwater caters nearly 80 percent of the rural domestic water needs, and 50 percent of the urban drinking water needs in India. Natural groundwater pollution occurs primarily because of geogenic and anthropogenic activities. There are many sources of inorganic contamination of ground water. Arsenic, iron, nitrate and fluoride stands among prior inorganic contaminants of groundwater. Irrespective of the origin, the isolated and/or co- occurrence of these contaminants in drinking water sources is unavoidable and of grave concern throughout the globe (Lenntech, 2015).

2.1. Introduction, Source and Environmental Impact/Health Effects of Contaminants

2.1.1 Arsenic

Arsenic is a well-known toxic metalloid and is present ubiquitously in nature: in air, soil, water, rocks, plants, and animals. Arsenic mostly occurs in combined state rather than free state. Its presence in environment ranges from -3 , 0 , $+3$ and $+5$ oxidation states. The two highest oxidation states are the most common in nature, whereas the two lowest are rare (Oremland & Stolz, 2003). The presence of As(0) is very rarely reported, it is mostly found in combination with sulphur, oxygen and iron (Jain & Ali, 2000; Oremland & Stolz, 2003). Arsenides, arsenosulphides, arsenites, arsenates and organoarsenicals are major compounds of arsenic other than elemental form of arsenic (Henke, 2009). In water the major forms of arsenic include arsenious acids (H_3AsO_3 , H_2AsO_3^- , HAsO_3^{2-}), arsenic

acids (H_3AsO_4 , H_2AsO_4^- , H_3AsO_3^0), arsenites, arsenates, methylarsenic acid, dimethylarsinic acid, arsine, etc. (Smedley & Kinniburgh, 2002). In natural waters arsenic exists in oxyanionic form of trivalent arsenite or pentavalent arsenate. In reducing anoxic conditions of groundwater arsenite predominates while arsenate is majorly found in oxygen rich aerobic water environments (Greenwood & Earnshaw, 1984). The mobilisation of arsenic species in groundwater under reducing and oxidising conditions is pH dependent (pH 6.5-8.5). Arsenic speciation in natural waters is strongly controlled by redox potential (Eh) and pH (Fig.2.1) (Wang & Mulligan, 2006). At pH values less than 9.2 and in reducing conditions, the uncharged arsenite (H_3AsO_3^0) will be the dominating species. At low pH (< pH 6.9) and oxidising conditions, H_2AsO_4^- is dominant, while HAsO_4^{2-} dominates at higher pH values (> pH 6.9). In highly acidic and alkaline conditions, H_3AsO_4^0 and AsO_4^{3-} are representing species respectively (Yan et al., 2000). Arsenic has been found to be a common contaminant of fresh water and sea water in many parts of the world. It can exist both in organic and inorganic forms.



(Ref.: Wang and Mulligan 2006)

Figure 2.1 Eh–pH diagram for arsenic at 25°C and 101.3 kPa.

2.1.1.1 Sources and Occurrence in Water Environment

Arsenic distribution and mobilisation in environment is complex process, occurs through continuous cycling of different forms of arsenic through air, soil and water. It is introduced in soil and groundwater during weathering of rocks followed by leaching and run off. Natural processes of arsenic transport includes mineral weathering, biologically aided mineralisation, and volcanic emissions (Sharma et al., 2014a). However, it can also be introduced as a result of many anthropogenic activities such as wood preservatives, paints, alloys, semi-conductors, fossil fuel combustion, mining wastes, smelting operations, landfilling, sewage, and agricultural applications (pesticides and fertilizers) (Mondal et al., 2013; Singh et al., 2015). Contribution of anthropogenic sources to groundwater arsenic contamination is much less compared to the natural sources, still their contribution cannot be ignored. Most of the arsenic transport in natural aquifers is due to the physical, geochemical conditions (especially reducing conditions) and water-rock interactions. That's why most of the reported arsenic poisoning, throughout the world is due to groundwater As exposure rather than surface water (Smedley & Kinniburgh, 2002).

Geogenic presence of arsenic in groundwater ranging from 0.5 to 5,000 $\mu\text{g/L}$ (Smedley & Kinniburgh, 2002) has been reported around the world (Ravenscroft et al., 2009). The source of As in the groundwater may be volcanic ash as in the southern Gulf Coast aquifer system in Texas (USA) (Gates et al., 2011), reductive dissolution of Fe-oxhydroxide minerals as in lower Fraser River Delta, British Columbia, Canada (Bolton & Beckie, 2011) and Bengal Basin (Uddin et al., 2011), weathering of ultramafic rocks as in bedrock aquifers of Rowe-Hawley Belt of northern Vermont, (USA), Ryan et al. (2011). In a geochemical and hydrological study of groundwater in Bihar, India, high As is attributed to recharging of deep aquifers through the Pleistocene deposits (Saha et al., 2011).

High As Concentrations are reported in groundwater from many parts of the world such as Africa, Bangladesh (up to 1000 $\mu\text{g/L}$), Brazil, China (up to 850 $\mu\text{g/L}$), India (up to 23mg/L), Italy, Mexico, Chile (up to 770 $\mu\text{g/L}$), Argentina (up to 3810 $\mu\text{g/L}$), Latin America, Canada, Germany, Ghana, Greece, Korea, Mexico, Mongolia (up to 1800 $\mu\text{g/L}$), Nepal (2660 $\mu\text{g/L}$) Poland, South Thailand, UK, USA (>3000 $\mu\text{g/L}$), Vietnam (up to 3050 $\mu\text{g/L}$) and Zimbabwe etc. (Singh et al., 2015; Smedley & Kinniburgh, 2002; Smedley et al., 2003; Van Halem et al., 2009)

2.1.1.2 Environmental Impact

Arsenic is extremely poisonous. International Agency for Research on Cancer has classified arsenic as a human carcinogenic substance, group 1. (IARC, 2004) According to the United Nations Synthesis report, arsenic poisoning is the second most important health hazard in the world related to drinking water after pathogenic contamination (Singh et al., 2015). More than 150 million people all over the world, including nearly 110 millions of South and South-east Asian countries are at risk of arsenicosis due to arsenic contamination in drinking water (Ravenscroft et al., 2009). Irrigation with As-enriched groundwater increases inorganic arsenic exposure through food, especially rice and vegetables thus lead to enter As in human food chain (Bhattacharya et al., 2012).

Arsenic poisoning in humans may cause melanosis, leuco-melanosis, keratosis, hyperkeratosis, dorsum, nonpetting edema, gangrene and skin problems including cancer (Singh et al., 2015). As(III) is more toxic because it can bind to sulfhydryl groups of cysteine residues in proteins and inactivates them (Cavalca et al., 2013). Long term high arsenic intake can cause peripheral vascular disease, gastrointestinal disturbances, and possibly diabetes, high blood pressure and reproductive disorders including cancers of lung, kidney, liver and bladder (WHO, 2011).

Scientific studies from China and Bangladesh have shown neurological problems, mental retardation and developmental disabilities such as physical, cognitive, psychological, sensory and speech impairments among arsenicosis patients. Moreover, arsenicosis not only affect its victims but also their families by social instability, social discrimination, marriage-related problems, refusal of victims by community and families (Brinkel et al., 2009). The drinking water standard for arsenic is reduced to 10 ppb from 50 ppb by most of the developed nations as WHO directive, because of serious health impacts on humans. However, some countries including Bangladesh and China still following the earlier WHO guideline of 50 ppb (Sharma et al., 2014a; WHO, 2011).

2.1.2 Nitrate

Nitrate (NO_3^-) is a nitrogenous compound that occurs naturally in moderate concentrations in many environments. Nitrate is an important ion for the growth of plants and micro-organisms. NO_3^- , due to its high water solubility, is the most ubiquitous chemical contaminant in the world's aquifers. It represents the stable end product of the nitrification process. Nitrates are very stable unless they undergo biological denitrification under anoxic conditions or consumed by plants. As it has no detectable colour, smell or taste, they remain undetected at typical concentrations in water. Raising concentration levels of NO_3^- in potable water is of prime concern on a global scale. The factors controlling distribution of NO_3^- in groundwater includes availability of electron donor, dissolved oxygen level, available sources, thickness and composition of the vadose zone, precipitation, irrigation, ground water flow and aquifer heterogeneity.

Nitrate nitrogen (NO_3^- -N) concentrations greater than about 3 mg/L are usually caused by human activities such as waste and effluent disposal, or leaching from normal farming activities (Daughney & Reeves, 2005). Today, NO_3^- contamination of groundwater has become a severe environmental problem in many parts of the world (Mohseni-Bandpi et al., 2013).

2.1.2.1 Sources and Occurrence in Water Environment

Nitrate contamination in groundwater may be attributed to geogenic and anthropogenic sources. Geogenic sources of NO_3^- in surface and groundwater include nitrogen bedrocks, sediments of arid environment and coal deposits. Geogenic nitrate in aquatic environments is reported from Mokelumne River watershed of California (Holloway et al., 1998), Chile (Motzer, 2006) and Cameroon (Ako et al., 2014). Major anthropogenic sources includes agricultural runoff, unsafe domestic/industrial effluent discharge, timber harvesting practices, animal manure, NO_x air stripping waste from air pollution control devices (Bhatnagar & Sillanpaa, 2011; Mohseni-Bandpi et al., 2013). Majority of the reported ground and surface water NO_3^- contamination appear to be related to irrigated agriculture and the use of chemical fertilizers or to domestic sewage (Mallick & Banerji, 1981; Rao & Puttanna, 2000). Wakida and Lerner (2005) found sewage and mains leakage, septic tanks, industrial spillages, contaminated land, landfills,

river or channel infiltration, fertilizers used in gardens, house building, storm water and direct recharge are major non-agricultural NO_3^- sources in urban groundwater.

Typically, industrial regions have greater concentrations of nitrates in waters than rural areas (WHO, 2011). Many industries like plastic, fuel additives and nitric acid, produce high nitrate containing wastes that contributed to the increase of nitrate level in water environments. Nitrate wastes containing more than 1,000 mg/L NO_3^- -N are generated in mobile, explosives, fertilizer, pectin, and in metals furnishing industries (Glass & Silverstein, 1999). The nuclear industry wastewater containing excess nitrates up to 50,000 mg/L NO_3^- -N. Huge amount of NO_3^- is leached into groundwater from such waste before treatment and disposal (Ghafari et al., 2008). Additionally, airborne nitrogen compounds given off by industry and automobiles are deposited on the land in precipitation and dry particles. NO_3^- concentration up to 53.0 mg/L is found in industrial area of Cuddalore (India) (Devi & Premkumar, 2012).

NO_3^- contamination of surface water and especially in groundwater has become a significant environmental problem in Australia, Canada, China, Europe, India, Japan, Saudi Arabia, USA and many other parts of the world (Gayle et al., 1989; Kapoor & Viraraghavan, 1997). High NO_3^- level in aquatic environment of 12 countries of European Economic Community (EEC) is reported. NO_3^- concentration in range of 50 mg/L to 250 mg/L in surface and groundwater sources is reported from United kingdom, Luxemburg, Germany, Denmark and Belgium (Kuzelka & Ennenga, 2013). High NO_3^- up to 127-1038 mg/L is reported from Southern and South-Western districts of Haryana (Kakar, 1981).

2.1.2.2 Environmental Impact

Nitrate can persist in groundwater for decades and accumulate to high levels as more nitrogen is applied to the land every year. Elevated NO_3^- concentrations in water sources can lead to a potential risk to human, animal health and environment. High NO_3^- concentrations cause eutrophication in water bodies by stimulating heavy algal growth. Ingestion of high nitrate drinking water is associated with “blue-baby syndrome”(methaemoglobinaemia) in infants, and the potential formation of carcinogenic nitrosamines in humans (Majumdar & Gupta, 2000). Nitrate poisoning in cattles can cause death after ingestion of high nitrate water and/or plant (Bhatnagar & Sillanpaa, 2011). In humans, raised NO_3^- concentrations in drinking water have found to be linked

with diverse kinds of cancers, adverse reproductive problems, infectious diseases and diabetes (Chiu et al., 2007; Ward et al., 2005). Several public supply wells in the Huntington Town, New York, have been closed because the high nitrate concentration in drinking water (Bleifuss et al., 1998).

Keeping in mind the link between serious health problems and excessive concentration of nitrate in drinking water, WHO and the European Union recommended nitrate concentration limit of 50 mg NO_3^-/L (WHO, 2011). The US Environmental Protection Agency has set maximum contaminant level (MCL) of 10 mg NO_3^-/L in potable water (EPA, 2009). In Australia, the recommended limit is 50 mg NO_3^-/L for infants up to 3 months old and 100 mg NO_3^-/L for adults and children over the age of 3 months. South Africa stipulates a very low permissible limit of 20 mg NO_3^-/L (Loganathan et al., 2013b).

2.1.3 Iron

Iron is the second most abundant metal and the fourth most abundant element in the Earth's crust (WHO, 1996). Iron usually exists in two oxidation states, reduced soluble divalent ferrous (Fe^{+2}) and oxidised trivalent ferric (Fe^{+3}). In groundwater, iron may be present in the following five forms: i) ferrous iron, ii) inorganic complexes, iii) organic complexes, iv) colloidal, and v) suspended. The form and stability of the iron in water depends mainly on the pH and the redox potential (Eh). The predominant form of iron is the soluble Fe^{+2} species in the absence of an electron acceptor such as oxygen and under the pH range of 5 to 8 (Hem, 1985). High alkalinity waters often have lower iron content than water of low alkalinity. The iron concentration in natural waters is often limited by the solubility of its carbonate (AWWA, 1990). Groundwater iron normally ranges from a few hundredths to about 50 mg/L with the majority containing <5 mg/L (Davis, 1997; Hem, 1985).

2.1.3.1 Sources and Occurrence in Water Environment

Natural sources of groundwater iron may include weathering of iron bearing rocks as earth's underground rock formations contain about 5% iron. Iron is also released in groundwater due to the dissolution of iron bearing minerals, mainly oxides, sulphides, carbonates and silicates under anaerobic conditions in the presence of reducing agents like organic matter and hydrogen sulphide (Sharma, 2001). Anthropogenic sources of iron in

groundwater may include industrial effluents, landfill leakages, acid mine drainage, well casing, pump parts, piping (Zhang et al., 2014a) and storage tanks (NovaScotia, 2008).

The iron contamination of groundwater is worldwide problem. Many countries including India (Bordoloi et al., 2013), Canada (7-15 mg/L) (Ellis et al., 2000) Denmark (Ankrah & Søggaard, 2009), Egypt (El-Naggar, 2009), Finland (Hatva, 1989) Greece (Katsoyiannis et al., 2008), Malaysia, Netherlands (0-30 mg/L), Nepal (Sharma, 2001), Russia (0.8-4.0 mg/L), Nigeria (0.03-2.38 mg/L) (Ocheri, 2010), Serbia (0.6-2.2 mg/L) and South Africa (Demlie et al., 2014) is characterized by presence of high iron in groundwater. Iron is widely distributed in aquifer systems of India, more than 23 states having >1 mg/L of iron in groundwater (CGWB, 2014). More than 10 mg/L iron is reported from Darrang, Kamrup, Sibsagar (Assam), Madhepura, Siwan (Bihar) and Gurgaon, Sonipat (Haryana) (Borah et al., 2010; Bordoloi et al., 2013; CGWB, 2010; Singh et al., 2008).

2.1.3.2 Environmental Impact

Iron is not considered to cause severe health problems in humans; rather its presence in potable water can cause different types of nuisance problems. The colour and flavour of food and water can be affected by iron because it can react with tannins in coffee, tea and alcoholic beverages which produce black sludge. Iron can cause reddish-brown staining of laundry, utensils, dishes and glassware. The other problem associated with iron in water is iron bacteria. However, iron bacteria are not responsible for any health issues, but they can cause an increase in the friction loss and power consumption, require higher chlorine dosage, deplete dissolved oxygen and clogging of water systems by forming red brown (iron) slime in toilet tanks (Wilson et al.). The iron precipitation reduces softening efficiency of home softeners by clogging (Tekerlekopoulou & Vayenas, 2007).

Excess iron accumulates in the heart, liver, brain and other vital organs (Albretsen, 2006). Recently, due to regular intake of high iron containing groundwater, some adverse health effects like hemochromatosis, liver cirrhosis and siderosis is observed in people of Assam, India (Chaturvedi et al., 2014). Iron overload in the body may result in fatigue, headache, irritability and lowered work performance in day-to-day activities. Moreover, it may cause joint pain, abdominal pain, bronzing of skin, arthritis, loss of body hair,

amenorrhea, impotence, diabetes and heart diseases, if remain untreated, and typically affects men more often than the women (Ronald, 2013). WHO recommends that the iron concentration in drinking water should be less than 0.3 mg/L (WHO, 2011). The EC directive recommends that the iron in water supplies should be less than 0.2 mg/L (Sharma, 2001).

2.1.4 Fluoride

The fluoride is member of the halogen group and a natural constituent of the environment. Fluoride is the most electronegative and reactive among all chemical elements and is never found in nature in the element form. In nature, it occurs in combination with other minerals and geochemical deposits (Ibrahim.M, 2011; Jagtap et al., 2012). It occurs naturally in reduced form and enters food chains through either drinking water or eating plants and cereals. Fluoride is an essential element for life which needs to be monitor in drinking water carefully. It is an important element for humans in preventing cavity and in facilitating the mineralization of arduous tissues when taken in optimum amount (Singh et al., 2016).The low concentrations lead to fluoride deficiencies while high fluoride concentrations may impose other deleterious effects. High fluoride concentration in the ground water and surface water in many parts of the world is a cause of great concern. Fluorides are mainly derived by the solvent action of water on the rocks and the soil of the earth's crust.

2.1.4.1 Sources and Occurrence in Water Environment

Fluoride-bearing rocks such as fluorspar, fluorite, cryolite, fluorapatite and hydroxyl apatite are the main source of fluoride in groundwater. Besides the natural geological sources, the anthropogenic activities also greatly contribute in fluoride contamination in groundwater. Many industries like glass and ceramic production, semiconductor and integrated circuits manufacturing, electroplating, coal fired power stations, beryllium extraction plants, brick manufacturing plants, hydrofluoric acid plants, phosphatic fertilizer plants, and aluminium smelters are also contributing to significant fluoride in surface waters. Also the fluoride content in groundwater is a function of many factors such as availability and solubility of fluoride minerals, velocity of flowing water, pH, temperature, concentrations of calcium and bicarbonate ions in water. (Bhatnagar et al., 2011; Jagtap et al., 2012). Groundwaters have high fluoride concentrations because of

long residence times in the host aquifers. Surface waters and hand-dug wells usually have low concentrations, as they represent young, recently infiltrated, rainwater (Edmunds & Smedley, 2013; Jagtap et al., 2012).

Fluoride is one of the most abundant anions present in groundwater worldwide. More than 27 developed and developing countries including Algeria, Argentina, Australia, Bangladesh, Canada, China, Egypt, Ethiopia, India, Iran, Iraq, Japan, Jordan, Kenya, Libya, Mexico, Morocco, New Zealand, Palestine, Pakistan, Senegal, S. Africa, Sri Lanka, Syria, Tanzania, Thailand, Turkey, Uganda, United Arab Emirates and U.S.A. etc. have been reported with high fluoride concentrations in groundwater (Jagtap et al., 2012; Meenakshi & Maheshwari, 2006).

2.1.4.2 Environmental Impact

Fluoride concentrations around 1 mg/L in drinking water is considered as beneficial especially to young children for calcification of dental enamel. However, long term consumption of water above 1.5 mg/L fluoride is detrimental to health. The WHO guideline for fluoride in drinking water is 1.5 mg/L (WHO, 2011). Many countries are following this value as drinking water standard. More than 200 million people around the globe are consuming drinking water beyond the guideline value of WHO (Edmunds & Smedley, 2013). There are different regulations and recommendations have been adopted for drinking water fluoride by different country and regulatory authorities.

High fluoride in drinking water causes dental fluorosis and/or skeletal fluorosis. Nearly 90 million people including 6 million children in 17 states of India the country are most affected with dental, skeletal and/or non-skeletal fluorosis (Singh et al., 2016) Continuous intake of excess fluoride may results in more health problems. The common problems associated with chronic fluoride poisoning are respiratory failure, fall of blood pressure, general paralysis, loss of weight, anorexia, anaemia, wasting, increased rates of bone fractures, decreased birth rates, increased urolithiasis (kidney stones), impaired thyroid function, muscle fibre degeneration, low haemoglobin levels, reduced immunity, lower intelligence in children and cohexia. Continuous intake of nonfatal dose of fluorides causes permanent inhibition of growth. Fluoride ions forms complexes with magnesium ions and other metal ions thus causes inhibition and even destruction to many enzymes (Ibrahim.M, 2011; Meenakshi & Maheshwari, 2006; Ozsvath, 2009). Due to

adverse health effects on humans and animals the fluoride has been classified as a priority pollutant by the United States Environmental Protection Agency and the German Research Council (Singh et al., 2016).

2.2 Simultaneous Co-occurrence of Multiple Pollutants in Groundwater

In many cases the natural water bodies are not only contaminated with single contaminant, but presence of two or more contaminants has also been reported (Fytianos & Christophoridis, 2004; Guha et al., 2005; Reddy, 2014; Xin et al., 2009). The co-occurrence of multiple contaminants is adding complexity to the problem of groundwater contamination at many locations in the world. The co-occurrence of multiple contaminants in groundwater can be due to geogenic and/or anthropogenic sources.

2.2.1 Co-occurrence due to Various Industrial Activities

Industrial effluents of many industries are a major anthropogenic source for the simultaneous occurrence of multiple contaminants in drinking water sources. Activities associated with Pesticides, Pharmaceuticals, Petroleum refining, Thermal power plants, Aluminium plant, Organic chemicals industries, mining and mineral processing operations have significant potential to pollute groundwater either directly or indirectly. High arsenic and fluoride concentrations in groundwater at Kalalanwala in the Kasur District of Pakistan was due to local brick factories (Farooqi et al., 2007). Unmanaged discharge of super acid system and waste water may also enhance combined occurrence of As and F (Chouhan & Flora, 2010). Exceeding level of Fe, F and NO_3^- (As per BIS standards) were found in groundwater of nearby industrial areas of Angul-Talcher (Orissa) and Drain Basin Area, Najafgarh (Delhi). High F and Fe (Korba (M.P.), Singrauli (U.P.), Fe and NO_3^- (North Arcot (Tamilnadu), Jodhpur (Rajasthan)), NO_3^- and F (Vishakhapatnam (Andhra Pradesh), Manali (Tamilnadu)), Fe and As (Bolaram-Patancheru (Andhra Pradesh) were also attributed to industrial activities in surrounding areas (CPCB, 2007). High levels of As, NO_3^- and thallium was found in surrounding water-supply wells of California as a result of oil industry waste (Kretzmann, 2014).

2.2.2 Co-occurrence due to Geogenic Sources

The co-occurrence of chemical constituents in drinking water also depends on the geology and on the physical and chemical conditions affecting solubility. In areas near the Gangetic plains and the Padma-Meghna-Brahmaputra basin, arsenic is present naturally due to the geological activities of these Rivers. Climate and environmental factors also has an important role in affecting the breakdown of rocks and the extent to which minerals are leached into rivers or groundwater (WHO, 2004a). The co-occurrence of these pollutants in drinking water sources is also reported from several parts of the world which is described in detail below.

Co-occurrence of Nitrate and Arsenic

Geogenic simultaneous occurrence of nitrate and arsenic from groundwater is reported various locations around the world, For example, in Northern Chile (Tellez et al., 2005), in Northern Greece (Fytianos & Christophoridis, 2004) and the Ogallala aquifer of Texas contain both nitrate and arsenic along with perchlorate (Venkataraman & Uddameri, 2012) in California (Seidel et al., 2008) Borrego Valley southern California (Rezaie-Boroon et al., 2014), Oakland County (Michigan) (Aichele, 2004) Duero River Basin (Spain) (Mayorga et al., 2013). Depth-specific profile studies have shown arsenic and nitrate contamination in Kathmandu Valley (Nepal) (Khatiwada et al., 2002) and West Bengal (India), (Guha et al., 2005). Exceedance of nitrate and arsenic in Southern Ogallala aquifer is due to intense agricultural activities (Venkataraman & Uddameri, 2012).

Iron and Arsenic

High concentrations of Fe and As in groundwater of the India (Darrang, Assam) (up to 0.95 mg/L and 11.25 µg/L) (Borah et al., 2010), Vietnam and Cambodia (Mekong delta floodplain) (up to 56 mg/L and 1300 µg/L) (Buschmann et al., 2008), China (Yunnan Province) (Xin et al., 2009), Pakistan (groundwater as well as surface water of Jamshoro), (0.09-4.28 Fe mg/L, (3.00-106.0 As µg/L) (Baig et al., 2009). Moreover, in the Chiang Mai basin of Northern Thailand, the co-occurrence of fluoride and iron were found at concentrations exceeding the national standards (Margane & Tatong, 1999).

Arsenic and Fluoride

The co-contamination of arsenic and fluoride in drinking water sources is very common in many countries of the world falling in arid or semi-arid regions. The geogenic dissolved As and F concentrations show a significant co-occurrence in Argentina (Padilla & Saitua, 2010) Central and Northern México (Rocha-Amador et al., 2007), Pakistan (Farooqi et al., 2007), China (Yuncheng Basin and Datong, up to 1550 µg/L As and 10.4 mg/L F) (Currell et al., 2011; Wang et al., 2009), Korea (Mankyeong River floodplain) (Kim et al., 2012b) Mangolia (Huhhot and Hetao Basin with concentrations up to 720 µg/L As and 2.57 mg/L F) (Guo et al., 2012; Smedley et al., 2003). Alarcón-Herrera et al. (2013) investigated genesis, mobility and remediation of co-occurrence of As and F, in groundwater of semi-arid regions of Latin America including, Chaco-Pampean plain of Argentina, ELTatio geothermal water system of Chile (1.0-2.0 mg/L arsenic and 0.85-8.5 mg/L F) and Mexico (up to 0.12 mg/L As and 16 mg/L F). The co-occurrence is reported from oxidizing as well as reducing aquifers, while it is less common in reducing ones. The co-occurrence of As and F was explained as desorption of As and F from Fe-(hydr)oxides due to raised pH in aquifers (Kim et al., 2012b). AsF₆ and KAsF₆ which has been used as a super acid system for organic synthesis, an electrolyte in rechargeable gel batteries, in acid-polishing process of crystal glass and pesticide respectively, were reported as main source of As and F co-occurrence from a lake (Daus et al., 2007).

Sulphate and Nitrate

In anoxic environments NO₃⁻ and SO₄²⁻ serve as important electron acceptors in aquatic systems. Their occurrence in groundwater is often controlled by bacterially-mediated redox reactions (e.g. denitrification and bacterial SO₄²⁻ reduction), Compared to NO₃⁻ free (uncontaminated) groundwater, NO₃⁻ rich groundwater can accelerate the oxidation of pyrite in aquifers and thus can produce elevated SO₄²⁻ concentrations and acidity. This process is known as denitrification using pyrite (as an electron donor) or pyrite oxidation by NO₃⁻ (Schwientek et al., 2008). Lipfert et. al., (2007) also reported the Ground water with high arsenic concentrations has enriched sulphate in the Kelly's Cove watershed, Northport, Maine and Goose River, Maine watershed USA.

Nitrate and Fluoride

Co-occurrence of fluoride and nitrate in groundwater as a result of geogenic and anthropogenic activity is also reported from some aquifers (Reddy, 2014). High concentrations of nitrate and fluoride co-exists in groundwater of several states in India, including Andhra Pradesh (Reddy, 2014) West Bengal (Kundu et al., 2009) Punjab (Sharma et al., 2014b), Haryana (Khurshid, 2013), Rajasthan (Suthar, 2011), U.P. (Raju et al., 2009), M.P. (Avtar et al., 2013), Maharastra (Sangole et al., 2012) and Karnataka (Shankar et al., 2008), High fluoride and nitrate concentrations (upto 10.6 mg/L and up to 90 mg/L respectively) have been reported in drinking water of Bathinda, Faridkot, and Firozpur districts of Punjab (Sharma et al., 2014b). Nitrate and fluoride co-occurrence in drinking groundwater was a function of lithology, soil characteristics and agricultural activities in Nadia (West Bengal), (Kundu et al., 2009) while was a result of industrial activities in Peenya industrial area, Bangalore, India (Shankar et al., 2008).

2.2.3 Co-existence of Multiple Contaminants

The co-occurrence of more than two contaminants in drinking water sources is also reported from several parts of the world including India. The simultaneous presence of As, NO₃-N and F (<4-5300 µg/L, <0.2-140 mg/L and 0-29 mg/L respectively) along with Fe and other elements from La Pampa province (Smedley et al., 2008); As, F and Fe (7-1990 µg/L, 0.1-4.20 mg/L and 0-2 mg/L respectively) along with 23 other elements from Chaco Province, Argentina, (Giménez et al., 2013); As, Fe, F along with manganese and uranium in Myingyan Township, Myanmar (Bacquart et al., 2015); Fe, NO₃, and F in Guwahati, India (Chakrabarty & Sarma, 2011; Das et al., 2003); As, Fe and F in North-eastern states of India (Singh et al., 2008) is reported in exceedance of drinking water guidelines.

2.2.4 Environmental Impact of Co-occurrence of Multiple Contaminants

Little is known about the toxic effects stemming from a co-exposure of multiple contaminants through drinking water (Chouhan & Flora, 2010). Individual contaminant may not pose appreciable risks to human health, there are concerns about potential risks of exposures to mixtures (Silva et al., 2002). For example, co-occurrence of arsenic and fluoride in groundwater can adversely affect IQ and growth in children (Rocha-Amador et al., 2007; Wang et al., 2007), alter the expression of apoptosis and inflammatory genes by immune cells (Salgado-Bustamante et al., 2010).

2.3 Review of Removal Techniques

Many treatment technologies are available to meet the drinking water standards, as suggested by the global and local regulatory agencies for the removal of arsenic, iron, nitrate and fluoride. Phase transfer by formation of insoluble precipitate with other elements or the transformation as volatile compounds, is considered as only option for arsenic removal from contaminated drinking water. Traditionally, arsenic can be treated using several technologies including adsorption, oxidation, co-precipitation, coagulation-flocculation, ion exchange and membrane processes (Jain & Singh, 2012; Leupin & Hug, 2005; Zouboulis & Katsoyiannis, 2002a; Zouboulis & Katsoyiannis, 2002b). In view of the lowering the drinking water standards by regulatory bodies, several hybrid and advance arsenic removal technologies have been developed, such as direct contact membrane distillation (Manna et al., 2010; Yarlagaadda et al., 2011), oxidation of As(III) to As(V) using KMnO_4 followed by nano filtration (Sen et al., 2010) integrated reverse osmosis and membrane distillation, (Macedonio & Drioli, 2008). The selection and effectiveness of a technique is dependent on form of arsenic species, total dissolved solids, water characteristics, pH of water and presence of competing ions (sulphate, phosphate, silicate, and fluoride) and cost involved. At near neutral pH, Arsenate exists in mono- or divalent anionic form, while arsenite remains unchanged. Hence, pre-oxidation of As (+3) to As (+5) is a necessary step for an efficient and effective As (+5) removal from water by several existing technologies (adsorption, ion-exchange, and co-precipitation). Recently, arsenic bioremediation of contaminated drinking water shows a great potential for future implications due to its environmental compatibility and possible cost-effectiveness. Arsenic bioremoval from contaminated water can be achieved by arsenic absorption to biomass (Mondal et al., 2008; Say et al., 2003) and/or coprecipitation with biogenic hydroxides (Katsoyiannis & Zouboulis, 2004) or precipitation with sulphides (Kirk et al., 2010; Upadhyaya et al., 2010), either in-situ or ex-situ (Onstott et al., 2011a).

Iron removal from groundwater can be accomplished by several ways like, oxidation-floc formation-filtration, adsorptive filtration, lime softening, ion-exchange, sub-surface iron removal and phosphate treatment (Sharma, 2001). The type of treatment largely depends on the raw water quality, iron form (dissolved or particulate) and treatment cost. Alternative processes include membrane treatment, enhanced conventional

treatment (Knocke & Association, 1990) and biological removal are frequently practiced for high amounts of iron and operational facilitation (Ellis et al., 2000).

High solubility and stability of nitrate ion make its removal difficult through coprecipitation or adsorption. Hence, conventional water treatment technologies such as lime softening and filtration, are not at ease for nitrate removal (Kapoor & Viraraghavan, 1997). Nitrate removal from groundwater on full-scale is achieved by ion exchange, reverse osmosis and biological de-nitrification processes (Sharma & Sobti, 2012).

The most commonly used methods for the defluoridation of water are chemical additive methods (precipitation and co-precipitation) (Reardon & Wang, 2000), contact precipitation, adsorption (Sujana et al., 2009), ion exchange (Vaaramaa & Lehto, 2003) and membrane techniques (reverse osmosis, nanofiltration, dialysis, and electro dialysis) (Hu & Dickson, 2006). Adsorption, a conventional technique, deals with adsorbents such as alumina/aluminium-based materials, clays and soils, calcium based minerals, synthetic compounds, and carbon-based materials, is most commonly used methods for the defluoridation of water (Jagtap et al., 2012; Mohapatra et al., 2009). Even though membrane techniques successfully reduce fluoride concentration to acceptable levels, adsorption is widely practiced option because of its lower cost and operational simplicity. Defluoridation efficiency varies according to many site-specific chemical, fluoride concentration, geographical, and economic conditions. In purview of co-existence of multiple contaminants in drinking water sources, researcher have been developed composite and polymeric adsorbents (Jing et al., 2012; Kumar et al., 2011), hybrid and integrated treatment options (Hristovski et al., 2008; Ingallinella et al., 2011; Mekonen et al., 2001) that provide simultaneous removal of multiple contaminants.

The review provided below presents brief descriptions of each of the treatment technologies available for arsenic, iron, nitrate and fluoride removal from drinking water sources, in isolated and/or co-occurrence. The removal method practiced for industrial effluents will not be a part of present review.

2.3.1 Oxidation

The oxidation process involves conversion of soluble As (+3) to As (+5), which is followed by precipitation of As (+5). Since As (+3) is the predominant form at near neutral pH, this is necessary for anoxic groundwater. As (+5) adsorbs more easily onto

solid surfaces than As (+3) and thus, oxidation followed by adsorption is effective for the removal of arsenic (Ghurye & Clifford, 2004). Several oxidants have been used for arsenic removal which includes manganese dioxide, iron containing compounds (Bajpai & Chaudhuri, 1999), permanganate, chlorine, hydrogen peroxide, chloramines and others (Mondal et al., 2013). Solar oxidation (Hug et al., 2001), In-situ oxidation (DPHE, 2001) and biological oxidation also received considerable attention in arsenic removal from drinking water. Oxidation is not considered as an effective method for arsenic removal because of need of another treatment step, formation of toxic by products and treatment of generated solid waste.

The oxidative iron removal may achieved via natural oxidation in presence of air or add of some oxidants (chlorine, ozone, potassium permanganate or hydrogen peroxide etc.) or biological oxidation. In the presence of oxygen, soluble iron (II) get oxidised and forms flocs of iron(III) hydroxide, thus precipitated iron is removed by filtration (Ankrah & Sogaard, 2009)

2.3.2 Coagulation-Flocculation

Soluble arsenic is precipitated/co-precipitated onto the flocs formed after coagulant addition and thus removed from aqueous solution. Commonly used chemical coagulants includes iron based (ferric chloride, ferric sulphate) (Lacasa et al., 2011; Lakshmanan et al., 2010), alum based salts ((aluminium chloride, polyaluminium chloride and kaolinite) (Hu et al., 2012; Pallier et al., 2010), manganese sulphate, copper sulphate and ammonium sulphate. Arsenic (+3) removal depends on the coagulant dose and pH of the solution as compared to arsenic (+5), which adsorbs better at near neutral pH. Iron salts provides better removal, as positively charged iron hydroxides are more stable over a wide range of pH and also having high affinity for negatively charged As (+5), than the alum based salts (Hering et al., 1997; Kay, 2011). Arsenic removal is also dependent on raw water quality like initial As concentration, pH (Wickramasinghe et al., 2004) and presence of organic matter (Yuan et al., 2003). The major drawback in field applications is management of contaminated sludge generation.

2.3.3 Ion Exchange

In this technique, contaminants are effectively removed from water, based on their affinity towards the charged functional groups of the resin bed of synthetic or natural

organic and inorganic or polymeric materials. Arsenate, iron, nitrate and fluoride can be removed through the use of strong-base anion exchange resin in chloride or hydroxide form, chloride or bicarbonate ions and chloride ions respectively. Ion exchange (IX) has been widely used to remove arsenic (An et al., 2010; Donia et al., 2011; Kim & Benjamin, 2004; Kim et al., 2003), nitrate (Clifford & Liu, 1993; Samatya et al., 2006) and fluoride (Ho et al., 2004; Meenakshi & Viswanathan, 2007; Rao & Bhaskaran, 1988) from water. The IX process have following demerits (i) pre-oxidation step for As (+3), (ii) need for pH adjustment (iii) competition with non contaminants (iv) resin fouling (v) hazardous waste generation (vi) high cost involved (Höll, 2010; Kemper et al., 2008).

2.3.4 Membrane Technology

The membrane processes involves forcing the contaminated water across a membrane under high pressure and leaving contaminants and other ionic species behind on the influent side of the membrane. There are four different types of membrane processes, i.e., reverse osmosis (RO), nanofiltration (NF), microfiltration (MF), and ultra filtration (UF) which are commonly employed for treatment of contaminated water. High pressure (50-150 psi) membrane techniques, NF and RO effectively removes (up to 99%) dissolved arsenic (+3 and +5) from contaminated water in pH range of 4-8 (Waypa et al., 1997). NF and RO membranes are having high removal rate for charged As (+5) as compared to uncharged As (+3), and the process is largely affected by pH of feed water and operating pressure rather than feed water concentration (Akin et al., 2011; Geucke et al., 2009; Seidel et al., 2001). Seidel et al. (2001) reported charge exclusion is predominant over the size exclusion mechanism for rejection of targeted ions. RO fails to remove As (+3) from natural anoxic groundwater at <10 pH value, as As (+3) is predominating in reducing ambience (Walker et al., 2008). Large pore size UF and MF membranes successfully removes all category size arsenic, particulate (>0.45 μm), colloidal (<0.45 μm and >3 kDa) and dissolved (<3 kDa) (Brandhuber & Amy, 1998). UF provides better removal but decreased removal efficiencies, attributed to the larger molecular weight-cut off feature in UF membrane. UF and MF requires particle size increasing techniques such as coagulation and flocculation for arsenic removal from water, as the particulate forms of arsenic are scarce in natural aquatic environment (Ghurye et al., 2004). Among membrane processes NF/RO can be used to remove dissolved iron while MF/UF to remove iron flocs.

Reverse osmosis (RO) can also be used to remove nitrate and fluoride from water. Guter (1982) reported nitrate removal up to 65% for influent NO_3^- -N concentrations ranging from 18 to 25 mg/L, provided 25% percent of the influent water became waste brine. Clifford et al. (1987) found polyamide membranes more effective than cellulose triacetate membranes for nitrate rejection in an RO system in presence of antiscalants in influent stream. In a recent study Epsztein et al. (2015) used Sulphuric acid and sodium hexamethaphosphate as antiscalants to minimize chemical fouling in hybrid NF/RO system for nitrate removal. RO is rarely used for nitrate removal because of scaling and high brine waste generation. Additionally, hydrophilic properties and monovalent nature of NO_3^- ion makes RO less effective for nitrate removal. Other membrane processes like MF and UF are ineffective for nitrate removal except when employed as part of an MBR. However, the usage of these processes has been limited as they are very costly and merely displace nitrate into concentrated waste brine that may pose a disposal problem.

Membrane separation such as RO, NF, dialysis and electro dialysis (ED) are very promising defluoridation methods used for drinking water supply (Mohapatra et al., 2009; Singh et al., 2016; Singh et al., 2013). Electrical effects (charge repulsion, Donnan exclusion and dielectric exclusion) and steric effects are the main governing factors for fluoride retention by RO/NF (Shen & Schäfer, 2014). Recently, Pontie et al. (2013) reported NF process as efficient process over RO in his study with worlds first defluoridation plant based on the NF. RO and NF are documented to have up to 90-98% fluoride removal efficiencies but fluoride retention is strongly affected by recovery and feed water composition, mainly ionic strength, fluoride concentration and to some extent natural organic matter concentration (Shen & Schäfer, 2014; Singh et al., 2013). Donnan dialysis was shown to remove high fluoride (>30 mg/L fluoride) from ground waters to below 1.5 mg/L even in presence of other ions (Mohapatra et al., 2009).

2.3.5 Adsorption Processes

Various adsorbents have been discussed for arsenic, iron, nitrate and fluoride removal in the literature. The criteria for selection of a suitable adsorbent media for contaminant removal from drinking water includes: medium cost, initial arsenic concentrations, adsorption capacity, ease of operation and maintenance, optimization of adsorbent dose, potential for regeneration and reuse, other elements and their

concentration in water etc. (Mohan & Pittman Jr, 2007). Mohan and Pittman Jr (2007) listed all potential adsorbents for arsenic removal and suggested that iron Based adsorbents are most widely used adsorbents. Aluminium, iron, titanium and low magnesium based substance have been shown very high arsenic removal efficiency. Activated alumina, granular ferric hydroxide and granular TiO₂ in the form of metal, metal oxides and/or hydroxides are commercially available arsenic adsorbents. In recent years, cerium (Ce) and zirconium (Zr), added adsorbents such as granular Fe-Ce oxide (Zhang et al., 2010), Ce-Ti oxide (Deng et al., 2010), Fe-Zr binaryoxides (Ren et al., 2011), Zr(IV)-loaded ligand exchange fiber (Awual et al., 2012) etc. have been used to enhanced As adsorption performance because of their increased surface areas, surface hydroxyl group, and pore accessibility. Very recently, Hassan et al. (2014) used potassium hydroxide activated carbon based apricot stone (C), calcium alginate beads (G) and calcium alginate/activated carbon composite beads (GC) for adsorption of arsenic. The adsorption capacity was found to be 27.0, 42.4 and 66.7 mg/g (at 30°C) for C, G and GC respectively for an initial arsenic dose of 75mg/L. Türk et al. (2009) reported arsenic adsorption to below 5.0 µg/L from 300 µg/L at optimum pH 7.1 using commercially available nanomagnetite. Bibi et al. (2015) studied industry based adsorbents such as hydrated cement, bricks powder and marble powder and reported removal >90% for arsenic and >75% for fluoride from an initial concentration of 1000 µg/L of arsenic and 30 mg/L of fluoride at pH 7.0 and 8.0, contact time of 60 min and a dose of 30 g/L. The major disadvantage of using adsorption process for drinking water is the disposal of both the spent media and the wastewater produced during regeneration/cleaning of the column.

Several adsorbents such as carbon and clay based, naturally occurring, chitosan, zeolites, double layered hydroxides, agricultural wastes, industrial wastes, bio sorbents and other synthetic organic and inorganic compounds have been used by previous researchers for nitrate removal from water (Bhatnagar & Sillanpaa, 2011; Loganathan et al., 2013a). Bhatnagar and Sillanpaa (2011) and Loganathan et al. (2013a) reviewed most of the nitrate adsorbents and their characteristics thoroughly and suggested that double layered hydroxide type compounds and modified chitosan have shown better adsorption compared to other conventional adsorbents. Surface modified agricultural wastes and other modified adsorbents have also been shown considerable potential for nitrate adsorption with only disadvantage of cost modification. Modified adsorbents have been

shown 4-11 times higher nitrate adsorption capacity than unmodified adsorbents thus they can be applied in remediation of high nitrate containing waters and where ultra-pure waters are required (Loganathan et al., 2013a). These reviewers have shown that most of the nitrate adsorption experiments were done in batch mode and most of the adsorbents were satisfactorily following the Langmuir equilibrium model and pseudo-second-order kinetic model. In most cases, the maximum Langmuir capacities were 1.7-92.1 mg/g and 125-363 mg/g for unmodified and modified adsorbents respectively.

A diverse range of adsorbents have been used so far to remove fluoride from water and wastewater. Most of them includes multivalent metal oxides and hydroxides, clay and soils, synthetic resins, layered double hydroxides (LDHs), zeolites, carbon materials, calcium materials, biopolymers, natural industrial by products, and organic wastes (Bhatnagar et al., 2011; Loganathan et al., 2013b; Mohapatra et al., 2009). Loganathan et al. (2013b) suggested multivalent metal oxides and hydroxides and layered double hydroxides as most promising because of their high fluoride adsorption capacities (1.08-28.0 mg/g). The WHO and USEPA classified activated alumina adsorption as one of the best available technologies for fluoride removal. The carbon-based adsorbents have been found less efficient however after some modifications they have been shown improved water defluoridation. Similarly natural materials such as different types of clays and biosorbents have been found less efficient under high fluoride concentrations and also difficult to regenerate (Singh et al., 2016). However, the adsorption capacities of these substances could be increased by modifying the surface by incorporating organic functional groups or multivalent metallic cations. In spite of having low adsorption capacities, some waste materials (e.g., red mud, slag, and sludge), natural and industrial by products could be used for defluoridation in rural areas, especially in developing countries because they are low-cost alternative adsorbents.

Recently, Yu et al. (2015) developed highly efficient Fe-Mg-La metal composite for fluoride adsorption. The adsorption capacity was found to be 270 mg/g, which is much higher than most reported adsorbents. Nath and Bhattacharyya (2015) studied adsorption of arsenite and fluoride on untreated and treated bamboo dust and found acid activation of bamboo dust increases adsorption capacity. Ippolito et al. (2011) reviewed the use of water treatment residuals (WTR) and suggested WTR successfully removes potential environmental contaminants such as arsenic, selenium, perchlorate and mercury etc. WTR

adsorbs a variety of anions due to their porosity, amorphous nature and the presence of Al and Fe (hydr)oxides. Chiang et al. (2012) studied WTR as alternative sorbents for multi-heavy metal removal from synthetic solutions, contaminated sediments, and surface waters. The WTR surpassed the adsorption capacity of commercially available goethite by 100-400% for single contaminant tests and by 240% for total sorption in multi-contaminant tests.

2.3.6 Small Scale/Household Technologies

Several small-scale and household level water treatment technologies have been developed worldwide for removal of arsenic, iron and fluoride from groundwater. Most of them have been successfully adopted and applied in developing as well as developed nations by low-income people, villages, small cities, periurban populations and towns. Some of these technologies are using conventional methods like coagulation–filtration, or adsorption, using very cheap materials, while some are based on new approaches such as biological, solar or photochemical processes.

In Peru, ALUFLOC, a mixture of an oxidant (chlorine), activated clays (adsorbents and/or ion exchangers) and a coagulant ($\text{Al}_2(\text{SO}_4)_3$ or FeCl_3), successfully removing dissolved As to the drinking water norms from an initial concentration of 1 mg/L and applied as low-cost, household scale As removal method (Bedolla et al., 1999). Similarly, hydrogel made up of activated aluminium hydroxide, hydrated aluminium sulphate, powdered calcium hypochlorite, ammonium hydroxide and demineralised water was tested for As removal at household-scale in Argentina. It successfully removes As below 10 $\mu\text{g/L}$ from an initial groundwater concentration of 40-800 $\mu\text{g/L}$ As (Luján, 1999). A number of filters namely Star Filter, Kanchan Arsenic Filter (Ngai et al., 2007), Household Sand Filter (Berg et al., 2006), IHE Arsenic Removal Family Filter (Petrusevski et al., 2008), and Sono 3-Kolshi (Munir et al., 2001) filter have been developed and deployed by for arsenic remediation.

Massachusetts Institute of Technology (MIT), Environment and Public Health Organization (ENPHO), Kathmandu, Nepal and Centre for Affordable Water and Sanitation Technology (CAWST) together developed household Kanchan Arsenic Filter (KAF) for arsenic removal. KAF successfully removed 85-90% arsenic, 90-95% iron, 80-95% turbidity, and 85-99% total coliforms in a two two-year technical and social

evaluation in rural Nepal (Ngai et al., 2007). UNESCO-IHE developed an arsenic removal family filter with a capacity of 100 L/day based on arsenic adsorption onto iron oxide coated sand- a by product of iron removal plants. Arsenic level was found below the WHO guideline value in long term field operations for 30 months in rural Bangladesh, in addition iron present in groundwater was also removed effectively (Petrusevski et al., 2008).

Recently Maiti et al. (2013) developed laterite based household filters which successfully removed arsenic to below 10 mg/L from an initial concentration of 70-250 µg/L for about a year when deployed in arsenic affected area of Barasat, West Bengal, India.

National Environmental Engineering Research Institute (NEERI), Nagpur, India developed hand pump attachable iron removal filtration unit and domestic iron removal unit (DIRU) for iron removal. During passage of water through the unit the ferrous iron got oxidized and converted to insoluble precipitates which were removed through filtration. The unit had been removed more than 15 mg/L soluble ferrous form iron to almost zero level in the field tests.

Devi et al. (2008) modified homemade filter using pebbles, gravels, sand and crushed brick as media for removal of fluoride, arsenic and coliform bacteria from drinking water. The maximum reduction of fluoride, arsenic and coliform bacteria was 85%, 93% and 100% with residual values of 0.72 mg/L, 0.009 mg/L and 0 coliform cells/100 mL respectively after 10 h treatment period. Birhane et al. (2014) studied the efficiency of locally available filter media on fluoride and phosphate removal for household water treatment and suggested that bone char has a good fluorine removal capacity, followed by pumice, calcined clay, scoria and sand.

2.4 Biological Processes

Biological drinking water treatment is based on the ability of indigenous microbes, specifically non-pathogenic bacteria to efficiently catalyze the biochemical oxidation/reduction of drinking water contaminants and produce biologically stable water (i.e., treated water that does not support microbial growth in the distribution system (Rittmann & Snoeyink, 1984). It involves the acclimatization and maintenance of microbial biomass in aerobic and/or anaerobic suspended or attached growth bioreactors. The process

involves addition of a carbon source (electron donor) such as acetic acid and nutrients (e.g., phosphate, if required) to water to promote biochemical reduction of inorganic contaminants such as perchlorate, nitrate, arsenic, iron etc., which serve as the terminal electron acceptors for respiration by these bacteria. The acclimatized microbial populations, thus can be harnessed for contaminants removal in natural or engineered environments.

Microbially mediated redox reactions can be effectively controlled by providing suitable electron donors and acceptors (Lovley & Chapelle, 1995). The establishment of various terminal electron accepting zones (TEAPs) enable microorganisms to use a number of suitable electron donors present in the system for their energy generation process sequentially. This is based on the thermodynamic favourability of the reaction, thus by gaining or losing electrons, compounds get converted to different, often innocuous, thermodynamically more stable forms than the original compounds. In groundwater systems, under anoxic conditions the ecological succession of terminal electron-accepting processes is O_2 followed by NO_3^- , Mn(IV), Fe(III), SO_4^{2-} , and finally CO_2 . As most of the O_2 get depleted along aquifer flowpaths in ground water systems, nitrate is next most energetically favoured electron acceptor. The ecological succession of TEAPs may change depending up on variation in concentration thresholds of electron acceptors, microbial species and electron donor availability. For example, the O_2 concentration threshold required for the onset of denitrification vary from 0.2 to more than 1 mg/L, depending up on bacterial strain and natural or controlled laboratory conditions (McMahon & Chapelle, 2008). Additionally, facultative microbes can utilize oxygen under aerobic conditions, while growth can still be sustained utilizing nitrate in the absence of oxygen. However, obligate anaerobes are inhibited in an aerobic environment. Generally, when DO, nitrate, iron(III), sulphate, and arsenate are present and an electron donor (e.g., acetate) is available, a series of sequential and energetically favourable TEAPs will be established in a biological system, starting with aerobic respiration (Upadhyaya et al., 2010). Such engineered systems can be employed in various configurations including fixed beds, fluidized beds, and membrane systems.

2.4.1 Aerobic Respiration

Aerobic respiration is defined as use of oxygen as a terminal electron acceptor by bacteria for the energy generation process. This is thermodynamically the most favourable

of the TEAPs. Both aerobic as well as facultative bacteria can mediate this reaction and are ubiquitous in natural environments. Such bacteria have the capability of complete oxidation of a large range of organic substrates ranging from natural to manmade compounds (Lovley & Chapelle, 1995). Interestingly, some of these microorganisms can also utilize inorganic electron donors, such as iron (II), manganese (II), elemental sulphur, and ammonium (Lovley & Chapelle, 1995).

2.4.2 Biological Denitrification

The microbial reduction of nitrate to gaseous nitrogen, a method used in the treatment of nitrate contaminated groundwater, is termed dissimilatory denitrification or nitrate respiration. Biological denitrification of drinking water is often favoured considerably due to the lower running costs on a large scale to other methods. In this process, nitrate is used instead of oxygen as a terminal electron acceptor in presence of an electron donor, for energy generation. Nitrate is finally converted to innocuous nitrogen gas through a series of four steps ($\text{NO}_3^- \rightarrow \text{NO}_2^- \rightarrow \text{NO} \rightarrow \text{N}_2\text{O} \rightarrow \text{N}_2$). Each step is catalyzed by different functional enzymes which includes nitrate reductase (Nar), nitrite reductase (Nir), nitric oxide reductase (Nor), and nitrous oxide reductase (Nos) respectively (Rich & Myrold, 2004). Denitrifiers, a phylogenetically diverse group of facultative anaerobic bacteria are found widely in the environment and display a variety of different characteristics in terms of metabolism and activities (Mateju et al., 1992; Soares, 2000). Nearly 130 species of bacteria including archaeobacteria can reduce NO_3^- to N_2 . The ability of denitrification is also reported in certain fungi (Zumft, 1997). Major genera of denitrifying bacteria includes *Achromobacter*, *Alcaligenes*, *Azospirillum*, *Bacillus*, *Chromobacter*, *Corynebacterium*, *Desulfovibrio*, *Flavobacterium*, *Halobacterium*, *Methanomonas*, *Moraxella*, *Paracoccus*, *Propionibacterium*, *Pseudomonas*, *Spirillum*, *Thiobacillus*, and *Xanthomonas* (Mateju et al., 1992; Myrold, 1998). The majority of denitrifiers are heterotrophic but several autotrophic denitrifying bacteria have been identified, using H_2 (Karanasios et al., 2010) or iron (Jha & Bose, 2005) and various reduced-sulphur compounds (H_2S , S , S_2O_3 , S_4O_6 , SO_3) as electron donors (Zhang et al., 2012). Many organic or inorganic compounds including liquids, solids, and gaseous (CH_4 and H_2) can be used as electron donor/carbon source for denitrification (Mateju et al., 1992). Major factors affecting the choice of a carbon source are: cost, pretreatment, denitrification rates, kinetics, degree of utilization, sludge

production, handling and storage safety/stability (ÆsØy et al., 1998). Solid substrates include wheat straw, plant pruning, reed, birch wood, and biodegradable polymers etc. Recently, water-insoluble biodegradable polymers such as Poly 3-hydroxybutyrate (PHB), polylactic acid (PLA), polycaprolactone (PCL) and polylactic acid/Poly (3-hydroxybutyrate-co-3-hydroxyvalerate) blend (PLA/PHBV) have been tested for denitrification in drinking water (Xu et al., 2011b). A wide spectrum of liquid organic carbon sources such as methanol, ethanol, glucose, glycerol, acetic acid, and lactic acid have been employed in water treatment (Akunna et al., 1993; Mohseni-Bandpi et al., 2013). The use of liquid or gaseous compounds are preferred and advantageous due to their easier uptake by bacterial cells and faster degradation, resulting in higher denitrification rates (Mohseni-Bandpi & Elliott, 1998). Methanol, ethanol and acetate are the most commonly used carbon sources for denitrification processes related to drinking water treatment (Calderer et al., 2010; Khardenavis et al., 2007). Methanol, being cheapest used in full-scale wastewater treatment plants but not used in drinking water treatment because of its toxicity in treated water (Jensen et al., 2012). However, ethanol is a better alternative to escape methanol toxicity since it is largely produced in some countries from sugarcane and costs less than other carbon sources, and there is no set permissible limit for ethanol in potable water. The acetic acid was found to be more effective in removal of nitrate as it reduces chlorine demand by preventing the growth of non-denitrifying biomass (mostly coliforms) which may cause clogging in reactors (Silverstein, 1997), more yield for denitrifiers, higher denitrification rate, high buffering capacity, low intermediate nitrite in the effluent, moreover, readily metabolised than methanol and glucose (Mohseni-Bandpi & Elliott, 1998). Therefore, use of acetic acid is more suitable over methanol and other fermentable substrates that may result in formation of alcohols and carboxylic acids. In a recent study, Yang et al. (2012) reported preferential use of acetate and citrate with minimal intermediate products accumulation and high nitrate reduction by *Pseudomonasstutzeri* D6. Heterotrophic denitrification is preferred over autotrophic as slower growth rate, complex process control and need of post treatment for degasification and biomass removal (Mohseni-Bandpi et al., 2013).

Like electron donors, denitrifiers can also use wide array of electron acceptors DO, nitrate, sulphate, selenate, chromate, chlorate, perchlorate, arsenate (Chung et al., 2007; Nerenberg & Rittmann, 2002), bromate (Hijnen et al., 1999), and iron (III).

Similarly a diverse group of bacteria including SRBs, DAsRBs, DIRBs and PCRBs which includes *Desulfovibrio desulfuricans* (Dalsgaard & Bak, 1994) *Desulfovibrio desulfuricans* strain 27774 (Marietou et al., 2009), *Chrysiogenes arsenatis* gen. nov., sp. nov. (Macy et al., 1996), *JMM-4* (Santini et al., 2002), *MIT-13*, *SES-3* strains (Newman et al., 1997), *E1HT*, *MLS10T*, *BAL-1T*, *Desulfitobacterium hafniense DCB-2T* and *Desulfitobacterium frappieri PCP-1T* (Niggemyer et al., 2001), arsenic reducers and *Geobacter metallireducens* is strictly anaerobic, dissimilatory iron-reducer (Murillo et al., 1999), *Dechloromonas* spp. Perchlorate reducer, can use nitrate as an electron acceptor.

Now days the N_2O emissions from wastewater treatment plants are of great concern among world urban water authorities. NO and N_2O can cause depletion of the ozone layer as its greenhouse effect is 300 times more potent than CO_2 (Ravishankara et al., 2009). N_2O is produced as an intermediate in the heterotrophic as well as in autotrophic nitrifying process, mainly ammonia-oxidizing bacteria (AOB) (Kampschreur et al., 2007). In contrast to AOB, the N_2O produced by heterotrophic denitrifiers emits less N_2O as it remains dissolved in absence of stripping and get time to reduced in to N_2 (Law et al., 2012). Other factors that promotes N_2O emission are low nitrate levels, active stripping, aerated zones, DO (Ahn et al., 2010), change in operational conditions such as pH, electron donor limitation, increased nitrite concentrations, and DO (Law et al., 2012). Generally, higher nitrate concentrations lead to the complete extent of denitrification, with nitrogen gas as more desirable final product however, relative contributions could be dependent on process conditions.

Environmental Factors Affecting Denitrification

DO is having inhibitory effect on denitrification, as later is thermodynamically less favourable biochemical reaction. In fact, oxygen presence in water inhibits nitrous oxide reductase, thus limits nitrous oxide conversion to nitrogen gas (Baumann et al., 1996). Recently, Hocaoglu et al. (2011) observed complete nitrate removal within the DO range of 0.15-0.35 mg/L in an MBR, while it was inhibited at 0.5 mg/L DO.

The pH range preferred by heterotrophic denitrifiers for complete reduction of nitrate to nitrogen gas is considered to be between 6 and 8 (Rust et al., 2000). At low pH ($pH < 5$) inhibition is due to the accumulation of nitrite or N_2O in solution (Glass & Silverstein, 1998). High pH ($pH 8.3$) may also arrests the denitrification (Rust et al.,

2000), the optimal pH is site-specific because of the effects of acclimation and adaptation on the microbial biomass in the system.

Denitrifiers can be found in diverse environments from arctic regions to hot springs. In most scientific studies, temperature impact was more significant on denitrification. Denitrification rate gradually increases within the optimal temperature range from 25 to 40°C. However, denitrification has been observed in the range of 2–50°C and beyond, microbial populations evolves to cope with specific environmental conditions on prolonged incubation such as high temperatures (Braker et al., 2010; Sprent, 1987). However, the effect of temperature on denitrifying microbial communities is limited to a few studies. Hollocher and Kristjánsson (1992) found two denitrifiers *Pseudomonas aeruginosa* (mesophilic) and *Bacillus* (thermophilic) that grow at 70°C in water samples, able to reduce nitrate to N₂.

2.4.3 Biological Iron Removal

In nature, iron oxidizing bacteria (IOB) and dissimilatory iron-reducing bacteria (DIRB) are widespread. Fe(II) can serve as an electron source for IOB under both oxic and anoxic conditions and Fe(III) can serve as a terminal electron acceptor under anoxic conditions for DIRBs. They are prevalent in groundwater, swamps, hot springs, ponds, lakes, sediments, soils, wells and water-distribution systems. Fe(III) and Fe(II) can be rapidly interconvert in subsurface environments because of high redox potential of Fe(III). Because of universal abundance, Fe(III) is top most electron acceptor in soils and next to sulphate in marine sediments. Iron reducing microbes exhibits great diversity in nature which includes aerobic bacteria, anaerobic bacteria as well as fungi (Frankel & Blakemore, 1991).

Iron removal from natural groundwater by IOB includes oxidation and precipitation of dissolved iron under optimal pH, redox potential (Eh) and DO (Mouchet, 1992). Biological iron removal has been reported to be employed for hand pump water supplies (Tyrrel et al., 1998) and in slow sand filters (Hatva, 1989), around the world for a wide range of iron concentrations (up to 16 mg/L), and temperatures (11-31°C) at good filtration rates (8-30 m/h). however, Twort et al. (2000) reported the inhibition of the process at high pH, DO, H₂S, chlorine, NH₄ and some heavy metals. Most of the freshwater IOB belong to the genera *Gallionella*, *Leptothrix*, *Crenothrix*, *Clonothrix*,

Siderocapsa, *Sphaerotilus*, *Ferrobacillus* and *Sideromona Sideroxydans* (Emerson et al., 2010; Sharma et al., 2005).

The iron and sulphate reduction are generally the most important terminal electron acceptors of TEAP processes in the upper anoxic zone of groundwaters (Lovley & Chapelle, 1995; McMahon & Chapelle, 2008). McMahon and Chapelle (2008) reported coexistence and sequential activity of DIRB and SRB in groundwater environments because of iron and sulphate zonation in such hydrologic system. This also removes iron and/or other metals by precipitating/coprecipitation/adsorption on to ferrous sulphides in these aquifers.

In subsurface groundwater environments, facultative (*Shewanella*) or strictly anaerobic (*Desulfuromonas acetooxidans*, *Geobacter metallireducens*) DIRB catalyze microbial reduction of Fe(III) minerals and play an important role in remediation of many metals (like As and U) in association with biogenic sulphides (Ehrlich & Newman, 2008; Lovley et al., 1991). The phylogenetically diverse DIRB are widespread across the Bacterial and Archaeal domains. Most studied DIRB includes strains of *Geobacter metallireducens*, *Geobacter sulfurreducens*, *Shewanella oneidensis* and *Shewanella putrefaciens* (Luef et al., 2013). Some members of DIRB are capable of complete oxidation of an organic substrate while some lead to incomplete oxidation, which includes *Geobacter*, *Geovibrio*, *Desulfuromonas*, and *Desulfuromusa* and *Pelobacter* and *Shewanella* species respectively (Coates et al., 1996). DIRB can respire on a wide range of organic compounds (e.g. lactate, acetate, propionate, isobutyrate, succinate, toluene, phenol, benzoate, glycerol, glucose) or H₂ (Finke et al., 2007; Lovley et al., 1989; Luef et al., 2013), as an electron donor and DO, nitrate, manganese (Mn(IV)) (Kawaichi et al., 2013; Lovley et al., 2004), sulphate (Ramamoorthy et al., 2006), chromate (Wielinga et al., 2001), uranium (Petrie et al., 2003) as electron acceptors. Many iron reducers like *Defferibacter thermophilus* (Slobodkin et al., 1999) and recently isolated *Ardenticatena maritima* (Kawaichi et al., 2013), are capable of iron reduction in moderate to extreme thermo biotic environments (up to 85°C), the later is facultative aerobic can also utilize DO and nitrate as electron acceptor (Zhang et al., 1997).

2.4.4 Microbial/Biological Arsenic Removal Mechanisms

Biological arsenic removal relies on microbially mediated redox and biochemical processes like oxidation–reduction, mobilization, or immobilization through sorption, biomethylation and complexation. These microbial processes have the potential to promote arsenic removal from contaminated soils/waters when used as intended.

2.4.4.1 Microbial Arsenic Oxidation

Arsenic oxidizing microbes (AOM), both heterotrophic and chemolithoautotrophic, are wide spread in the domain of Bacteria and Archaea. (Oremland & Stolz, 2003; Stolz et al., 2010). Many isolates of AOM have been reported from various environments such as from arsenic rich waters, soil, and mines etc. regardless of arsenic contamination (Yamamura & Amachi, 2014). Phylogenetically diverse strains of AOM belongs to *Alpha-*, *Beta-*, *Gamma- Proteobacteria* and genus *Thermus*. Arsenite oxidation for energy generation or as a detoxification mechanism is catalyzed by arsenite oxidase, which is present in heterotrophic (Vanden Hoven & Santini, 2004) as well as chemolithoautotrophic AOM.

Heterotrophic oxidation of As(III) may be used as a supplemental energy source, is primarily considered as a detoxification reaction (Vanden Hoven & Santini, 2004). While chemolithoautotrophic AOM derive metabolic energy by coupling the oxidation of As(III) (e.g., electron donor) to the reduction of either oxygen or nitrate to fix CO₂ into organic cellular material and achieve growth (Rhine et al., 2006). A chemolithoautotroph *Pseudomonas arsenitoxidans NT-26*, uses As(III) and oxygen as electron donor and acceptor respectively, and carbon dioxide or bicarbonate as the carbon sources is reported by (Santini et al., 2000). Many workers reported anaerobic As(III) oxidation in presence of nitrate in lieu of oxygen, like Oremland et al. (2002) reported a facultative chemoautotrophic strain *MLHE-1* isolated from anoxic bottom of Mono Lake (USA), strain showed both nitrate dependent autotrophic growth with H₂ or sulphide and heterotrophic growth with acetate. Recently, Dong et al. (2014) isolated a new facultative chemolithoautotrophic arsenite oxidizing bacterium, *KGO-5* strain of *Sinorhizobium* sp., from arsenic-contaminated industrial soil in Japan, capable of oxidizing arsenite either in the presence or absence of organic matter. Similarly Rusch et al. (2015) isolated a new facultative chemolithotrophic bacterium, *Burkholderia insulsa* sp., from an arsenic-rich

system of Papua New Guinea. The bacterium shown heterotrophic growth in presence of O_2 and NO_3^- as electron acceptors as well as aerobic lithoautotrophic growth was with thiosulphate or nitrite as electron donors.

Gihring et al. (2001) reported thermophilic AOM signifying detoxifying role of As(III) oxidation, namely *Thermus aquaticus* and *Thermus thermophilus*, oxidized As(III), but not used it as sole energy source. Interestingly, Gihring and Banfield (2001) isolated another *Thermus* strain (HR13) from an arsenic-rich terrestrial geothermal environment, capable of both As(III) oxidation for detoxification under aerobic conditions and dissimilatory As(V) reduction under anaerobic conditions. Muller et al. (2007) reported presence of both As(V) oxidation and As(III) reduction in *Herminiimonas arsenicoxydans* bacterium. The biological oxidation of As(III) to As(V) by iron and manganese oxidizing microbes is widely reported and it well established for efficient As(III) removal without any additional chemical usage in this bioprocess (Casiot et al., 2003).

2.4.4.2 Microbial Arsenic Reduction

Microbial arsenic reduction is a microbial mechanism for detoxification and resistance or for metabolic energy generation (Macy et al., 1996). As(V) reduction under aerobic conditions is more likely a detoxification mechanism. Many bacteria can reduce As(V) to As(III) by mean of detoxification systems. while some microbes can reduce As(V) as an electron acceptor in anaerobic respiration known as arsenic (V)-resistant microbes (ARMs) and (dissimilatory As(V) respiring prokaryotes (DARPs) respectively. Both mechanisms of Arsenic reduction have been described briefly.

Microbial Arsenic Reduction: As Metabolic Energy Generation

DARPs utilize As(V) as a terminal electron acceptor in their respiratory process for energy generation. They have been isolated from freshwater sediments, estuaries, soda lakes, hot springs and gold mines (Oremland & Stolz, 2003). DARPs are phylogenetically diverse bacteria distributed in the Gamma-, Delta- and Epsilon-proteobacteria, Aquificae, Deferribacteres, Chrysiogenetes, Firmicutes and in the Archaea, including obligate and facultative anaerobes (Cavalca et al., 2013). Diversified DARPs include several strains of *Sulfurospirillum spp.*, *Desulfitobacterium spp.*, *Bacillus spp.*, *Geobacter spp.*, *Shewanella spp.*, *Chrysiogenes arsenatis* and *Anaeromyxobacter sp. PSR-1* (Yamamura & Amachi,

2014). These microbes can use a variety of electron donors including hydrogen, acetate, formate, pyruvate, butyrate, citrate, succinate, fumarate, malate and glucose. Furthermore, most of them can use sulphate, nitrate, nitrite, Fe(III), Se(VI), Mn(IV), U(VI), elemental sulphur, thiosulphate, fumarate and oxygen (microaerobic) as the electron acceptors (Newman et al., 1997; Niggemyer et al., 2001) other than As(V) except strain *MLMS-1* (Hoeft et al., 2004).

Few sulphate reducing bacteria have been shown to mediate dissimilatory arsenate reduction (Blum et al., 2012; Newman et al., 1997). Anaerobic microbes can display As(V) reduction abilities both as As(V)-respiring heterotrophs gaining energy from the oxidation of small organic molecules or aromatic compounds (Liu et al., 2004), and as chemolithoautotrophs gaining energy from hydrogen and sulphide (Stolz & Oremland, 1999). Chung et al. (2006) and Xia et al. (2014) studied arsenic removal from groundwater by acclimated sludge under autohydrogenotrophic conditions.

The enzyme arsenate respiratory reductase (ARR), which is believed to mediate the As(V) reduction in solid phase, belongs to DMSO reductase family. ARR is a heterodimer, periplasmic protein consists of a larger (ArrA) molybdenum and a smaller (ArrB) iron-sulphur containing subunits encoded by *arrA* and *arrB* genes of the *arr* operon (Afkar et al., 2003). ARR, is a bidirectional enzyme acting as an oxidase or reductase depending on its electron potential and the constituents of the electron transfer chain (Richey et al., 2009). They also reported the reversible functionality of ARR, capable of both As(III) reduction and As(V) oxidation in in-vitro conditions. Many microbes other than DARPs have been reported with ARR respiratory systems, including DIRB *Shewanella ANA-3* strains (Saltikov et al., 2003), *Geobacter lovleyi* (Giloteaux et al., 2013), SRB *Desulfohalophilus alkaliarsenatis* (Blum et al., 2012) and dechlorinating bacteria *Desulfitobacterium spp.* (Kim et al., 2012a).

The purification and characterization of ARR has been reported for *Chrysiogenes arsenatis* (Krafft & Macy, 1998), *Bacillus selenitireducens* (Afkar et al., 2003), and *Shewanella sp.* strain *ANA-3* (Malasarn et al., 2008). In *Shewanella sp.* *ANA-3*, presence of genes encoding for ArsA, ArsB, ArsD and ArsC subunits, which is responsible for As resistance is observed (Saltikov et al., 2003). Vaxevanidou et al. (2015) suggested that microbial arsenate reduction is not related with pre-existing high arsenic pollution and

microbial biomass do not require long term acclimation with arsenic to carry such type of metabolism.

Microbial Arsenic Reduction: As Detoxification Mechanism

Arsenic (V)-resistant microbes (ARMs) are widespread among different bacterial phyla, carry out As(V) reduction to As(III) mediated by an enzyme cytoplasmic As(V) reductase (ArsC) (Silver & Phung, 2005). Bacterial arsenic detoxification mechanism is based on the expression of the *ars* operon (*arsRBC*), consists of minimum three genes encoding a transcriptional repressor *arsR*, a transmembrane efflux pump *arsB* and an arsenate reductase *arsC* respectively (Mukhopadhyay & Rosen, 2002). ArsC gene is responsible for the reduction of As(V) while *arsA* and *arsB* control the release of As(III) from the cytoplasm (Villegas-Torres et al., 2011). The *ars* genes are widespread in nature and found encoded in genome of a large number of Gram-negative *alpha* and *gamma* Proteobacteria as well as in Gram-positive Firmicutes. The *arsC* gene is widely also used for the detection, quantification and diversity analysis of ARM in arsenic contaminated environmental samples (Kaur et al., 2009; Sun et al., 2004). In some ARMs, an enlarged operon configuration (*arsRDABC*) contains the additional presence of *arsA*, for providing energy to ArsB efflux pump, *arsD* to enhance the efficiency of the ArsAB efflux pump is present providing resistance to organisms in high arsenic concentrations. As (III) is sequestered in intracellular compartments, either as free As(III) or as conjugates with glutathione or ferredoxin or other thiols. Which is finally excreted out of the cell via ArsAB arsenic chemiosmotic efflux pump and by ATPase membrane system (Rosen, 2002; Silver & Phung, 2005). Macur et al. (2001) suggested As(V) reduction under aerobic conditions as a detoxification mechanism.

2.4.4.3 Arsenic Biomethylation

Arsenic methylation followed by volatilisation is ubiquitous phenomenon to detoxify inorganic arsenic by some microorganisms in aquatic environments (Kosolapov et al., 2004; Qin et al., 2006). Biomethylating organisms includes bacteria, yeast, fungi, algae and other eukaryotes, which can convert As to gaseous arsines, but is less known in bacteria (Páez-Espino et al., 2009). Arsines are highly volatile and toxic compounds formed under extremely reducing and anoxic conditions (Frankenberger Jr, 2001). Despite being a very slow process, it has been found in several aerobic and anaerobic

bacteria including *Clostridium collagenovorans*, *Desulfovibrio vulgaris*, *Desulfovibrio gigas*, *Methanobacterium formicium* etc. and in strains of *Proteus*, *Escherichia*, *Flavobacterium*, *Corynebacterium* and *Pseudomonas* genera (Páez-Espino et al., 2009). The As(V) reduction via methylation pathway(s) involves oxidative addition of a methyl group (Dombrowski et al., 2005) which results in a sequential generation of less toxic pentavalent methylated arsenicals like methyl arsenite (MMA), dimethyl arsenate (DMA-V) and trimethyl arsine oxide (TMAO) (Challenger, 2006). S-adenosylmethionine (SAM) is methyl groups donor in methylation reactions (Dombrowski et al., 2005). Arsenic(III) S-adenosylmethionine methyltransferase (*arsM* gene), is responsible for SAM-dependent methylation has been identified and characterized in many prokaryotes including bacteria, has been identified and characterized in many prokaryotes including archaea (Wang et al., 2014a) and bacteria (Qin et al., 2006). Anaerobic arsenic biomethylation only proceeds to dimethylarsine, which can be rapidly oxidized back to less noxious water-soluble species under oxygenated conditions (Wang & Zhao, 2009).

Despite their release in to atmosphere, arsine formation provides an effective mitigation for As poisoning in soils and water toward human or animals (Wang et al., 2014b). However, the role of arsenic biomethylation as a detoxification process is still controversial.

In some innovative techniques microbes have been used to promote the precipitation/co-precipitation of arsenic for its removal from contaminated water. The microbial biomass is either attached to a submerged solid substrate or suspended in the water. Such types of biological system are currently employed to remove arsenic from water in two ways. Which are described in detail in section 2.4.4.4 and 2.4.4.5.

2.4.4.4 Microbially Mediated Adsorption/Co-precipitation on Biogenic Oxides

In this method, arsenic is removed by adsorption/co-precipitation to the iron and manganese oxides which are formed by indigenous bacteria that oxidise and precipitate iron and manganese in water. The process relies on the fact that arsenic contaminated groundwater is usually reducing and containing iron and manganese concentrations. In such systems, i) the oxidation of Mn, Fe and As followed by precipitation ii) abiotic oxidation of As by manganese and iron oxides and iii) finally As(V) sorption by manganese and iron oxides, takes place sequentially. Katsoyiannis and Zouboulis (2004)

investigated arsenic removal during biological iron oxidation in a fixed-bed upflow filtration unit containing polystyrene beads. They reported that the iron-oxidizing bacteria *Gallionella ferruginea* and *Leptothrix ochracea*, led to the formation of iron oxides, providing a favorable environment for arsenic adsorption and consequently removal from the aqueous streams. The system was capable of 95% arsenic removal from an initial arsenic concentrations of 200 mg/L. In a similar type of system Pokhrel and Viraraghavan (2009) reported arsenic removal from 100 µg/L to 5 µg/L in the groundwater treating bioreactor grown with iron oxidizing bacteria. Katsoyiannis et al. (2004) also reported the kinetics of microbial As(III) oxidation and subsequent As(V) removal by sorption onto biogenic manganese oxides and suggested that the role of microbes is important in both oxidation of As(III) and in the generation of reactive manganese oxide surfaces for the removal of dissolved As(III) and As(V) during groundwater treatment. Later, Katsoyiannis and Zouboulis (2006) reported the simultaneous removal of iron, manganese and arsenic from contaminated ground water by using iron and manganese oxidizing bacteria.

In-situ oxidation by pumping the oxygenated water into aquifer to reduce As concentration in the pumped groundwater was investigated by (Gupta et al., 2009; Van Halem et al., 2010). Gupta et al. (2009) created an oxidizing zone in the aquifer by passing aerated water, which in turn oxidized iron and arsenic and resulted in As(V) removal by adsorption on to hydrous ferric oxides (HFO) (also termed as Fe(III) oxyhydroxides/oxides). The process relies on promoting the growth of iron and chemoautotrophic arsenic oxidizing bacteria (CAOs) by suppressing the growth of anaerobic As reducers in an aquifer. The In-situ oxidation of arsenic and iron in the aquifer has been also used for As(V) removal in Danida Arsenic Mitigation Pilot Project (DPHE, 2001). The aerated tube well water is stored in a tank and released back into the aquifers through the tube well in order to oxidize As(III) and Fe(II) by the dissolved oxygen content in water. This causes the reduction in arsenic content of tube well water.

Anaerobic CAOs have been widely used in the process which utilizes pre-oxidation of As(III) before its removal by adsorption and/or co-precipitation. Andrianisa et al. (2008) isolated an aerobic chemoautotrophic arsenic oxidizing (CAO) bacteria from activated sludge collected from a treatment plant receiving no arsenic contaminated wastewater, was able to oxidized As(III). They found an effective removal of oxidized

arsenic by co precipitation with HFO. Ito et al. (2012) carried out biological oxidation of AS(III) as a pretreatment step for As removal from synthetic groundwater in an immobilized aerobic continuous-flow bioreactor. Simultaneous removal of arsenic and nitrate in a single system is demonstrated in anaerobic continuous flow sand columns where oxidation of As(III) and Fe(II) was coupled with denitrification by As(III)-oxidizing denitrifying sludge bacteria. The arsenic removal was attributed to adsorption on to the mixture of biogenic iron oxides formed as a result of Fe(II) oxidation (Sun et al., 2009; Sun et al., 2010c) and activated alumina (Sun et al., 2010b). Several studies are available on the biological oxidation of As(III) followed by adsorption of As(V) on an adsorbent kutnahorite (Lièvrement et al., 2009), zero valent iron or activated charcoal (Mokashi & Paknikar, 2002) in a two stage process. These processes were successfully removing influents arsenite concentration 100 mg/L to 1 mg/l. While in other methods anaerobic bacterial population including sulphate-reducing bacteria have been employed to remove arsenic from solution as insoluble arsenosulphides precipitates.

2.4.4.5 Microbial Arsenic Precipitation, Co-precipitation and/or Adsorption onto Biogenic Sulphides

These methods use anaerobic, sulphate-reducing bacteria, and arsenic reducing bacteria, to precipitate arsenic from solution as insoluble arsenic-sulphide complexes. Sulphate reduction controls arsenic levels in many naturally reducing aquifers through arsenic co precipitation with biogenic sulphide minerals (Kirk et al., 2004) and/or through the formation of As-bearing sulphide minerals as in acid mine drainage (Altun et al., 2014; Battaglia-Brunet et al., 2012), sediments (Kirk et al., 2010), as well as in field (Saunders et al., 2008) under sulphate reducing environments.

The arsenic removal in such systems was mainly attributed to formation of As-bearing iron sulphides (FeAsS) (Altun et al., 2014; Saunders et al., 2008), arsenosulphides precipitation, e.g. orpiment (As_2S_3) and realgar (AsS) (Battaglia-Brunet et al., 2012; O'Day et al., 2004; Rodriguez-Freire et al., 2014), as well as co-precipitation and/or adsorption during the interaction between iron sulphides (FeS, FeS_2) and arsenic species (Bostick & Fendorf, 2003; Upadhyaya et al., 2010; Wolthers et al., 2005). The *in situ* applications have also been shown that As concentrations in groundwater can be greatly reduced by biogenic arsenosulphides in presence of sulphate-reducing bacteria (SRB)

(Keimowitz et al., 2007). The removal of arsenic also coincides the removal of dissolved iron from the water in the same precipitation/co-precipitation processes.

Sulphate Reduction Biotechnology

Dissimilatory sulphate-reducing prokaryotes (SRP) are a wide spread heterogeneous group of archaea and bacteria capable of reducing sulphate to sulphide (H_2S , HS^-) by using sulphate as electron acceptor (Castro et al. 2000; Garrity et al., 2003). SRP are spread in 60 genera including 220 species (Barton and Fauque, 2009). As most of the SRP species belongs to bacteria, they are oftenly termed as sulphate reducing bacteria (SRB). SRB gain energy for cell synthesis and growth by coupling oxidation of various organic compounds or molecular hydrogen (H_2) to the sulphate (SO_4^{2-}) reduction (Rabus et al., 2013). SRP are categorized in six different classes: *Archaeoglobi*, *Clostridia*, *δ -Proteobacteria*, *Nitrospira*, *Thermoprotei*, and *Thermodesulfobacteria* (Garrity et al., 2003). Most of SRB identified are mesophilic in terms of optimal growth temperature, but thermophilic, hyperthermophilic and psychrophilic species have also been reported (Knoblauch et al., 1999; Jeanthon et al., 2002). All SRB contain genes for the proteins mediating sulphate reduction, including sulphate transporters, ATP sulfurylase (*sat*), APS reductase (*aprAB*), and dissimilatory sulphite reductase (*dsrAB*) (Rabus et al., 2013).

Sulphate reducers can use a variety of electron acceptors, including sulphate, sulphite, thiosulphate, elemental sulphur (Kaksonen et al., 2007), DO (Barton & Tomei, 1995), nitrate (Barton & Tomei, 1995; Dalsgaard & Bak, 1994; Sorokin et al., 2013) (Moura et al., 1997), arsenate (Macy et al., 2000; Newman et al., 1997; Sorokin et al., 2013), and iron(III) (Sorokin et al., 2013; Tebo & Obraztsova, 1998), Cr(VI), U(VI), and Mn(IV) (Tebo & Obraztsova, 1998).

Factors Affecting SRB Activity

pH

Most engineering applications utilizing SRB have been carried out at neutral pH because of faster microbial growth and activity (Willow & Cohen, 2003). However, SRB can exhibit sulphate reduction even at low pH 3 (Kimura et al., 2006), but low pH can exert toxic effects resulting in cytoplasm acidification, accumulation of VFA and sulphide (Thauer et al., 1977) in the cells.

Temperature

Most of the sulphate-reducing applications have been run at room temperature or under mesophilic conditions (25-45°C) (Madigan et al., 1997) because at low temperatures, the kinetics of chemical and biological reactions sensibly slows down. Generally, the growth and the conversion rates are higher at elevated temperature, but the energy needed to heat a bioreactor contributes to increase the costs. Several species have been found to immediately respond and acclimatize to quick temperature decrease (Bakermans et al., 2007), even if it results in a decrease of the enzymatic activity (Feller & Gerday, 2003).

Oxygen

Presence of oxygen inhibits SRB metabolism, although the inhibition is reversible. Some SRB species (like *Desulfovibrio aerotolerans*) are capable to tolerate low levels of oxygen (Mogensen et al., 2005) or transform HS^- to partially oxidized species like $\text{S}_2\text{O}_3^{2-}$, which is reduced back to sulphide on reestablishment anaerobic conditions (Wall et al., 1990). The capability of aerobic respiration was also detected in *Desulfovibrio vulgaris*, *D. sulfidismutans*, *Desulfobacterium autotrophim*, *Desulfobulbus propionicus*, and *Desulfococcus multivorans* (Dilling & Cypionka, 1990).

Metal and Sulphide Toxicity

At low concentrations heavy metals can be stimulatory for SRB activity and, at the same time, inhibitory or even lethal at high concentrations (Sani et al., 2003). The metals toxicity can cause bacterial growth inhibition, extension of the lag phase in sulphide production, decrease of sulphate reduction efficiency and even death of the bacteria by deactivating enzymes and denaturation of proteins (Cabrera et al., 2006). But it depends on many factors such as biomass quantity, pH, temperature and initial metal concentration (Hao, 2000).

In anaerobic reactors small quantities of sulphide is advantageous since it decreases the bioavailability of some toxic metals by producing insoluble metal sulphides (Mizuno et al., 1994). Sulphide is inhibitory to some anaerobic trophic groups. The H_2S is toxic form of sulphide because it passes through the cell membrane and inhibits the metabolic enzymes of the cells (O'Flaherty et al., 1998). H_2S concentrations are related to the temperature, the pH and its solubility in water. The decrease in temperature and pH

increases the H_2S proportion. At low pH (4 and 5) values almost all the sulphide is present as H_2S . H_2S easily tends to strip out from liquid phase because it has a low solubility in water. However, not all the scientific studies on the sulphide toxicity towards SRB report similar results. For example, (Greben et al., 2007) observed increased sulphate reduction efficiency at high sulphide concentrations of 1424 mg/L. On the contrary, Visser et al. (1993a) reported the process failure even at sulphide concentration as low as 50 mg/L.

Biogenic Iron Sulphide (FeS) Precipitation

Biogenic iron-sulphides are abundant in freshwater and marine sediments attributed to microbial sulphate reducing activity in such naturally reducing aquifers. Biogenic FeS solids play an important role in sequestration of many metals and some metalloids including arsenic, from contaminated groundwater and soil (Kirk et al., 2004; O'Day et al., 2004; Ramamoorthy et al., 2009). Several studies have shown iron sulphide as a good scavenger for arsenic (III) under anoxic conditions. The mackinawite (FeS) and pyrite (FeS_2) can remove the arsenic by co-precipitation, and their generation controls the sulphide concentration in a system up to certain extent. (Gallegos et al., 2008; Gallegos et al., 2007; Wolthers et al., 2005).

Iron sulphide precipitation occurs when metal- and sulphate-reducing microbes use Fe(III) and sulphate, respectively, as electron acceptors either in succession or simultaneously (Postma & Jakobsen, 1996). Poorly crystalline mackinawite (FeS) and greigite (Fe_3S_4) are the major biogenic iron-sulphide solids in sedimentary pyrite formation studies. When dissolved iron comes in contact with sulphide, mackinawite is usually the first precipitate that forms in anoxic and sedimentary environments (Remoundaki et al., 2008; Wolthers et al., 2003). Aging period may vary from a few days to two years to form well crystalline mackinawite from amorphous mackinawite (Rickard, 1995). Mackinawite is also considered as pyrite precursor. Additionally, iron monosulphides have also been identified in bacterial diagenesis pathways to pyrite formation (Donald & Southam, 1999). Greigite (Fe_3S_4), smythite (Fe_9S_{11}), and pyrrhotite ($Fe_{1-x}S$) are the intermediate Fe-sulphides which may exist in ambient anaerobic environments during the transformation of disordered mackinawite to crystallized pyrite (Richard, 1969). Zhou et al. (2014) reported initial pH, electron donor, and sulphide

availability affects FeS bio precipitation in their experiments with *Desulfovibrio vulgaris*, a widely studied SRB. Larger-sized mackinawite and further its transformation to greigite (Fe_3S_4) is observed in presence of excess free sulphides, while excess Fe (II) resulted in vivianite [$\text{Fe}_3(\text{PO}_4)_2 \cdot 8\text{H}_2\text{O}$] formation. Benning et al. (2000) found that mackinawite was stable in a reducing atmosphere or up to 16 weeks over a range of pH from 3 to 12 at temperatures below 100°C . Recently, Gramp et al. (2010) reported improved crystallinity of biogenic mackinawite at increasing incubation temperatures from 22 to 60°C (22, 45 and 60°C), under experimental laboratory conditions. They also reported mackinawite (FeS) and greigite (Fe_3S_4) as dominant iron sulphide phases formed in sulphate-reducing conditions. Recently, Omoregie et al. (2013) observed arsenic removal as biogenic arsenic sulphide precipitation and sorption on surface of biogenic FeS formed in a biological system having iron and arsenic reducing bacteria (*Geobacter* sp. and *Sulfurospirillum* sp.). They also suggested that prolonged sulphidogenesis in the microcosms may lead to the formation of realgar-like surface precipitates on the surface of FeS, which provides efficient arsenic removal.

Biogenic Arsenosulphide Precipitation

Simultaneous formation of arsenite and sulphide in natural and engineered systems is an alternative way to remove arsenic as sulphidic minerals. As(III) can be removed from solution by its precipitation or complexation with sulphide or sulphide-containing materials such as orpiment (As_2S_3) and/or realgar (AsS) (Battaglia-Brunet et al., 2012; Newman et al., 1997; Onstott et al., 2011b; Xia et al., 2014; Xu et al., 2011a). Many bacteria can precipitate arsenosulphides including dissimilatory arsenate reducing (Newman et al., 1997), sulphate reducing bacteria (Jong & Parry, 2003; Luo et al., 2008; Teclu et al., 2008) and iron-reducing bacteria (Lee et al., 2007; Lim et al., 2008). Newman et al. (1997) demonstrated both intra- and extracellular bioprecipitation of orpiment particles, under sulphate-reducing conditions. They also suggested that the orpiment stability is dependent of small changes in pH and sulphide, and its precipitation is also dependent on the rate and extent of As(V) and sulphate reduction by a given microorganism. Microbial arsenate reduction may lead to arsenic removal by bio precipitation (sufficient sulphide) or its dissolution and enhanced mobility (insufficient sulphide). O'Day et al. (2004) through his reaction path model suggested that realgar (AsS) precipitates first in high- sulphate, iron reducing environment while orpiment

(As₂S₃) will be the second dominant form in low-iron environment, due to the absence of effective H₂S buffering. Teclu et al. (2008) observed a decrease in the dissolved arsenic availability due to formation of an arsenic sulphide precipitate. The biogenic sulphide was produced as a result of metabolic activity of the SRB and its interaction with the dissolved arsenic species.

Battaglia-Brunet et al. (2012) reported arsenic removal orpiment precipitation from acidic waters, in a glycerol and hydrogen fed fixed bed bioreactor using SRB containing mixed microbial consortium. They observed that excess sulphide induces orpiment dissolution in the reactor when reactor was fed with hydrogen instead of glycerol. The predominating bacterial genera in the reactor was *Desulfosporosinus* which is known to use As(V) and sulphate as a respiratory electron acceptor. Xia et al. (2014) reported arsenic bioremoval as arsenosulphides precipitation under autohydrogenotrophic conditions in batch studies conducted with synthetic groundwater. In their study they used anaerobic sludge as inoculum, collected from anoxic pond a sewage treatment plant. They also observed optimum pH ranges of 6.5-7.0 and temperature of 30-40°C for As(V) removal. Biogenic realgar and orpiment formation was observed in anaerobic granular biofilm batch reactors, when operated at pH conditions ranging from 6.1 to 7.2 in Fe-poor environments. In ethanol fed batch reactors, which were amended with As (v) and sulphate, the biogenic minerals were formed as a result of combined As(v) and sulphate reduction (Rodriguez-Freire et al., 2014). More recently Drewniak et al. (2015) reported the self cleaning of arsenic contaminated drinking water source by *Shewanella* sp. as (As₂S₃) bio precipitation, which also enhanced sorption of arsenic by the microbial mats.

Interaction between Biogenic Sulphide Phases and Its Role in Arsenic Sequestration

The importance of microbial iron and arsenic sulphide phases in combination on arsenic regulation is well established in anoxic environments. The association of pyrite and arsenic is apparent because it favours arsenic precipitation as arsenopyrites (FeAsS) and orpiment (Bostick & Fendorf, 2003). Selective extraction also suggested that formation of FeAsS occurs on FeS and FeS₂ mineral Diaz and Morse, 1992; Cooper and Morse, 1996). Mackinawite is also capable of arsenic reduction, as As(III) is known to get reduced to an As-S mineral in the presence of mackinawite (Gallegos et al., 2008; Gallegos et al., 2007). Kirk et al. (2010) suggested, in a reducing system containing iron,

arsenic, and sulphate, the difference in the solubility of iron and arsenic sulphides results in the precipitation of iron sulphides, which govern the arsenic removal through adsorption and co-precipitation mechanisms.

Recently, Omoregie et al. (2013) suggested the formation of realgar-like surface precipitates on the surface of FeS or of arsenic sulphide mineral formation under prolonged sulphidogenic environments, which may lead to more efficient arsenic removal. Altun et al. (2014) also reported the arsenic precipitation as As_2S_3 and arsenic co-precipitation with FeS, FeS_2 or FeAsS as arsenic removal mechanisms in the AMD treating bioreactor.

2.5 Arsenic Containing Solids Treatment and Management

Drinking water treatment plants produce arsenic containing solid residuals (ACSR) after arsenic removal from the water which may contain concentrated amounts of arsenic. The lower arsenic MCL imposes stricter limits on the handling procedures and disposal of arsenic containing residuals. However, the possibility of arsenic leaching from the sludge/waste generated from the treatment processes is dependent on the type of removal mechanism and the ultimate sludge disposal method. The disposal options include land application, stabilization, cow dung, passive aeration systems, ponds, soil and landfilling (Clancy et al., 2013).

Only non-hazardous waste can be disposed of in municipal solid waste landfills (Itle, 2001). The characterization and toxicity testing of the ACSR are important, because disposal options and selection of treatment option are ruled by these two properties. Waste containing less than 41 mg/kg arsenic can be subjected to land with no limitations, while waste containing 75 mg/kg arsenic or less can be applied in limited quantities.

In developing countries, ACSRs are often disposed by mixing with livestock waste, incorporating wastes into construction materials and sometimes left open in nearby fields and ponds (Clancy et al., 2013; Sullivan et al., 2010). Mohapatra et al. (2008) observed only 10% volatilization and 32% leaching of arsenic in 40 days period when arsenic-bearing ferrihydrite (18.5 mg As/g) was mixed with cow dung. A recent study conducted with ACSRs of drinking water treatment in West Bengal (India), have been

shown that ACSRs mobilizes arsenic into the liquid phase (~5%) more than volatilization (0.02%) (Clancy et al., 2014).

In developed countries, ACSRs of water treatment systems are often disposed in municipal solid waste landfills. A number of materials have been used for arsenic stabilization to minimize the leaching from ACSRs which includes iron sulphate, lime, cement, concrete and polymeric matrices (Camacho et al., 2009; Leist et al., 2003). Arsenic leaching from stabilized wastes is affected by environmental factors such as pH, relative humidity, and wetting and drying cycles. In many developing countries, mixing of ACSRs from drinking water treatment with brick and road construction material is widely practiced.

Raghav et al. (2013) highlighted arsenic crystallization technology (ACT) as an effective and eco-friendly technology for stabilization of ACSRs generated during water treatment. The ACSRs are getting converted into minerals of high arsenic capacity and long-term stability in mature, municipal solid waste landfills. They included scorodite, arsenate hydroxyapatites, ferrous arsenates, and arsenated-schwertmannite as potential candidate minerals for ACT based on ease of synthesis, their applicability and arsenic leachability. Onstott et al. (2011b) examined the stability of Fe and As-bearing biogenic sulphides by long term (115 days) column leaching tests with aerobic groundwater. On the basis of laboratory and field studies, they reported that biogenic minerals were resistant to dissolution under aerobic conditions and will remain stable for many decades. Arsenic leaching from the iron rich sludges is favoured at high pH (alkaline) and low redox conditions. Shafiquzzaman et al. (2010) reported arsenic leaching was 35-45 times higher at high pH (pH 11) as compared to lower pH (pH 3) based on toxicity characteristic leaching procedure (TCLP) and pH leaching tests conducted with sludge's taken from laboratory scale As removal columns. As leached were below the TCLP limit from an initial concentrations of 1270 mg/kg, 705 mg/kg and 313 mg/kg of As in the three test sludge respectively. Ghosh et al. (2014) reported that there was no significant arsenic leaching from the arsenic containing residuals which were stored on the coarse-sand filters of a community-scale arsenic removal units in West Bengal, India. They monitored the groundwater quality of nearby wells for over four years and reported no further contamination of wells from small amount of arsenic leached through the filter.



CHAPTER 3

AIM AND SCOPES OF THE STUDY

Aim of study:

The primary aim of the present study is to develop a bioreactor system for simultaneous removal of arsenic, nitrate, iron and fluoride from groundwater at wide range of temperature to meet the drinking water standards, leaving a non-hazardous and stable solid waste.

Scopes of the Study:

The following scopes have been identified to achieve the above objective:

1. Collection and acclimatization of mixed bacterial consortia in presence of arsenic, nitrate and sulphate.
2. Batch shake flask studies (in *absence* and *presence* of iron) to evaluate the efficiency of acclimatized mixed bacterial culture on simultaneous removal of pollutants.
3. Fabrication and performance evaluation of two semi-batch bioreactors (SmBRs) on simultaneous removal of pollutants, in *absence* (SmBR-1) and *presence* (SmBR-2) of iron.
4. Collection, characterization and performance evaluation of waste activated carbon (WAC) on arsenic adsorption from simulated groundwater in absence of iron.
5. Fabrication of two laboratory scale biological attached growth reactors (AGRs) using WAC as the packing material for simultaneous removal of target pollutants arsenic, nitrate and fluoride in absence (AGR-1) and presence of iron (AGR-2). The bioreactors will have multiple sampling ports along the depth of the beds for profile sampling to understand the terminal electron accepting process (TEAP).

6. Optimization of bioreactor process parameters such as empty bed contact time (EBCT), backwash frequency and electron donor.
7. Performance evaluation of AGR-1 on simultaneous removal of pollutants *in absence of iron* at varying feeding and operating conditions.
8. Performance evaluation of AGR-2 on simultaneous removal of pollutants *in presence of iron* at varying feeding and operating conditions.
9. Collection, characterization and treatment of arsenic contaminated real groundwater in the developed AGR systems.
10. Characterization of AGR treated water through “chemical analysis”, “Whole Effluent Toxicity (WET)” and “Most Probable Number (MPN)” tests.
11. Collection, preparation, characterization and performance evaluation of an adsorbent from residues of a water treatment plant (WTR) on fluoride removal from AGR treated water to evaluate its potential as a post treatment unit.
12. Microbial population diversity analyses of bacterial species present in the AGRs.
13. Characterization of biosolids of SmBRs and AGRs through FESEM/EDX, XRF, XRD, TEM and XAS analysis to understand the mechanisms of arsenic removal in absence and presence of iron.
14. Stability check of the biosolids and the spent WAC under aerobic as well as anoxic conditions through “Ageing test”, “Toxicity Characteristics Leaching Procedure (TCLP) test” and “Long Term Leaching test”.

CHAPTER 4

MATERIALS AND METHODS

In this section various materials and equipment used and different methodologies exercised in the present investigation are described.

4.1 Materials

All the glassware used in this study was of Borosil and plasticware was of Tarson products. Double distilled water or milliQ water was used to prepare all the reagents. The glassware used in this study was kept immersed overnight in chromic acid solution (2.25 g $K_2Cr_2O_7$ and 20 ml concentrated H_2SO_4 per litre of distilled/milliQ water) followed by washing with tap water and then distilled/milliQ water. Cleaned glassware was kept in oven for drying at 70-75°C for about 4 hours before being used for any experiment. Glassware was autoclaved as and when it required. All the chemicals used were either of analytical reagent (AR) or laboratory reagent (LR) grades. Sodium arsenate ($Na_2HAsO_4 \cdot 7H_2O$; 98.5% assay) and sodium nitrate ($NaNO_3$; 99% assay) used in the study were of AR grade and procured from Hi-media (India) and Sigma Aldrich, USA, respectively. HPLC grade (99.5% purity) acetone and ethanol were used as solvent during mineralogical analysis of backwash solids. Several instruments and equipments were used in this project work are given in Table 4.1.

Table 4.1 Instruments and equipment used in the present investigation.

Instrument/ Equipments	Parameters tested/measured	Model/ Manufacturer/ Specification
Magnetic Stirrer	Mixing	SPINIT ML 02, Tarsons, India
Autoclave	Sterilization	Equitron , Medica Instrument Co., India
COD Digester	COD	Hach DRB 200, Hach, USA
Digital Nephelo-Turbidity Meter	Sulphate	132, Systronics , India
DO meter	DO measurement	DO 32 A, DKK-TOA Corporation, Japan
Hot air oven	Drying , MLSS	ICT, Calcutta, India
Electric Muffle Furnace	MLVSS	ICT, Calcutta, India
pH meter	pH	Systronics μ pH system, India
Centrifuge	Remove settleable solids	R-24 REMI, Mumbai, India
Shaking incubator	For mixing and temperature control	Labtech, LSI-100 SR, Korea
Weighing balance	Weight	SL-234, Denver Instrument
BOD Incubator	For MPN test	ICT, Calcutta, India
Laminar flow	For MPN test	CLEANAIR SYSTEMS, Chennai, India
Refrigerator	For sample preservation	MRC Scientific instruments, India
Peristaltic pump	Feeding in to bioreactor	Miclins India Limited
Temperature controlled water bath	Maintain constant temperature	LAUDA, ALPHA RA 8, USA
Field Emission Scanning electron microscope	For images of bacteria and WAC particles	Zeiss, Sigma, Germany
Transmission electron microscope	For biosolids characterization	JEOL, JEM- 2100Plus, Japan
Atomic absorption spectrophotometer	Arsenic measurement	SpectrAA 55B, Varian
UV-Visible spectrophotometer	Nitrate measurement	CARY50BIO, Varian

4.2 Waste Activated Carbon (WAC)

WAC granules were obtained from house hold water purifiers. KENT RO Systems limited, India, marketed water purifier with the brand name of KENT ULTRA in India. These days hospitals, households, commercial and educational institutes are commonly

using such type of water purifiers to purify tap water. This type of a water purifier generally contains 200-300g activated carbon depending upon its size and capacity. The grain size of waste activated carbon is around 2 mm. After its useful life of about 6 months to 1 year, the exhausted activated carbon is replaced with fresh activated carbon. The exhausted activated carbon become a waste which, was collected and used as supporting material for biomass growth in flow through bioreactors used in this project. The collected carbon granules were washed by rinsing twice with deionized water and overnight oven drying at 70°C before use to eliminate previous contamination with organic matter which could have been attached on the surface of the granules. The carbon granules were then sieved through 2 mm and retained on 1.5 mm. The WAC granules were autoclaved (20 min, 121°C) to remove any possible microbial contamination prior to use as bio-support material in the AGRs. Approximately, 203 g of WAC was put inside the reactor to occupy 17 cm of bed height.

4.2.1 Microscopic Analysis of WAC

The dried waste activated carbon (WAC) granules were subjected to FESEM/EDX analysis prior to inoculation. Similarly, WAC granules harbouring biofilms were carefully taken from the attached growth reactor (AGR) and analysed for the presence of microbial biofilm. The biofilm cells were fixed with 1.25% glutaraldehyde and 1.3% osmium tetroxide. After that cells were dehydrated using a graded series of ethanol solutions, and finally dried. The resultant specimen was mounted on aluminium stubs and then coated with gold using sputter coater (Edward, UK). The specimen was then observed under an S4500 FESEM (Hitachi).

4.2.2 Bulk Density of WAC

Bulk density of WAC was determined to estimate the packing volume in column studies as described (CEFIC, 1986). A dry, clean and graduated measuring cylinder and an aluminium plate were each weighed. The volume of the sample was determined with a graduated cylinder (50 ml). WAC was put into the cylinder and reweighed. The WAC granules were transferred into an aluminium plate and put into an oven so as to dry it to constant weight at a temperature of 105°C for one hour. The bulk density (D_b) was calculated using the following expressions and given in gm/cm^3 .

$$D_b = M / V \quad \dots \quad \text{Eqn. (4.1)}$$

Where,

M = Mass of WAC (gm).

V = Volume of the WAC, measured under test conditions (ml).

4.2.3 Evaluation of WAC Adsorption Capacity on Arsenic Removal

Characterization of waste activated carbon (WAC) and its adsorption behaviour on removal of arsenic from simulated groundwater in absence of iron was evaluated. The experiment was carried out at constant temperature of 30°C at 150 rpm. The pH of the solution was maintained at 7.00±0.10 and the adsorbent dose was kept 2.0 g/L.

4.3 Analysis of Liquid Samples

In this section, different analytical techniques and methodologies used for the present investigation have been described. In general, standard techniques as described in Standard Methods for the Examination of Water and Wastewater (APHA, 2005) has been followed unless otherwise specified. pH was measured using a digital pH meter with a sensitivity of 0.01 with temperature correction facility. The instrument was calibrated periodically with standard buffer solutions. Chemical oxygen demand (COD) of samples was measured by closed refluxed method. Digestion was carried out using a COD thermoreactor fitted with temperature controller and timer. Quantification of biomass in mixed culture samples was done by measuring its concentration and expressed as mg/L of mixed liquor suspended solids (MLSS) and/or mixed liquor volatile suspended solids (MLVSS). Nitrate was measured by colorimetric method using a UV-Visible spectrophotometer. Sulphate concentration in aqueous samples was measured following turbidimetric method using a nephelo turbidity meter. Fluoride measurements were done by SPADNS colorimetric method. Iron content was determined in a spectrophotometer by following phenanthroline method and/or in an AAS.

Aqueous samples were analysed for total arsenic concentrations in an atomic absorption spectrophotometer (AAS) equipped with a vapour generation assembly (VGA-77) in the form of As(III) with an electrodeless discharge lamp as the radiation source at a wavelength of 193.7 nm. Before estimation of arsenic concentrations in the samples, both the standards and samples were treated with 1(M) HCl and ensured that any analyte

present as As(V) is reduced to As(III) as arsine gas, by the action of potassium iodide at a concentration of 1% w/v. The reduction completes in about 50 minutes at room temperature. Necessary amount of distilled water was added to the standards and the samples to produce appropriate dilution and arsenic concentrations of the solutions were quantified using AAS. Arsenic concentrations of the solutions were estimated according to the guideline of AAS user manual. Collected samples for arsenic analysis were filtered through 0.2 mm filters (GE health care, UK) and stored at 4°C before being analysed in AAS. Unfiltered samples were also analysed to know the total arsenic concentration.

Standard calibration curves prepared for nitrate, sulphate, fluoride and iron are shown in Figure A1, A2, A3, and A4, respectively in the Appendix.

4.4 Experimental Methodologies

4.4.1 Seed sludge and Its Acclimatization in Reactor BR-0

A glass aspirator bottle of 2.0 L capacity with 1.0 L working volume was used as reactor (BR-0) for the purpose to prepare acclimatized seed sludge. Biomass used as seed sludge for the present study was mainly the bio sludge collected from the bottom of the wastewater treatment plant of IIT Guwahati (Figure A5, appendix). The sludge of 0.75 L (MLSS: 3780 mg/L and MLVSS: 2560 mg/L) was mixed with small amount of (< 5% as MLSS) biosolids collected from two nos. laboratory scale bioreactors treating perchlorate and nitrate (Ghosh, 2013) and sulphate (Brahmacharimayum, 2014) respectively. The mixed bacterial biomass thus prepared was fed with contaminated drinking water spiked with 200 µg/L of arsenic, 50 mg/L of sulphate and nitrate and other macro and micronutrients as given in Table 4.2. The composition given in Table 4.2 is considered as simulated groundwater for the entire project. The bicarbonate alkalinity added in the reactor was to maintain pH of the content near to 7.0. Nitrogen gas was supplied intermittently to remove DO, if any, present in the reactor. One third of the supernatant was replaced by fresh medium in every 7 days cycle. The performance of seed sludge was analyzed on the same day. The mixed microbial culture was then acclimatized, over a period of 35 days.

4.4.2 Experimental Set-up and Bio-reactors

The experimental works carried out in different laboratory scale reactors are broadly grouped in to two categories viz., the reactors operated in absence of iron, and the reactors operated in presence of iron (in the contaminated water). A series of experiments were carried out with the acclimatized sludge in batch and semi batch modes of operations with the aim to evaluate their performance at different initial arsenic and nitrate concentration, in absence as well as presence of iron. Experiments in semi batch mode were also carried out at different hydraulic retention time (HRT) supplemented with a variety of carbon sources. In all the cases the pH was maintained at 7.0 ± 0.2 . Studies in semi batch mode were carried out at room temperature. In this section, detailed description of the procedures followed for various experiments, experimental set-up, specification and feeding and operating conditions of various reactors used in this project are given.

Table 4.2 Composition of feed of synthetic groundwater and trace mineral solution.

Component	Concentration (mg/L)	Trace mineral solution**	
		Component	Concentration (mg/L)
NaNO ₃ (as NO ₃ ⁻)	50-250 [#]	ZnSO ₄ ·7H ₂ O	100
Na ₂ SO ₄ (as SO ₄ ²⁻)	25-75 [#]	MnCl ₂ ·4H ₂ O	30
Na ₂ HAsO ₄ ·7H ₂ O (as As)	0.2-1.5 [#]	H ₃ BO ₃	300
NaHCO ₃ (as HCO ₃ ⁻)	25-45 [#]	CoCl ₂ ·6H ₂ O	200
K ₂ CO ₃ (as CO ₃ ²⁻)	1.5	CuCl ₂ ·2H ₂ O	10
NaCl (as Cl ⁻)	13.1	NiCl ₂ ·6H ₂ O	10
CaCl ₂ (as Cl ⁻)	13.1	Na ₂ MoO ₄ ·2H ₂ O	30
MgCl ₂ ·6H ₂ O (as Cl ⁻)	13.1		
H ₃ PO ₄ (as P)	0.5		
CH ₃ COOH (as C)	35-90 ^{#*}		
FeCl ₂ (as Fe ²⁺)	2-10 [#]		

Variable

* Different carbon sources were used.

** 1.0 ml of this solution was added in 10 L of water.

4.4.3 Batch Studies

4.4.3.1 Adsorption Studies in Batch Shake Flasks

Studies were conducted to assess the removal of arsenic by mixed bacterial seed sludge through adsorption from 500 µg/L of arsenic spiked in distilled water as well as simulated groundwater (excluding iron and sulphate) as given in Table 4.2. In both the cases 100 mg/L of acclimatized seed sludge, measured as MLVSS, was added in a series of 250 ml conical flasks with working volume of 100 ml. The purpose of conducting experiment on arsenic spiked distilled water was to eliminate the effects of the other ions present in simulated groundwater. The purpose of conducting experiments with simulated groundwater excluding iron and sulphate was to assess the arsenic adsorption efficiency of the seed sludge excluding the possibility of removal as any precipitates, as there is a possibility of formation of arsenosulphides (Battaglia-Brunet et al., 2012) and/or co-precipitation with sulphides of iron (Altun et al., 2014). To assess the loss due to adsorption by the flask material and/or volatilization, a blank containing arsenic spiked simulated groundwater (excluding iron and sulphate) without any seed sludge was also run.

4.4.3.2 Bio-removal Studies in Batch Shake Flasks

Batch studies were carried out in an incubator shaker at pH 7.0±0.2, 120 rpm, and 30°C in a series of shake flasks (High density polyethylene Erlenmeyer flasks) of 250 ml capacity containing 100 ml of media, 100 mg/L (as MLVSS) biomass and acetate as carbon source. Amount of carbon source added was calculated based on the stoichiometric requirement for all the electron acceptors (nitrate, arsenate and sulphate), assumed average biomass yield (0.4 g MLVSS/g COD utilized) and a safety factor of 1.5. The mouth of each of the flasks was sealed with a butyl rubber cork with the provision to supply nitrogen gas. The outer surfaces of the flasks were wrapped with aluminium foils to prevent algal growth. After addition of reactants, the flasks were purged with nitrogen gas from a nitrogen cylinder for about 10 minutes to expel out dissolved oxygen, if any, from the liquid. All experiments were conducted in triplicate and average values were used in data analysis. The screw capped flasks were sealed with parafilm after nitrogen purging and shaken for seven days. Samples were collected at an interval of 24h in self scarifying mode. The contents were centrifuged and analyzed for residual arsenic, nitrate,

sulphate, iron (in case of iron addition), COD, MLSS, MLVSS and pH. Simulated groundwater with the composition given in Table 4.2, was added into the flasks with sterile syringes and the following experiments were carried out:

Batch studies in absence of iron:

Effects of initial arsenic concentration:

Effect of initial arsenic concentration on the efficiency of the mixed culture was investigated with four different arsenic concentrations of 250 µg/L, 350 µg/L, 450 µg/L and 550 µg/L, maintaining sulphate and nitrate concentration of 25 mg/L and 50 mg/L respectively.

Effects of initial nitrate concentration:

The initial nitrate concentrations for this study were kept as 50 mg/L, 100 mg/L and 150 mg/L. The arsenic and sulphate concentration was kept constant at 500 µg/L and 25 mg/L respectively.

Batch studies in presence of iron:

Similar studies were carried out in batch mode in presence of iron. In addition to the studies carried out in absence of iron (i.e., effects of initial arsenic and nitrate concentrations), effects of initial iron concentration, was also investigated.

Effects of initial iron concentration:

The batch studies with iron concentration of 1, 2, 3, 4 and 5 mg/L was done to assess the iron as well as arsenic removal capacity of the mixed culture. During this study the initial arsenic, nitrate and sulphate concentration was kept at 500 µg/L, 50mg/L and 25 mg/L respectively.

Effects of initial arsenic concentration:

Effect of initial arsenic concentration on the efficiency of the mixed culture was investigated with arsenic concentrations of 500 µg/L, 600 µg/L, 750 µg/L and 1000 µg/L, maintaining iron, sulphate and nitrate concentration of 3 mg/L, 25 mg/L and 50 mg/L respectively.

Effects of initial nitrate concentration:

Effect of initial nitrate concentration of 50 mg/L, 100 mg/L and 150 mg/L on arsenic removal efficiency was also investigated in batch studies. The iron, arsenic and sulphate concentration was kept constant at 3 mg/L, 1000 µg/L and 25 mg/L respectively.

4.4.4 Semi-Batch Reactors (SmBR-1 & SmBR-2)

Feeding and operating conditions of the reactors (each of 1 L capacity, 600 ml working volume, polypropylene reagent bottles) used in this project operated in semi-batch mode in absence (SmBR-1) and presence of 2 mg/L of iron (SmBR-2) in the contaminated water are listed in Table 4.3 and 4.4, respectively. Both the reactors were of anaerobic suspended growth type operated at room temperature ($30\pm 4^{\circ}\text{C}$), inoculated with mixed bacterial population (MLVSS: 1150 mg/L) that was acclimatized in BR-0. The schematic representation of SmBR reactors set up used in this study is shown in Figure 4.1. Before inoculation, the reactor content was deoxygenated by supply of nitrogen gas.

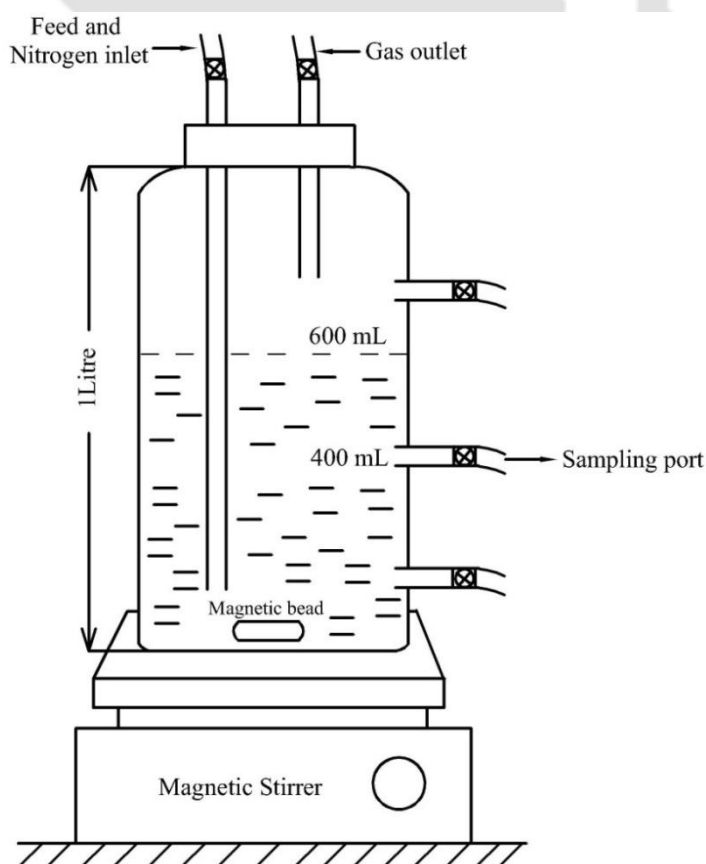


Figure 4.1 Schematic diagram of semi-batch reactor set-up.

A heater was used to increase the room temperature ($30\pm 4^\circ\text{C}$) during winter. The reactors were filled up with 600 ml of fresh simulated groundwater, which in this project refers to as medium. They were sealed, covered with black film to prevent any activity of phototrophic bacteria and algal growth before being mounted on magnetic stirrers. Initial concentration of arsenic, nitrate and sulphate in both the reactors were maintained at 200 $\mu\text{g/L}$, 50 mg/L and 25 mg/L respectively. The dose of carbon source was supplemented more than the stoichiometric requirement of all electron acceptors present in the feed. Both the reactors were operated at an HRT of 3 days except during first 34 and 40 days of SmBR-1 and SmBR-2 operation respectively, when the HRT was of 6 days. HRT of 6 day was maintained by removal of 200 ml of the supernatant (treated water after settlement of biomass) at an interval of 2 days and replacing the equal volume of untreated water. Similarly HRT of 3 day was maintained by replacing 200 ml of the supernatant daily. The reactors were allowed to stand for 20 min without mixing, to allow biomass settling to prevent any loss of biomass during effluent collection. The effluent was directly collected in Erlenmeyer flasks which were made anoxic by purging nitrogen gas from a nitrogen gas cylinder and analysed for nitrate, arsenic, sulphate, COD and pH. The experiments carried out in both the reactors are explained below.

Operation of SmBR-1

After inoculation, the SmBR-1 was operated at 6 days HRT for first 34 days. Then after, the following experiments were carried out in semi batch mode at 3 days HRT:

Effects of initial arsenic concentration:

In order to evaluate the effect of arsenic concentration on its removal, the arsenic concentration in the feed was increased stepwise from 200 $\mu\text{g/L}$ to 300 $\mu\text{g/L}$, 400 $\mu\text{g/L}$, 500 $\mu\text{g/L}$, 600 $\mu\text{g/L}$, 700 $\mu\text{g/L}$ and 800 $\mu\text{g/L}$.

Effects of initial nitrate concentration:

The effect of nitrate concentration on reactor performance in terms of nitrate and arsenic removal was evaluated at stepwise increasing influent nitrate concentration of 50 mg/L , 100 mg/L , 150 mg/L , 200 mg/L and 250 mg/L .

Effects of various carbon sources:

The performance of SmBR-1 on removal of arsenic and nitrate was evaluated by using different carbon sources as electron donor. The effectiveness of acetate, malate, succinate, lactate and glucose as the sole sources of carbon and energy were tested.

Operation of SmBR-2

After inoculation, the SmBR-2 was operated at 6 days HRT for first 40 days. Then after, the SmBR-2 was operated at HRT of 3 days to evaluate the followings.

Effects of initial arsenic concentration:

In order to evaluate the arsenic removal efficiency of mixed culture, arsenic concentration in the feed was increased stepwise from 250 µg/L to 350 µg/L, 450 µg/L, 550 µg/L, 750 µg/L and 1000 µg/L.

Effects of initial nitrate concentration:

The effect of initial nitrate concentration on reactor performance in terms of nitrate and arsenic removal was evaluated by stepwise increasing the influent nitrate concentration from 100 mg/L to 150mg/L, 200mg/L and 250 mg/L.

Effects of various carbon sources:

The performance of SmBR-2 was evaluated using various carbon sources such as acetate, malate, succinate, lactate and glucose.

Table 4.3 The operational schedule of semi batch reactor (SmBR-1) operated in absence of iron.

Purpose of operation	Days of operation	HRT (Days)	Influent characteristics		
			Arsenic ($\mu\text{g/L}$)	Nitrate (mg/L)	COD (mg/L)
(Phase-1) Effect of HRT	1-34	6	200	50	107
	35-56	3			
(Phase-2) Effect of initial arsenic concentration	35-56	3	200	50	107
	57-79		300		
	80-101		400		
	102-124		500		
	125-146		600		
	147-168		700		
	169-191		800		
(Phase-3) Effect of initial nitrate concentration	192-213	3	600	50	107
	214-235			100	150
	236-257			150	194
	258-279			200	240
	280-301			250	285
(Phase-4) Effect of carbon source	Acetate	302-332	600	200	240
	Malate	333-365			
	Succinate	366-396			
	Lactate	397-427			
	Glucose	428-459			

Sulphate concentration in feed was 25 mg/L for entire SmBR-1 operation

Table 4.4 The operational schedule of semi batch reactor (SmBR-2) operated in presence of iron.

Purpose of operation		Days of operation	HRT (Days)	Influent characteristics		
				Arsenic ($\mu\text{g/L}$)	Nitrate (mg/L)	COD (mg/L)
(Phase-1) Effect of HRT		1-40	6	250	100	150
		41-69	3			
(Phase-2) Effect of initial arsenic concentration		41-69	3	250	100	150
		70-90		350		
		91-112		450		
		113-134		550		
		135-156		750		
		157-178		1000		
(Phase-3) Effect of initial nitrate concentration		157-178	3	1000	100	150
		179-201			150	194
		202-223			200	240
		224-244			250	285
(Phase-4) Effect of carbon source	Acetate	224-244	3	1000	250	285
	Malate	245-275				
	Succinate	276-307				
	Lactate	308-338				
	Glucose	339-369				

Iron and sulphate concentration in feed was 2 mg/L and 25 mg/L respectively for entire SmBR-2 operation

4.4.5 Flow through Reactors (AGR-1 and AGR-2)

Two nos attached growth reactors (AGR), designated as AGR-1 & AGR-2, were fabricated with transparent perspex cylinders with waste activated carbon as supporting material for the growth of bacterial species on their surface to assess the performance of the mixed microbial culture on multipollutants removal from groundwater, were operated in continuous (flow through) mode. These reactors were operated in down flow mode to treat groundwater in absence (AGR-1) and presence of iron (AGR-2), respectively at different feeding and operating conditions. Specification of both the reactors was the same having overall height of 32cm and internal diameter of 5cm. Schematic diagram and the actual photograph of the reactor with details of various components are shown in Figure 4.3a and 4.3b respectively (page 70). The specification is given in Table 4.5. Feeding and operating schedule of AGR-1 and AGR-2 at different phases are given in Table 4.6 (page 74-75) and 4.7 (page 78-79) respectively.

4.4.5.1 Reactor Configuration and Experimental Set-up

The following are the main components of the AGRs:

A) *Untreated water (feed) inlet and distribution system:*

For uniform and efficient distribution of feed, an L- shape tube was used. One end of the tube was vertically downward along the reactor and the other end was kept horizontal connected to the feed pumps.

Table 4.5 Specifications of AGRs.

Parameter	Specification
Material	Transparent Perspex tube
Height	32 cm
Inner-diameter	5 cm
Volume	628 cm ³
Packed bed volume	333 cm ³
Fixed bed height	17
Packing media	WAC
Waste activated carbon (WAC)	Passed through 2 mm and retained on 1.5 mm size sieves

B) Raw water flow regulation system:

Peristaltic pumps (Model: PP10, Miclins India) were used to regulate the influent flow rate in AGR systems. Flow rate maintained for empty bed contact time (EBCT) of 90, 60, 45 and 30 min. were 3.7, 5.6, 7.4 and 11.0 ml/min. respectively. EBCT calculation was made based on packed volume of reactor. In addition to peristaltic pumps a syringe pump (Model: SP10, Miclins India) was used to feed iron solution to the AGR-2 so that the carbon source (acetic acid) and Fe(II) supply could be varied independently and without any interference. The iron stock solution was loaded into a syringe by filtering through a 0.2 μm filter. The syringe was placed on the syringe pump and the iron solution was pumped into the reactor.

C) Screens:

Two nos. perforated (about 70% perforation, 1 mm diameter holes) circular perspex discs of 5 cm diameter (equal to the internal diameter of the main reactor) were placed at the top and the bottom of the reactor bed (Fig. 4.2a). The purpose of the bottom perforated disc is to support the WAC granules from being washed out along with the treated water. The purpose of the top perforated disc was to prevent WAC from being washed out during backwashing as well as to help raw water distribute more uniformly throughout the cross section of the reactor.

D) Deflector beam:

A hollow perspex disc, with external diameter of 5 cm (same as the internal diameter of the main reactor) and internal diameter of 2.5 cm, tapered from the outside was fitted inside the main reactor, at a depth of 11cm from the top, was used as deflector beam (Fig. 4.2b).

E) Sampling Ports:

Five nos. sampling ports (namely P1 to P5) were provided for collection of samples at different depths of the reactor at centre to centre distance of 3 cm starting from 15 cm from the top. The ports were kept closed with metallic lab clips except during sampling.

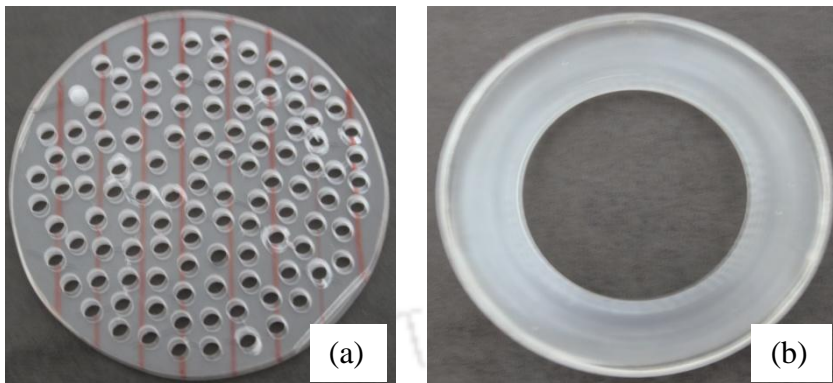


Figure 4.2 Photographs of a screen (a) and deflector beam (b) used in the reactor.

F) Backwash outlet and effluent port:

An outlet was provided above the top normal water level in the reactor during operation, as effluent port as well as to remove backwash solids.

G) Biogas release system:

The gas release system adopted in this study consisted of 2 nos. conical flasks of 250 ml capacity. The biogas from a reactor was first allowed to pass through an empty conical flask and then through the other, partially filled up with acidified water, before being released into the atmosphere. The system prevents contamination of the reactor content from atmospheric gas as well as accidental mixing up of acidified water in the second flask with the reactor content.

H) Arrangement for temperature control:

The temperature inside the reactor was maintained between 20 ± 0.5 and $50\pm 0.5^{\circ}\text{C}$ during the study. Desired temperature with a variation of $\pm 0.5^{\circ}\text{C}$ was maintained by circulating warm water from a thermostat installed temperature controlled water bath (LAUDA, RA-8, Germany) through silicon pipes wrapped over the reactor throughout its depth.

I) Water level adjuster:

The reactor was connected to a water level adjuster to maintain a constant liquid level in the reactor.

J) Feed composition:

Simulated ground water spiked with varying concentration of pollutants such as arsenic, nitrate, fluoride, iron and sulphate supplemented with carbon source and mineral salt media (MSM) was used as feed for the AGRs. The composition of simulated groundwater is given in Table 4.2.



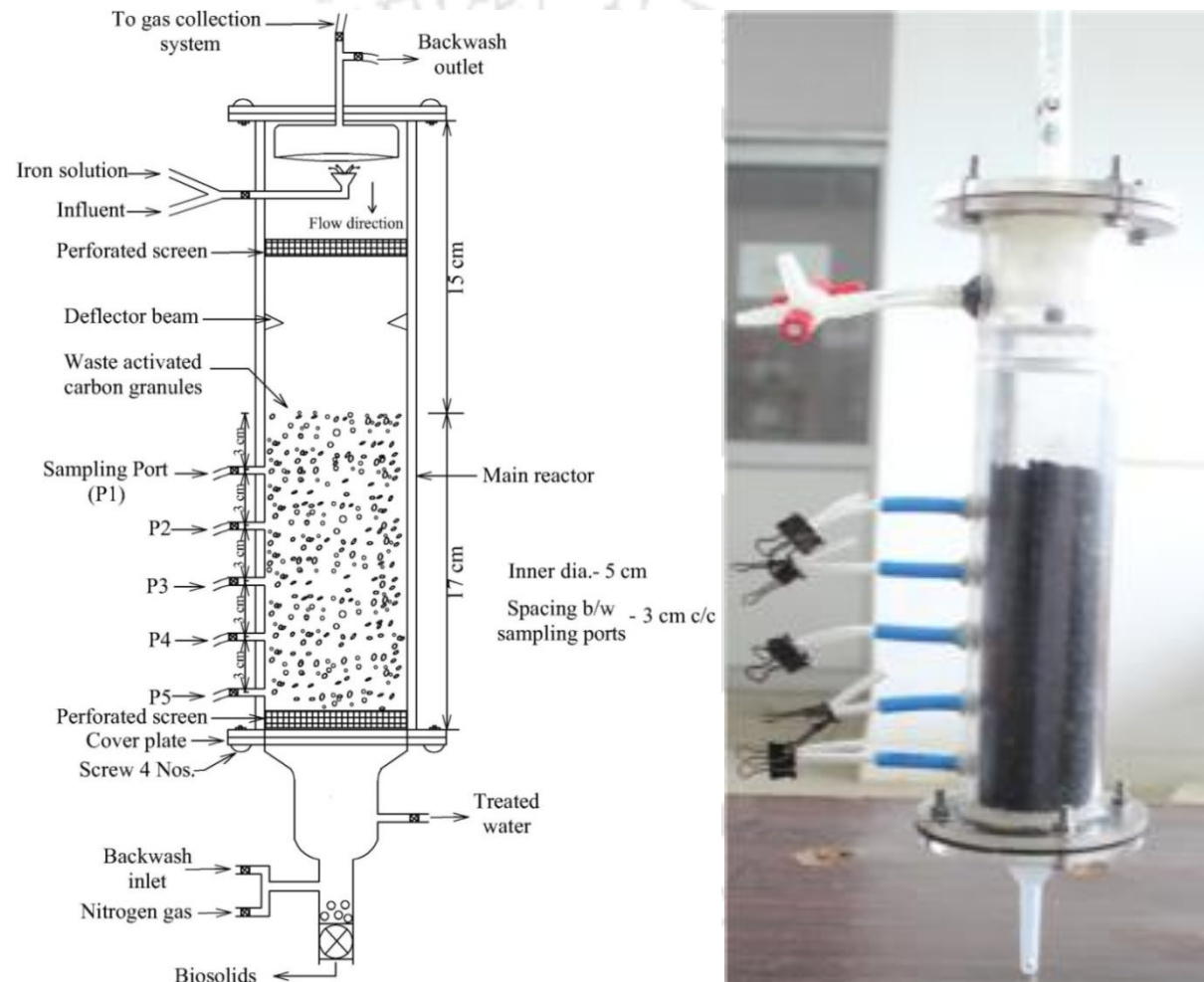


Figure 4.3 (a) Schematic diagram and (b) actual photograph of an attached growth reactor (AGR).

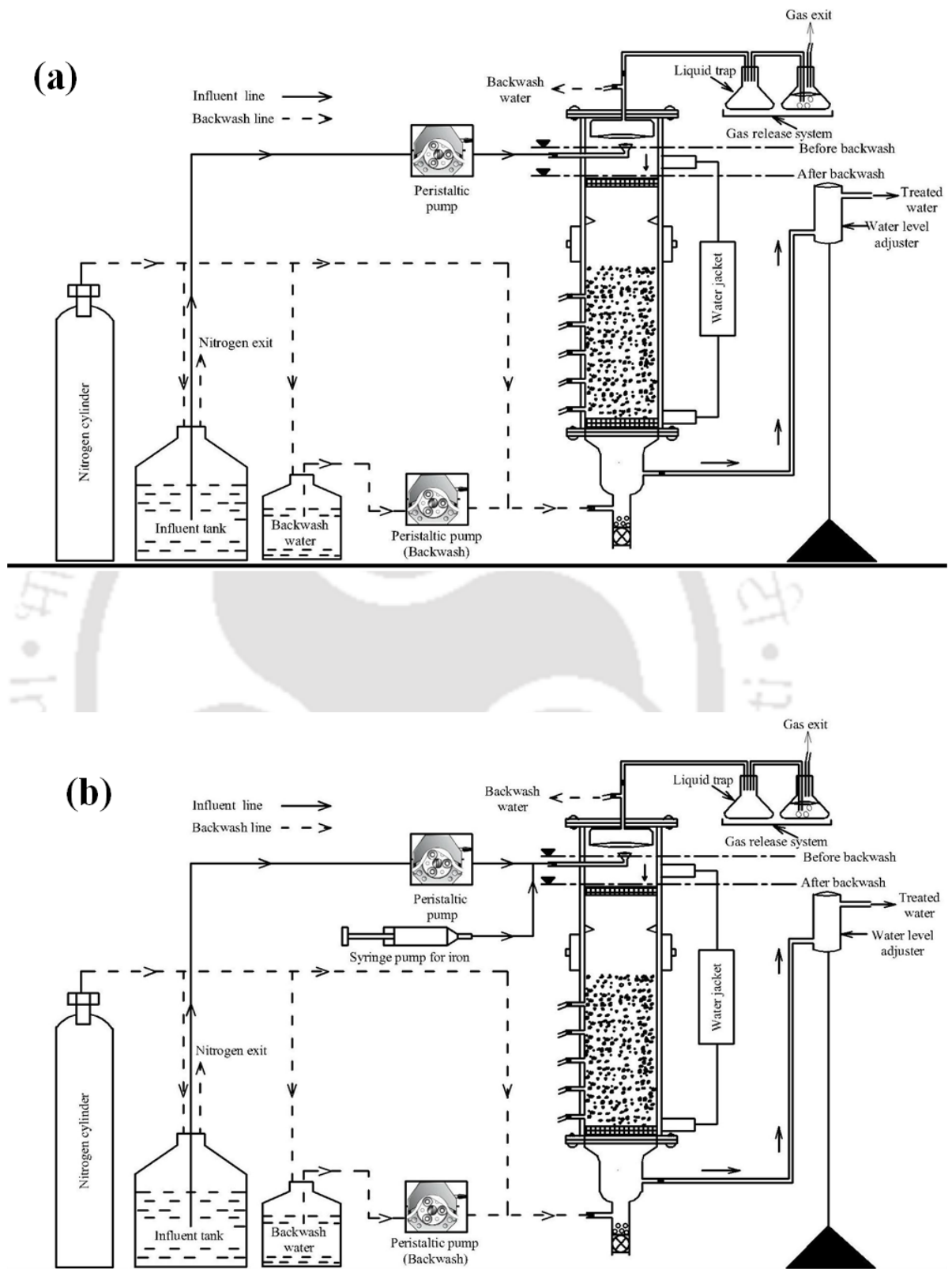


Figure 4.4 Lab scale schematic diagram of flow through reactors set-up AGR-1 (a) and AGR-2 (b).

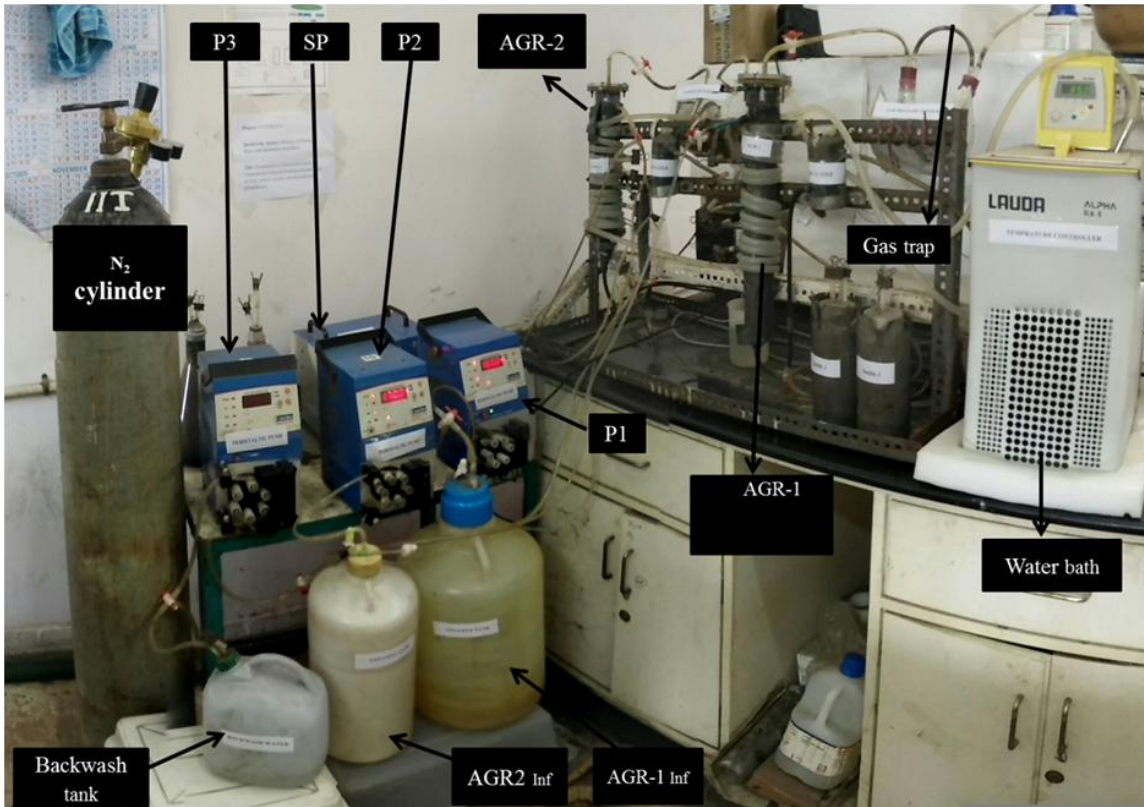


Figure 4.5 Photographs of the lab scale reactor set-up of flow through reactors AGR-1 and AGR-2.

4.5.2 Operation of AGR-1

4.5.2.1 Inoculation and Start-up of AGR-1

After inoculation with the acclimatized mixed bacterial consortia, during start-up the AGR-1 was purged with oxygen free N₂ gas for 30 minutes to establish anoxic conditions. The reactor was fed continuously with influent having 200 µg/L arsenic, 50 mg/L nitrate, 25 mg/L sulphate and 91 mg/L of COD as carbon source for 43 days maintaining an EBCT of 90 min. Any biomass washed out of reactor along with the effluent was recycled back. From 44th day the COD was increased to 105 mg/L on the basis of the performance of the reactor. All the subsequent experiments were performed with an addition of 105 mg/L of COD or higher. The overall operating schedule of AGR-1 is given in Table 4.6.

After start-up, AGR-1 was operated to evaluate its performance on arsenic, nitrate and/or fluoride removal efficiencies and effects of EBCT, initial arsenic, nitrate, pH,

temperature and fluoride. For discussion and better understanding, the whole reactor operation has been divided into the following eight phases:

4.5.2.2 Phase-1: Effects of EBCT and Backwash Frequency

The AGR-1 was operated at varying EBCT of 90, 60 and 45 min to get the optimum EBCT. EBCT was changed by adjusting influent flow rate to AGR-1.

Backwashing operation is necessary for effective removal of excess biomass sludge and biogenic precipitates which may lead to head loss development and clogging of WAC bed (Slavik et al., 2013). Backwashing reduces/minimizes the head loss development in the reactor which is an important consideration in AGR operation. Hence, backwashing of reactor was carried out regularly under mixed flow of deoxygenated-DI water (60 mL/min) and nitrogen gas to fully fluidize the WAC bed for 2-3 min followed by a flow of only (deoxygenated) DI water (500 mL/min) for 2-3 min to maintain the treatment efficiency. Performance of AGR-1 was evaluated at different backwash frequencies of 2, 3, 4 and 7 days starting from day 115 of reactor run. The backwash frequencies were selected based on previous findings where backwash frequencies of 1 to 7 days were practiced (Boller et al., 1997; Choi et al., 2007; Upadhyaya et al., 2010).

4.5.2.3 Phase-2: Effects of Influent Arsenic Concentration

In this phase of operation the AGR-1 was fed with influent containing varying arsenic concentration of 200, 250, 350, 450, 550, 650 and 750 $\mu\text{g/L}$. The reactor was operated at an EBCT of 45 min, nitrate 50mg/L, sulphate 25 mg/L and a carbon dose of 105 mg/L COD. At 750 $\mu\text{g/L}$ of influent arsenic concentration, the reactor performance was also evaluated at elevated dose of sulphate (50 mg/L) and longer EBCT of 60 min. The COD was kept 121 mg/L during this period of operation.

4.5.2.4 Phase-3: Effects of Influent Nitrate Concentration

In the 3rd phase of operation, the AGR-1 was fed with influent containing varying nitrate concentration of 50, 100, 150 and 200 mg/L. The reactor was operated at an EBCT of 45 min, arsenic 500 $\mu\text{g/L}$, sulphate 25 mg/L and a varying carbon dose as per the requirement for increased nitrate concentration. At 200 mg/L of influent arsenic concentration, the reactor performance was also evaluated at longer EBCT of 60 min.

Table 4.6 Operational schedule of AGR-1.

Purpose of operation	Days of operation	Influent characteristics				EBCT (Min.)	Remarks
		Arsenic ($\mu\text{g/L}$)	Nitrate (mg/L)	Sulphate (mg/L)	COD (mg/L)		
Start-up	1-43	200	50	25	91	90	
	44-114				105	90	First backwashing - day 49
(Phase-1) Effects of EBCT and backwash frequency	44-114	200	50	25	105	90	
	115-136					60	Backwash frequency 2 days
	137-168					45	Backwash frequency 3 days
	169-196						Backwash frequency 4 days
	197-231						Backwash frequency 7 days
(Phase-2) Effect of influent arsenic concentration	197-231	200	50	25	105	45	Profile sampling on day 228
	232-263	250					
	264-290	350					
	291-313	450					
	314-340	550					
	341-369	650					
	370-398	750					
	399-426	750					
	427-457	750					50
(Phase-3) Effect of influent nitrate concentration	458-480	500	50	25	105	45	Profile sampling on day 480
	481-510		100		150		Profile sampling on day 508
	511-541		150		194		Profile sampling on day 540
	542-572		200		240		Profile sampling on day 570
	573-604						60

(Phase-4) Effect of pH	605-637	500	50	25	105	45	pH = 6.6
	638-668						pH = 7.2
	669-699						pH = 8.4
(Phase-5) Effect of temperature (°C)	700-732	500	50	25	105	45	Temp.= 20°C
	733-763						Temp.= 30°C
	764-791						Temp.= 40°C
	792-839						Temp.= 50°C
	840-861						Temp.= 30°C
(Phase-6) Removal and effects of fluoride	862-896	500	50	25	105	45	5 mg/L of F ⁻ is introduced
(Phase-7) Performance at Low EBCT	897-934	500	50	25	105	30	
(Phase-8) Performance after shutdown	942-969	500	50	25	105	30	

* AGR-1 was operated at 30°C and pH of 6.8 throughout experiment except during effect of temperature and pH studies.

4.5.2.5 Phase-4: Effects of Influent pH

The normal range for pH in surface water systems is 6.5 to 8.5 and for groundwater systems 6.0 to 8.5 (Jordana & Piera, 2004). Although, microorganisms can grow in a wide range pH, their performance depends upon the pH at which they are subjected to. In the 4th phase, performance of the AGR-1 was evaluated by introducing influent of pH 6.5, 7.0 and 7.5. The pH was adjusted with varying sodium bicarbonate and potassium carbonate in the influent solution.

4.5.2.6 Phase-5: Effects of Operating Temperature

The change in temperature is one of the common diurnal and seasonal variable parameter of water. Temperature plays a key role in the selection of both the overall bacterial diversity present and the efficiency of the biological process. The impact of these variations with temperature-specific bacterial consortia on the efficiency of anaerobic water treatment remains unknown. The objectives of this study were to investigate the effects of temperature on the performance of the AGR-1. The AGR-1 was operated at 20°C, 30°C, 40°C and 50°C in phase-5. The reactor was operated at an EBCT of 45 min, arsenic 500 µg/L, nitrate 50 mg/L, sulphate 25 mg/L and COD of 105 mg/L. After the study at 50°C, the temperature was reduced to 30°C to bring back the AGR-1 in normal condition for future operation.

4.5.2.7 Phase-6: Effects of Influent Fluoride Concentration

The objective of this experiment was to evaluate the efficiency of the bioreactor on fluoride removal as well as its effects on removal of other pollutants. Fluoride of 5 mg/L was introduced into the AGR-1 for this purpose.

4.5.2.8 Phase-7: Performance at Low EBCT

AGR-1 was operated at lower EBCT of 30 min. in order to evaluate its effect on arsenic removal and overall performance of the reactor.

4.5.2.9 Phase-8: Performance After Shut down

In order to test the response of the bioreactor system to any emergent and/or accidental shutdown periods, the influent feed was stopped on day 935 and remained off for seven days. The reactor was restarted after a seven day shutdown and fed with influent arsenic 500 µg/L, nitrate 50 mg/L, and sulphate 25 mg/L, at an EBCT of 30 min.

4.5.3 Operation of AGR-2

4.5.3.1 Inoculation and Start-up of AGR-2

Inoculation of AGR-2 was done following the same procedure to that of AGR-1. The reactor was inoculated with the acclimatized mixed bacterial consortia (from BR-0) and the sludge from AGR-1 collected as backwash solids, purged with oxygen free N₂ gas for 30 minutes and recycled back the washed out biomass into the reactor with the help of a peristaltic pump. The reactor feed solution contained 250 µg/L of arsenic, 50mg/L of nitrate, 25 mg/L of sulphate and 2.0 mg/L of iron during the initial period of the start-up. The reactor was operated at 90 min EBCT with the addition of 115 mg/L of acetate as COD. Arsenic concentration in the influent was increased to 500 µg/L and EBCT was reduced to 45 minutes in the final stage of the start-up period. After start-up, AGR-2 was operated to evaluate its performance on iron, arsenic and/or nitrate removal as well as effects of influent iron, arsenic and nitrate concentrations, pH and temperature on its performance. The operating schedule of AGR-2 is given in Table 4.7.

For discussion and better understanding, the whole reactor operation has been divided into the following eight phases:

4.5.3.2 Phase-1: Effects of Influent Iron Concentration

The AGR-2 was operated at varying influent iron concentration of 2.0, 3.0, 4.0, 5.0, 7.5 and 10 mg/L at an EBCT of 45 min. Although influent arsenic of 500 µg/L and nitrate of 50 mg/L was kept constant, sulphate concentration was varied between 25 mg/L and 75 mg/L with the application of higher concentration with higher iron in the influent. As sulphide was thought to be the main agent for removal of arsenic either as arsenosulphide precipitate in absence of iron or through adsorption by iron sulphide that form in presence of iron, sulphate concentration was always added more than the stoichiometric requirement for the added iron in the influent for iron sulphide formation. Furthermore, COD was also increased from 105 mg/L to 134 mg/L to meet the requirement for additional added sulphate. Performance of the reactor fed with 10.0 mg/L of iron was also evaluated at EBCT of 90 min.

Table 4.7 Operational schedule of AGR-2.

Purpose of operation	Days of operation	Influent Characteristics					EBCT (Min.)	Remarks	
		Arsenic ($\mu\text{g/L}$)	Iron (mg/L)	Nitrate (mg/L)	Sulphate (mg/L)	COD (mg/L)			
Start up	1-58	250	2.0	50	25	115	90	Profile sampling on day 102	
	59-77	250				60			
	78-102	500	105	45					
(Phase-1) Effect of iron concentration	78-102	500	2.0	50	25	105	45	Profile sampling on day 181	
	103-125		3.0						
	126-154		4.0						
	155-181		5.0		50	50	121	60	Profile sampling on day 208
	182-208		5.0						
	209-233		7.5		75	134	90	Profile sampling on day 265	
	234-265		7.5		75				
	266-294		10.0		75				
	295-326		10.0		75	90	Profile sampling on day 326		
(Phase- 2) Effect of arsenic concentration	295-326	500	10.0	50	75	134	90	Profile sampling on day 382	
	327-353	750							
	354-382	1000							
	383-413	1250							
	414-444	1500							
(Phase- 3) Effect of nitrate concentration	414-444	1500	10.0	50	75	134	90	Profile sampling on day 474	
	445-474			100		179	90		
	475-505			150		225	90		Profile sampling on day 505
	506-533			200		270	90		Profile sampling on day 533
	534-561			270		120	Profile sampling on day 561		

(Phase- 4) Effect of pH	562-592	500	3.0	50	25	105	45	pH = 6.6
	593-623							pH = 7.2
	624-658							pH = 8.4
(Phase- 5) Effect of temperature (°C)	659-695	500	3.0	50	25	105	45	Temp. = 20°C
	696-726							Temp. = 30°C
	727-757							Temp. = 40°C
	758-792							Temp. = 50°C
	793-817							Temp. = 30°C
(Phase- 6) Operation with real groundwater	818-828	226	8.3	50	75	134	90	Profile sampling on day 839 Real groundwater pH-6.6
	829-836	295	13.2	50	75	134	90	
	837-856	295	13.2	50	100	150	120	
(Phase- 7) Performance at low EBCT	857-891	500	3.0	50	25	105	30	
(Phase- 8) Performance after shut down	899-926	500	3.0	50	25	105	30	

* AGR-2 was operated at 30°C and pH of 6.8 throughout the experiment except during effect of temperature and pH studies.

4.5.3.3 Phase-2: Effects of Influent Arsenic Concentration

In this phase of operation the AGR-2 was fed with influent containing varying arsenic concentration of 500, 750, 1000, 1250 and 1500 $\mu\text{g/L}$. The minimum concentration of 500 $\mu\text{g/L}$ was selected based on the performance of the reactor under lower arsenic concentration of influent arsenic. The reactor was operated at an EBCT of 90 min, nitrate of 50mg/L, sulphate 75 mg/L and a carbon dose of 134 mg/L COD and iron of 10.0 mg/L. EBCT of 90 minutes was selected based on the results of the previous studies on effects of iron concentration.

4.5.3.4 Phase-3: Effects of Influent Nitrate Concentration

In the 3rd phase of operation, the AGR-2 was fed with influent containing varying nitrate concentration of 50, 100, 150 and 200 mg/L. Influent iron, arsenic and sulphate concentration was kept constant at 10 mg/L, 1500 $\mu\text{g/L}$ and 75 mg/L, respectively. The reactor was operated at relatively longer EBCT of 90 min and 120 min, a varying carbon dose to match with the nitrate concentration was also maintained. The feeding and operating condition was changed based on the stoichiometric requirement as well as performance of the reactor in the previous condition. The influent COD of 134, 179, 225 and 270 mg/L was maintained for 50, 100, 150 and 200 mg/L of influent nitrate concentration respectively.

4.5.3.5 Phase-4: Effects of Influent pH

The objective of this study was to determine the effect of the pH on the removal of arsenic as biogenic sulphides formation in iron-rich environments. In order to achieve this objective, performance of the AGR-2 was evaluated by introducing influent of pH between 6.5 and 8.5 in the 4th phase of the reactor run. The pH was adjusted with varying sodium bicarbonate and potassium carbonate in the influent solution as done for AGR-1. The influent concentration of nitrate, sulphate, arsenic and iron was kept 50 mg/L, 25 mg/L, 500 $\mu\text{g/L}$ and 3 mg/L respectively.

4.5.3.6 Phase-5: Effects of Operating Temperature

The AGR-2 was operated at different temperature of 20°C, 30°C, 40°C and 50°C in final phase-5 to assess its performance on simultaneous removal of the target pollutants in presence of 3 mg/L of iron. After the study at 50°C, the temperature was reduced to

30°C to bring back the AGR-2 in normal condition for future operation with real contaminated groundwater.

4.5.3.7 Phase-6: Operation with Real Groundwater

The AGR-2 operation with arsenic contaminated real groundwater is discussed separately in section 4.6.

4.5.3.8 Phase-7: Performance at Low EBCT

AGR-2 was operated at lower EBCT of 30 min. in order to evaluate its effect on arsenic removal and overall performance of the reactor. The reactor was fed with influent arsenic 500 µg/L, iron 3.0 mg/L, nitrate 50 mg/L, and sulphate 25 mg/L.

4.5.3.9 Phase-8: Performance after Shut down

The AGR-2 performance was also assessed after a seven day shutdown periods similar to AGR-1. The influent feed was stopped on day 877 and remained off for 7 days. Throughout the AGR-1 operation, synthetic groundwater and nutrient solution were supplied to the bioreactor on nights, weekends and holidays. From days 935 to 941, the AGR-2 was shut down for seven days, during which no synthetic groundwater and nutrient solution were supplied to the bioreactor.

4.6 AGR-2 operation with Real Groundwater

To examine the efficiency of laboratory scale flow through reactors on the arsenic and iron removal, studies were conducted using real-life groundwater sample collected from the arsenic affected area. Real groundwater was collected from the well of two locations at (26°16.74'N and 90°40.79'E; 26°23.22'N and 90°43.47'E, depth of well 100 ft.) New Bongaigaon area, Assam (India) (Fig A6 and A7 appendix), where arsenic and iron concentrations were varied in the range of 20.5-300 µg/L and 8.0-14.0 mg/L respectively. For the present study, groundwater was sampled in February, 2015 at the end of the annual rainy season.

Groundwater collected after adequate purging (10-15 min.) were stored in pre-rinsed and pre-acidified (with HCl at pH 2) high-density polyethylene containers for metal analysis. The characterization of other water quality parameters is done with non-acidified groundwater sample which was also stored in high-density polyethylene container. The real groundwater quality parameters are given in Table 4.8. Containers were filled to overflowing and sealed with thread seal tape immediately to further

minimize introduction of oxygen. All groundwater samples was transported to the Environmental Engineering Laboratory, IIT Guwahati, with in 8 h and subsequently kept at 4°C until analysis. A multiparameter water quality monitoring system (Professional plus: YSI, USA) was used for onsite pH, ORP, DO and conductivity of the groundwater while a visual arsenic detection kit (Wagtech, UK) was used to determine onsite arsenic determination (Fig. A8 appendix)

Groundwater from one location was contaminated with arsenic of 226 µg/L and iron of 8.3 mg/L, which is designated as real groundwater type-1. The groundwater collected from another location (type-2) consists of 295 µg/L of arsenic and 13.2 mg/L of iron. AGR-2 was first fed with groundwater of type-1 before type-2. There was no nitrate or nitrite present in either groundwater but 3-4 mg/L of sulphate was present. AGR-2 was fed solely with type-1 real groundwater for 11 days except an addition of sulphate, nitrate and COD at the rate of 75 mg/L, 50 mg/L and 134 mg/L respectively. From day 829, AGR-2 was run for 8 days with type-2 real groundwater at an EBCT of 90 min. The AGR-2 was operated at increased sulphate and COD of 100 mg/L and 150 mg/L at an increased EBCT OF 120 min for next 19 days (from day 837 to day 856) and effluent was analysed for its efficiency on arsenic and iron removal.

Table 4.8 Characteristics of raw groundwater.

Components	Unit	Concentration	
		Type -1 RGW	Type -1 RGW
Temperature	°C	25.8°C	24.5
pH	-	6.65	6.8
EC	µs/cm	932	842
ORP	mv	88.3	89
Fe _{tot}	mg/L	8.3	13.2
SO ₄ ²⁻	mg/L	3.2	4.8
As _{tot}	µg/L	226	295
PO ₄ ³⁻	mg/L	1.14	0.86
Cl ⁻	mg/L	10.6	12.4
HCO ₃ ⁻	mg/L	107	84
CO ₃ ²⁻	mg/L	19.2	17.6
Na	mg/L	12.8	16.4
Ca	mg/L	17.8	18.2
Mg	mg/L	4.82	5.1
Mn	mg/L	0.023	0.021
D.O.	mg/L	4.1	4.3

4.7 Microbial Population Identification and Diversity Analyses

4.7.1 Biofilm formation on WAC

The colonization by mixed microbial communities on WAC granules was examined on a Hitachi S-4500 field emission SEM (FE-SEM) in the central instrument facility at the IIT Guwahati. Both types of WAC granules, virgin as well as those harbouring biofilms were subjected to FESEM. The WAC granules were collected after backwashing to give a complete representation of bacterial population of the AGR from sampling port with the help of a tweezers in a centrifuge tube prior filled up with N₂ gas. After careful isolation from AGR, biofilm containing WAC granules were fixed with 0.1M phosphate buffer (pH 7.0) containing 4% (vol/vol) glutaraldehyde and 1.3% osmium tetroxide for 1h and washed with 0.1 M phosphate buffer for 10 min. After fixation, cells were dehydrated using a graded series of ethanol solutions (20, 40, 60, 80 and 100% ethanol) (Massol-Deya et al., 1995). The samples were then critical point dried and coated with gold using a coating device (Hitachi) and mounted on a copper specimen stub and fixed using carbon tape. FE-SEM micrographs were obtained with a JSM35C FE-SEM (JEOL, Ltd., Tokyo, Japan)

4.7.2 T-RFLP analysis

T-RFLP (terminal restriction fragment length polymorphism) analysis is used to test environmental samples of soil, fresh, and marine water origin, to know structure and spatial distribution of bacterial communities using the 16S rRNA gene or other functional genes (Schütte et al., 2008). In this project T-RFLP analysis was used to explore the composition of the predominant microbial populations present in AGR-1. The other objective of generating Terminal Restriction Fragment (T-RF) patterns (presence/absence of peaks and area of peaks) was to determine bacterial species richness, diversity index and functional diversity in microbial communities. T-RF numbers has been shown to be effective indicators of microbial communities richness and microbial ecology in a range of environments (Denaro et al., 2005; Zhang et al., 2008). On 250th day, WAC granules from the AGR-1 were collected after backwashing of AGR-1. Then it was sent to Geneombio Technologies Private Limited, Pune (India) for T-RFLP analysis.

4.7.3 Metagenomic analysis

Metagenomic analyses of mixed bacterial populations of AGRs were performed on V3-V4 variant regions of the 16 S rRNA genes. The primary goal of metagenomic analysis was to identify microbial diversity present in complex polybacterial populations of AGRs. In prokaryotes, 16S ribosomal RNA (rRNA) amplicons have been widely used in the classification of uncultured bacteria inhabiting environmental samples (Wang & Qian, 2009).

WAC granules harbouring biofilm were collected from the AGRs after backwashing, to give a complete representation of bacterial population in the reactors. The WAC granules were collected in polyethylene bottles in an anoxic environment and sealed immediately on 752th and 720th day of operation of AGR-1 and AGR-2, respectively. The sealed bottles were then packed properly with an ice gel pack, which was then shipped to SciGenom Labs Private Limited, Kerala, India for metagenomic analysis.

4.8 Whole Effluent Toxicity (WET) Test of Treated Water

The WET test is a form of biological monitoring that determines/predicts the aggregate toxic effect of an effluent or its potential impact on receiving (ambient) waters on to aquatic organisms. The test method is based on the effect on the test organism's ability to survive in terms of mortality and gross morphological deformities (growth and reproduction) (Hollenkamp 2012, USEPA 2004). Due to several limitations of chemical analysis in assessment of complex natured effluents, the biological toxicity was added as a correctional approach. For this reason the WET testing was done as it focuses on acute toxicity. Moreover it also takes an account for the uncharacterized sources of toxicity, and additionally, shows that known toxicants to aquatic organisms may become either less or more toxic (antagonistic or synergistic respectively) due to particular characteristics of the effluent matrix or stream chemistry (Ra et al., 2007; Tonkes et al., 1999).

The main aim of this study is to evaluate the acute toxicity of AGR treated water on the freshwater fish in context of mortality. To determine the acute toxicity of the AGR effluents, WET test was performed on fresh water fishes because EPA has not provided an acute toxicity test for plants, effluents can only be tested for acute toxicity with a

fish and an invertebrate (Marshall, 2016). The freshwater fish, *Puntius*, were collected from local market as a freshwater species can be typically used for acute freshwater WET test as per EPA guidelines. The test species has local importance and found abundantly in the river Brahmaputra and water bodies in and around Kamrup district of Assam. They were brought to the laboratory in large plastic troughs and acclimatized for one week in tap water (pH 7.3 ± 0.05 , DO 7.5 ± 1.0 mg/L, total hardness 215.3 ± 7.0 mg/L as CaCO_3 and alkalinity 133.2 ± 5.0 mg/L as CaCO_3). The fish having average body length of 2-3 cm and body weight of 2.6 ± 0.3 g were selected for the present study. Acute toxicity of treated water on test fish was measured in static and static-renewal bioassay procedures, as outlined by USEPA (2002). The test was carried out on absolute and 50% diluted treated water along with control which was containing only river water. The mortality rate of fish along with other physiological responses (change in behaviour, growth) was recorded at 24, 48, 72 and 96 h of exposure to the treated water as a measure of toxicity.

4.9. MPN test of Treated Water

The MPN test, intended to check the usability and presence of potential disease-causing microorganisms, was conducted on treated water from AGRs. The MPN method is a commonly used traditional protocol for screening of a test sample for bacterial prevalence and concentration. Original effluent sample was subjected to serial decimal dilutions up to three dilutions (i.e., 10^{-1} , 10^{-2} and 10^{-3}). One ml aliquots from each dilution including original sample were placed into three MPN tubes each containing lauryl tryptose broth medium for bacterial enrichment. After 48 hours incubation periods, each tube is evaluated for bacterial presence (APHA, 2005). The most probable number of microorganisms in the original sample is subsequently estimated from the number of positive tubes for the individual serial dilutions (i.e., the MPN pattern).

4.10 Characterization of Biosolids

The solids collected from the SmBRs and backwash solids from AGRs were characterized using FESEM-EDX and TEM-EDX, XRF, XRD and XAS.

4.10.1. Collection and Preservation of Biosolids

The biosolids from AGRs were collected from backwash suspension after a backwash. During backwash nitrogen gas was supplied along with distilled water to maintain anoxic condition. The backwash suspension was collected in anoxic condition in a container prefilled with nitrogen gas. The suspension was collected through the inlet port and the gas from the container was allowed to exit through the exit port. Schematic diagram of a container used to collect backwash suspension is shown in Figure 4.6. The backwash suspension, thus collected, was transferred to centrifuge tubes to separate solids for their various characterizations. The backwash solids (BWS) were centrifuged at 6000 rpm for 10 min to obtain wet paste, which was freeze dried and preserved at 4°C in sealed specimen tubes in a double zip locked plastic bags. All necessary practical steps were taken to minimize contact between the solids and atmospheric air.

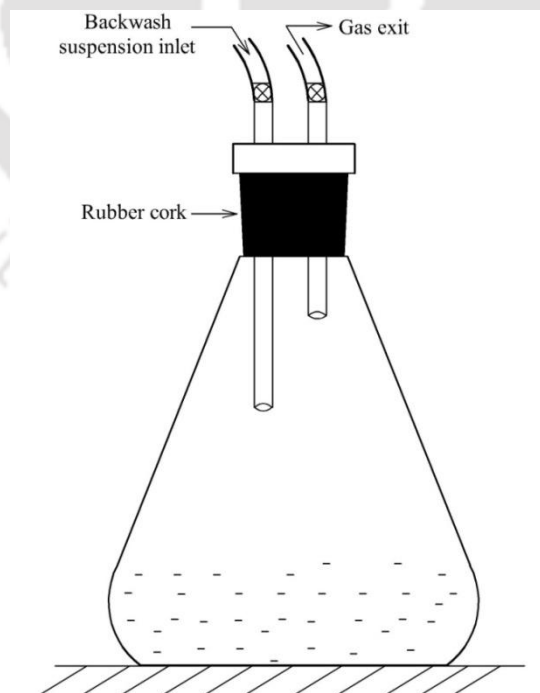


Figure 4.6 Schematic diagram of container used for collecting backwash suspension.

4.10.2 X-ray Fluorescence (XRF)

The qualitative elemental composition of biosolids generated in SmBRs was performed by AXIOS X-ray Fluorescence Spectrometer of PANalytical make (Model DY840). The XRF qualitative analysis is done by scanning the pressed pellet. 1g of finely ground sample is mixed with 0.5g of Boric acid (binder) and given a load of 50kN for 2 minutes. Pressed pellets made in the aforesaid method are scanned by qualitative XRF (SuperQ) software program in the XRF machine, which showed presence of As, Fe and S.

4.10.3 Microscopic Methods

FESEM and EDX

Field emission scanning electron microscopy (FESEM) (Zeiss, Sigma, Germany) equipped with energy dispersive X-ray microanalysis system (EDX) (INCA 300, Oxford, UK) was used for topographical characterization and elemental confirmation of arsenic, iron and sulphur in the biosolids. Before the examination, the freeze dried backwash solids was lightly dusted onto the carbon tape of the SEM stub surface and coated with gold using a Scancoat Six SEM sputter coater system.

TEM and EDX

The detailed morphology, microstructure and chemical composition of BWS were examined by transmission electron microscopy (TEM), using a JEOL, JEM 2100 microscope operated at 200 kV, equipped with an energy dispersive X-ray spectrometry (EDX). Specimens for TEM observations were prepared using an ultrasonic vibration method. First, the powdered samples were immersed in acetone solution and subjected to ultrasound vibration (Vibra-Cell model VC 505, Sonics, USA) to disperse the sample homogeneously. Then, one drop of the suspension was dropped with a micropipette to holey carbon supporting film (TEM Grids). After being well dried under ambient conditions, the grid was mounted on the TEM specimen holder for examination. Samples were investigated thoroughly by TEM selected-area electron diffraction (SAED), high resolution imaging (HRTEM) and EDX. A series of Fast Fourier Transform (FFT) patterns calculated from the HRTEM images of samples was used to help identify their crystal structure.

4.10.4 X-Ray Diffraction (XRD)

X-ray powder diffraction was used to check the existence and crystalline form of the solid phase generated in the bioreactors. The analysis was carried out with a PANalytical X'pert PRO-MPD diffractometer equipped with a monochromator in the diffracted beam. The X-ray powder diffraction spectra were recorded in the 2θ range from 10° to 80° using Cu K_α (wavelength = 1.54 \AA , 40 mA, 40 kV) radiation with a step size of 0.05° and a step duration of 1 sec. The freeze dried backwash solids were used as a sample in XRD pattern recording.

4.10.5 X-ray Absorption Spectroscopy (XAS)

X-ray absorption spectroscopy (XANES and EXAFS) were used to determine the arsenic and iron oxidation state and local structure of the back wash solids. The characterization was performed at Raja Ramanna Centre for Advanced Technology (RRCAT), Indore, India. The samples for XAS analyses were filtered through $0.22 \mu\text{m}$ nylon filters and the filtered paste of back wash solids were transferred into airtight, crimp-sealed serum bottles without drying and then shipped to Indus Synchrotron Radiation Laboratory of RRCAT for XAS analysis. XAS samples were prepared for analysis by applying wet sample pastes onto a double layer of Kapton tape in anaerobic conditions. XAS spectra were collected at Indus-2 beamline (BL-9) (3 GeV, $\sim 100 \text{ mA}$ of maximum current) with an unfocused beam. The beam line mainly consists of Rh/Pt coated meridional cylindrical mirror for collimation and Si (111) based double crystal monochromator to select excitation energy. XANES and EXAFS measurements were carried out in transmission mode. The energy range of EXAFS was calibrated simultaneous measurements on a commercial Fe and Au foils. XAS spectra were also collected for $\text{Na}_2\text{HAsO}_4 \cdot 7\text{H}_2\text{O}$ and NaAsO_2 powders to use as As(V) and As(III) standards. Model compounds such as metallic iron foil (Fe(0)), amorphous FeS, and amorphous Fe_2O_3 . The EXAFS data has been analysed using FEFF 6.0 code (Zabinsky et al., 1995), which includes background reduction and Fourier transform to derive the $\chi(R)$ versus R spectra from the absorption spectra (using ATHENA software) (Ravel & Newville, 2005), generation of the theoretical EXAFS spectra starting from an assumed crystallographic structure and finally fitting of experimental data with the theoretical spectra using ARTEMIS software (Ravel & Newville, 2005).

4.11 Stability Check of Biosolids

To investigate the stability of arsenic immobilized as a result of biomineralization in AGRs, the aging test, toxicity characteristic leaching procedure (TCLP) test, and long-term aerobic leaching tests were conducted. TCLP is the most widely used regulatory protocol to test the leachability of solid wastes in landfilling environments and to classify a solid waste as a hazardous waste (USEPA, 1992).

The findings of the present study are important for the understanding of arsenic mobility from precipitates generated as a result of anaerobic sulfidogenic water treatment and in determining the disposal criteria.

4.11.1 Batch Ageing Test of Backwash Suspension

Ageing test of backwash solids of AGR-1 and AGR-2 were conducted in batch mode to evaluate their stability against leachability under anoxic as well as oxic conditions. Collections of backwash suspensions from both the reactors for this test were started after studying the effects of temperature on performance of the reactors. The feeding and operating conditions of the reactors were as follows: Arsenic = 500 µg/L; Nitrate = 50 mg/L; Sulphate = 25 mg/L; iron = 3.0 mg/L (AGR-2 only) with other components as mentioned in Table 4.2; EBCT = 45 min; temperature = 30°C and backwash frequency = 48 h.

Backwash suspensions from the AGRs were collected after each backwash for a period of about 1½ months. Fresh suspension samples were collected in a container as described in section 4.10.1. The solids in each suspension were allowed to settle for 2 h. The supernatant was then carefully decanted and the bottom 250 ml, containing settled solids, was transferred into a 250 ml high-density polyethylene (HDPE) screw cap conical flask (test vessel). For ageing test in anoxic environment, the test vessels were prefilled with nitrogen gas and no headspace was left out.

The oxic aging test was conducted in 250 ml HDPE beaker (test vessel) without capping and N₂ supply. The test vessels for anoxic aging were kept in dark at room temperature (30±2°C) whereas, for oxic aging vessels were kept open for approximately 90 days of test period (Meng et al. (2001)). Ageing tests in both the conditions were conducted in self scarifying mode using 22 test vessels. The aliquots of suspension were periodically monitored for pH, arsenic, iron and dissolved oxygen (DO) during the aging

period. After completion of an ageing test, the supernatant was carefully decanted and the wet solid paste was freeze dried.

4.11.2 Toxicity Characteristics Leaching Procedure (TCLP) test

Leaching tests were outlined to estimate the leaching potential of a waste in a time period much shorter than that of disposal. Though various leaching tests are designed in time duration ranging from 1 hr to 13 weeks, the TCLP test is conducted either for 18 hours, known as standard TCLP test (USEPA, 1997) or extended period termed by several researchers as extended TCLP test (Hooper et al., 1998). It has been observed that standard TCLP test for 18 hours is not always sufficient to evaluate the toxicity characteristics of the waste. The TCLP extraction has been tested for longer period (up to 84 hours) and greater arsenic leaching has been found for longer test durations (Clancy et al., 2013; Hooper et al., 1998). Therefore, extended TCLP tests for up to 84 hours have been suggested by several researchers (Hooper et al., 1998; Sima et al., 2015). In this project extended TCLP tests were conducted on backwash solids of AGRs for an extraction period of 84 hours.

Backwash solids used in TCLP

The backwash solids used for TCLP tests were collected by following the procedure as described in section 4.10.1. Triplicate samples of 1g of dry backwash solids, after being dried at 60°C, was digested in a mixture of acids of HNO₃ and HClO₄ (1:4, v/v) to extract out arsenic and iron present in the solids (Jong & Parry, 2005). Concentration of arsenic and iron in the digested extract were measured in AAS. Average concentration of arsenic or iron in backwash solids were calculated and expressed as mass (µg or mg) of arsenic or iron per kg of dry solids. Concentrated HNO₃ (1 ml) was added to 1.0 g of backwash solids in a digestion tube. When effervescence of brown NO₂ subsided, conc. HClO₄ (4 ml) was added and digested under reflux at 160°C, 220°C and 250°C for 30, 220 and 180 min, respectively, to reduce the final volume to 2 ml. After the digested samples cooled, the contents were diluted to 20 ml with DI water, mixed using a Vortex mixer (Remi Instruments, India) and allowed to settle overnight at 4°C. The supernatant was then carefully decanted into a 10 ml polypropylene tube (Tarsons) and stored at 4°C until analysis. Total suspended solids (TSS) and volatile suspended solids

(VSS) were measured according to the methods described in Standard Methods for the Examination of Water and Wastewater (APHA, 2005).

TCLP leaching tests

The TCLP test was conducted on stored freeze dried backwash solids in accordance with SW 846 test Method 1311 (USEPA, 1997). To decide on the TCLP leachant as extraction liquid, pH of the backwash solids was measured by adding 96.5 ml of DI water to 1 g of the test material (backwash solid) in a glass beaker after vigorous stirring for 5 minutes (USEPA, 2004). The pH of the backwash solid was between 6.8 and 7.2, and therefore, glacial acetic acid buffered at pH 4.93 ± 0.05 with 1N sodium hydroxide was selected as TCLP leachant (USEPA, 1997). The TCLP tests were conducted in Teflon screw cap bottles (test vessels) keeping a specific leachant-to-solid mass ratio (on wt/wt basis) of 20 in the mixture. All experiments were carried out in triplicate to ensure the reproducibility. The agitated mixture was centrifuged at 5000 rpm for 10 min. The supernatant was filtered through 0.45 μm filter paper, and the filtrate was analysed for arsenic and/or iron. Kinetic and extended TCLP tests were conducted either in nitrogen filled vessels (screw cap Teflon bottles) leaving 50% head space of the gas above the mixture or in vessels (beakers) exposed to air. To take more accurate account for anaerobic landfill conditions, TCLP tests were conducted in nitrogen filled vessels (screw cap Teflon bottles) whereas, vessels (beakers) exposed to air were used to represent aerobic condition. The following are the experiments conducted related to TCLP tests:

(i) Kinetic TCLP leaching test

Experiments of kinetic TCLP leaching test were conducted with the aim to determine the rate of leaching of arsenic and/or iron from the backwash solids of AGR-1 and AGR-2. Kinetic experiments were conducted by gentle mixing of TCLP extraction solution and 1g backwash solid samples (leachant-to-solid ratio of 20) in a test vessel for a period of 24 h. The test vessels were open to air or filled up with nitrogen gas during the mixing. The kinetic TCLP extractions in presence of air were carried out in a 100 ml Teflon beaker with a magnetic flea and the beakers were exposed to air during the mixing. On the other hand, the kinetic TCLP extractions were carried out in 100 ml Teflon screw cap bottles filled up with nitrogen gas. The mixture in the screw cap bottles was agitated

in an end-over-end rotary shaker at 30 ± 1 rpm. Both sets of experiments were conducted at a temperature of $30 \pm 2^\circ\text{C}$. Samples were taken at the end of the desirable extraction period and filtered samples were analyzed for arsenic and/or iron. A duplicate blank extraction, containing extraction solution but no test solids was also run.

(ii) Extended TCLP test

The extended TCLP test (for 84 ± 1 h) was conducted by extracting the contaminants from a 1g sample of test material with an appropriate extraction fluid.

(iii) Effects of dissolved oxygen (DO) on TCLP leaching characteristics

TCLP test was also conducted to determine the effects of oxygen on arsenic leaching. The headspace in the vessels was varied by varying the headspace-to-leachant volume ratio ($V_{\text{air}}/V_{\text{L}}$) at a constant leachant-to-solid ratio of 20. The $V_{\text{air}}/V_{\text{L}}$ ratios of 0.25, 0.50, 1.0 and 1.25 were used. As the size of the extraction vessels were not specified in TCLP test protocol, thus extraction vessels of different sizes were used in order to maintain $V_{\text{air}}/V_{\text{L}}$ ratio of 0.25, 0.50, 1.0 and 1.25. Filtered samples were taken at the end of the extraction period and analysed for arsenic and/or iron. A duplicate blank extraction, containing extraction solution but no test solids was also taken.

4.11.3 Long term Aerobic Leaching Test

After useful life of WAC filter bed it needs to be disposed off and replaced by fresh WAC bed. The exhausted WAC bed may behave like a layer of soil. There are several reports on leaching of arsenic from exhausted resins and adsorbents (Henke, 2009; Jing et al., 2005). After successful operation of flow through reactors for approximately 1000 days, the experiments on long term stability check was conducted on the arsenic and/or iron bearing solid-precipitates and exhausted WAC filter bed, whilst it was still intact in the flow-through reactors. The experiment was intended to simulate the in situ leaching of uncontaminated groundwater through the arsenic bearing solid-precipitate with virtually no physical disturbance in a subsurface environment. The AGRs were operated for 20 days without backwashing prior to this test in order to keep solid phase sulphides remain in the system. The feeding and operating conditions of the reactors were as follows: Arsenic = $500 \mu\text{g/L}$; Nitrate = 50 mg/L ; Sulphate = 25 mg/L ; iron = 3.0 mg/L (AGR-2 only) with other components as mentioned in table 4.2. After 20 days of

operation, the original influent media was drained to maximum possible extent and the columns were subjected to a sequential leaching process by passing aerobic water through it. The new influent media of pH 7.0 ± 1 , prepared in DI water without addition of any metal was charged into the AGRs through the influent port using a syringe pump (200 $\mu\text{L}/\text{min}$). The dissolved oxygen was maintained between 4.6-5.4 mg/L in the new influent and intermittent supply of oxygen was also done in order to maintain the DO level constant in the aerobic water. The sample was collected in every 24 hr and the parameters were analyzed for pH, arsenic and iron concentrations in the leachate. Aerobic leaching test was stopped after 110 days, which is equivalent to 220 pore volumes. After completion of test, the solids were collected under a flow of nitrogen by backwashing and freeze dried. The freeze dried solids were stored at 4°C and subjected to XAS analysis for their characterization.

4.12 Fluoride Removal by Water Treatment Residues (WTR)

4.12.1 Water Treatment Residues (WTR)

The water treatment residues (WTR), generated during the drinking water treatment was collected from the water treatment plant at IIT Guwahati, India. The WTR was collected from the clariflocculator drain of the treatment plant. The WTR was Sun-dried and grinded to fine powder using mortar-pestle to a particle size range of 0.5-0.8 mm and stored in airtight containers until further use. This material was used as an adsorbent to investigate fluoride removal in batch shake flasks.

4.12.2 WTR Characterization

Brunauer–Emmett–Teller (BET) surface area measurement of WTR was done using Quantachrome automated gas sorption system (Autosorb, Quantachrome, Germany). The surface morphology and elemental composition of the WTR was examined with FESEM and EDX respectively. The Fourier transform infrared spectrometer (FT-IR) (IR Prestige-21, Shimadzu, Japan) spectra was also recorded for qualitative identification of chemical groups and compounds present in WTR. X-ray diffraction (XRD) pattern was collected to identify detailed structure of adsorbent. Both

fresh and spent WTR were subjected to FESEM/EDX, FT-IR and XRD analyses to understand the fluoride removal mechanism.

4.12.3 Batch Adsorption Experiments

Experiments on removal of fluoride by WTR as adsorbent were carried out in batch mode in are described in a series of 250 ml HDPE screw capped conical flasks in self-sacrificing mode. Effects of WTR dose, contact time, agitation speed, initial fluoride concentration, operating temperature and pH were studied to determine the optimum experimental conditions. The pH of the solution was kept primordially without any adjustment except the experiments conducted for studying pH effect where the pH of the solution was adjusted using either HCl or NaOH. All the experiments were carried out at room temperature of $(30\pm 2)^{\circ}\text{C}$ except experiment on studies of effect of temperature. Initial fluoride concentration was maintained at 5.0 mg/L for all experiments except during studies on effects of initial fluoride concentration.

The experiments on effects of WTR dose were carried out by taking 4, 8, 12, 16, 20, 24, and 28 g/L WTR in a series of conical flasks, agitated at 100 rpm for 120 min. at room temperature. The kinetic studies were conducted by adding fixed dosage (16 g/L) of WTR into a set of flasks containing 100 mL sodium fluoride with fluoride concentration of 5.0 mg/L. The mixtures were agitated at 100 rpm at room temperature. The effect of agitation speed on fluoride adsorption was examined at 50, 100, 150, 200 and 250 rpm at WTR dosage of 16 mg/L. The mixtures were agitated at desired speed for 120 min. The effect of initial fluoride concentration was conducted at initial fluoride of 5, 6, 7, 8, 9 and 10 mg/L at fixed WTR dosage of 16 g/L. The mixtures were agitated at 200 rpm for 120 min. Adsorption experiments were also carried out at 15, 25, 35, 45 and 55°C at 200 rpm for 120 min to investigate the effect of temperature. The effect of pH on F^{-} adsorption was evaluated by adjusting solution pH to 5, 6, 7, 8 and 9 respectively at WTR dose of 16 g/L at 200 rpm for 120 min. Samples were filtered and filtrates were analyzed for fluoride by SPADNS method (APHA, 2005). Fluoride removal efficiency (%) by WTR in the batch reactors was defined as:

$$\text{Fluoride removal (\%)} = \frac{\text{initial fluoride (mg/L)} - \text{final fluoride (mg/L)}}{\text{initial fluoride (mg/L)}} \times 100$$

4.12.4 Adsorption Equilibrium Study

In order to optimize the design of a sorption system for the removal of fluoride ions from aqueous solution by WTR, three different isotherm equations have been used in the present study. These are Freundlich isotherm, Langmuir isotherm, and Temkin isotherm. Langmuir, (Eq. (4.2)) Freundlich, (Eq. (4.4)) and Temkin (Eq. (4.6)) isotherms were plotted by using standard straight-line equations and corresponding parameters were calculated from their respective graphs. Comprehensively various adsorption isotherm models are discussed as follows:

Langmuir adsorption isotherm

The Langmuir equations is based mainly on the assumptions that molecules are adsorbed on definite sites on the surface of the adsorbent, each site can accommodate only one molecule (monolayer) and the adsorption energy is the same at all sites. The Langmuir adsorption isotherm is expressed as:

$$q_e = \frac{q_m BC_e}{1 + BC_e} \quad \dots\dots\dots \text{Eqn. (4.2)}$$

Where,

$$q_e = \frac{X}{M} = \frac{C_0 - C_e}{m}$$

q_m = amount of solute adsorbed per unit weight of adsorbent required for monolayer coverage of the surface, also called monolayer capacity. This represents the total capacity of the adsorbent for a specific adsorbate.

B = a constant related to the heat of absorption.

Langmuir isotherm can be written in linear form as:

$$\frac{1}{q_e} = \frac{1}{q_m} + \frac{1}{Bq_m C_e} \quad \dots\dots\dots \text{Eqn. (4.3)}$$

Equilibrium parameter (R_L) is a dimensionless constant, defined by

$$R_L = \frac{1}{1 + BC_0}$$

Where, B is the Langmuir constant and C_0 is the initial adsorbate concentration (mg/L), R_L values indicate the type of isotherm to be irreversible ($R_L = 0$), favourable ($0 < R_L < 1$), linear ($R_L = 1$), or unfavourable ($R_L > 1$) (Nigussie et al., 2007).

Freundlich adsorption isotherm

The Freundlich isotherm is expressed as: $q_e = KC_e^{1/n}$ Eqn. (4.4)

Where,

$$q_e = \frac{X}{M} = \frac{C_0 - C_e}{m}$$

X = weight of solute adsorbed (mg)

M = weight of adsorbent (g)

C_0 = Initial concentration of solute (mg/L)

C_e = final concentration remaining in solution (mg/L)

m = Adsorbent added in, (g/L)

The linearized form of Freundlich adsorption isotherm is of the form:

$$\log q_e = \log K_f + \frac{1}{n} \log C_e \quad \text{.....} \quad \text{Eqn. (4.5)}$$

K_f = minimum sorption capacity (mg/g)

$1/n$ = adsorption intensity

K_f and n are constants depending on temperature, the adsorbent and the substance to be adsorbed.

By plotting $\log (q_e)$ versus $\log C_e$, a straight line is obtained with a slope of $1/n$, and $\log K_f$ as the intercept.

Temkin adsorption isotherm

Temkin isotherm contains a factor that explicitly takes into account of adsorbing species and adsorbent interactions. The heat of adsorption of all the molecules in the layer would decrease linearly with coverage due to adsorbate/adsorbent interactions. This isotherm assumes that (i) the heat of adsorption of all the molecules in the layer decreases linearly with coverage due to adsorbent and adsorbate interactions, and that (ii) the adsorption is characterized by a uniform distribution of binding energies, up to some maximum binding energy (Nigussie et al., 2007). A plot of q_e versus $\ln C_e$ enables the

determination of the isotherm constants B_1 and K_T from the slope and the intercept, respectively. K_T is the equilibrium binding constant (L/mol) corresponding to the maximum binding energy and constant B_1 is related to the heat of adsorption.

Temkin isotherm is given as: $q_e = \frac{RT}{b} \ln (K_T C_e)$ Eqn. (4.6)

A linearized form of Temkin isotherm is: $q_e = B_1 \ln K_T + B_1 \ln C_e$ Eqn. (4.7)

Where,

$$B_1 = \frac{RT}{b}$$





CHAPTER 5

RESULTS AND DISCUSSION

The discussions on the experimental results are made as per the following sequence in accordance with the aim and scopes of the study.

The discussions on the experimental results are made as per the following sequence:

- **Seed sludge preparation**
 - 5.1 Acclimatization and seed sludge preparation in BR-0
- **Performance evaluation of batch, semi-batch and flow through bioreactors**
 - 5.2 Performance evaluations of batch shake flasks
 - 5.3 Performance evaluation of semi-batch bioreactor SmBR-1 in absence of iron
 - 5.4 Performance evaluation of semi-batch bioreactor SmBR-2 in presence of iron
 - 5.5 Performance evaluation of flow through reactors AGR-1 in absence of iron
 - 5.6 Performance evaluation of flow through reactor AGR-2 in presence of iron
 - 5.7 Performance evaluation of AGR-2 on treatment of real groundwater
- **Characterization of bioreactor treated water**
 - 5.8.1 MPN test
 - 5.8.2 Toxicity test
- **Post treatment of bioreactor treated water (effluent)**
 - 5.9 Fluoride removal using water treatment plant residues
- **Microbial characteristics**
 - 5.10.1 Biofilm formation
 - 5.10.2 TRFLP analysis
 - 5.10.3 Metagenomic analysis
- **Biosolids characterization**
- **Stability tests on biosolids**

5.1 Seed Sludge Collection and Acclimatization

Enrichment of the mixed microbial consortium was carried out in reactor BR-0 by adding a fixed amount of 200 $\mu\text{g/L}$ arsenate and 50 mg/L of NO_3^- and SO_4^{2-} respectively in simulated groundwater. The detailed enrichment phase is presented in Figure 5.1. It could be observed that NO_3^- was completely removed while SO_4^{2-} removal rate was improved at each and every stage of acclimatization. After 35 days of acclimatization period, almost 50% SO_4^{2-} depletion of the initial 50 mg/L was achieved. This acclimatized mixed bacterial consortium was used as seed sludge for all further experiments.

5.2 Performance Evaluation of Batch Shakes Flasks

Arsenic adsorption on to biomass, effects of initial arsenic, initial iron and initial NO_3^- concentration on arsenic removal were performed in batch shake flasks as described in section 4.2.3.

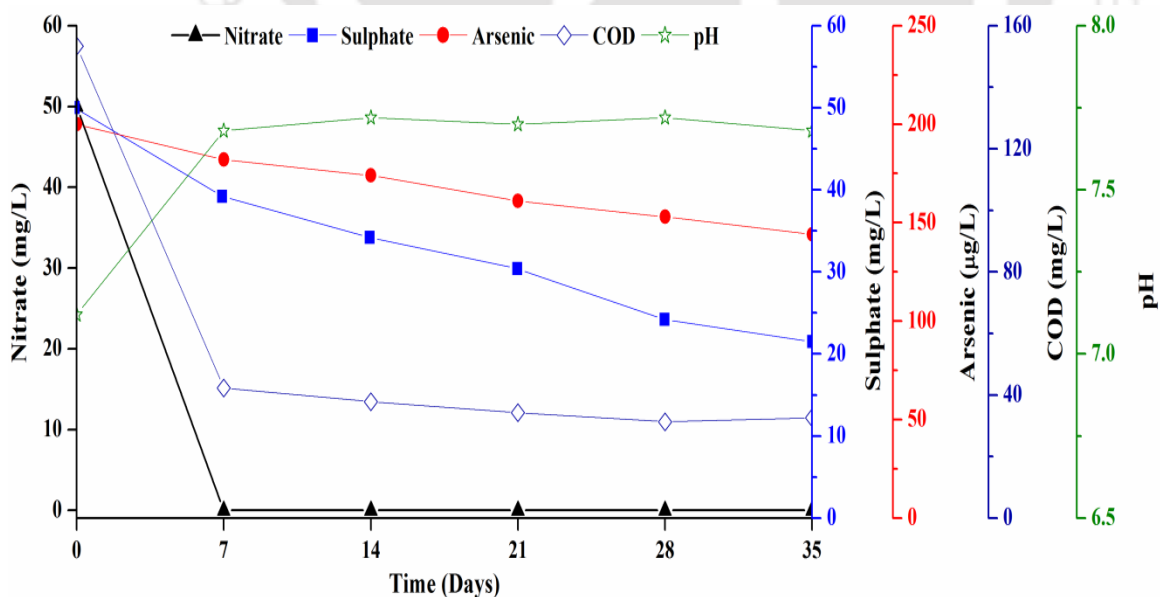


Figure 5.1 Enrichment of mixed microbial consortium.

5.2.1. Adsorption Studies in Batch Shake Flasks

Time series profiles of average residual arsenic concentration after adsorption by 100 mg/L of inoculum (MLVSS) from the “control” (i.e., batch shake flasks containing no inoculum), arsenic spiked distilled water and media (Table 4.2) excluding iron and sulphate, have been shown in Figure 5.2. After 7 days, from an initial 500 µg/L, only about 1%, 2% and 3% removal of arsenic was noticed from control, arsenic spiked distilled water, and the media, respectively. Reduction in arsenic concentration in the “control” might be due to loss of arsenic by adsorption on the flask material and/or volatilization. Teclu et al. (2008) reported about 6.5% and 10% bio-sorption of As(III) and As(V), respectively, from an initial of 1000 and 5000 µg/L in high sulphate (about 1650 mg/L) and iron (100 mg/L) containing Postgate medium. Low removal of arsenic through bio-sorption could have been due to the near neutral pH at which the experiments were conducted. Seki et al. (2005) reported that the isoelectric point of most microbes is around pH 2 and their surfaces should be negatively charged at near neutral pH. Therefore, bio-sorption of arsenic oxyanions at near neutral pH was very low (Teclu et al., 2008). In fact, in the present study, arsenic bio-sorption was even lower than that reported by Teclu et al. (2008). This could have been due to absence of sulphate and iron in the media used in this study. It has been reported that arsenic removal in presence of sulphate in anaerobic condition would be possible either through precipitation as arsenosulphide and/ or co-precipitation with iron sulphides in presence of iron (Altun et al., 2014).

Time series profile of COD and nitrate concentration from media also has been shown in Figure 5.2. Complete nitrate reduction was observed within 24 hours of reaction. Nitrite was not observed in any of the samples, indicating complete denitrification of the media. Although 57% of COD reduction was observed in 7 days of experiment, 51% was removed within first day of operation. Slow rate of COD reduction might be due to absence of sulphate and/or methanogens in the inoculum. There was no reduction of nitrate or COD was observed from the control batch shake flasks, indicating necessity of the presence of microbes for their bioconversion.

5.2.2 Adsorption of Arsenic by WAC

Figure 5.3 shows adsorption capacity of WAC on arsenic removal. Characterization of waste activated carbon (WAC) and its adsorption behaviour on removal of arsenic from simulated groundwater in absence of iron was evaluated. Batch studies with WAC (@ 2.0 g/L) showed that the removal of As(V) by adsorption was less than 10% from an initial of 250 µg/L after 12 h of agitation at 150 rpm and 30°C.

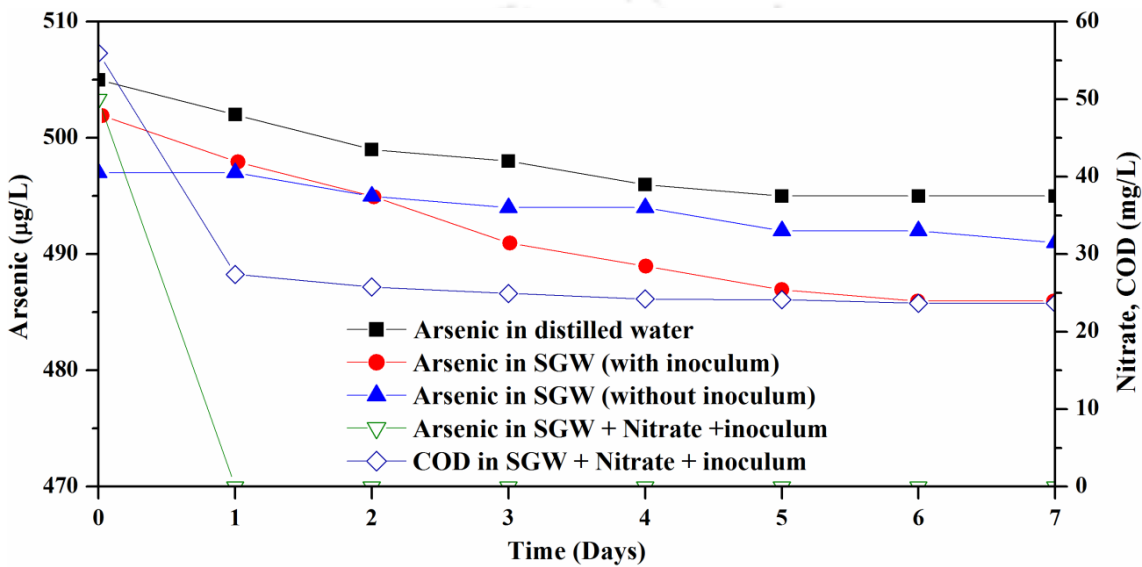


Figure 5.2 Time series profile of average residual arsenic, nitrate and COD concentration after adsorption by 100 mg/L of inoculum (MLVSS). (SGW = simulated groundwater without sulphate and iron as defined in Table 4.2)

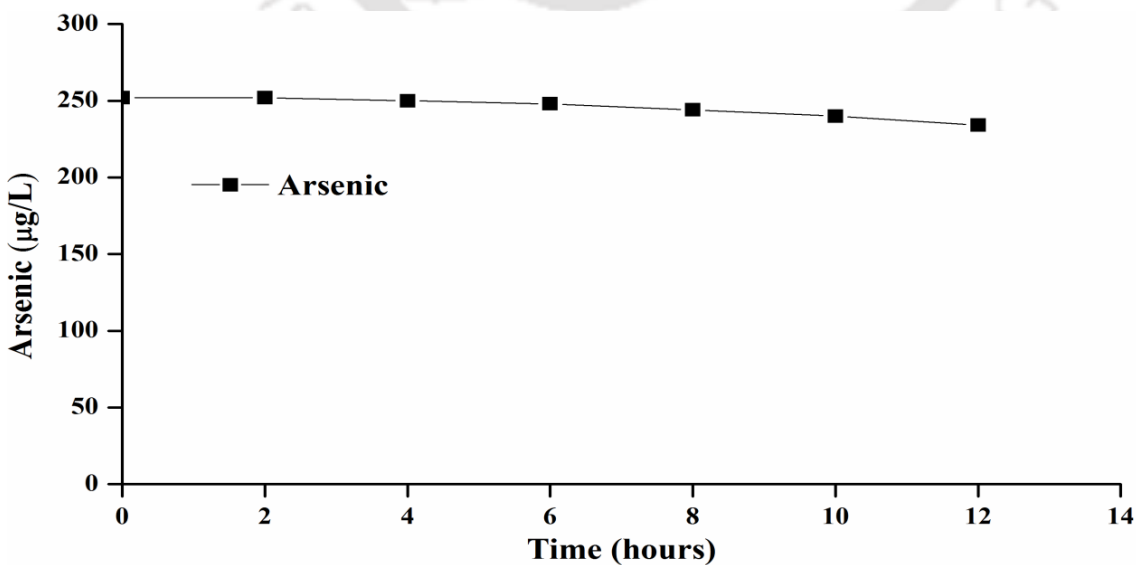


Figure 5.3 Arsenic adsorption on to WAC.

5.2.3 Bioremoval Studies in Batch Shake Flasks

5.2.3.1 Batch Studies in Absence of Iron

Effects of initial arsenic concentration:

Figure 5.4, 5.5, 5.6, and 5.7 represents the performance of mixed bacterial culture in batch shake flasks at four different initial arsenic concentrations of 250, 350, 450 and 550 $\mu\text{g/L}$, respectively. Although sulphate and COD were gradually reduced during entire period of 7 days operation, reduction rate decreased after about 3-4 days of reaction. COD of only 22-24 mg/L and 16-18 mg/L remained in the effluent after 4 days and 7 days of operation respectively. pH of the effluent (Fig. 5.4) increased with the biodegradation of sulphate. This could have been due to formation of alkalinity due to reduction of sulphate. Microbial mass (MLVSS) concentration started decreasing after initial increase for first 3-4 days of operation. This might be due to unavailability of sufficient food (COD) in the media leading to net growth negative. In all the cases complete removal of nitrate from its initial 50 mg/L was noticed within first day of operation and therefore it has not been plotted in any of the above mentioned figures. With respect to arsenic, the mixed bacterial culture performed well in batch shake mode. Irrespective of initial concentration, arsenic in the treated water reduced below permissible limit (10 $\mu\text{g/L}$) in 5-6 days of reaction.

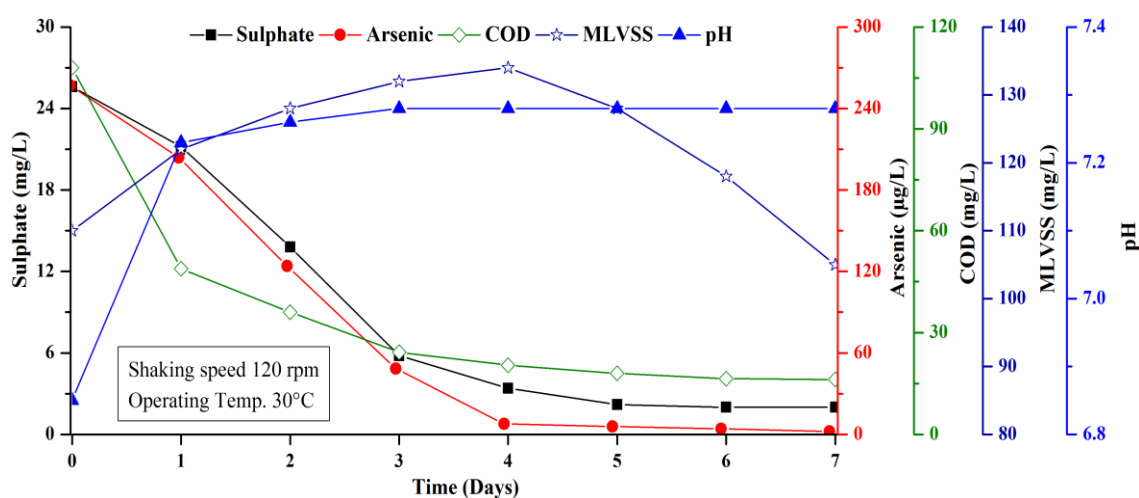


Figure 5.4 Performance of batch shake flasks in absence of iron at initial arsenic = 250 $\mu\text{g/L}$, nitrate = 50 mg/L and sulphate = 25 mg/L.

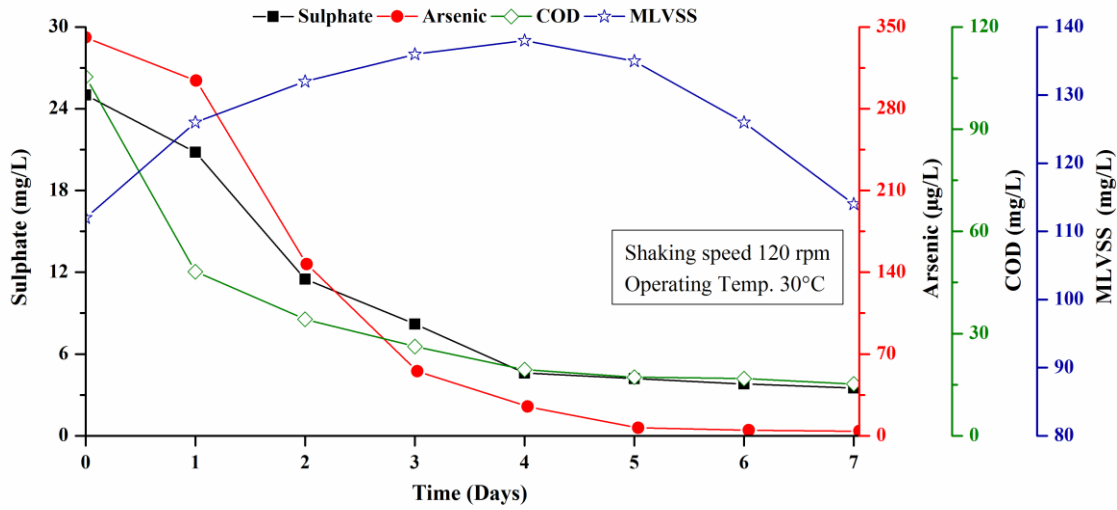


Figure 5.5 Performance of batch shake flasks in absence of iron at initial arsenic = 350 µg/L, nitrate = 50 mg/L and sulphate = 25 mg/L.

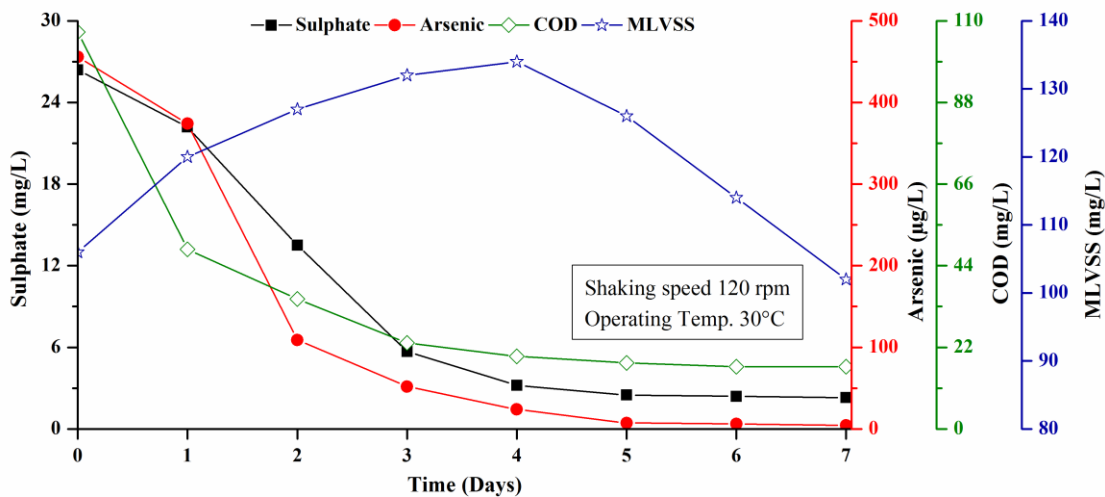


Figure 5.6 Performance of batch shake flasks in absence of iron at initial arsenic = 450 µg/L, nitrate = 50 mg/L and sulphate = 25 mg/L.

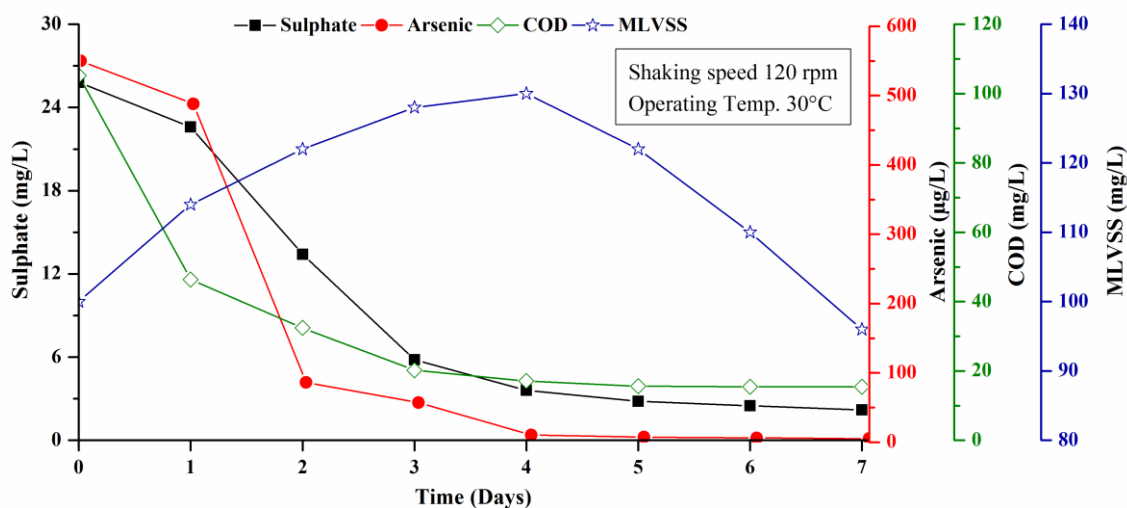


Figure 5.7 Performance of batch shake flasks in absence of iron at initial arsenic of = 550 µg/L, nitrate = 50 mg/L and sulphate = 25 mg/L.

Effects of initial nitrate concentration:

Figure 5.7, 5.8 and 5.9 represents effects of initial nitrate concentration of 50, 100 and 150 mg/L on performance of mixed bacterial culture in batch shake flasks. Irrespective of initial nitrate concentration (up to 150 mg/L), arsenic in the treated water was found to be below 10 µg/L within first 4 days of operation. Nitrate in the treated water was always less than the detection limit and therefore, not shown in the figures. Variation in sulphate and MLVSS concentration followed similar trend as observed at varying arsenic concentration. Little increase in pH with time would have been due to alkalinity formation during nitrate and sulphate reduction.

As arsenic cannot be removed from the system by biological processes, the reduction in arsenic concentration could be possible due to either adsorption on the microbial mass or precipitation as arsenosulphide. As arsenic removal by adsorption on biomass was almost nil, the only possibility of removal could be due to formation of arsenosulphides precipitation. However, formation of arsenosulphides precipitation could not be proved due to unavailability of sufficient amount of such solids in batch shake flasks, which were used for the study only with 50 ml of contaminated water. Analysis of

solids of a semi batch reactor (SmBR-1) and flow through reactor (AGR-1) were done to confirm the formation of arsenosulphides.

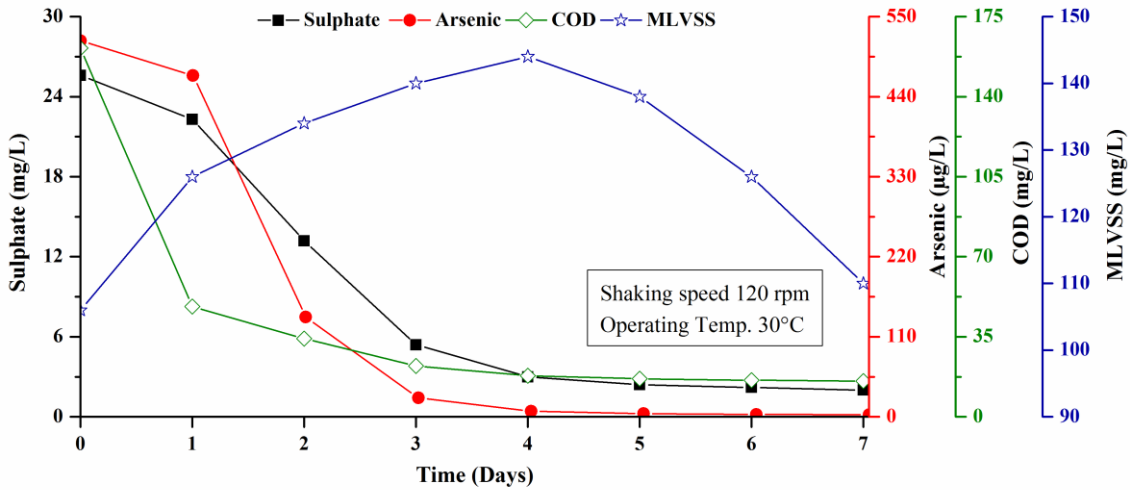


Figure 5.8 Performance of batch shake flasks in absence of iron at initial arsenic = 500 µg/L, nitrate = 100 mg/L and sulphate = 25 mg/L.

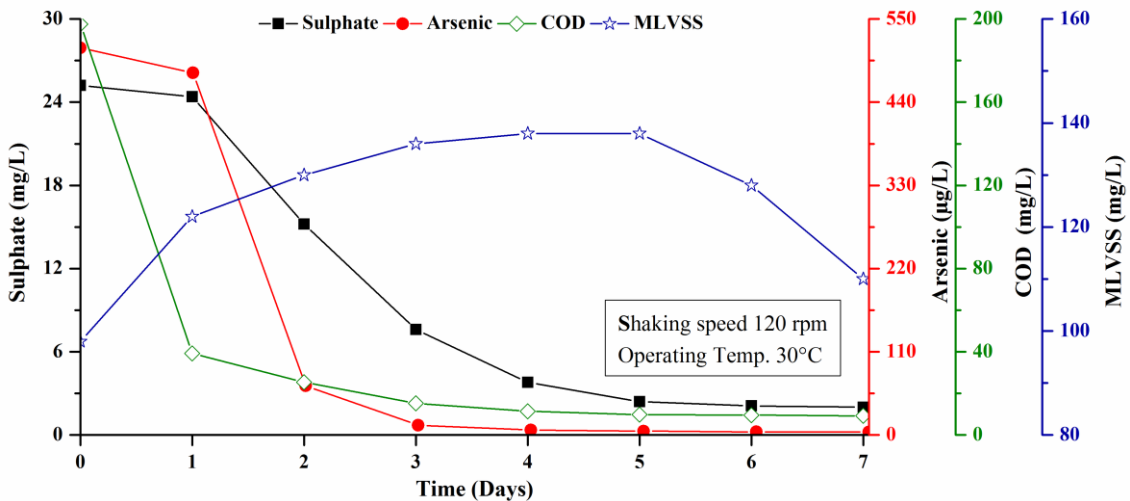


Figure 5.9 Performance of batch shake flasks in absence of iron at initial arsenic = 500 µg/L, nitrate = 150 mg/L and sulphate = 25 mg/L.

5.2.3.2 Batch Studies in Presence of Iron

Effects of initial iron and sulphate concentration:

Figure 5.10, 5.11, 5.12, 5.13 and 5.14 represents effects of initial iron concentration of 1.0, 2.0, 3.0, 4.0 and 5.0 mg/L, respectively. Irrespective of initial iron concentration (up to 5.0 mg/L), nitrate and arsenic removal was not affected in batch reactors. Up to an initial 3.0 mg/L, iron in the treated water was always below detection limit. However, 0.23 mg/L (94% removal) and 0.48 mg/L (90% removal) of iron concentration was observed in the treated water at 4.0 mg/L and 5.0 mg/L of initial iron. The possible reason for this higher iron concentration (0.48 mg/L) in treated water might be due to unavailability of sufficient sulphides for precipitation as iron sulphides. Therefore another set of experiment was conducted with an increased initial sulphate concentration of 50 mg/L (Figure 5.15). Iron in the treated water now reduced below 0.3 mg/L at initial sulphate of 50 mg/L. Better removal of iron with the increase in influent sulphate was due to availability of sufficient sulphide to react with iron to form iron sulphide precipitate. Although sulphate and COD were gradually reduced during entire period of 7 days operation, reduction rate decreased after about 3-4 days of reaction. COD of only 27-30 mg/L and 22-25 mg/L remained in the effluent after 4 days and 7 days of operation, respectively. The pH of the effluent increased with the biodegradation of sulphate. This could have been due to formation of alkalinity due to reduction of sulphate. Microbial mass (MLVSS) concentration started decreasing after initial increase for first 2-3 days of operation. This might be due to unavailability of sufficient food (COD) in the media leading to net growth negative. In all the cases complete removal of nitrate from its initial 50 mg/L was noticed within first day of operation and therefore it has not been plotted in any of the above given figures.

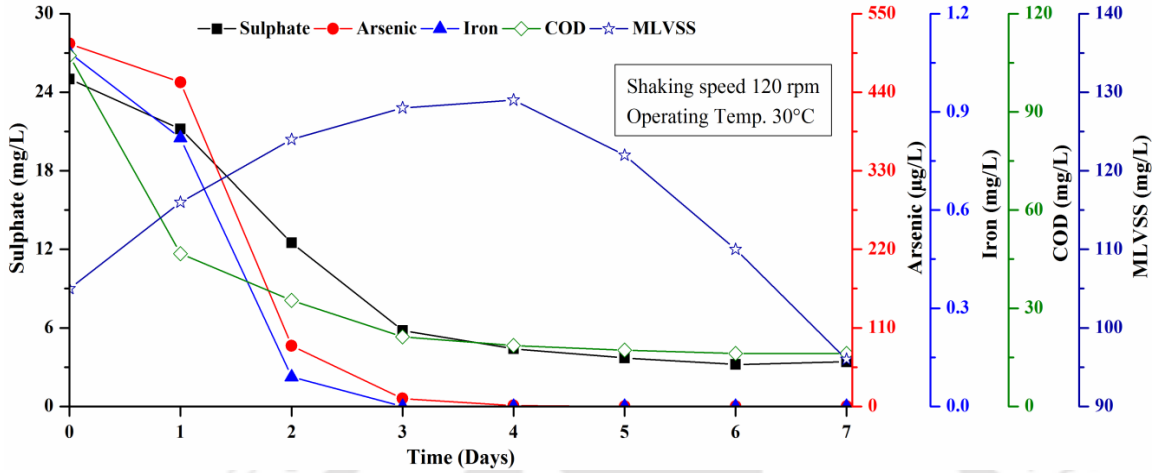


Figure 5.10 Performance of batch shake flasks in presence of iron at initial iron = 1.0 mg/L, arsenic = 500 µg/L, nitrate = 50 mg/L and sulphate = 25 mg/L.

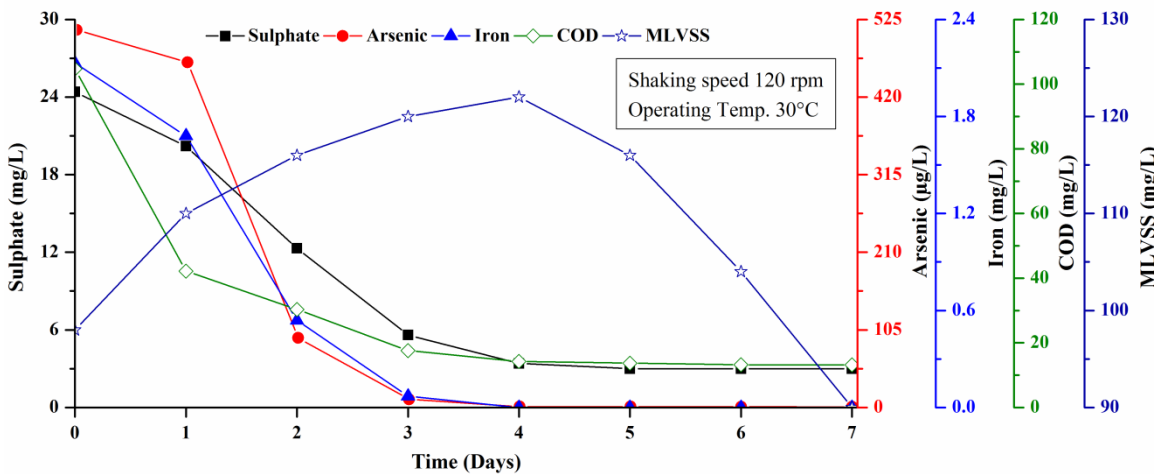


Figure 5.11 Performance of batch shake flasks in presence of iron at initial iron = 2.0 mg/L, arsenic = 500 µg/L, nitrate = 50 mg/L and sulphate = 25 mg/L.

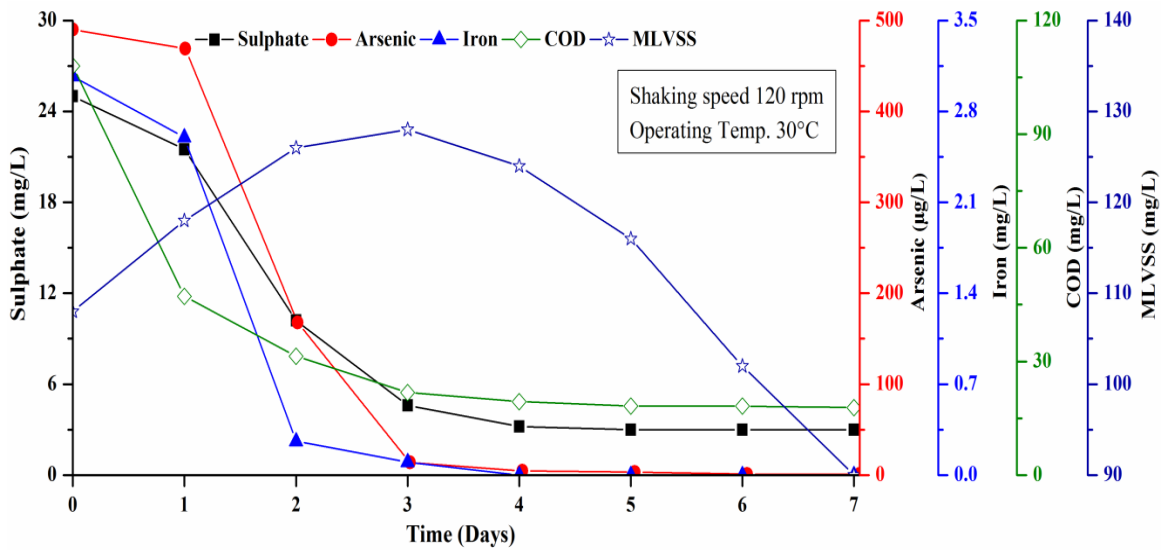


Figure 5.12 Performance of batch shake flasks in presence of iron at initial iron = 3.0 mg/L, arsenic = 500 µg/L, nitrate = 50 mg/L and sulphate = 25 mg/L.

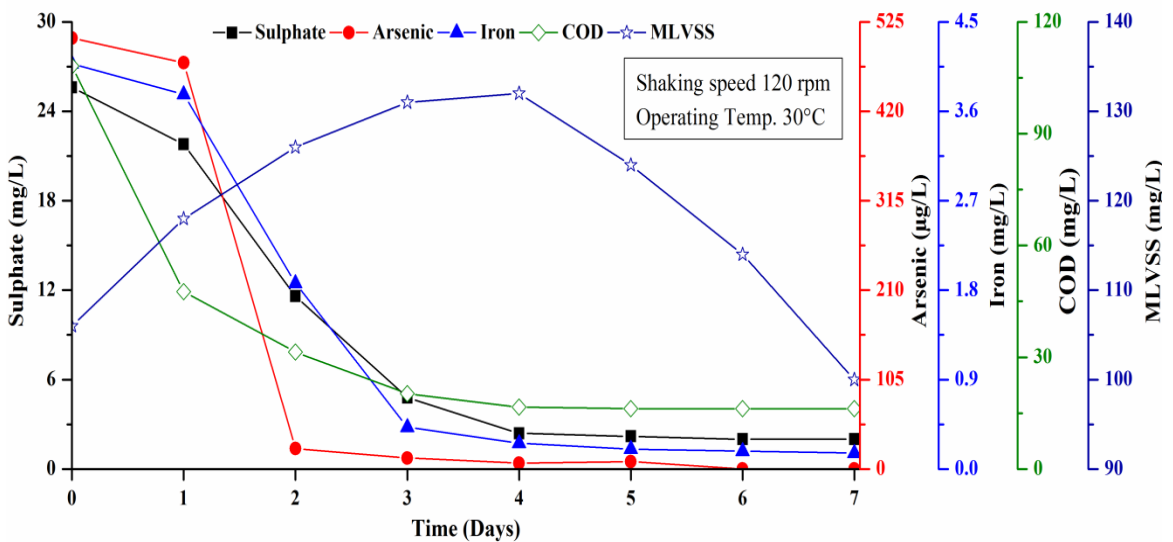


Figure 5.13 Performance of batch shake flasks in presence of iron at initial iron = 4.0 mg/L, arsenic = 500 µg/L, nitrate = 50 mg/L and sulphate = 25 mg/L.

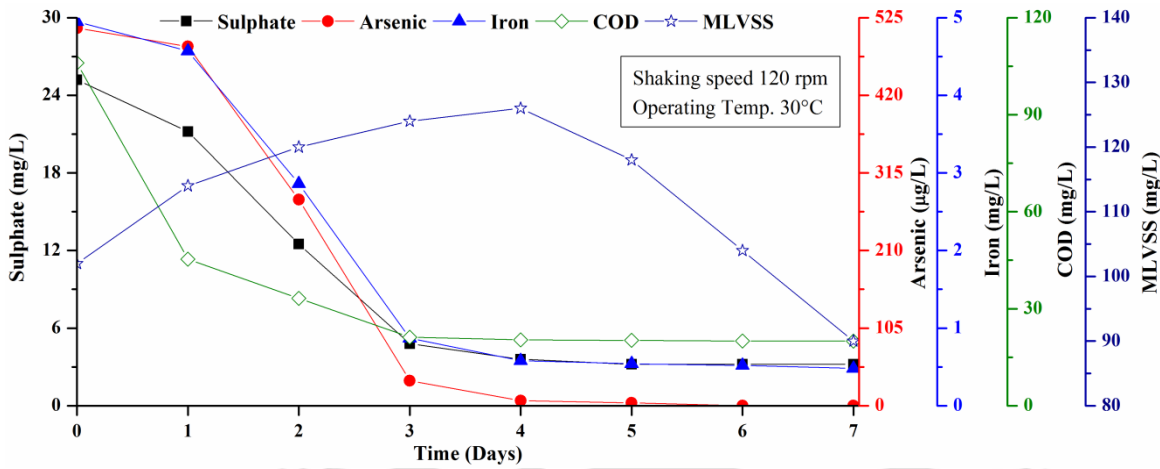


Figure 5.14 Performance of batch shake flasks in presence of iron at initial iron = 5.0 mg/L, arsenic = 500 µg/L, nitrate = 50 mg/L and sulphate = 25 mg/L.

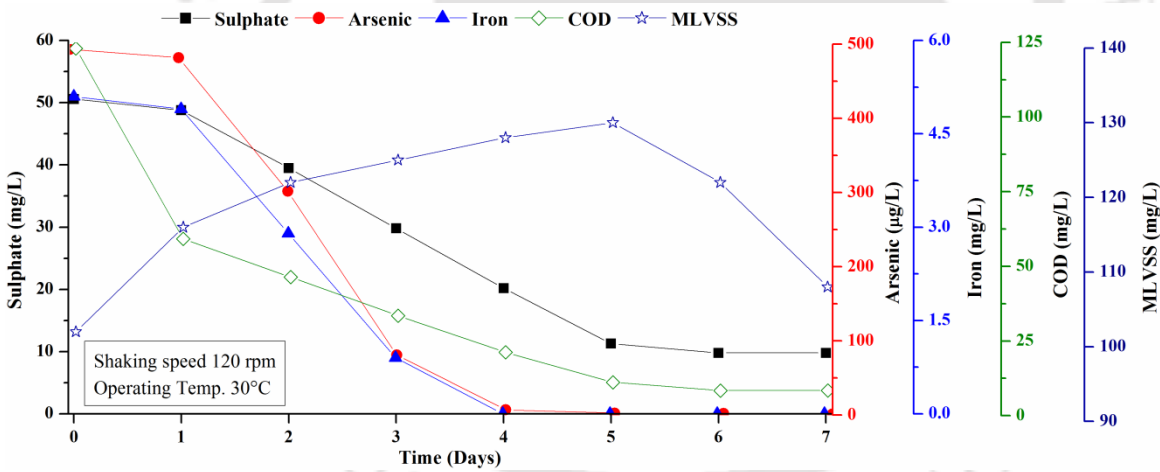


Figure 5.15 Performance of batch shake flasks in presence of iron at initial iron = 5.0 mg/L, arsenic = 500 µg/L, nitrate = 50 mg/L and sulphate = 50 mg/L.

Effects of initial arsenic concentration:

Figure 5.12, 5.16, 5.17 and 5.18 represent the performance of mixed bacterial culture in batch shake flasks at four different initial arsenic concentrations of 500 µg/L, 600 µg/L, 750 µg/L and 1000 µg/L, respectively. Irrespective of initial concentration, arsenic in the treated water was reduced below permissible limit (10 µg/L) in 3-5 days of reaction and finally averaged 7 ± 2 µg/L with 98.5% removal efficiency. Variation in

COD, sulphate, pH and MLVSS concentration followed similar trend as observed in previous experiments. The higher arsenic removal is possibly due to formation of arsenosulphides as well as co-precipitation and/or adsorption with iron sulphides in presence of iron (Altun et al., 2014).

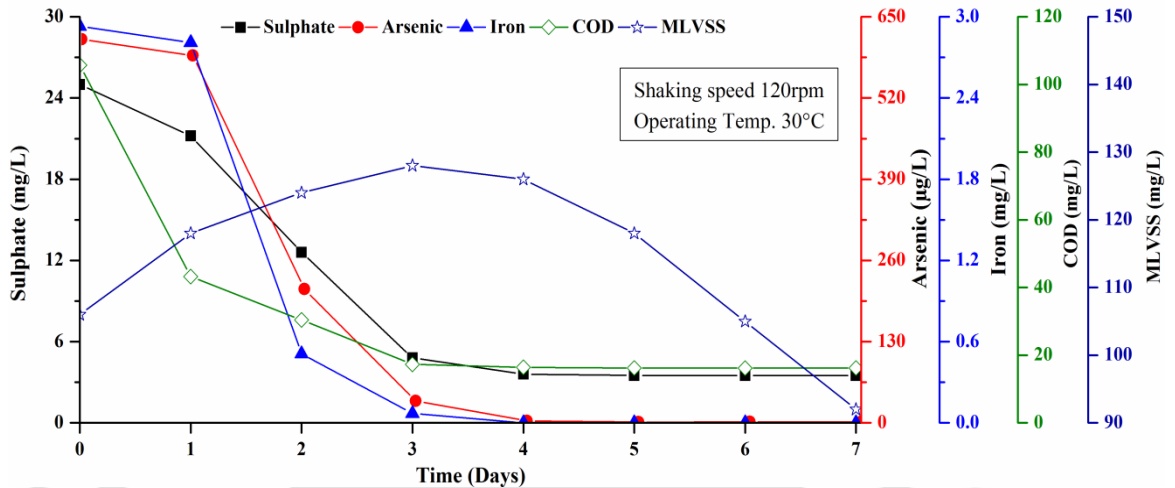


Figure 5.16 Performance of batch shake flasks in presence of iron at initial iron = 3.0 mg/L, arsenic = 600 µg/L, nitrate = 50 mg/L and sulphate = 25 mg/L.

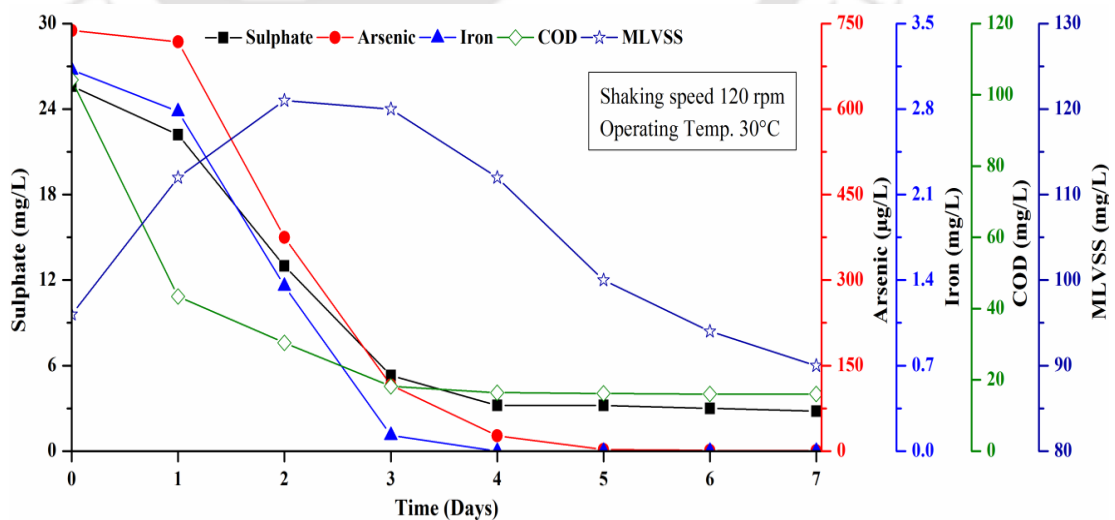


Figure 5.17 Performance of batch shake flasks in presence of iron at initial iron = 3.0 mg/L, arsenic = 750 µg/L, nitrate = 50 mg/L and sulphate = 25 mg/L.

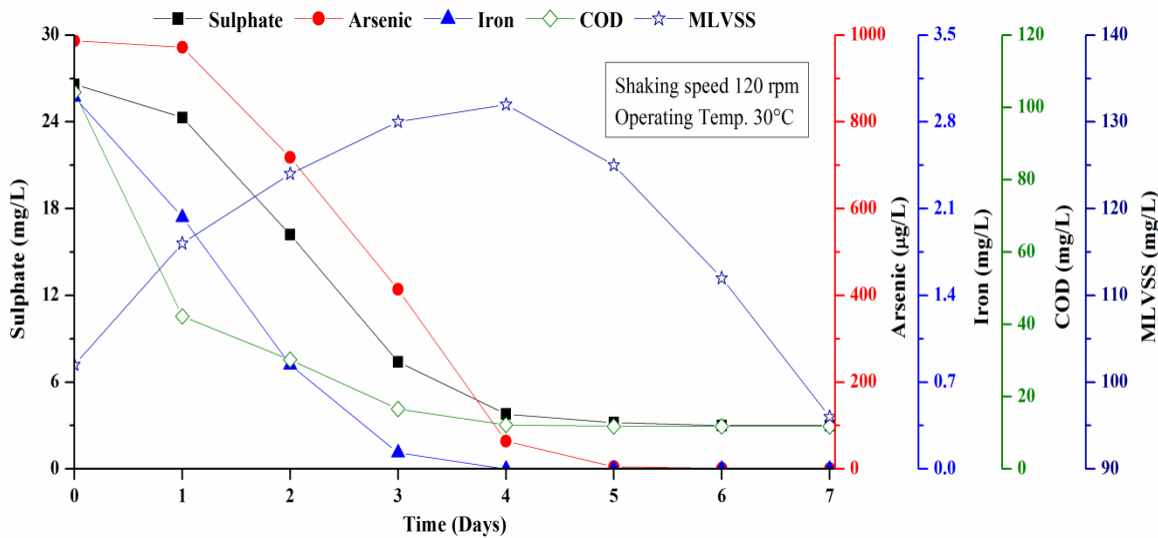


Figure 5.18 Performance of batch shake flasks in presence of iron at initial iron = 3.0 mg/L, arsenic = 1000 µg/L, nitrate = 50 mg/L and sulphate = 25 mg/L.

Effects of initial nitrate concentration:

Figure 5.12, 5.19 and 5.20 represents effects of initial nitrate concentration of 50, 100 and 150 mg/L on performance of mixed bacterial culture in batch shake flasks. Irrespective of initial nitrate concentration (up to 150 mg/L), arsenic in the treated water was found to be below 10 µg/L within first 4-6 days of operation. Nitrate in the treated water was always less than the detection limit within one day for all the tested concentrations and therefore, not shown in any of the figures. Variation in sulphate and MLVSS concentration followed similar trend as observed at varying arsenic concentration. Slight increase in MLVSS formation was observed and this is expected due to more biomass formation at higher nitrate concentrations of 100 and 150 mg/L. Similarly little more increase in pH with time was also noticed due to more alkalinity formation at higher nitrate concentrations.

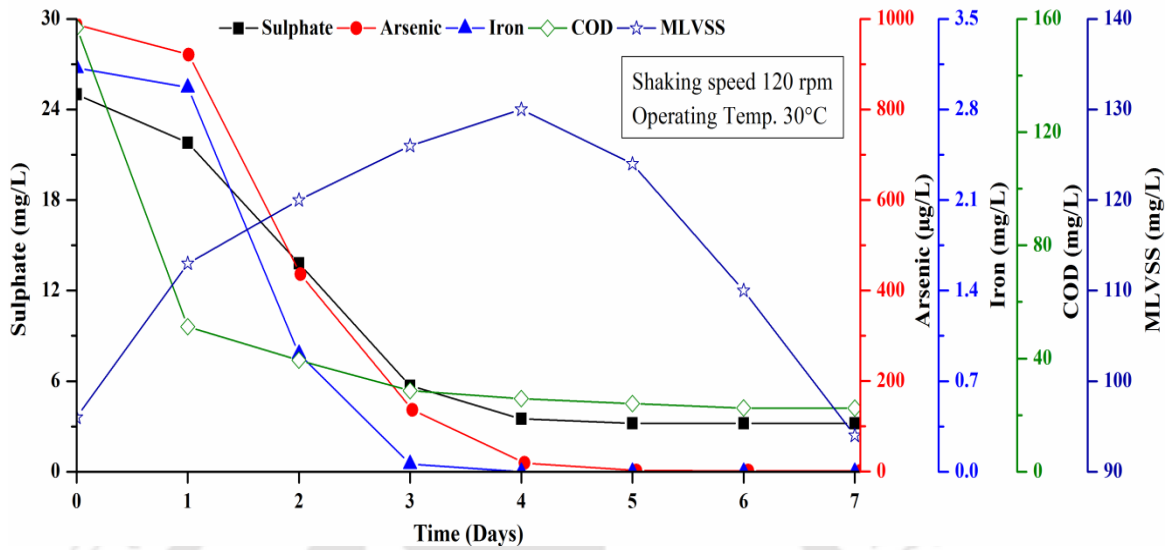


Figure 5.19 Performance of batch shake flasks in presence of iron at initial iron = 3.0 mg/L, arsenic = 1000 µg/L, nitrate = 100 mg/L and sulphate = 25 mg/L.

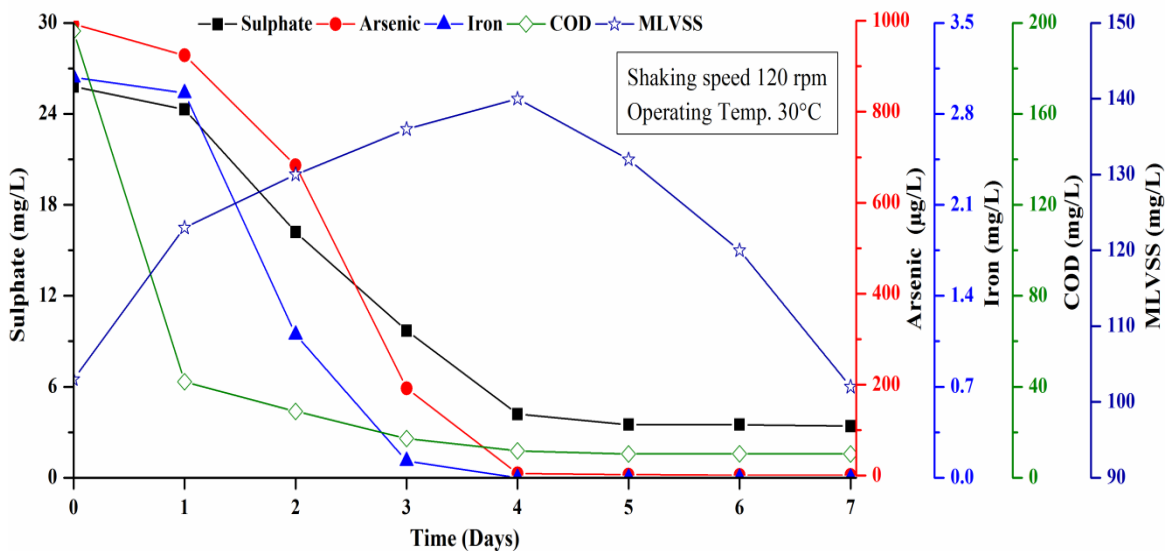


Figure 5.20 Performance of batch shake flasks in presence of iron at initial iron = 3.0 mg/L, arsenic = 1000 µg/L, nitrate = 150 mg/L and sulphate = 25 mg/L.

5.3 Performance Evaluation of Semi-batch Bioreactor SmBR-1 in Absence of Iron

Removal of arsenic, effects of HRT, initial arsenic, initial NO_3^- concentration and different carbon sources on the performance of mixed bacterial consortia in semi-batch bioreactors in absence of iron are studied at different phases as given in Table 4.3, and the results are discussed in this section.

5.3.1 SmBR-1 Phase-1: Effect of HRT

The performance of SmBR-1 in phase-1 is given in Figure 5.21. The SmBR-1 was first operated at 6 days HRT. Arsenic, SO_4^{2-} and COD were gradually decreased with time and become almost constant after about 30 days of operation. Arsenic concentration reduced by about 94% to slightly more than the permissible limit of in drinking water. No nitrate or nitrite was found in the treated water indicating complete removal of nitrate. Although, sulphate reduction was poor in first few days, it improved after 21 days of operation. This might be due to slower adaptation of SRBs than other microbial population in the heterogeneous mixed microbial consortia during the start-up period (first 10-15 days) in the SmBR-1 (Kalyuzhnyi & Fedorovich, 1998). The overall SO_4^{2-} and COD removal was 70% and 88% respectively at the end of 6 days HRT.

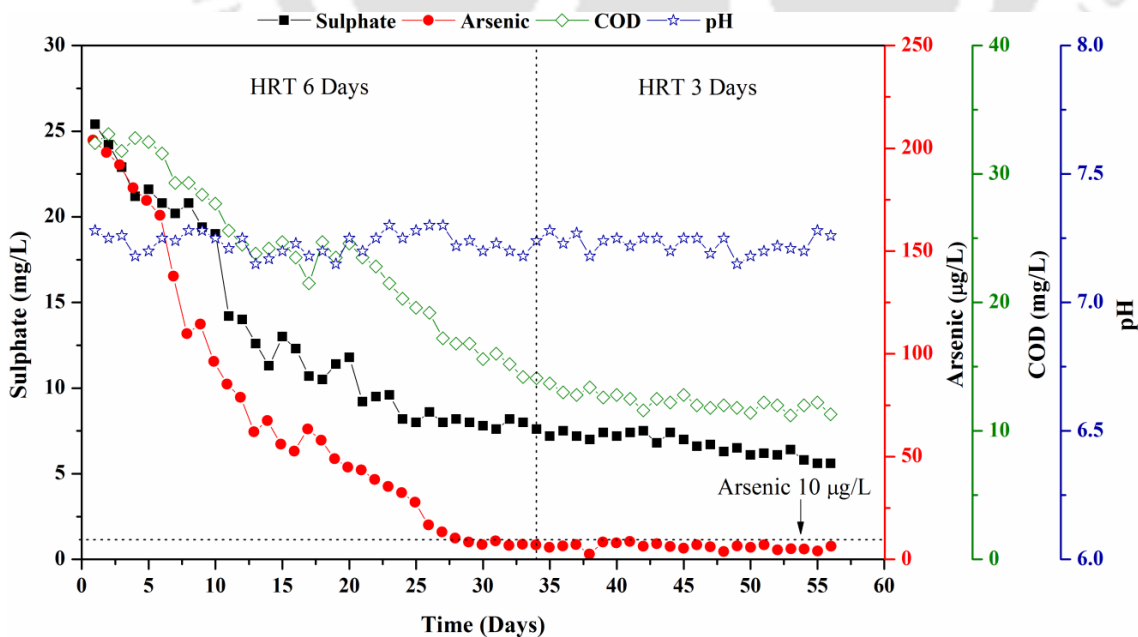


Figure 5.21 Performance evaluation of SmBR-1 in phase-1 at initial arsenic = 200 µg/L, nitrate = 50 mg/L and sulphate = 25 mg/L.

After attaining the stability in the reactor performance, the HRT was changed to 3 days. The SmBR-1 performance was not negatively affected at 3 days HRT from day 34 to day 56. This might be due to well adaption of microbial communities in the reactor. The maximum and minimum arsenic and COD in the treated water were 8 and 4 $\mu\text{g/L}$ and 13 and 11 mg/L during last 20 days of operation. The average values were 6 ± 1.5 $\mu\text{g/L}$ and 12 ± 0.5 mg/L, respectively. The pH of treated water remained between 7 and 7.5 during the entire period of operation.

5.3.2 SmBR-1 Phase-2: Effect of Initial Arsenic Concentration

Figure 5.22 represents the effects of initial arsenic concentration of 200, 300, 400, 500 600, 700 and 800 $\mu\text{g/L}$ in SmBR-1. As observed at 200 $\mu\text{g/L}$ of initial arsenic, complete nitrate removal occurred within 24 hours of operation concludes no adverse effects even up to an initial arsenic concentration 800 $\mu\text{g/L}$. Performance on SO_4^{2-} and COD removal was also remained same to that in the previous phase with only 6 ± 0.5 mg/L and 12.5 ± 0.6 mg/L in the treated water, irrespective of the initial arsenic concentrations studied.

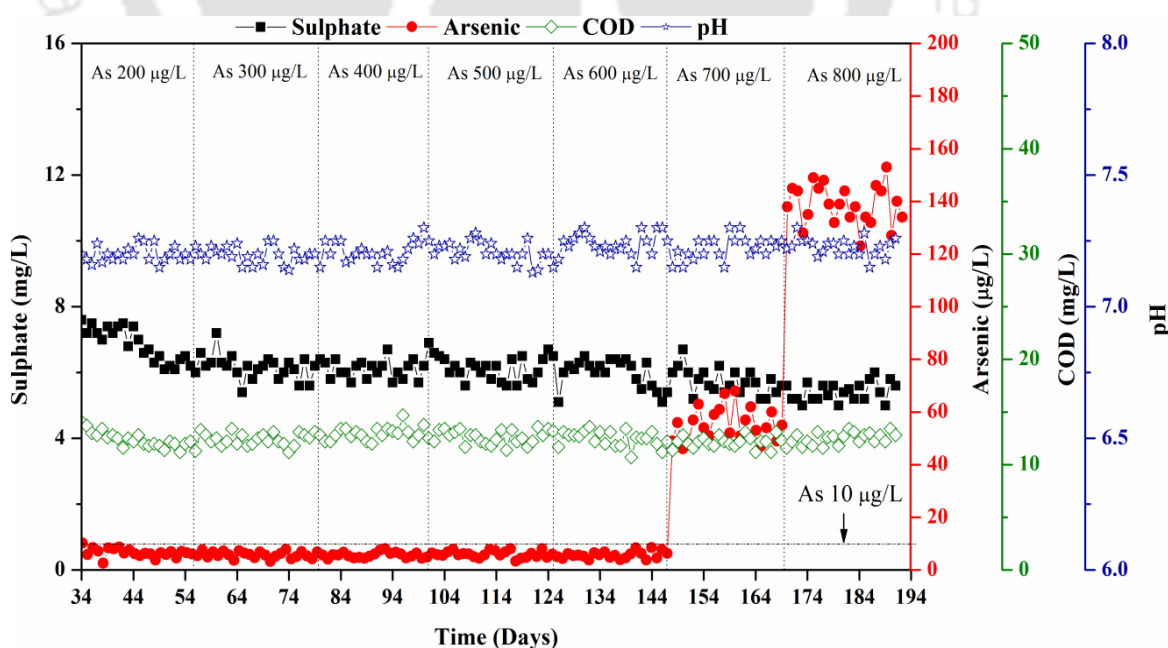


Figure 5.22 Performance evaluation of SmBR-1 in phase-2 at initial arsenic = 200-800 $\mu\text{g/L}$, nitrate = 50 mg/L and sulphate = 25 mg/L.

Arsenic in the treated water remained below permissible limit of 10 $\mu\text{g/L}$ when the initial arsenic was 600 $\mu\text{g/L}$ or less. Whereas arsenic in treated water averaged 55 and 138 $\mu\text{g/L}$ with 92% and 83% removal efficiency at initial arsenic concentration of 700 and 800 $\mu\text{g/L}$ respectively. The pH remained between 7.0 and 7.3 throughout the experiment.

5.3.3 SmBR-1 Phase-3: Effect of Initial Nitrate Concentration

The effects of initial nitrate concentration of 50, 100, 150, 200 and 250 mg/L is summarised in Figure 5.23. Irrespective of initial NO_3^- concentration (up to of 250 mg/L) arsenic in the treated water was found always below 10 $\mu\text{g/L}$. Efficient arsenic removal (up to 98%) was seen even at highest NO_3^- concentration of 250 mg/L. However, the nitrate in the treated water was always less than the detection limit and therefore, not shown in the figure. SO_4^{2-} and COD concentration in the treated water was remained between 6 and 8 mg/L, and 12 and 17 mg/L, respectively, in the treated water. Increase in pH was more in the reactor when initial nitrate concentration was higher justifying alkalinity formation during denitrification. However, pH in the reactor always remained below 7.5.

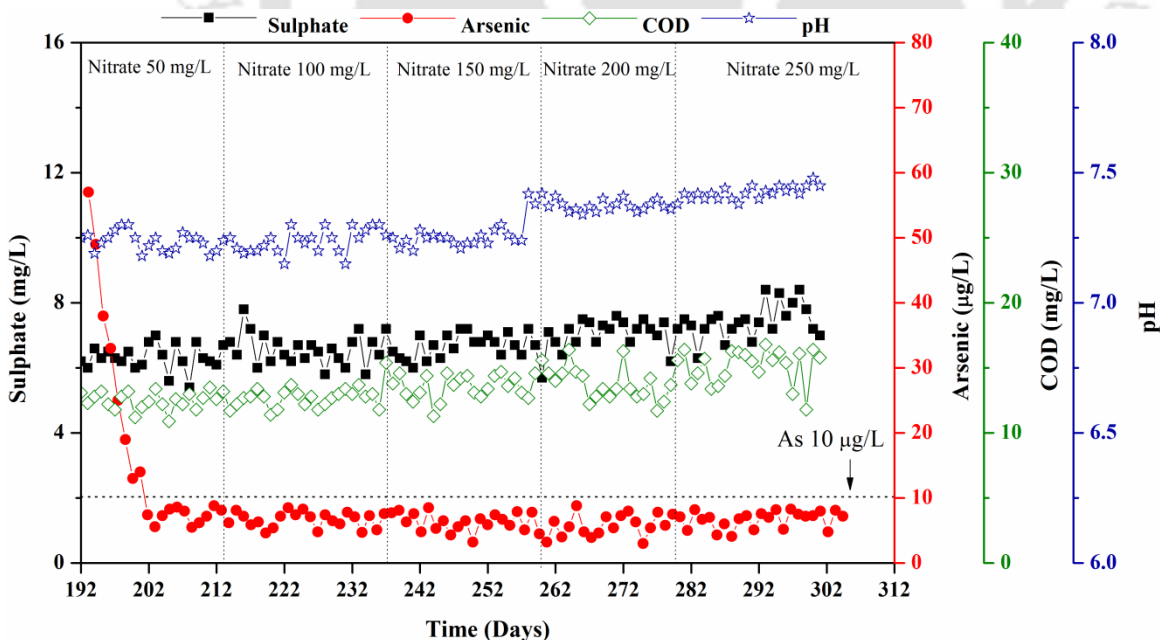


Figure 5.23 Performance evaluation of SmBR-1 in phase-3 at initial nitrate = 50-250 mg/L, arsenic = 600 $\mu\text{g/L}$ and sulphate = 25 mg/L.

5.3.4 SmBR-1 Phase-4: Effect of Different Carbon Sources

Among the five carbon sources used in reactor acetate, malate, succinate, lactate and glucose, the mixed bacterial culture showed the best performance by utilizing glucose as the sole carbon source. The performance of SmBR-1 with the five carbon sources on arsenic, sulphate, nitrate and COD removal is shown in Figure 5.24. Nitrate in the treated water was below detection limits with all the tested carbon sources. Arsenic removal was the best to below detection limit when glucose was used as the carbon source. The SO_4^{2-} and COD removal was 90% and 89.5%, respectively. Lactate and succinate was the second best carbon sources resulted in 98%, 84%, and 94% arsenic, sulphate and COD removal, respectively. Malate is also utilized effectively in our experiment for arsenic removal. Only 68% sulphate removal was seen with malate as carbon source, however, it was not affecting the arsenic and nitrate removal in SmBR-1. Lactate, succinate and malate are reported as preferred carbon sources for SRB among organic acids under mesophilic operating conditions (Costa et al., 1996; Hao et al., 1996; Liamleam & Annachatre, 2007). Kesserú et al. (2002) reported succinic acid as best carbon source for denitrification among succinic acid, acetic acid and ethanol.

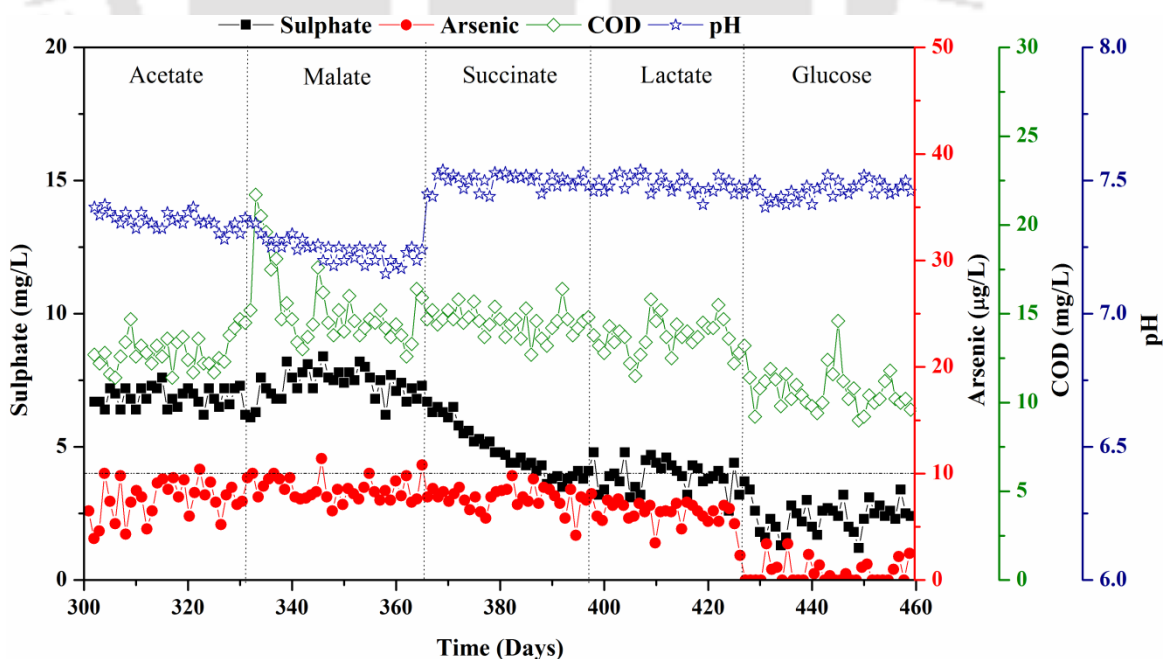


Figure 5.24 Performance evaluation of SmBR-1 in phase-4 at initial nitrate = 200 mg/L, arsenic = 600 µg/L and sulphate = 25 mg/L.

Around 72% sulphate removal efficiency was observed in the case of using acetate as the sole carbon source provided 98% arsenic removals. The poor efficiency of the mixed consortium to reduce sulphate using acetate could be due to inability of the SRB to completely oxidize acetate even with excess sulphate levels (Lens et al., 2002). SRB are generally poor competitors of methanogenic archaea (MA) for acetate. However, in a long-term operation, SRB gradually out compete MA in a sulphidogenic reactor due to their higher affinity for the substrate and higher substrate removal rate. Moreover, SRB also have a thermodynamic advantage over methanogens and acetogens in terms of the standard free energy change of the acetate oxidation. *Desulfotomaculum* genus among SRB generally consumes acetate. In addition most of the published research regarding drinking water denitrification involves the use of methanol, ethanol and acetic acid (Mohseni-Bandpi et al., 2013; Park & Yoo, 2009). Different species of *Pseudomonas* were found to be the dominant bacterial species in acetate fed denitrifying bioreactors. High sulphate and nitrate removal efficiency in the experimental results indicates the presence and growth of sulphate and nitrate reducers. The pH of the treated water was in the range of 7.2-7.5 for all carbon sources studied during the entire phase. For glucose as carbon source showing the best performance may be because of the fact that sugar is an effective electron donor that is easily degraded under anaerobic conditions and glucose supports the growth of a wide variety of nitrate as well as sulphate reducing bacteria leading to increased microbial diversity and treatment system resilience (Akunna et al., 1993; Liamleam & Annachatre, 2007; Mohseni-Bandpi et al., 2013). Similar performance in presence of other carbon sources might be due to the fact that the anaerobic degradation pathway of sugar such as glucose, fructose, and dextrose are also similar to that of many other organic compounds (Liamleam & Annachatre, 2007).

5.4 Performance Evaluation of Semi-batch Bioreactor SmBR-2 in Presence of Iron

Performance of semi batch reactor, SmBR-2, which was operated in presence of iron as per the schedule given in Table 4.4, is discussed in this section.

5.4.1 SmBR-2 Phase-1: Effect of HRT

Figure 5.25 represents the performance of SmBR-2 during phase-1 operation. The SmBR-2 was started with a HRT of 6 days and initial arsenic, NO_3^- and SO_4^{2-} concentration of 250 $\mu\text{g/L}$, 100 mg/L and 25 mg/L respectively with COD of 153 mg/L . Like SmBR-1, complete removal of NO_3^- was observed within one day of operation. Some instability in the treated water iron concentration observed in the initial periods of start-up might be associated with poor sulphate reduction in SmBR-2. Once sulphate reduction was well stabilized the iron in the treated water was always below detection limit. SmBR-2 showed a maximum arsenic, SO_4^{2-} and COD removal of 99%, 78% and 92% respectively at 6 days HRT. After attainment of steady state in terms of arsenic removal the HRT was changed to 3 days. The SmBR-2 performance was not negatively affected due to reduction in HRT (to 3 d) might be due to better adaptation of microbial population and attainment of steady state in the reactor. The treated water arsenic, SO_4^{2-} and COD values were averaged 1.5 \pm 1 $\mu\text{g/L}$, 5.7 \pm 0.3 mg/L and 11.5 \pm 0.5 mg/L corresponding to 99.4%, 77% and 92.5% removal respectively. The treated water pH remained between 7.0 and 7.4.

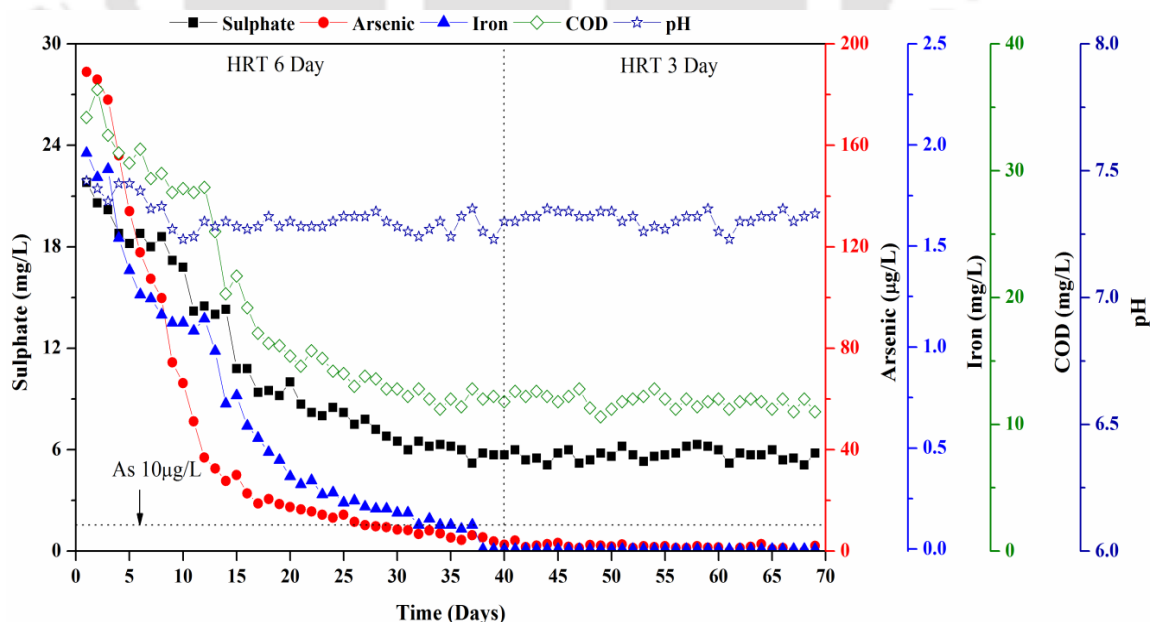


Figure 5.25 Performance evaluation of SmBR-2 in phase-1 at initial nitrate = 100 mg/L , arsenic = 250 $\mu\text{g/L}$, iron = 2 mg/L and sulphate = 25 mg/L .

5.4.2 SmBR-2 Phase-2: Effect of Initial Arsenic Concentration

Figure 5.26 represents the effects of initial arsenic concentration of 250, 350, 450, 550, 750 and 1000 $\mu\text{g/L}$ in SmBR-2. The SmBR-2 performance remained stable at all tested influent arsenic concentrations. Arsenic in the treated water was always reduced to below 10 $\mu\text{g/L}$ (99.5% removal) whereas iron and nitrate remained below detection limits. Moreover, increased initial arsenic concentration did not affect iron and/or NO_3^- removal. The COD and SO_4^{2-} removal did not showed significant differences during this phase. However, the SO_4^{2-} reduction was improved during this phase this might be due to well establishment of sulphate reducing communities in the reactor. The SO_4^{2-} and COD of only 5 ± 0.6 mg/L and 11.6 ± 0.6 mg/L remained in effluent at end of phase-2 operation of SmBR-2. The pH of treated water remained between 7.23 and 7.35 during the entire phase.

5.4.3 SmBR-2 Phase-3: Effect of Initial Nitrate Concentration

The effects of initial nitrate concentration of 100, 150, 200 and 250 mg/L is summarised in Figure 5.27. Irrespective of initial NO_3^- concentration (up to 250 mg/L), arsenic in the treated water was found below 10 $\mu\text{g/L}$, with more than 99% removal efficiency. Nitrate and iron in the treated water was always less than the detection limits.

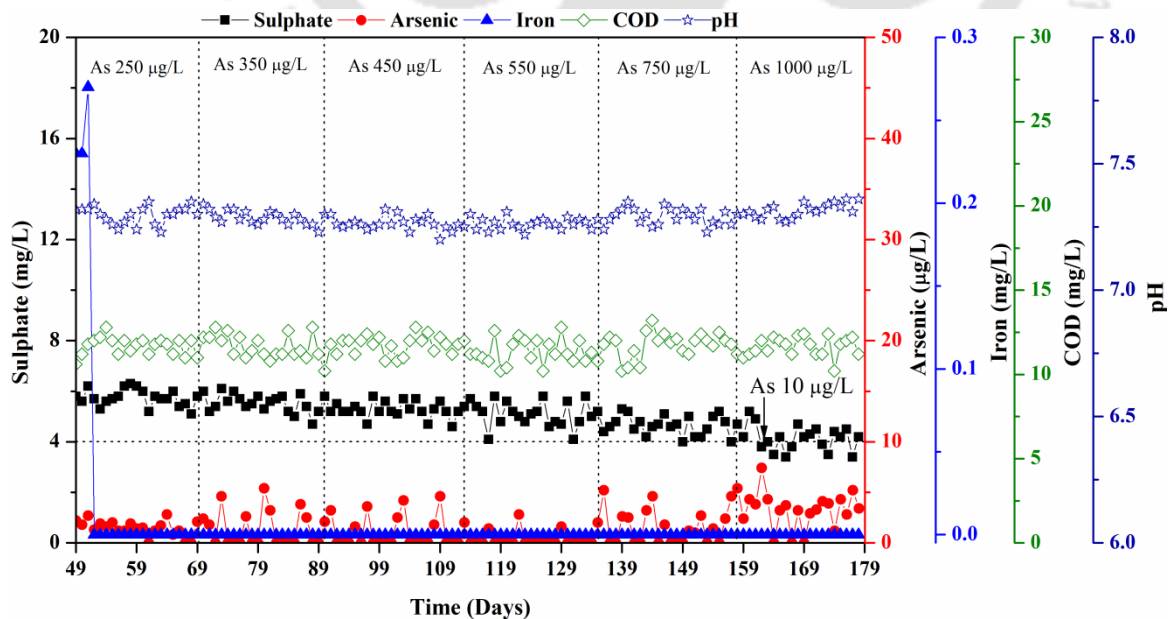


Figure 5.26 Performance evaluation of SmBR-2 in phase-2 at initial nitrate = 100 mg/L, arsenic = 250-1000 $\mu\text{g/L}$, iron = 2 mg/L and sulphate = 25 mg/L.

Thus the performance of SmBR-2 was stable in terms of arsenic and iron removal with the increase of the influent nitrate. Variation in SO_4^{2-} and COD concentration followed similar trend as observed in phase-2. The SO_4^{2-} and COD removal efficiencies remained on average values of 79.6% and 92.5% respectively. pH trend was varied between 7.3 and 7.5.

5.4.4 SmBR-2 Phase-4: Effect of Different Carbon Sources

The performance of SmBR-2 on arsenic, iron and nitrate removal with the five different carbon sources is shown in Figure 5.28. Among the five carbon sources used in SmBR-2, the mixed bacterial culture showed the best performance with glucose. Almost 100% nitrate, iron and arsenic removal was achieved with all the carbon sources. Glucose was found to be best electron donor in terms of sulphate and COD removal with 93% and 96% removal respectively. Despite of higher sulphate reduction with glucose, the arsenic, iron and nitrate removal remained unaffected with other carbon sources.

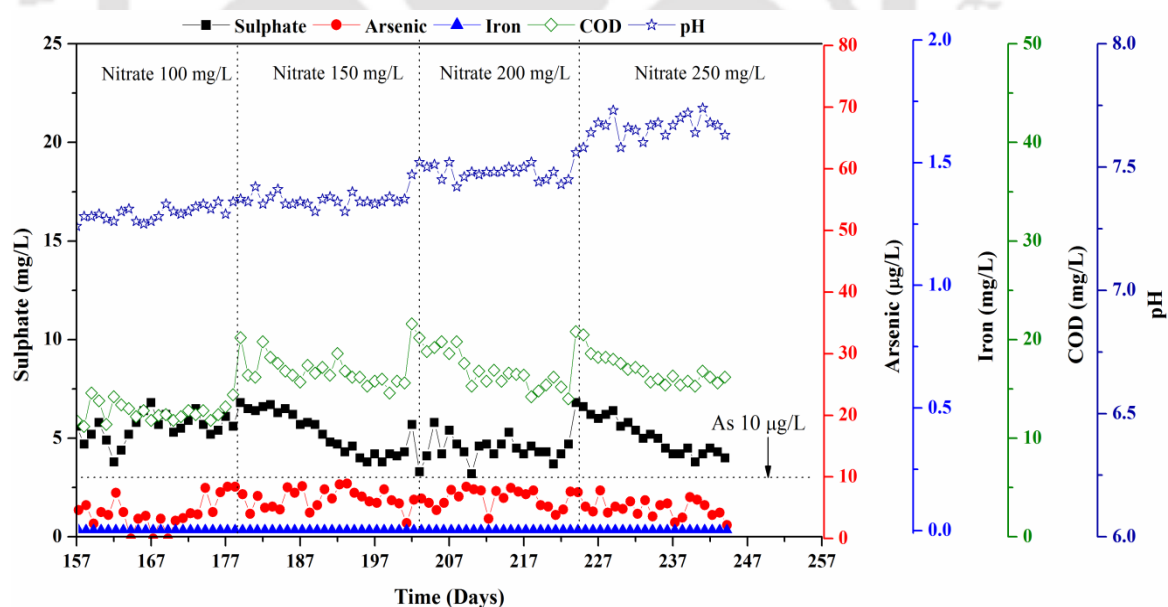


Figure 5.27 Performance evaluation of SmBR-2 in phase-3 at initial nitrate = 100-250 mg/L, arsenic = 1000 µg/L, iron = 2 mg/L and sulphate = 25 mg/L.

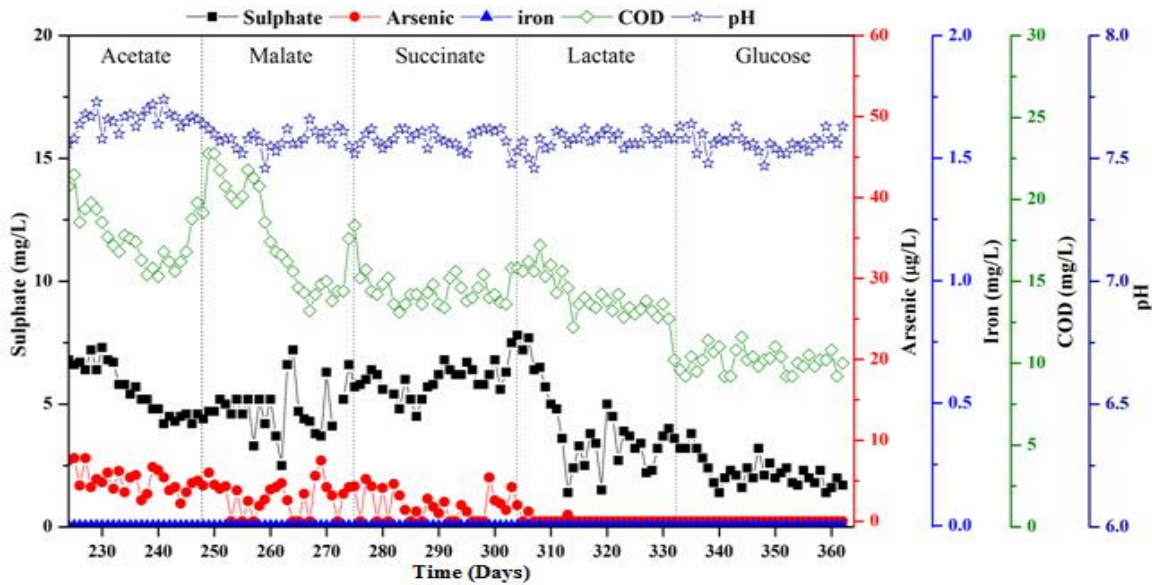


Figure 5.28 Performance evaluation of SmBR-2 in phase-4 at initial nitrate = 250 mg/L, arsenic = 1000 µg/L, iron = 2 mg/L and sulphate = 25 mg/L.

5.5 Performance Evaluation of the Flow through Attached Growth Reactor, AGR-1

The flow through attached growth reactor, AGR-1 was operated in absence of iron in the influent. After start-up, operation of AGR-1 was divided into 8 phases (Table 4.6). In this section performance of AGR-1 has been discussed in details.

5.5.1. AGR-1 Start-up

After inoculation, AGR-1 was operated for a period of 82 days to obtain an appreciable colonization of mixed microbial consortia on the WAC granules in the reactor as well as to get consistent performance. The performance of the reactor during this period was characterized by COD and sulphate removal efficiency. COD removal was gradually increased to 83-85% during the end of this period leaving about 12-16 mg/L of COD in the treated water (Figure 5.29), with 100% nitrate removal after the very first day. Arsenic removal started gradually with onset of sulphate reduction and reduced by about 95% on day 82 when sulphate removal was about 74%. Based on stoichiometric calculations to utilize all electron acceptors COD of 91 mg/L was used to carry out the start-up phase in the reactor. Low sulphate reduction efficiencies were observed during

this experimental period (i.e. average values of 35% in first 35 days and reached up to maximum 60% in next 27 days) and almost no arsenic removal was observed in first 35 days. This was probably due to the heterogeneous seed sludge used as source of inoculum. SRB showed a slower adaptation to the system than other active microorganisms in the biofilm (D'Acunto et al., 2011; Frunzo et al., 2012).

After 43 days operation, COD in the influent was increased to 105 mg/L to evaluate the performance of the reactor in terms of contaminants removal at 90 min EBCT. The increase in COD resulted in better sulphate removal and which in turn lead better arsenic removal in AGR-1. Arsenic concentration reduced to below the permissible limits in drinking water and only 3-7 $\mu\text{g/L}$ remained in the treated water after 82 days of operation. The reactor was continued to operate up to 114 days, under the same conditions when the overall arsenic and SO_4^{2-} removal was 97% and 80% respectively, at the end period of the start up phase of AGR-1. The result showed that arsenic removal followed sulphate reduction in the reactor. Apart from the permanent characteristic odour of the sulphide in the treated water samples, the establishment of the biofilm was indirectly checked by the systematic pH monitoring and analysis of nitrate, sulphate, arsenic and COD concentrations in the treated water.

5.5.2 AGR-1 Phase-1: Effects of EBCT and Backwash Frequency

The performance of AGR-1 during phase-1 is also shown in Figure 5.29. AGR-1 was first operated at 90 min EBCT when arsenic removal was around 97%. Complete NO_3^- removal was seen after the first day of the reactor operation hence nitrate profile has not been plotted in the given figure. Only about 2-5 mg/L of SO_4^{2-} and 11-14 mg/L of COD remained in the treated water after about 80% and 87% removal, respectively. After attaining the consistent results, the EBCT was reduced to 60 min. on day 115. The performance remained same and therefore, the EBCT was further reduced to 45 min. on day 137 of operation. During the above periods, the reactor was operated with 50 mg/L, 25 mg/L, and 200 $\mu\text{g/L}$ of initial NO_3^- , SO_4^{2-} and arsenic respectively, The effluent nitrate was remaining undetected while around 98% arsenic removal was observed. The effluent arsenic concentration was below the drinking water permissible limit of 10 $\mu\text{g/L}$. The SO_4^{2-} and COD removal were between 76% and 87% with an average value of 5.9 mg/L and 13.4 mg/L respectively at 45 min. EBCT. As no negative effect was observed on

reactor performance further experiments were carried out at 45 min EBCT and influent COD was 105 mg/L.

Effect of Backwash Frequency

The first backwashing was done on day 49, followed by backwashing of the reactor at an interval of 7 days till 114th day. The backwash frequency was kept 7 days during this period of operation because frequent backwashing in earlier stage of biofilm formation may cause loss of biomass from reactor. Thus, in order to promote a stable biofilm on WAC granules the backwashing of the reactor was done at an interval of 7 days till 114th day. Once the arsenic removal in the reactor was reached in steady state, the reactor performance was evaluated at different backwash frequencies of 2, 3, 4 and 7 days between day 115 and 231.

The effect of backwash frequency on arsenic, SO_4^{2-} , COD and pH variations in effluent samples is shown in Figure 5.28. Irrespective of backwash frequency, the effluent NO_3^- was found below detection limit at all times hence not plotted in figure. At backwash frequency of 2 days, the effluent arsenic concentration after backwashing event remained below 10 $\mu\text{g/L}$ in the samples collected after 24 hour. The COD and SO_4^{2-} in the treated water was remained between 15.0 ± 1.6 mg/L and 5.4 ± 1.1 mg/L respectively. At backwash frequency of 3, 4 and 7 days, no change in arsenic, NO_3^- , SO_4^{2-} and COD removal efficiency was observed to that of 2 days was noticed. The arsenic removal efficiency was also remaining the same with 1.2-6.5 $\mu\text{g/L}$ in the treated water whereas SO_4^{2-} and COD removal efficiency was remained between 5.9 ± 1.6 mg/L and 13.5 ± 1.7 mg/L respectively. We observed no upset in arsenic removal at all backwash frequencies tested. With time, backwashing had no influence on NO_3^- and arsenic removal in AGR-1.

Irrespective of backwash frequency (from 2 days to 7 days) the backwashing never resulted in reduced system performance. This might be due to the formation of healthy biofilm and rapid growth of microorganisms for reformation of biofilm on the WAC immediately after dislodging of it during backwashing. The results indicated that longer backwash intervals between can be feasible in AGR-1, at least if biological performance is the criterion used for evaluation. These results were in line with previous laboratory scale studies conducted on biofilm reactors used in drinking water treatment (Brown et al., 2003; Choi et al., 2007).

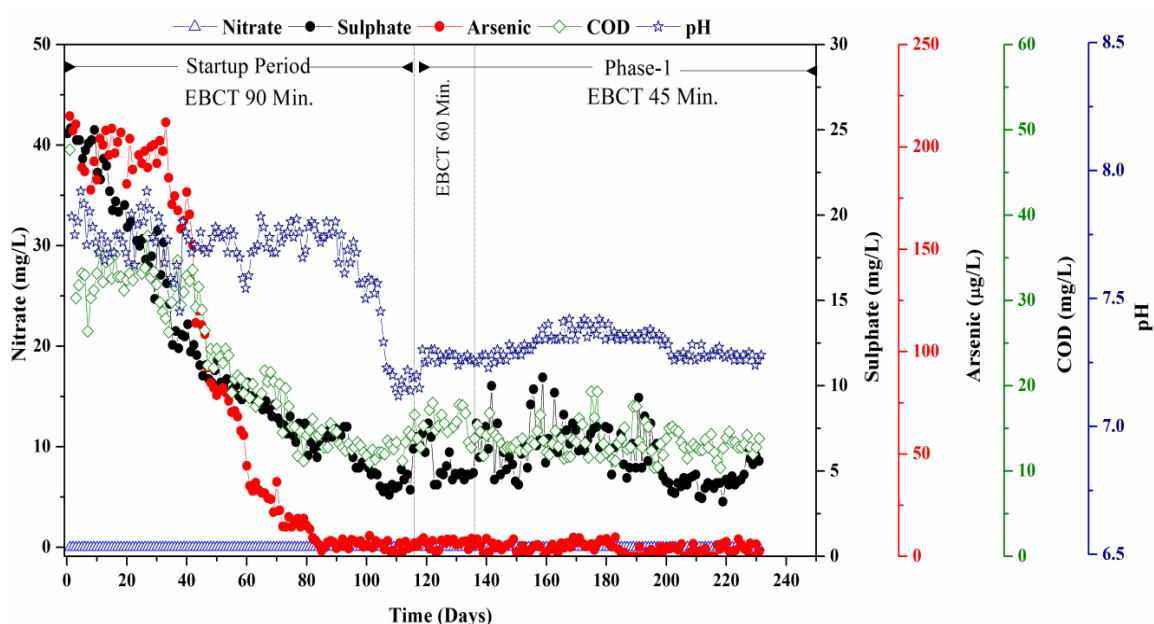


Figure 5.29 Performance evaluation of AGR-1 in start up and phase-1 at initial nitrate = 50 mg/L, arsenic = 250 µg/L, and sulphate = 25 mg/L.

Profile sampling: Profile samples taken during phase 1 on day 228, representing the concentration of various pollutants along the depth of the reactor is shown in Figure 5.30. Complete removal of NO_3^- and 17.5% SO_4^{2-} removal occurred in the 1st port. The significant sulphate removal (74.2%) was observed in the 3rd port. More than 90% arsenic removal was observed in the 3rd effluent port. A total of 99.2% arsenic and 82.8% sulphate removal were observed in 5th port. The COD removal also followed nitrate and sulphate removal and nearly 85.8% COD removal was observed in 5th port. Profile samples shows that only 1.8 µg/L arsenic, 3.4 mg/L of sulphate and 12.5 mg/L of COD were left in the final treated water.

Profile sampling data shows sequential utilization of electron acceptors present in the influent media was O_2 (if any residual DO present) followed by NO_3^{2-} , As(V) , and SO_4^{2-} . After nitrate reduction, arsenic removal was observed in port 3 because of formation of biogenic sulphides responsible for arsenic removal. Thus, arsenic removal in the reactor followed sulphate reduction. The sequential utilization of electron acceptors in the systems confirms the establishment of TEAP zones on the basis of thermodynamic favourability.

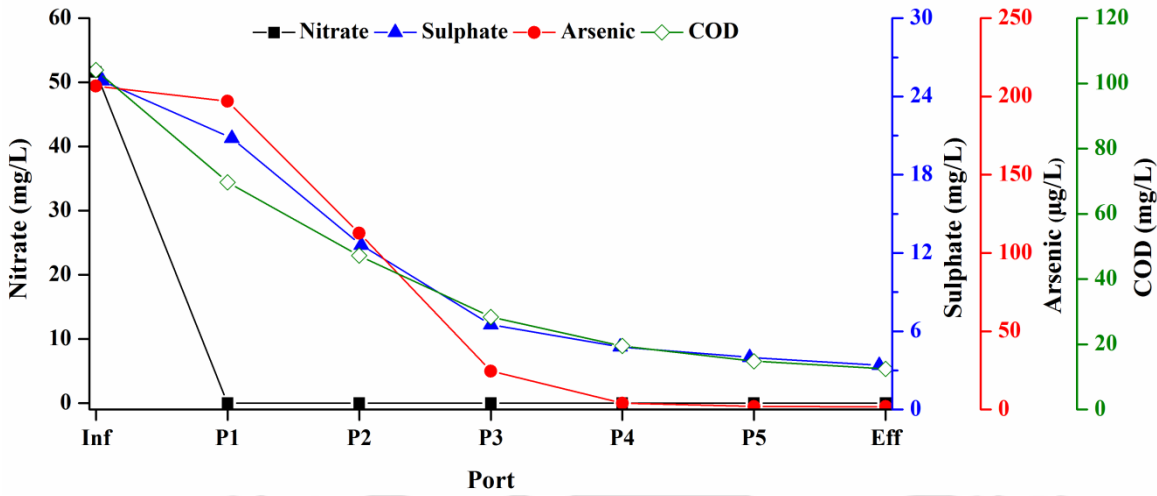


Figure 5.30 Sampling profile of the AGR-1 on day 228 (arsenic = 250 µg/L, nitrate = 50 mg/L, sulphate = 25 mg/L and EBCT 45 Min.).

5.5.3 AGR-1 Phase 2: Effect of Influent Arsenic Concentration

Figure 5.31 represents the effects of initial arsenic concentration of 200, 250, 350, 450, 550 650, and 750 µg/L on the performance of AGR-1.

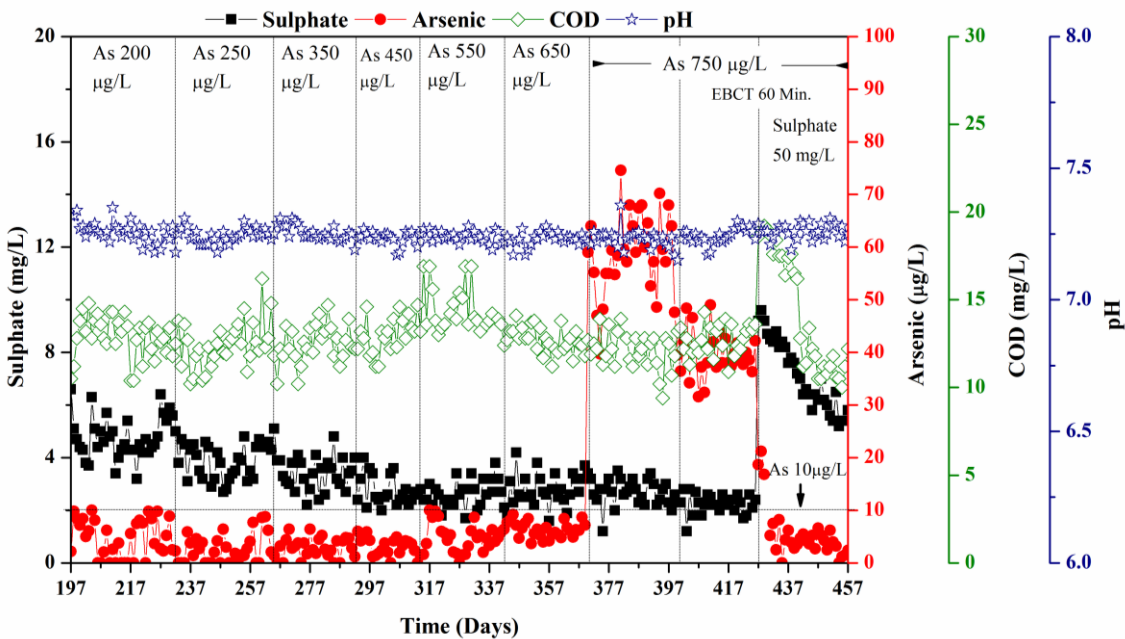


Figure 5.31 Performance evaluation of AGR-1 in phase-2 at initial nitrate = 50 mg/L, arsenic = 200-750 µg/L, and sulphate = 25 mg/L.

In the figure 5.31, initial arsenic concentrations in the influent are indicated at the top. The reactor could reduce to below 10 µg/L from an influent concentration of up to 650 µg/L. However, when the influent arsenic was 750 µg/L, 45 to 75 µg/L of it appeared in treated water. On increase in EBCT to 60 minutes (day 399-426, Table 4.6) arsenic concentration in the treated water was reduced but remained between 30 and 50 µg/L. On day 427, sulphate in the influent was enhanced to 50 mg/L, which results in decreasing arsenic concentration in the treated water well below drinking water standards of 10 µg/L. Sulphate concentration in the treated water gradually decreased with the increase in the influent arsenic concentration with the lowest of near about 2-3 mg/L remained during the operation of AGR-1 at 60 min EBCT and 750 µg/L of influent arsenic (day 427-457, Fig 5.31). As sulphate reduction leads to formation of sulphides that combines with arsenic to form arsenosulphide precipitates, non-availability of sufficient sulphides might be the reason for appearance of higher concentration of arsenic in the treated water. On increase in influent sulphate concentration to 50 mg/L from day 427, improvement in the treated water quality in terms of arsenic concentration is clearly visible.

COD in the treated water was found always between 10 and 13 mg/L except a few data that exceeded 15 mg/L. COD in the treated water on day 428 was 19 mg/L that gradually decreased to near 10 mg/L by 447th day of operation. High COD in the treated water could be due to higher influent COD (121 mg/L) added on day 427 to meet the requirement of carbon source due to addition of excess 25 mg/L (total 50 mg/L) of sulphate in the influent on the same day. pH of the treated water remained between 7.1 and 7.4 throughout this phase of study.

Profile sampling: Profile sampling in phase-2 were done on day 398 (Fig 5.32) and 457 (Fig 5.33) of reactor operation when the influent arsenic was 750 µg/L (Table 4.6). Day 398 and day 457 were the last days of running AGR-1 at 45 min and 60 min EBCT, respectively. Profiles of nitrate, sulphate and COD remained almost same along the depth of the reactor except arsenic, concentrations of which were higher at each sample port leaving 55 µg/L in the treated water. As mentioned before, nitrate was completely removed by the time it reached to the first sampling port. Results of profile sampling on day 398 revealed that the sulphate concentration at sample port 3 reduced to 4 mg/L, which further reduced to below 3 mg/L and remained constant without any further reduction. Arsenic reduction was followed by sulphate reduction suggesting arsenic

removal as arsenosulphide precipitates. However, arsenic reduction ceased somewhere between sampling post 3 and 4 suggesting non-availability of sufficient sulphides to combine to form its sulphide precipitates. In contrast, day 457 profile sample results clearly showed sulphate reduction continued even after port 5 leaving 5.8 mg/L in the treated water, This could be due to higher sulphate concentration (50 mg/L) introduced into the AGR-1. Arsenic removal followed sulphate reduction and came down to well below the permissible limit in port 5 and in the treated water.

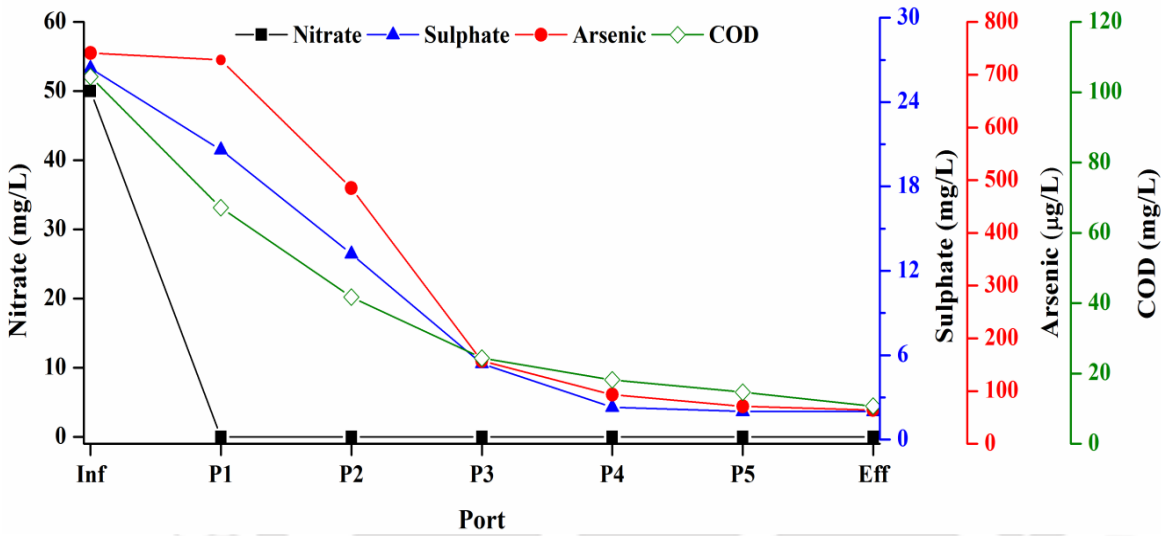


Figure 5.32 Sampling profile of the AGR-1 on day 398 (arsenic = 750 µg/L, nitrate = 50 mg/L, sulphate = 25 mg/L and EBCT 45 Min.).

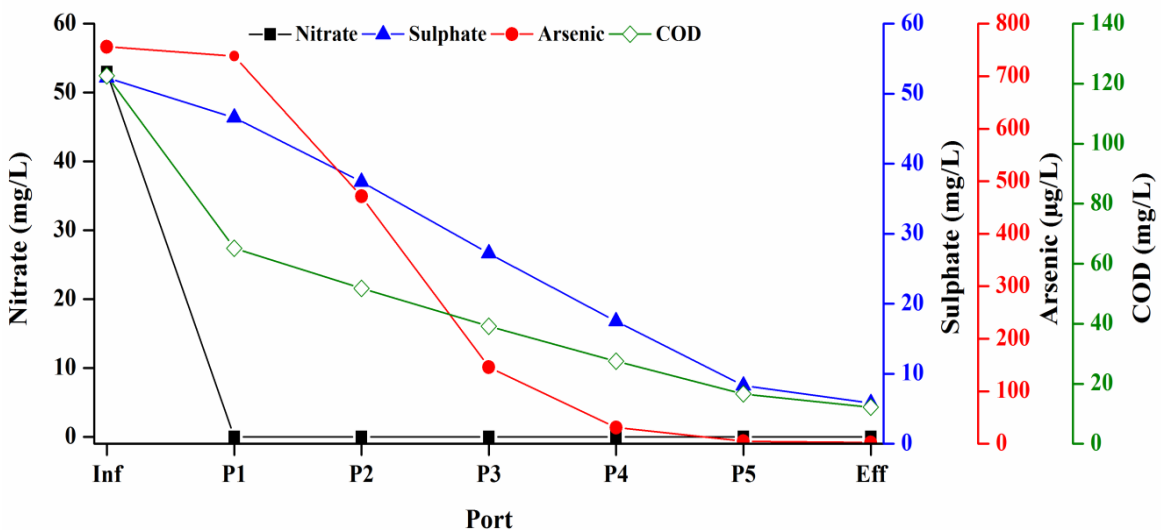


Figure 5.33 Sampling profile of the AGR-1 on day 457 (arsenic = 750 µg/L, nitrate = 50 mg/L, sulphate = 50 mg/L and EBCT 60 Min.).

The experimental results of the studies in phase-2 revealed that the reactor AGR-1 would be able to reduce 650 µg/L of arsenic to well below permissible limit, at 45 min EBCT. The reactor could also take care of higher initial arsenic concentration of 750 µg/L but required longer EBCT (60 min) and higher initial sulphate (50 mg/L) concentration. Based on the phase-2 experimental results, all the subsequent experiments with AGR-1 were carried out at 500 µg/L of influent arsenic concentration.

5.5.4 AGR-1 Phase 3: Effect of Influent Nitrate Concentration

After the experiments in phase-2 with initial arsenic of 750 µg/L, sulphate of 50 mg/L, COD of 121 mg/L and EBCT of 60 min, the AGR-1 was brought back to its operation at 45 min EBCT with 25 mg/L of sulphate and 105 mg/L of COD. However, the initial arsenic concentration was maintained at 500 µg/L for the next phase of study (phase-3) to evaluate the performance of AGR-1 at varying initial nitrate concentration. Effects of initial nitrate concentrations of 50, 100, 150 and 200 mg/L on performance of AGR-1 are shown in Figure 5.34. Corresponding COD in the influent was maintained at 105, 150, 194 and 240 mg/L respectively to meet the requirement of carbon source at elevated initial nitrate concentration. Irrespective of initial NO_3^- concentration (up to of 200 mg/L) NO_3^- in the treated water was found always below detection limits hence it is not plotted in the given figure. From day 458 to day 480, the performance of AGR-1 was stable and arsenic, sulphate and COD removal efficiencies remained near to 99.0%, 90% and 88% respectively. Treated water pH remained between 7.15-7.25 during this period. From day 481 to day 510, high removal efficiency of arsenic was observed as effluent arsenic was well below permissible limits (98.4% removal). During this period, the average COD and SO_4^{2-} reduction were 90.2% and 86.1% respectively. From day 511 to 541, the arsenic in treated water remained unaltered even at influent nitrate concentration of 150 mg/L and average COD and SO_4^{2-} reduction noticed were 91.3% and 74.2%, respectively.

Profile sampling: The profile sampling results of the day 480, 508 and 540 are shown in Figure 5.35, 5.36, and 5.37 respectively. The pH of treated water was between 7.80-7.86 during this period. The slight increase in treated water pH may be attributed to more alkalinity generated during reduction of higher influent nitrate of 150 mg/L.

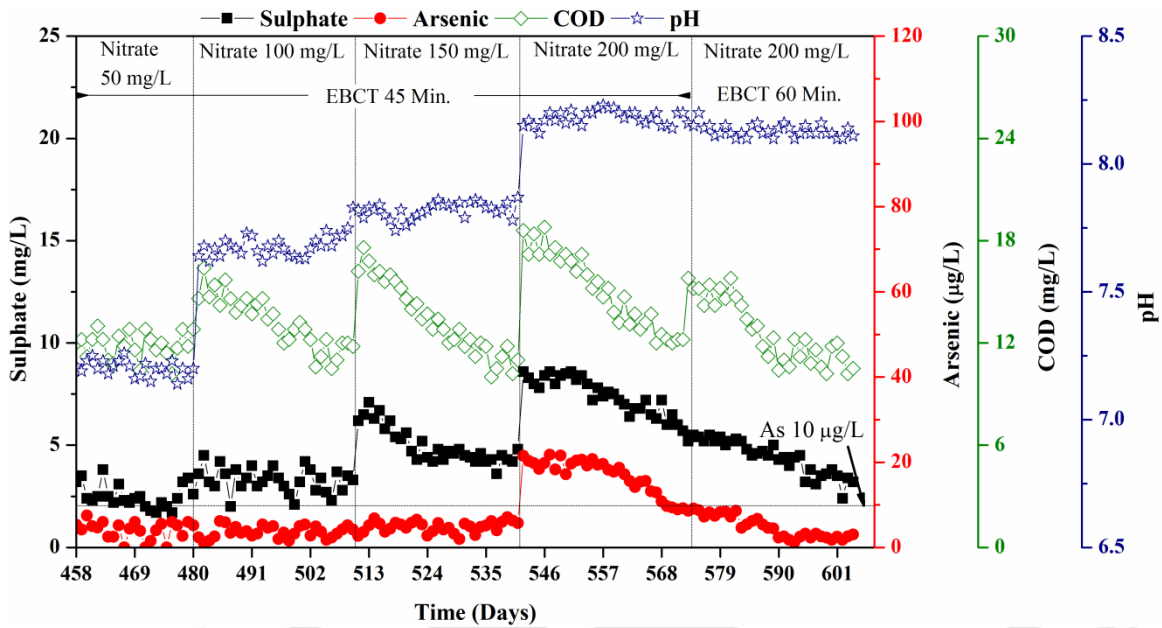


Figure 5.34 Performance evaluation of AGR-1 in phase-3 at initial nitrate = 50-200 mg/L, arsenic = 500 µg/L, and sulphate = 25 mg/L.

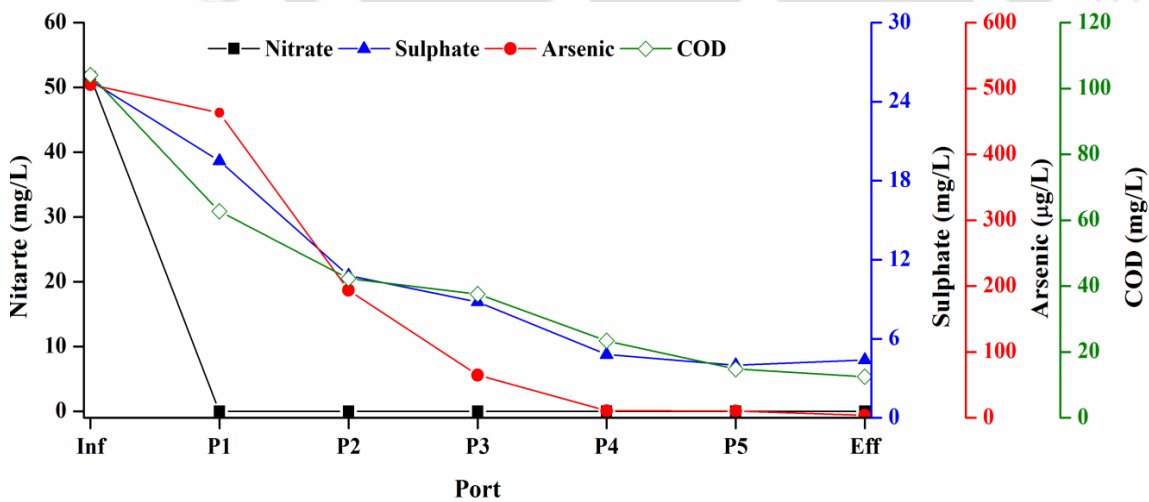


Figure 5.35 Sampling profile of the AGR-1 on day 480 (arsenic = 500 µg/L, nitrate = 50 mg/L, sulphate = 25 mg/L and EBCT 45 Min.).

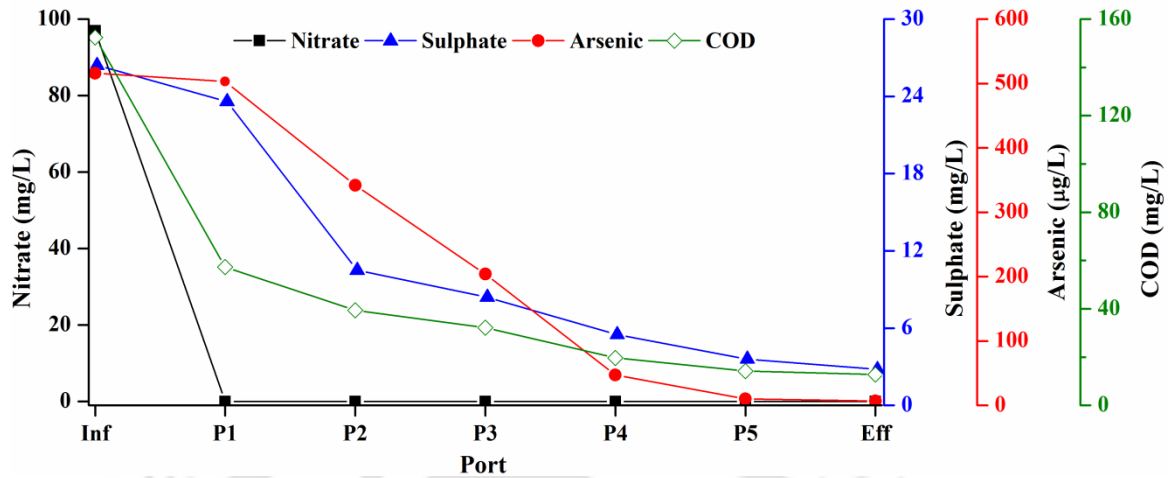


Figure 5.36 Sampling profile of the AGR-1 on day 508 (arsenic = 500 µg/L, nitrate = 100 mg/L, sulphate = 25 mg/L and EBCT 45 Min.).

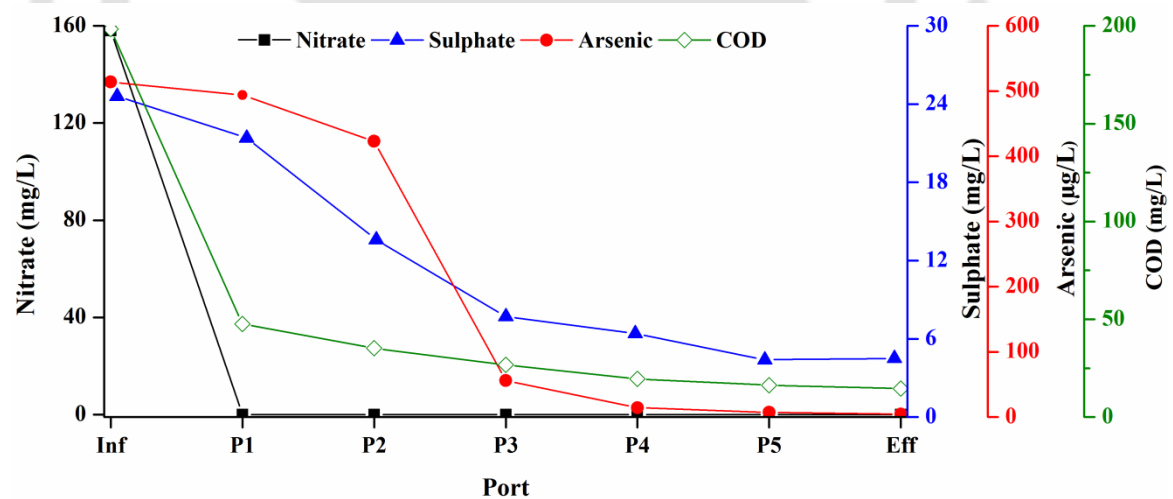


Figure 5.37 Sampling profile of the AGR-1 on day 540 (arsenic = 500 µg/L, nitrate = 150 mg/L, sulphate = 25 mg/L and EBCT 45 Min.).

The further increase in influent NO_3^- to 200 mg/L from day 542 caused a drop in the SO_4^{2-} as well as arsenic removal. The average SO_4^{2-} and COD removal was 70% and 92% respectively. The average arsenic concentration in the effluent rose to 18 ± 3.0 µg/L (about 96% removal). But the AGR-1 responded better to the 200 mg/L influent nitrate when EBCT was changed from 45 min. to 60 min., from day 573. The arsenic removal

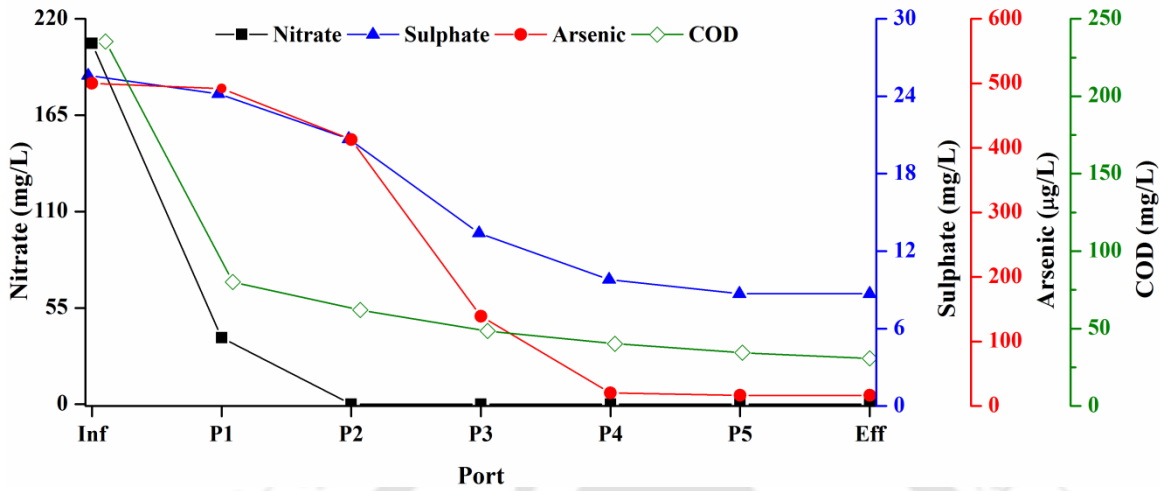


Figure 5.38 Sampling profile of the AGR-1 on day 570 (arsenic = 500 µg/L, nitrate = 200 mg/L, sulphate = 25 mg/L and EBCT 45 Min.).

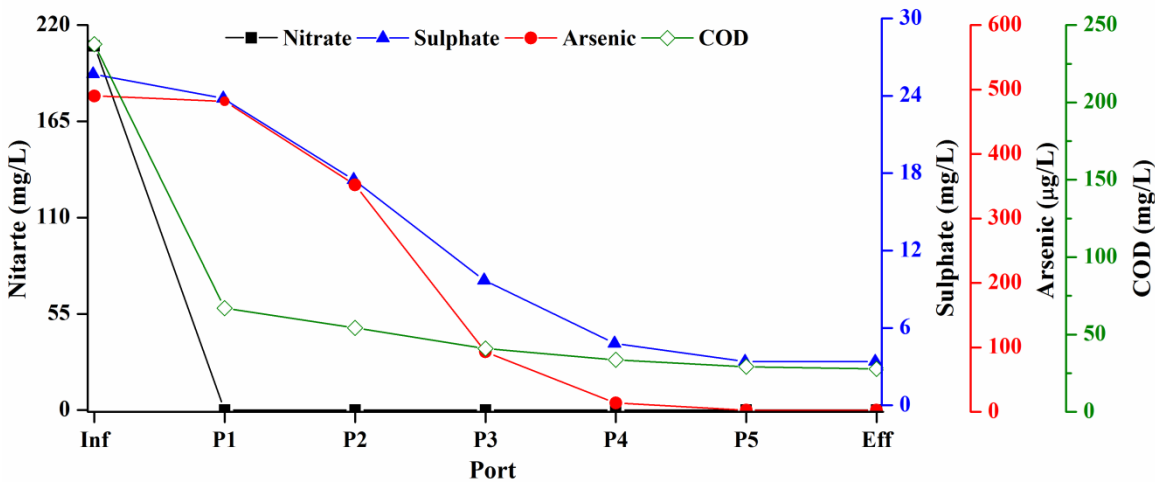


Figure 5.39 Sampling profile of the AGR-1 on day 603 (arsenic = 500 µg/L, nitrate = 200 mg/L, sulphate = 25 mg/L and EBCT 60 Min.).

efficiency improved in less than 10 days and resumed below permissible limit. This may be because of improved sulphate reduction at 60 min. EBCT. The profile sampling analysis was done on day 570 is shown in Figure 5.38 which shows only 81.5% nitrate removal was taken place till 1st port and no sulphate reduction was seen in 1st port. The noticeable sulphate reduction started from 2nd port and thereafter, this may be because of

shifting of TEAP zones in the AGR-1 at high nitrate concentration of 200 mg/L. The results of profile sampling done on day 603 at 60 min. EBCT is shown in Figure 5.39 confirmed that complete nitrate removal was taken place in 1st port. This confirms the results of Carollo Engineers (2008) who obtained 75 mg/L nitrate removal in 4 min. EBCT without nitrite accumulation in fixed bed reactor treating drinking water. The increased EBCT provided enough residence time for sulphate reduction and hence enough reaction time for arsenosulphide precipitation in the AGR-1. The profile sampling confirmed about a total of 86% and 88.0% SO_4^{2-} and COD removal respectively, was taken place till 5th port. The arsenic removal followed sulphate removal and up to 99% arsenic removal was seen in 5th port. The pH of treated water was in the range of 8.10-8.22 during this period.

Thus, gradual feed nitrate increase from 50 mg/L to 200 mg/L, did not affect the AGR-1 performance. The arsenic removal in the reactor was dependent on sulphate removal and also a function of EBCT. These results also suggested that nitrate addition did not inhibit SRBs permanently in a well established sulfidogenic bacterial community.

5.5.5 AGR-1 Phase 4: Effect of pH

Arsenic and nitrate removal in the AGR-1 by the mixed consortium over the initial pH range between 6.6 and 8.4 are shown in Figure 5.40. The pH in the reactor at different influent pH is shown in the figure. As shown, pH of the content in the reactor was always higher than the influent initial pH. However, at all the initial pH tested, the microbial consortia could substantially remove nitrate and arsenic. Nitrate in treated water remained below detection limit during the entire period of phase 4. From an initial of 12.5 mg/L of NO_3^- -N, 97% of nitrate removal in membrane biofilm reactor within 42 min has been reported by Lee and Rittmann (2003). In their study increased nitrate and nitrite removal was observed during pH increment from 7.2 to 8.4 while the removal percent decreased when pH was increased from 8.6 to 9.5. The treated water SO_4^{2-} and COD during the experimental period at initial pH of 6.6 and 7.2 was between 1.5-3.5 mg/L and 9.2-12.8 mg/L with an average 88.8% and 89% removal respectively. In the present study, very high percentage of arsenic removal (up to 99.2%) was observed at initial pH 6.6 within 5-6 days. The arsenic in treated water remained always between 1-6 $\mu\text{g/L}$.

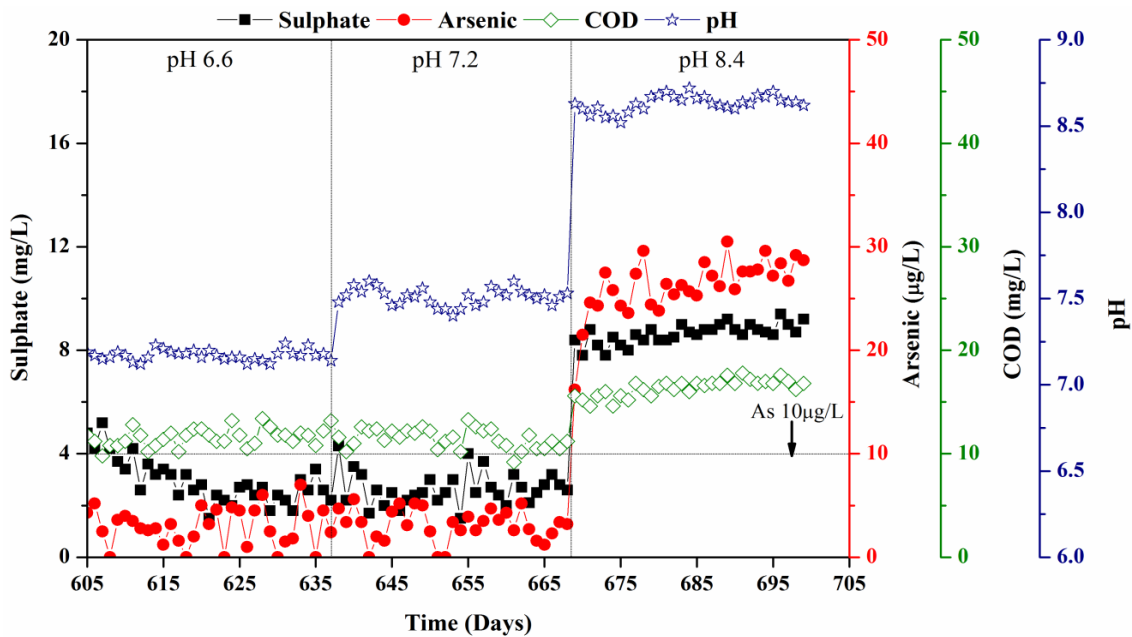


Figure 5.40 Performance evaluation of AGR-1 in phase-4 at initial nitrate = 50 mg/L, arsenic = 500 µg/L and sulphate = 25 mg/L.

It has been reported that high-arsenic waters are not expected in presence of high free sulphide concentration (Moore et al., 1988), as in reducing conditions SO_4^{2-} begins to play an important role which favours arsenic precipitation in the form of secondary sulphides like orpiment (As_2S_3) and realgar (AsS) and/or As rich pyrite (in presence of iron) in a wide range of pH (Cheng et al., 2009). In this case of present study treated water pH remained between 7.12-7.25.

At influent pH of 7.2, no change in SO_4^{2-} and COD removal to that at 6.6 was noticed. The arsenic removal efficiency was also remaining the same with 1-6 µg/L remaining in the treated water. Similarly, Rodriguez-Freire et al. (2014) obtained two fold higher arsenic removal at pH 6.1 than at pH 7.2 in batch reactors operated for assessing the effect of pH on arsenic sulphides precipitation. Also Rodriguez-Freire et al. (2014), suggested increased orpiment precipitation at circumneutral and higher pH values, with increasing pH over the realgar formation. The formation of thioarsenite species dominates at higher pH values and precipitation of arsenic sulphide minerals may be limited, even though any precipitation that does occur would be predominantly orpiment. The effluent pH was once again remained higher (between 7.4-7.6) than the influent due to alkalinity production because of denitrification of nitrate.

At pH 8.4, a slight decrease in SO_4^{2-} and COD reduction was observed with average mean values of 8.6 ± 0.4 mg/L and 16.4 ± 0.8 mg/L in the treated water corresponding to 66.2% and 84.5% removal, respectively. Gutierrez et al. (2009) also reported 30% and 50% reduction in SRB activity in an anaerobic biofilm reactor when pH was increased from 7.6 to 8.6 and 9.0 respectively. In the present study, the reactor pH remained between 8.52-8.70 at an influent pH of 8.4 due to alkalinity formation on denitrification. Average concentration of arsenic in the treated water during this period was 26 ± 2.7 $\mu\text{g/L}$. This decrease in the arsenic removal efficiency could be due to decreased sulphate removal efficiency in the reactor.

5.5.6 AGR-1 Phase 5: Effect of operating Temperature

With respect to the effect of temperature, the stability and efficiency of the reactor was evaluated in terms of the arsenic and nitrate removal. The effects of operating temperature of 20, 30, 40 and 50°C is summarised in Figure. 5.41. NO_3^- in the treated water was always remained undetected throughout the experimental period in all the temperature ranges studied. As observed the SO_4^{2-} reduction was slowly decreased for first 14-15 days of operation (from day 700 to 714) which was probably due to acclimation of the biomass at 20°C temperature. The SO_4^{2-} in treated water was in the range of 7.2-9.6 mg/L during this acclimation period. After acclimation period, SO_4^{2-} reduction in the AGR-1 was improved and SO_4^{2-} was remained between 5-7 mg/L for next 18 days operation at 20°C. COD of 19-21 mg/L was remained in the treated water during the reactor operation at 20°C. Except the acclimation period when arsenic in the treated water was between 15 and 22 $\mu\text{g/L}$, it was found always below 10 $\mu\text{g/L}$. The reactor performance was found to be improved slowly at higher temperature up to 40°C. SO_4^{2-} and COD in treated water remained between 1.5 and 4 mg/L, and 10 and 13 mg/L, respectively. Irrespective of operating temperature (up to 40 °C) arsenic in the treated water was found always below 10 $\mu\text{g/L}$. The results indicated that the system could tolerate the 10°C shock from the operating temperature of 30°C.

At 50°C, the reactor performed poorly for first 15 days but improved to some extent in next 10 days. SO_4^{2-} removal efficiency dropped and SO_4^{2-} in treated water increased up to 13-14 mg/L during this period. Although the pH remained between 7.2-7.35, treated water COD became as high as 19-20 mg/L. Arsenic in the treated water went

up to 58 $\mu\text{g/L}$. Poor performance of the AGR-1 during initial periods of 50°C could be due to lack in presence of thermophilic bacterial species as the reactor was in operation for long in 30°C. However, during the later periods of operation at this temperature (day 822 onwards), the mixed bacterial culture performed well and the arsenic in the treated water reduced to below 10 $\mu\text{g/L}$. This is also supported by previous studies on temperature shifts, which showed a loss of stability and change in the performance of the reactor when an operating temperature was raised over 45°C (Boušková et al., 2005). Because 45°C is at the edge between mesophilic and thermophilic temperature ranges, the AGR was more sensitive to the temperature shocks when operated at 50°C than at 40°C. Visser et al. (1993b) observed that a short term increase in temperature from 30°C to 45°C did not show any detrimental effect on, process recovery, process stability and particularly the competition among sulphate-reducing and methanogenic and acetogenic bacteria in a UASB reactor. However, at 55 and 65°C performance of the reactor reduced significantly. As the present study was conducted for drinking water treatment in presence of low substrate, nutrient and microbial population, AGR-1 showed more sensitivity towards temperature change than that reported by Visser et al. (1993b).

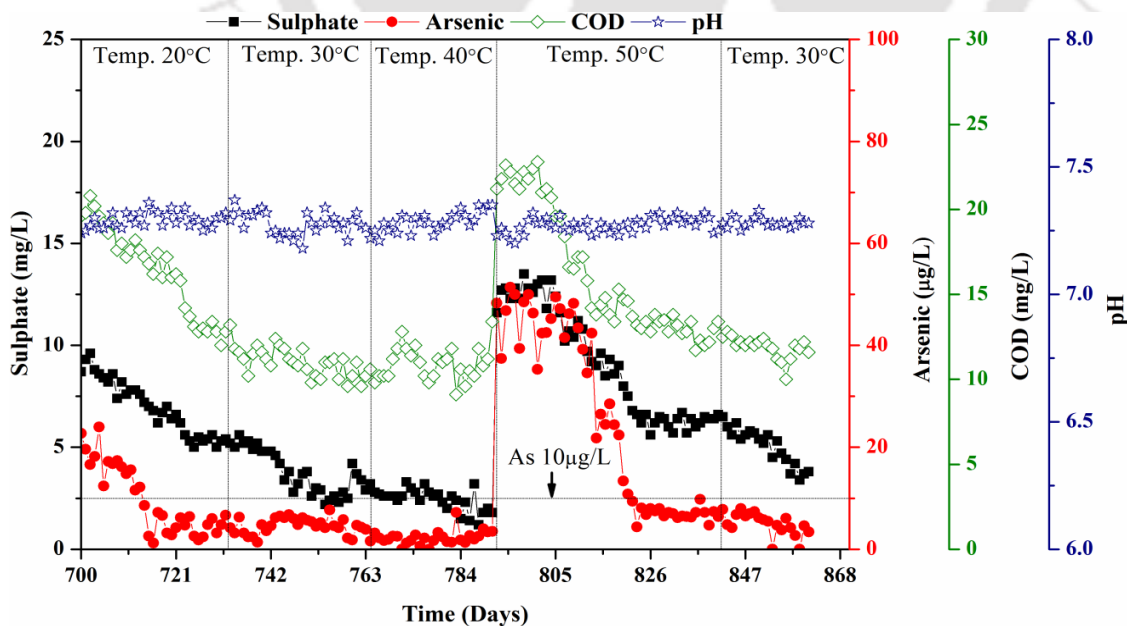


Figure 5.41 Performance evaluation of AGR-1 in phase-5 at initial nitrate = 50 mg/L, arsenic = 500 $\mu\text{g/L}$ and sulphate = 25 mg/L.

5.5.7 AGR-1 Phase 6: Removal and Effects of Fluoride

Figure 5.42 represents the removal and effect of fluoride on AGR-1 performance. Like previous phases NO_3^- in the treated water was always remain undetected during entire experimental period. Performance of AGR-1 did not affect due to introduction of 5 mg/L of fluoride. However, there was no fluoride removal was observed during the entire period of 34 days of operation. These results also indicated that presence of fluoride did not impose any inhibitory effect on reactor performance in terms of arsenic removal.

5.5.8 AGR-1 Phase 7: Performance at Lower EBCT

After a steady performance at 45 min. EBCT, the AGR-1 was tested for its contaminant removal efficiency at lower EBCT of 30 min. The performance of AGR-1 at 30 min. EBCT is shown in Figure 5.43. NO_3^- in the treated water remained below detection limit and therefore, not plotted in the figure.

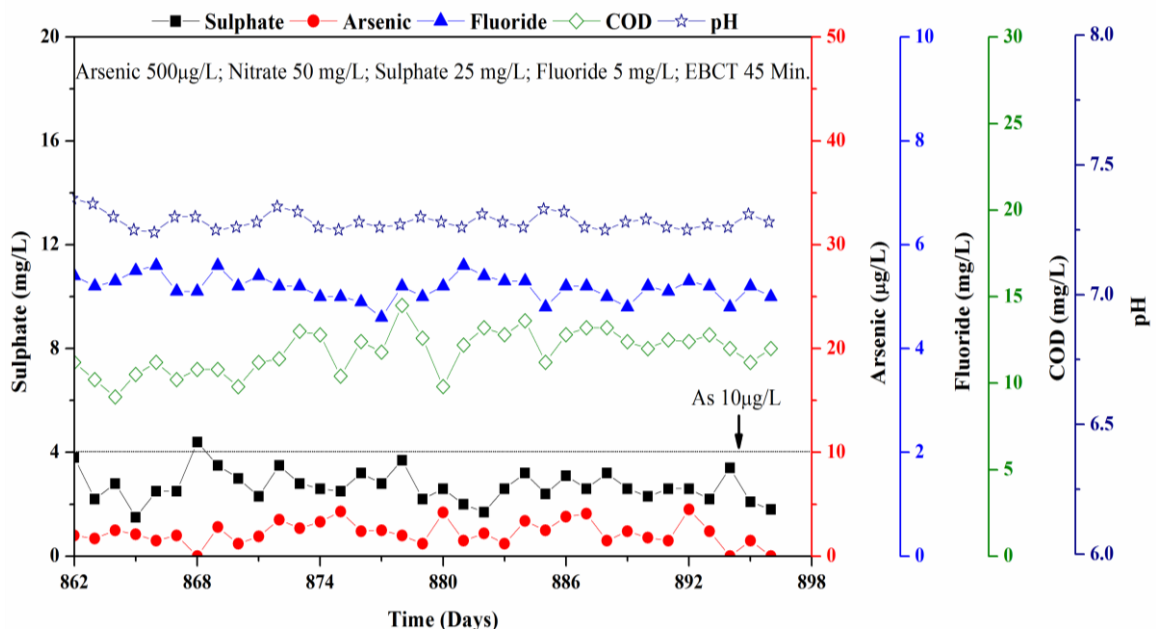


Figure 5.42 Performance evaluation of AGR-1 in phase-6 at initial nitrate = 50 mg/L, arsenic = 500 µg/L, sulphate = 25 mg/L and fluoride = 5 mg/L.

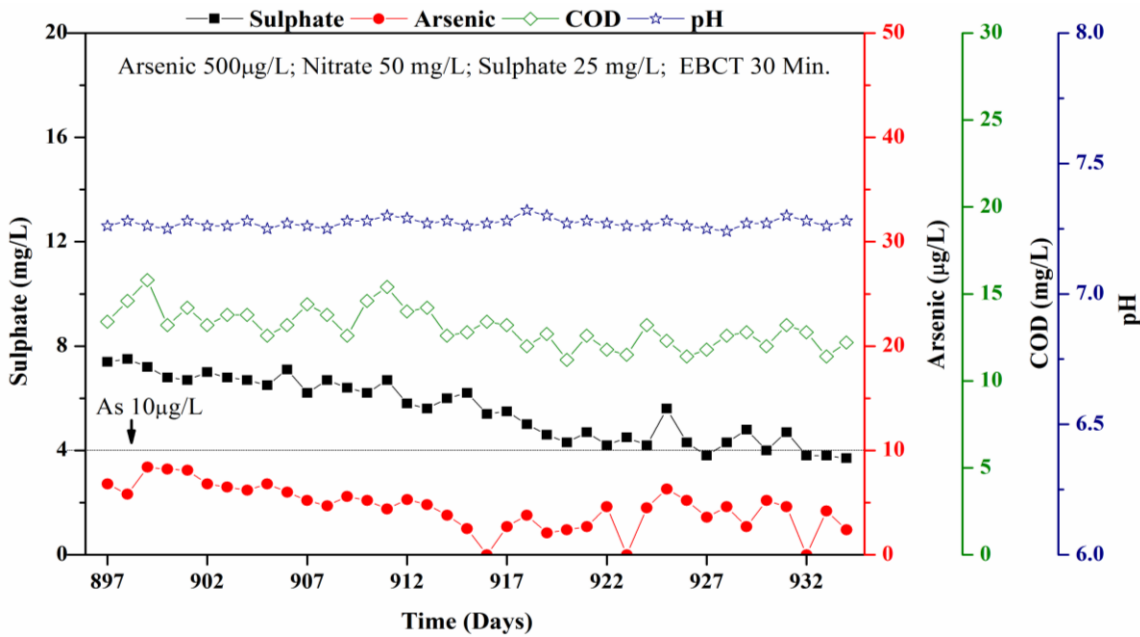


Figure 5.43 Performance evaluation of AGR-1 in phase-7 at initial nitrate = 50 mg/L, arsenic = 500 µg/L and sulphate = 25 mg/L.

There was no adverse effects on SO_4^{2-} , COD and arsenic removal efficiency, suggesting that the reactor would perform as good as at 45 min EBCT. The pH profile have not shown any remarkable changes in this phase and remained between 7.24 and 7.32. These results suggested that the WAC granules have good biomass growth and which enabled AGR-1 to perform effectively even at lower EBCT of 30 min.

5.5.9 AGR-1 Phase 8: Performance after Shutdown

Throughout the AGR-1 operation, synthetic groundwater and nutrient solution were supplied to the bioreactor on nights, weekends and holidays. From days 935 to 941, the AGR-1 was shut down for seven days, during which no synthetic groundwater and nutrient solution were supplied to the bioreactor. The performance of AGR-1 after shutdown period is given in Figure 5.44. After restart, the NO_3^- removal was completely recovered within few hours and it was found below detection limits in the treated water. The sulphate removal efficiency was restored to more than 65% within 7 days after shutdown. Whereas, arsenic in treated water was resumed to below 10 µg/L after 6 days of operation with 98% removal efficiency. Thus, the AGR-1 required a re-adaptation

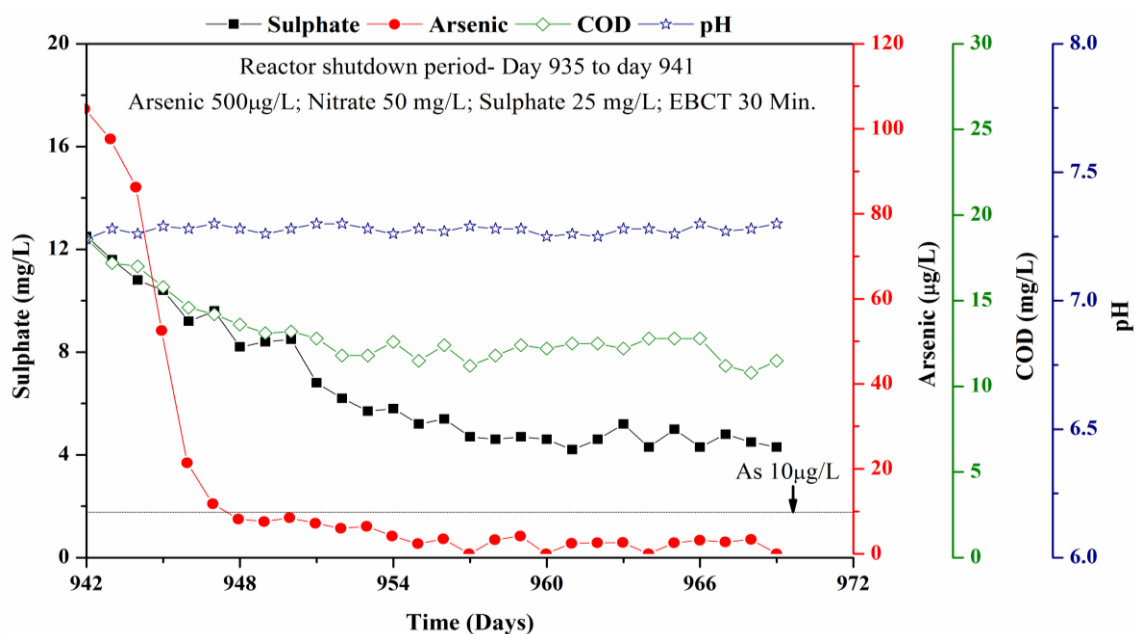


Figure 5.44 Performance evaluation of AGR-1 in phase-8 at initial nitrate = 50 mg/L, arsenic = 500 µg/L and sulphate = 25 mg/L.

period of only 6-7 days after one week-shutdown, even though no feed and nutrients were supplied to the bioreactor during the shutdown period. A potential explanation for this short re-adaptation period might be due to the higher water holding capacity of WAC and presence of high microbial biomass on the WAC surface (Devinny et al., 1998). The other possible reason is high survival efficiency of SRBs during starvation (Fukui et al., 1996). The results indicated there was no significant inhibition effect on the bioreactor performance was observed related to the seven days shutdown, and it can be operated with 100% comparable performance to that achieved before shutdown.

5.6 Performance Evaluation of the Flow through Attached Growth Reactor, AGR-2

The flow through attached growth reactor, AGR-2 was operated in presence of iron in the influent. After start-up, operation of AGR-2 was divided into 8 phases (Table 4.7). In this section performance of AGR-2 is discussed in details.

5.6.1 AGR-2 Start-up

The performance of AGR-2 during start-up phase is shown in Figure 5.45. After inoculation, AGR-2 was operated for a period of 36 days to obtain an appreciable colonization of mixed microbial consortia on the WAC granules in the reactor as well as to get consistent performance. The performance of the reactor during this period was characterized by COD, SO_4^{2-} and iron removal efficiency. Based on stoichiometric calculations to utilize all electron acceptors COD of 115 mg/L was used to carry out the start-up phase in the reactor. Low sulphate reduction efficiencies were observed during this experimental period (i.e. average values of 29% in first 18 days and reached up to 63% in next 18 days). This was primarily due to the heterogeneous seed sludge which was used as source of inoculum. Moreover, SRB are also reported to adapt slowly in a mixed microbial population containing system than other active microorganisms in the biofilm (D'Acunto et al., 2011; Frunzo et al., 2012). Complete nitrate removal was observed from first day of reactor operation. Iron removal in the reactor started after onset of sulphate removal. Treated water iron reduced to below the drinking water permissible limits of 0.3 mg/L after 36 days and remained within limits thereafter. Arsenic removal started gradually with onset of sulphate and/or iron reduction and reduced to below 10 $\mu\text{g/L}$ after 57 days of operation. The steady-state sulphate and COD concentration in the treated water after 58 days were averaged 7.0 ± 0.6 mg/L and 15.3 ± 1.5 mg/L with 72% and 85% of removal efficiency respectively. Treated water iron remained below detection limits, whereas arsenic in the treated water was found to be 7.6 ± 1.2 $\mu\text{g/L}$. The pH of the treated water during steady state was between 7.1-7.25. After attaining the stability in the reactor performance, the EBCT was changed to 60 min. from day 59 to day 77. The maximum and minimum arsenic in treated water was 8.7 and 3.6 $\mu\text{g/L}$, respectively. SO_4^{2-} and COD values were 6.7 and 3.5 mg/L and 16.8 and 11.4 mg/L respectively, during this period. Further decreasing the EBCT to 45 min did not adversely affect the AGR-2 performance in terms of arsenic and iron removal from day 78 to day 102. The average values of SO_4^{2-} and COD were 3.0 ± 1.0 mg/L and 12.5 ± 1.5 mg/L respectively during this period. Efficient arsenic removal (up to 99%) was seen even at lower EBCT of 45 min. The arsenic in the treated water was found always below 10 $\mu\text{g/L}$ with average values of 4.5 ± 2.0 $\mu\text{g/L}$. Irrespective of EBCT changes iron and nitrate in treated water remained below detection limit. Treated water pH was constant as well and stable between 7.05-7.23.

Profile Sampling: Figure 5.46 represents the profile sampling results of day 102. As observed complete NO_3^- removal and nearly 14% SO_4^{2-} removal occurred till the 1st sampling port. High sulphate removal (73%) occurred till 3rd effluent port and overall 85% sulphate removal was seen till 5th port. Efficient iron removal (72%) was seen till 2nd port and remains below detection limits thereafter. Most of the arsenic was removed in 2nd and 3rd port with 42% and 92% removal efficiency. The arsenic concentration in treated water was below 10 $\mu\text{g/L}$ in the 4th port with about 99% removal. In fact, no considerable arsenic removal was seen after 4th port. Arsenic removal followed sulphate reduction as most of the sulphate reduction took place in the 3rd port, most of the arsenic was removed from the reactor till the water reached 3rd port. Iron and arsenic removal followed sulphate reduction due to the availability of biogenic sulphides for formation of respective metal sulphides. A total of 85.5% and 99% sulphate and arsenic removal was seen in the 5th port. The COD values also followed nitrate removal and 56% COD removal was seen in 1st port whereas 85.5% COD removal noticed in 5th port. Moreover, the sequential utilization of electron acceptors in the systems confirms the establishment of TEAP zones on the basis of thermodynamic favourability. Profile samples shows that only 5.3 $\mu\text{g/L}$ arsenic, 3.7 mg/L of sulphate and 13.2 mg/L of COD were left in final treated water.

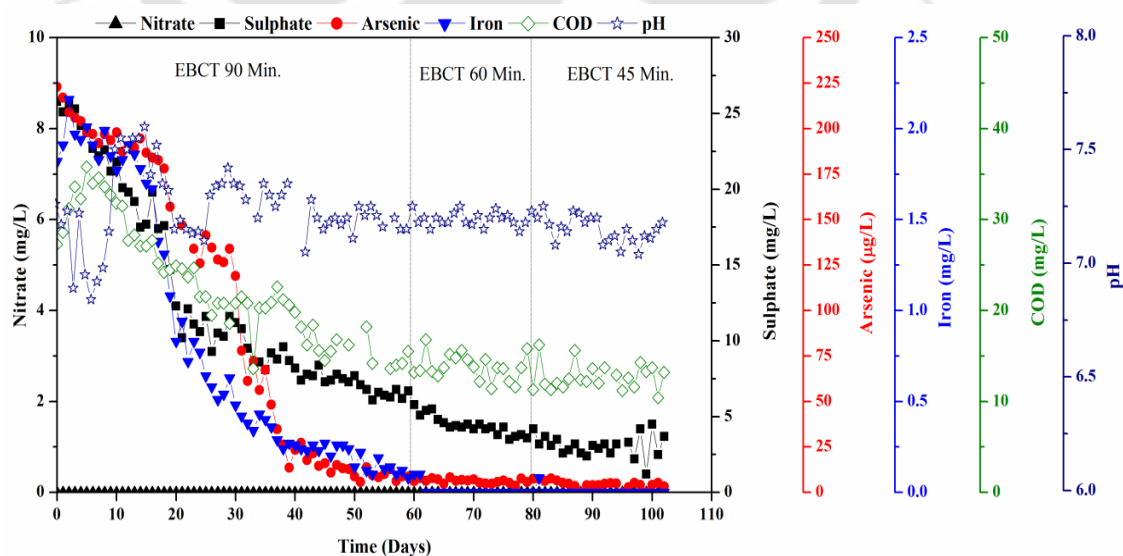


Figure 5.45 Performance evaluation of AGR-2 in start up phase at initial arsenic = 250 $\mu\text{g/L}$, iron = 2.0 mg/L, nitrate = 50 mg/L and sulphate = 25 mg/L.

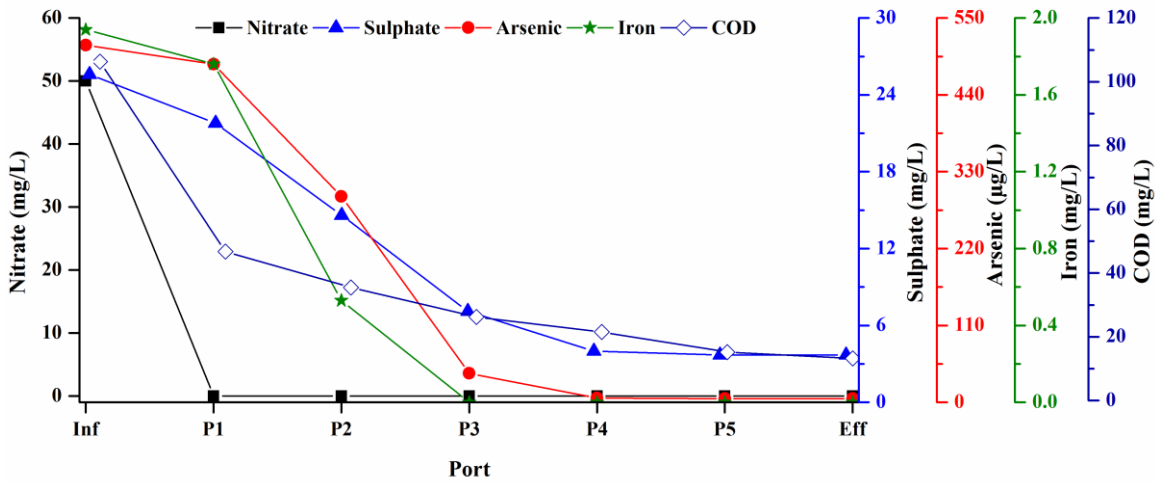


Figure 5.46 Sampling profile of the AGR-2 on day 102 (arsenic = 500 µg/L, iron = 2.0 mg/L, nitrate = 50 mg/L, sulphate = 25 mg/L and EBCT 45 min).

5.6.2 AGR-2 Phase-1: Effects of Influent Iron Concentration

The performance of AGR-2 on effects of initial iron concentration of 2, 3, 4, 5, 7.5 and 10 mg/L is summarised in Figure 5.47. Irrespective of initial iron concentration (up to 10 mg/L) nitrate in the treated water was always less than detection limits and therefore, not plotted in given figure. This also concludes no adverse effects on nitrate removal in reactor even at iron concentration up to 10 mg/L. Iron in the treated water remained below permissible limits of 0.3 mg/L when the influent iron was 4 mg/L or less whereas treated water iron averaged 0.82 mg/L with 83% removal efficiency at influent iron of 5 mg/L during day 155 to day 181. The possible reason for this higher iron concentration (0.82 mg/L) in treated water might be due to unavailability of sufficient sulphides for precipitation as iron sulphides. The average values of SO_4^{2-} and COD were 3.2 ± 0.8 mg/L and 10.8 ± 1.0 mg/L with 87% and 89.5% removal efficiency, respectively. The maximum and minimum SO_4^{2-} and COD in the treated water were 5.0 and 1.7 mg/L, 16.2 and 9.6 mg/L, respectively, during AGR-2 operation from day 79 to 181. The maximum and minimum values of arsenic in the treated water were 7.6 and 1.2 µg/L with average values of 4.0 ± 1.8 µg/L (99.2% removal) during above period. pH of treated water remained between 7.05 and 7.25 during this period.

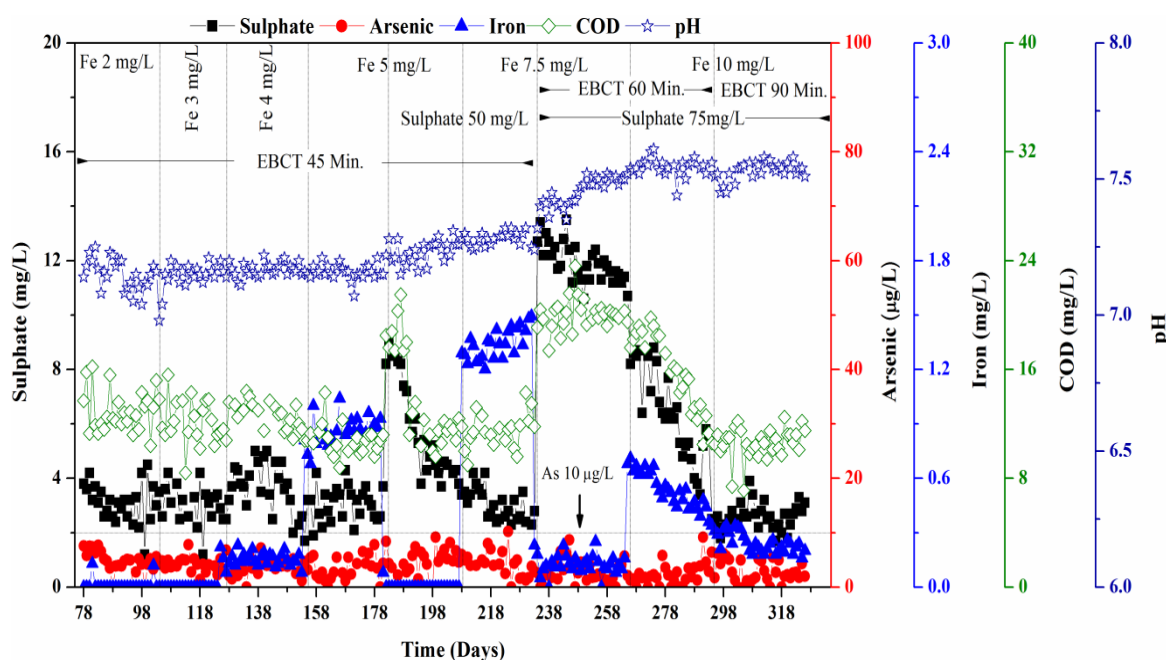


Figure 5.47 Performance evaluation of AGR-2 in phase-1 at initial arsenic = 500 µg/L, iron = 2.0 -10 mg/L, nitrate = 50 mg/L and sulphate = 25-75 mg/L.

Profile sampling: The profile sampling results of the day 181 is shown in Figure 5.48. Complete nitrate removal was observed in 1st port. Sulphate removal started from 1st port and almost 89% sulphate removal was observed in 5th port. Iron removal followed sulphate reduction and only 82% iron removal was occurred in 5th port. The iron concentration in treated water was found to be 0.9 mg/L. This might be due to unavailability of sulphides for iron sulphide precipitation. The arsenic in the treated water was below 10 µg/L in 4th port and remained undetected in the 5th port. Based on the profile sampling results, future experiments were conducted with increased influent sulphate of 50 mg/L in order to ensure the availability of sufficient sulphide for iron sulphides precipitation. Iron in the treated water was again resumed below 0.3 mg/L when the initial sulphate was raised to 50 mg/L from the day 182 to day 208.

The profile sampling results of the day 208 is shown in Figure 5.49. Sixty five percent of iron removal was observed in 3rd sampling port and became less than detection limits in port 4. Iron in treated water averaged 1.35 ± 0.08 mg/L from day 209 to day 233 of AGR-2 operation when influent iron was increased to 7.5 mg/L. However, reactor performance remained stable in terms of arsenic removal and other parameters such as SO_4^{2-} and COD removal during this period with average values of 4.3 ± 2.4 µg/L, 3.0 ± 0.5

mg/L and 11.5 ± 1.3 mg/L respectively. Iron concentration was again reduced to below permissible limits when influent sulphate was increased to 75 mg/L from day 234 till day 264.

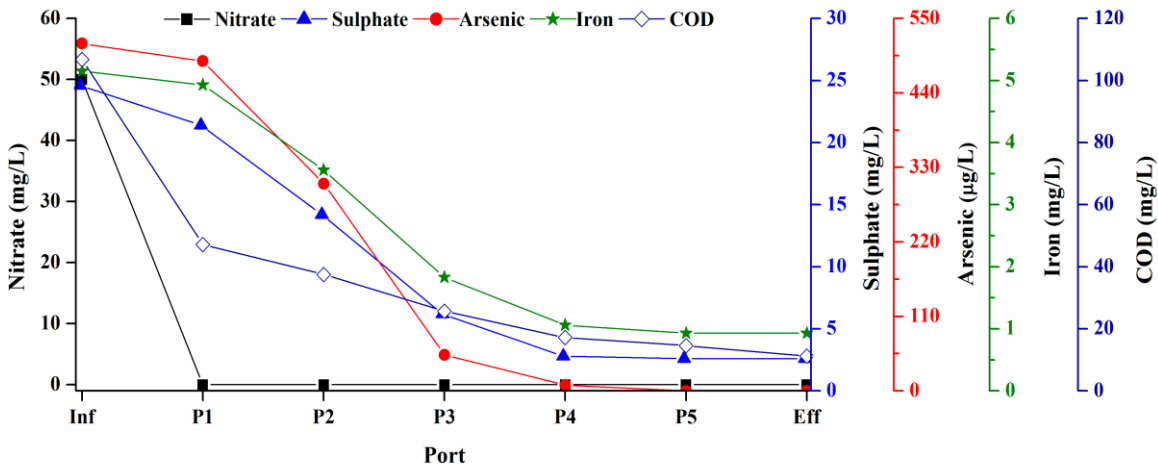


Figure 5.48 Sampling profile of the AGR-2 on day 181 (Iron = 5.0 mg/L, arsenic = 500 µg/L, nitrate = 50 mg/L, sulphate = 25 mg/L and EBCT 45 Min.).

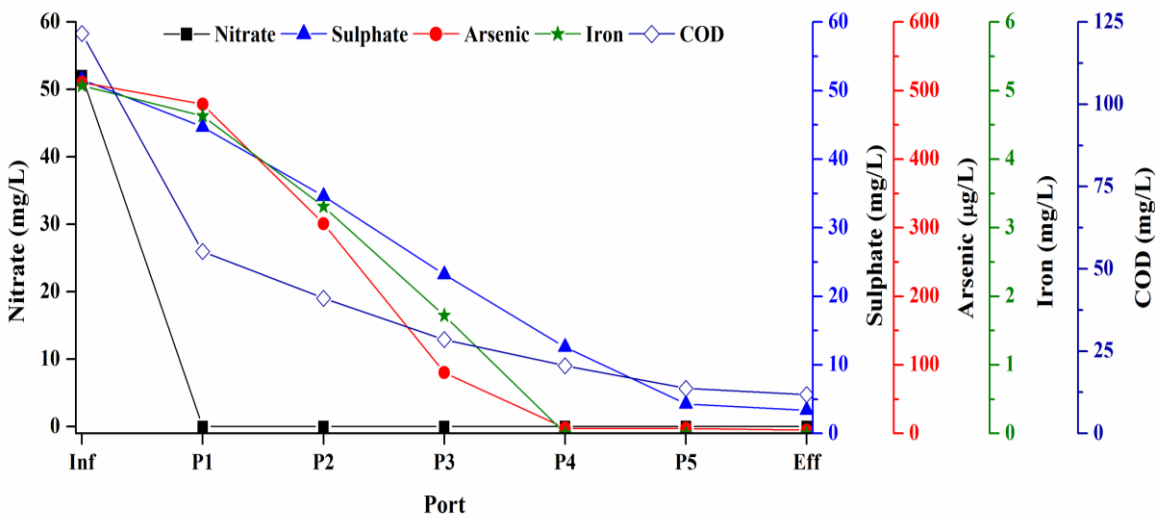


Figure 5.49 Sampling profile of the AGR-2 on day 208 (sulphate = 50 mg/L, iron 5.0 = mg/L, arsenic = 500 µg/L, nitrate = 50 mg/L and EBCT 45 Min.).

The profile sampling results of the day 264 is shown in Figure 5.50. These result showed that only 83% SO_4^{2-} removal was seen in the effluent indicating lower EBCT a reason for poor sulphate reduction in AGR-2. However, a total of 98% iron removal was observed in 5th port and only 0.16 mg/L iron was left out in final treated water from initial 7.5 mg/L. Arsenic in treated water was 5.7 $\mu\text{g/L}$ corresponding to 98.8% removal in the 5th port. Iron in treated water was found between 0.35-0.7 mg/L with an average value of 0.52 ± 0.1 mg/L between day 265 and 294 when influent iron was 10 mg/L. SO_4^{2-} and COD of only 6.3 ± 1.8 mg/L and 15.7 ± 2.8 mg/L, respectively, remained in the treated water during this period, whereas the maximum and minimum SO_4^{2-} and COD were between 9.3 and 2.5 mg/L, and 19.5 and 10.5 mg/L respectively. The change in EBCT to 60 min improved in SO_4^{2-} reduction with time as a result of which better COD removal was also seen in the reactor from day 266 to 294. Further increase in the EBCT to 90 min provided even better SO_4^{2-} removal leaving only an average of 2.4 mg/L in the treated water between day 295 and day 326. In treated water, iron concentration was dropped to below the drinking standards of 0.3 mg/L, and was found in the range of 0.18-0.26 mg/L during last 20 days of operation at 90 min EBCT. This was probably due to generation of enough sulphide to form iron sulphides in the system thus promoting iron removal in the system. Moreover, sulphate addition up to 75 mg/L to the synthetic feed did not adversely affect the system performance. Arsenic removal was stable during the entire period of operation.

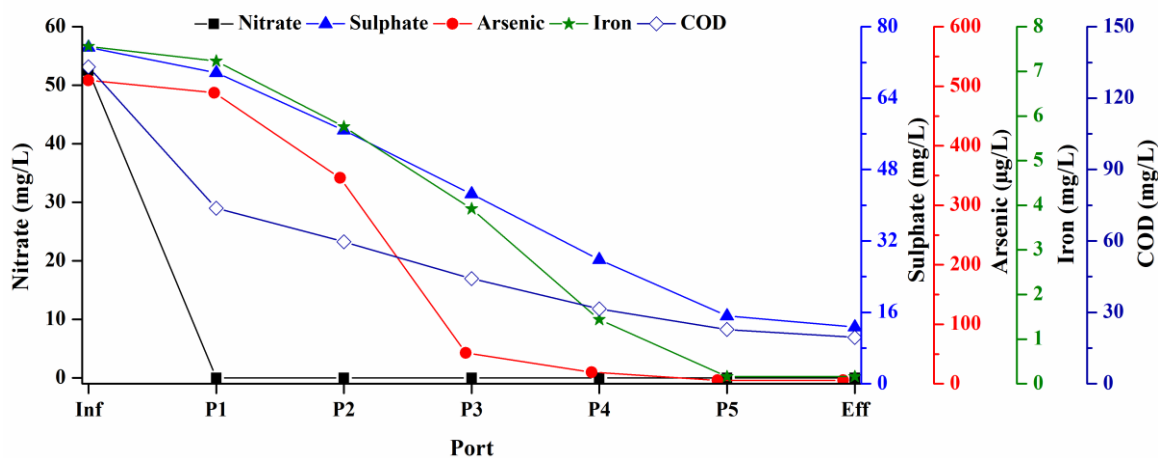


Figure 5.50 Sampling profile of the AGR-2 on day 264 (sulphate = 75 mg/L, iron = 7.5 mg/L, arsenic = 500 $\mu\text{g/L}$, nitrate = 50 mg/L and EBCT 60 Min.).

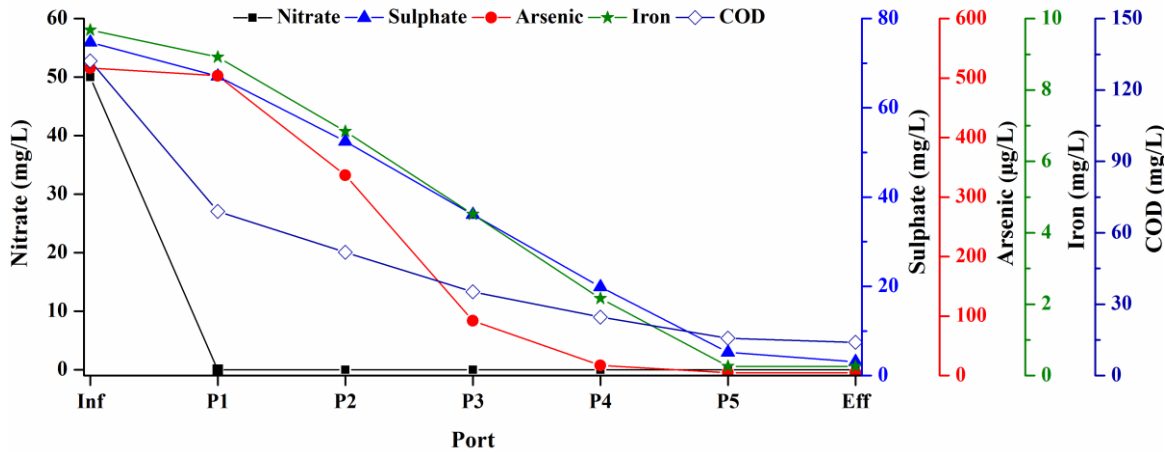


Figure 5.51 Sampling profile of the AGR-2 on day 326 (sulphate = 75 mg/L, iron = 10.0 mg/L, arsenic = 500 µg/L, nitrate = 50 mg/L and EBCT 90 Min.).

The pH of the treated water remained between 7.25 and 7.60 from day 182 to day 326. Slight increase in pH might be due to alkalinity generation resulting from reduction of increased SO_4^{2-} in influent. Higher EBCT improved the reactor performance in terms of iron removal because it prolongs the TEAP zone which results in improve sulphate reduction, which in turn provides more sulphides to form iron and arsenic sulphides.

The profile sampling results of the day 326 is shown in Figure 5.51. The results indicated better sulphate removal of up to 95% efficiency at higher EBCT of 90 min and only 3.1 mg/L of SO_4^{2-} was left out in treated water. Average iron concentration in the treated water was found to be 0.26 mg/L (97% removal) from an initial of 10 mg/L. Thus, increase in EBCT provided sufficient residence time for influent media to contact with biofilm which in turn resulted in enhanced sulphate and therefore higher iron removal in the reactor.

At the end of phase-1, the treated water arsenic, iron and nitrate was within the drinking water permissible limits with around 99.5%, 97.5% and 100% removal efficiency. Moreover, high iron concentration (up to 10 mg/L) did not adversely affect reactor performance in terms of arsenic removal. The SO_4^{2-} and COD removal efficiencies by mixed microbial consortia was around 96.5% and 91.5% during the last 20 days of operation. These results conclude that the microbial reduction became the predominant process in the system.

5.6.3 AGR-2 Phase 2: Effects of Arsenic

The effects of initial arsenic concentration of 500, 750, 1000, 1250 and 1500 $\mu\text{g/L}$ is summarised in Figure 5.52. The performance of AGR-2 remained stable at all tested influent arsenic concentrations introduced. The treated water nitrate was always found below detection limit and therefore, not plotted in the figure. Variation in SO_4^{2-} and COD concentrations followed similar trend as observed in phase-1. The SO_4^{2-} and COD removal efficiencies remained on average values of 96% and 91.5%, respectively and averaged 3.0 ± 0.8 mg/L and 11.3 ± 1.0 mg/L respectively. Irrespective of initial arsenic concentration, iron in treated water always remained less than permissible limits except one or two instances. Iron in treated water was found to be 0.2 ± 0.06 mg/L corresponding to 98% removal. Gradual increase of influent arsenic did not adversely affect reactor performance. The arsenic concentration in treated water during this phase decreased further to 3.5 ± 2.7 $\mu\text{g/L}$ corresponding to 99.7% removal. The treated water pH remained between 7.42-7.58 during entire phase-2 of reactor operation.

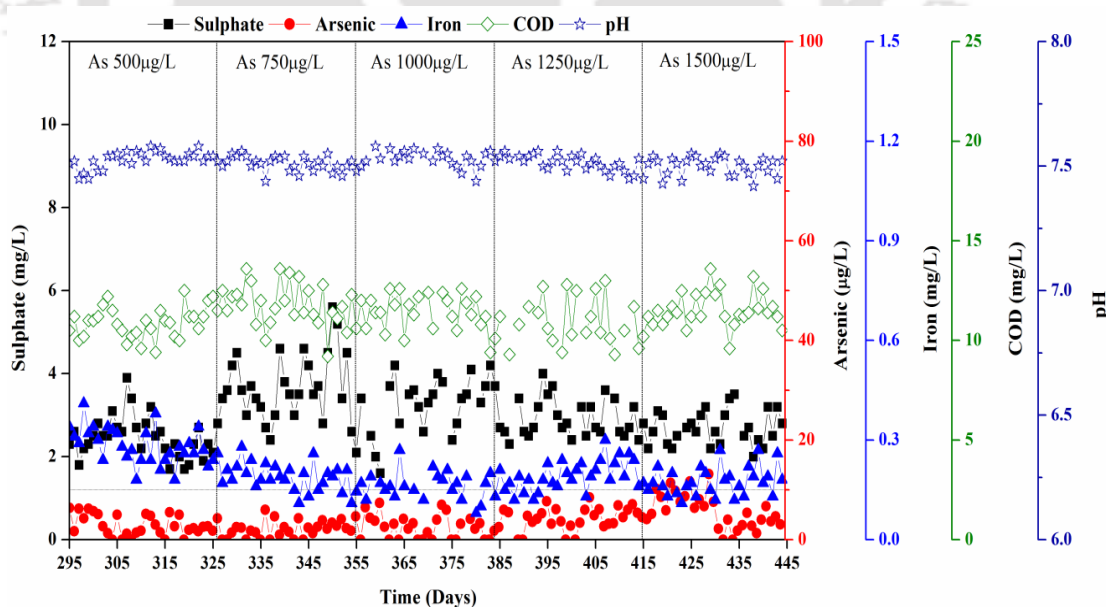


Figure 5.52 Performance evaluation of AGR-2 in phase-2 at initial arsenic = 500-1500 $\mu\text{g/L}$, iron = 10.0 mg/L, nitrate = 50 mg/L and sulphate = 75 mg/L.

Profile sampling: The profile sampling results of day 382 and day 444 are shown in Figure 5.53 and 5.54 respectively. Arsenic in treated water was below detection limits in port 4 from an initial arsenic of 1000 µg/L. Iron removal also followed similar trend and almost 79% iron was removed in 4th port from an initial concentration of 10 mg/L. Whereas, iron in treated water was found to be 0.17 mg/L with 98.3% removal efficiency. Similarly, the profile samples collected on day 444 shows 87% arsenic removal in port 4 and leaving only 3.1 µg/L in port 5 from initial arsenic of 1500 µg/L. The iron concentration in the 5th port was found to be 0.27 mg/L corresponds to 97.3% iron removal efficiency. The arsenic removal at higher concentrations (up to 1500 µg/L) may be due to the presence of iron in the influent and subsequent formation of its sulphide in the reactor.

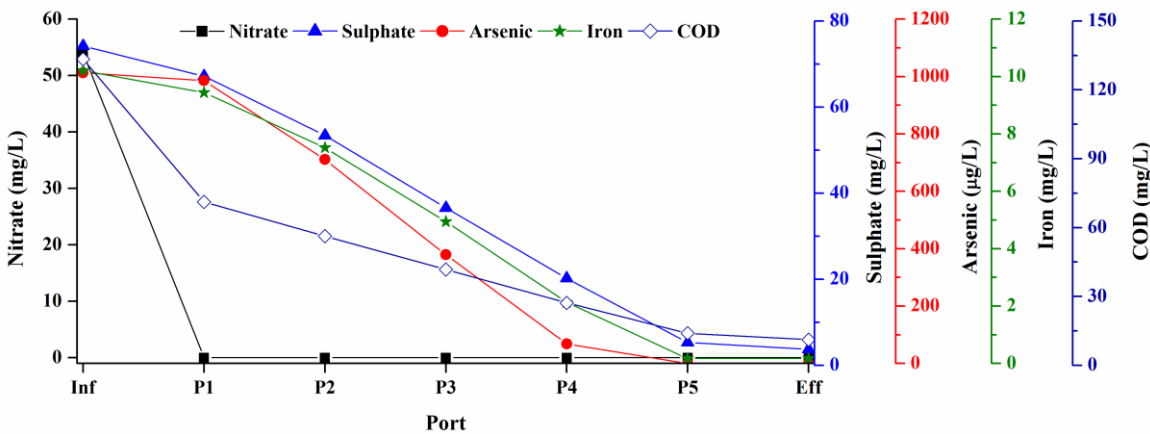


Figure 5.53 Sampling profile of the AGR-2 on day 382 (arsenic = 1000 µg/L, sulphate = 75 mg/L, iron = 10.0 mg/L, nitrate = 50 mg/L and EBCT 90 Min.).

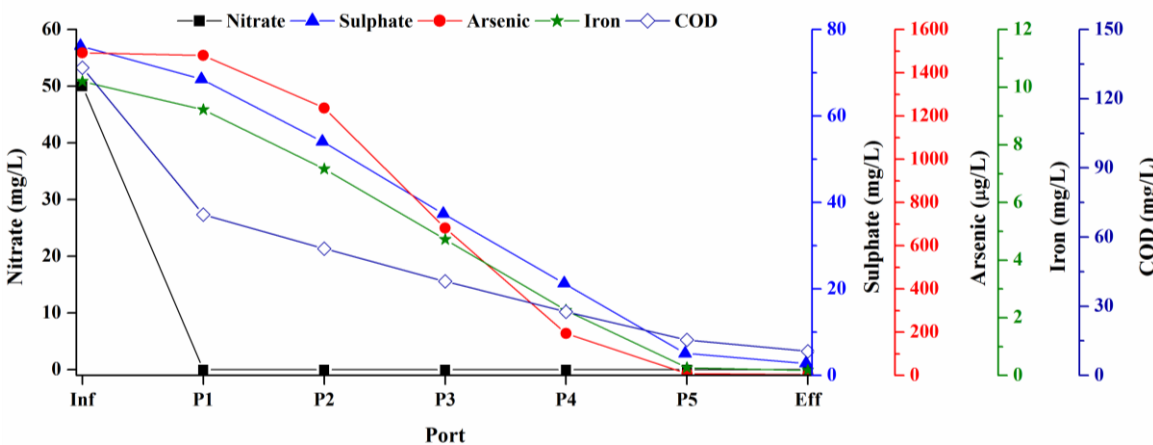


Figure 5.54 Sampling profile of the AGR-2 on day 444 (arsenic = 1500 µg/L, sulphate = 75 mg/L, iron = 10.0 mg/L, nitrate = 50 mg/L, and EBCT 90 Min.).

The influent As(V) which was reduced to As(III) by the microorganisms in the reactor resulting in arsenosulphides formation such as orpiment (As_2S_3), realgar (AsS) etc. in presence of biogenic sulphides. Moreover, presence of iron improves the removal of arsenic via adsorption on to the iron sulphides and/or co-precipitation as arsenopyrites in sulfidogenic environment, which results in an appreciable arsenic removal in the system. Similar results were obtained by Altun et al. (2014) in a sulphidogenic ethanol-fed reactor treating acid-mine drainage. They observed the highest arsenic removal of 95.4% with an influent arsenic concentration of 20 mg/L in presence of 200 mg/L Fe (II) in the influent, with the highest COD and SO_4^{2-} removal efficiency of 95% and 80% respectively. They also suggested that low sulphide concentration improves arsenic removal efficiency even at neutral to alkaline pH. Upadhyaya et al. (2010) also observed the arsenic removal to below 20 $\mu\text{g/L}$ from influent arsenic of 200 $\mu\text{g/L}$ in presence of 22.4 mg/L sulphate and 10 mg/L iron in a series of two acetate-fed bioreactors for drinking water treatment.

5.6.4 AGR-2 Phase 3: Effects of Influent Nitrate

Figure 5.55 depicts the effects of initial nitrate concentration of 50, 100, 150 and 200 mg/L on AGR-2 performance during phase-3 operation.

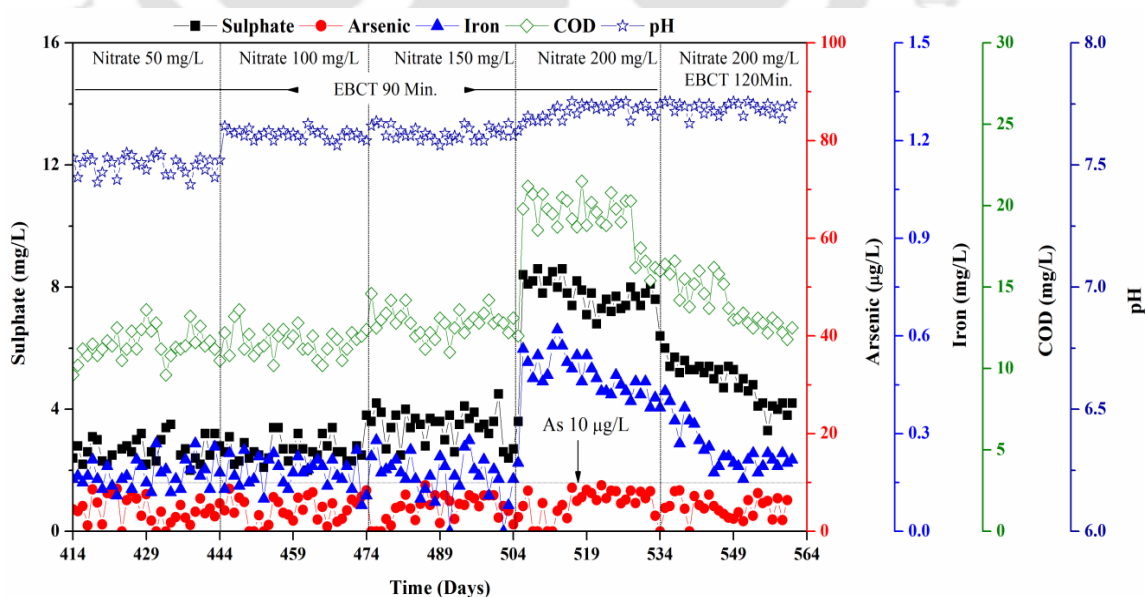


Figure 5.55 Performance evaluation of AGR-2 in phase-3 at initial arsenic = 1500 $\mu\text{g/L}$, iron = 10 mg/L, nitrate = 50-200 mg/L and sulphate = 75 mg/L.

AGR-2 responded better to the feed changes in terms of denitrification as well as arsenic and iron removal. Irrespective of initial NO_3^- concentration (up to 200 mg/L), NO_3^- in the treated water remained below detection limit therefore, not plotted in the Figure. From day 445 to 474, SO_4^{2-} and COD removal efficiencies were 96% and 92% with mean values of 2.7 ± 0.5 mg/L and 11.5 ± 0.8 mg/L respectively, at influent nitrate of 100 mg/L. The iron and arsenic removal in AGR-2 was remained stable during this period. With the increase in feed nitrate from 50 to 100 mg/L (day 414 to day 474) SO_4^{2-} and COD removal efficiencies were 96% and 92% with mean values of 2.7 ± 0.5 mg/L and 11.5 ± 0.8 mg/L respectively. Moreover, increase in NO_3^- concentration from 50 mg/L to 100 mg/L did not affect iron and arsenic removal in AGR-2. Iron and arsenic removal percentages were on average 98.2% and 99.7% respectively. The treated water pH varied between 7.44 and 7.67 during this period.

Profile sampling: The profile sampling results of day 474 are shown in Figure 5.56. It shows complete NO_3^- removal and just 7% SO_4^{2-} removal in the 1st sampling port. The SO_4^{2-} reduction lasted till 5th sampling port and a total of 89% sulphate removal was observed in port 5. Arsenic and iron removal was prolonged till port 5 with 99% and 97.5% removal efficiencies respectively. The arsenic and iron removal followed sulphate removal. From day 475 to day 505, the AGR-2 performance was stable.

In presence of 150 mg/L of NO_3^- in the influent, arsenic and iron in the treated water remained below 10 $\mu\text{g/L}$ and 0.3 mg/L, respectively. The average values of SO_4^{2-} and COD were at 3.4 ± 0.5 and 12.8 ± 0.8 mg/L with 95% and 94% removal efficiencies, respectively. Treated water pH was between 7.60 and 7.68. The profile sampling results of day 505 is shown in Figure 5.57.

An increase in iron, SO_4^{2-} and COD in the treated water was observed without any change in arsenic concentration when influent nitrate was 200 mg/L (day 506 to 533) at influent nitrate of 200 mg/L. During this period, the average concentration of iron, SO_4^{2-} and COD in the treated water were found to be 0.48 ± 0.05 mg/L, 7.8 ± 0.5 mg/L and 19.2 ± 1.6 mg/L, respectively. The decreased SO_4^{2-} reduction efficiency might be associated with higher influent nitrate due to which the SO_4^{2-} removal was delayed in the bioreactor. The increase in COD in treated water could be due decreased SO_4^{2-} reduction in the reactor. The profile sampling results (Fig 5.58) of day 533 also confirmed the same.

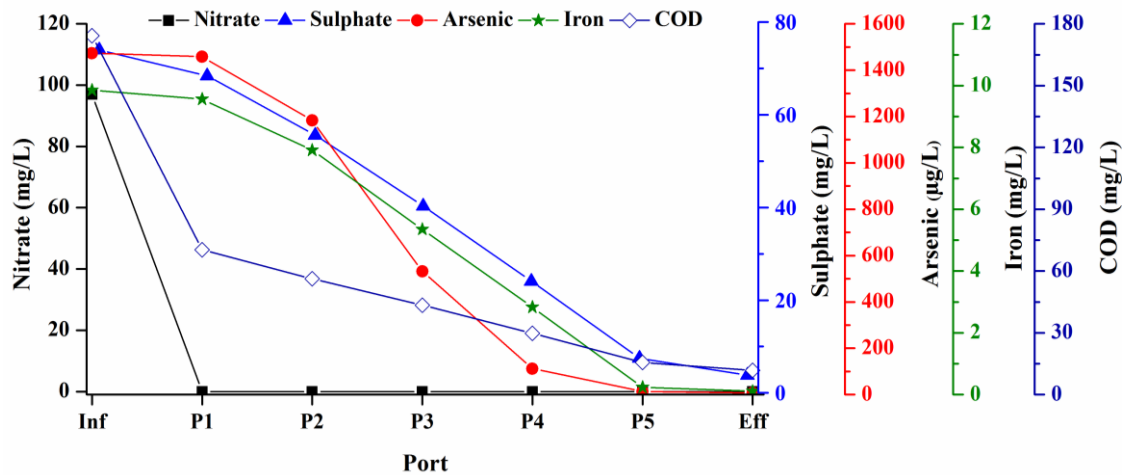


Figure 5.56 Sampling profile of the AGR-2 on day 474 (nitrate = 100 mg/L, arsenic = 1500 µg/L, sulphate = 75 mg/L, iron = 10.0 mg/L and EBCT 90 Min).

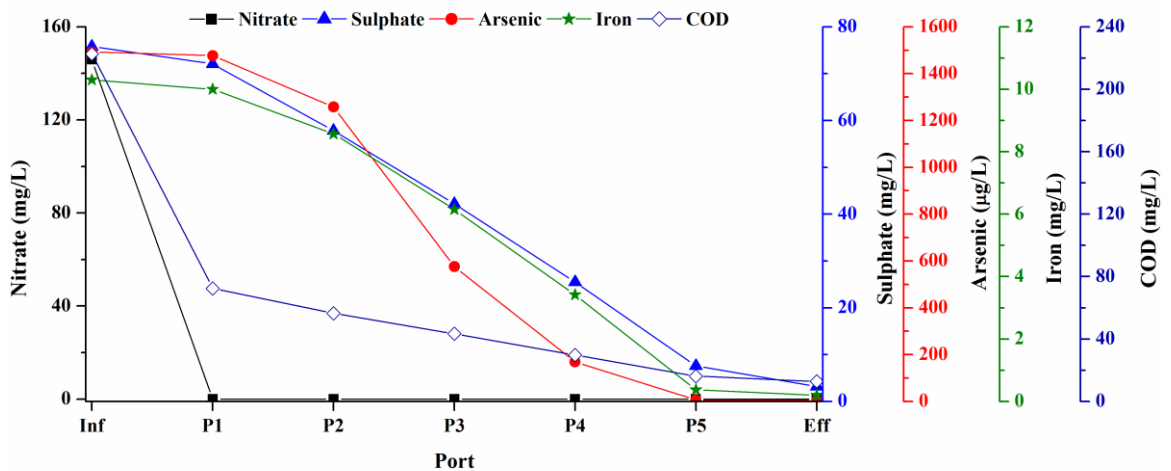


Figure 5.57 Sampling profile of the AGR-2 on day 505 (nitrate = 150 mg/L, arsenic = 1500 µg/L, sulphate = 75 mg/L, iron = 10.0 mg/L and EBCT 90 Min).

Hence, the reactor was operated at increased EBCT of 120 min from day 534 onwards. At longer EBCT (120 min) SO_4^{2-} in the treated water reduced to 4.9 ± 0.9 mg/L. This increased SO_4^{2-} reduction in turn improved iron removal. The iron in treated water was 0.28 ± 0.06 mg/L with 97.2% removal efficiency. COD in the treated water was also reduced to 16.8 ± 0.9 mg/L. The arsenic removal efficiency remained high (~ 99.6%) leaving 5.4 ± 3.0 µg/L in the treated water during last 55 days of operation of the AGR-2

fed with initial NO_3^- of 200 mg/L. The pH of the treated water remained in between 7.67 and 7.76 during this period. The profile sampling results of day 561 is shown in Figure 5.59.

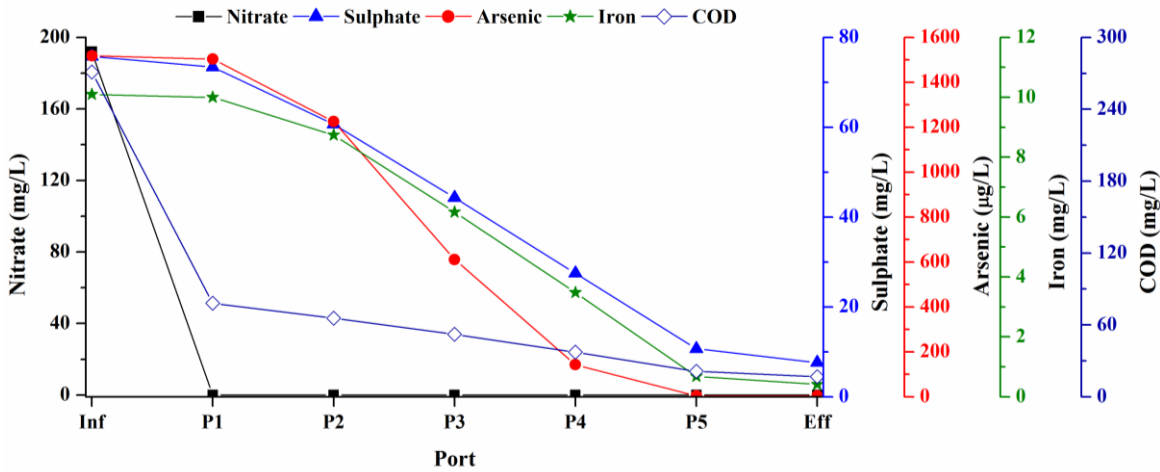


Figure 5.58 Sampling profile of the AGR-2 on day 533 (nitrate = 200 mg/L, arsenic = 1500 µg/L, sulphate = 75 mg/L, iron = 10.0 mg/L and EBCT 90 Min).

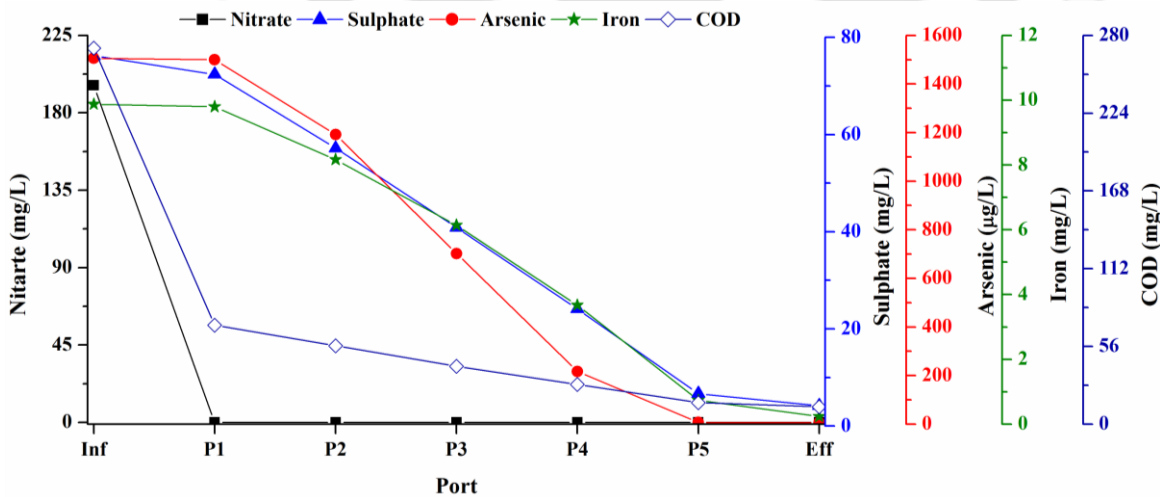


Figure 5.59 Sampling profile of the AGR-2 on day 561 (nitrate = 200 mg/L, arsenic = 1500 µg/L, sulphate = 75 mg/L, iron = 10.0 mg/L, and EBCT 120 Min).

Complete nitrate removal up to 200 mg/L in AGR-2 is giving evidence of the presence of different active denitrifying bacteria in the original seed. Chen et al. (2008) also observed similar results for simultaneous NO_3^- and SO_4^{2-} removal in a granular sludge bioreactor operated at pH 8. They have reported 78% and more than 99% SO_4^{2-} and NO_3^- removal respectively from an initial loading of $2.1 \text{ kgm}^{-3}\text{day}^{-1}$ and $1.7 \text{ kgm}^{-3}\text{day}^{-1}$. The microbial population in their reactor revealed presence of *Proteobacteria*, *Bacteroidetes*, *Chloroflexi* and *Fimicutes* which are also major microbial group found in our studied bioreactors (section 5.10.3.1). Gruyer et al. (2013) reported simultaneous removal of nitrate (300 mg/L) and sulphate (500 mg/L) with sulphate removal (98%) followed by denitrification (95-99%) in a constructed wetlands.

5.6.5 AGR-2 Phase 4: Effect of Initial pH

Effects of initial pH of 6.6, 7.2 and 8.4 on AGR-2 performance are shown in Figure 5.60. The system showed performance stability to the experiments done at pH 6.6 and 7.2 from day 562 to day 623. Irrespective of initial pH, treated water arsenic remained at mean value of $3.0 \pm 2.0 \text{ } \mu\text{g/L}$ with more than 99% removal efficiency during this period. The treated water NO_3^- was always below detection limits throughout the phase-4 operation and therefore, not shown in the figure. The iron in the treated water was below 0.3 mg/L with an average value of 0.13 ± 0.06 during the reactor operation at initial pH of 6.6 and 7.2. SO_4^{2-} and COD in the treated water were averaged $2.5 \pm 0.52 \text{ mg/L}$ and $11.8 \pm 0.8 \text{ mg/L}$ corresponding to 90% and 89 % removals, respectively. A little increase in pH was observed but it remained between 7.18-7.28 and 7.66-7.74 at an initial pH of 6.6 and 7.2. With the further increase in influent pH to 8.4 from day 624 to day 658, a little drop in SO_4^{2-} removal was seen and this contributed little increase in treated water COD in treated water. In AGR-2, SO_4^{2-} and COD removal percentages were on average 74.3% and 84.7%, respectively. Iron removal dropped to 84.5 % in the reactor leaving $0.47 \pm 0.04 \text{ mg/L}$ in the treated water. However, the arsenic removal remains unaffected and remains below 10 $\mu\text{g/L}$ during the reactor operation even at influent pH 8.4. The pH in the treated water was raised and remained between 8.48-8.62. Reduction in SO_4^{2-} removal could be due to slower adaptation of SRB at higher initial pH of 8.4 and would require some more time to adapt in new pH. Visser et al. (1996) reported that at high pH SRB growth is inhibited. Despite a little drop in iron removal, the result indicates the

stability of the process in a wider pH range. High removal efficiencies were achieved as treated water NO_3^- remained below their detection limits and arsenic met the drinking water standards.

Mixed microbial community showed to immediately adapt to the changing pH conditions at 6.6, 7.2 and 8.4. Moreover, the reactor performance remained stable at different pH values because the reactor pH was always between 7.2 and 9.0, which is between 1st and 2nd pKa values of H_2S ($\text{pK}_{a1}=7.04$ and $\text{pK}_{a2}=11.96$ at 25°C). Hence, most of the dissolved sulphide was as HS^- rather than H_2S , and the formation of H_2S can be considered low.

Results from AGR-2 demonstrated greater arsenic and iron removal than those reported in the literature. Jusoh et al. (2011) reported optimum iron removal as biogenic iron sulphide at pH between 7 and 8 in a bioreactor treating real groundwater. Hayes et al. (2014) also reported optimum pH for biogenic FeS formation was circumneutral pH (6.5-7.3) by SRB, *D. vulgaris*. They also suggested slightly alkaline pH is beneficial to form more-amorphous biogenic iron-sulphide. However, SRB growth was retarded at pH 5.6 and 8.9 but they observed fast adaptation of SRBs and suggested that mackinawite

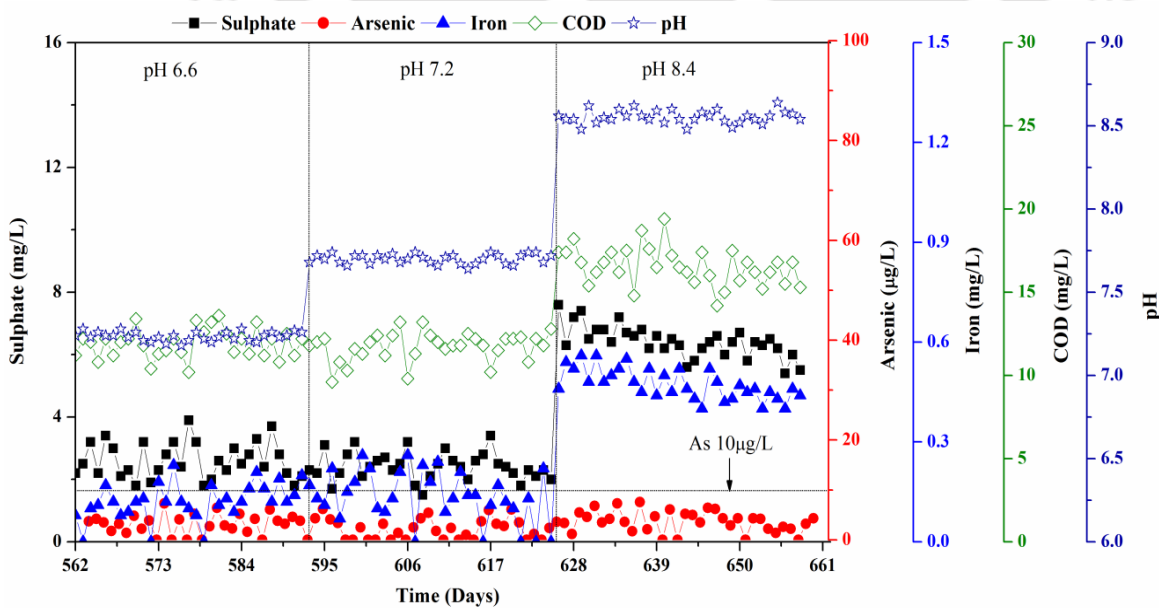


Figure 5.60 Performance evaluation of AGR-2 in phase-4 at initial arsenic = $500 \mu\text{g/L}$, iron = 3.0 mg/L , nitrate = 50 mg/L and sulphate = 25 mg/L .

formation was sensitive to pH and lower pH leading to more crystallinity. In the present study amorphous and nanocrystalline phases of iron as well as arsenic sulphides were formed (Refer section 5.11.4.1). Hayes et al. (2009) reported that biogenic FeS generated by *D.acetoxidans* is highly efficient in As(III) removal (100% removal efficiency) from water, especially, in pH range from 4.0 to 7.5 whereas beyond pH 9 As(III) removal was decreased. They suggested As(III) uptake at low pH was resulting from FeS dissolution and AsS precipitation, while at higher pH it was attributed to the adsorption of As(III) oxyacid species to surface sites on the FeS solid. The biogenic FeS was more efficient than synthetic mackinawite by 2.5 times in terms of arsenic uptake as biogenic FeS has high porosity and unique textural properties. They also suggested that biogenic FeS can be an efficient scavenger of As(III), even at low solution concentrations. At higher arsenic concentration, As(III) uptake increases gradually suggesting biogenic FeS has more accessible surface at higher pH and accessible sulphide at lower pH.

5.6.6 AGR-2 Phase 5: Effect of operating Temperature

Figure 5.61 shows AGR-2 performance on arsenic, iron and nitrate removal at operating temperature of 20°C, 30°C, 40°C and 50°C. Change in operating temperature did not negatively affect the system performance in terms of NO_3^- and arsenic removal. Irrespective of operating temperature (up to 50°C) treated water nitrate remained below detection limits during entire phase-5 operation and therefore, not shown in the figure. The average SO_4^{2-} and COD in the treated water were between 2.8-6.2 mg/L and 11.9-15.4 mg/L, with removal efficiencies of 83% and 87 %, respectively, at 20°C. Iron in the treated water was stable at mean values of 0.23 ± 0.04 with 92% removal efficiency. From day 659 to day 695, the treated water arsenic remained below 10 $\mu\text{g/L}$, with mean values of 5.6 ± 2.0 $\mu\text{g/L}$. AGR-2 responded better to the temperature changes of 30°C, 40°C and showed high removal efficiencies for arsenic, iron, SO_4^{2-} and COD with 99.2%, 96%, 88%, and 89% removal respectively.

During first 16 days of AGR-2 operation at 50°C (from day 758 to 774), slight increase in the concentrations of SO_4^{2-} and COD were observed in the treated water. The SO_4^{2-} and COD were found between 7.5-9.3 mg/L and 16.6-20.7 mg/L, respectively. Arsenic and iron in the treated water remained between 2.6-8.5 $\mu\text{g/L}$ and 0.24-0.36 mg/L

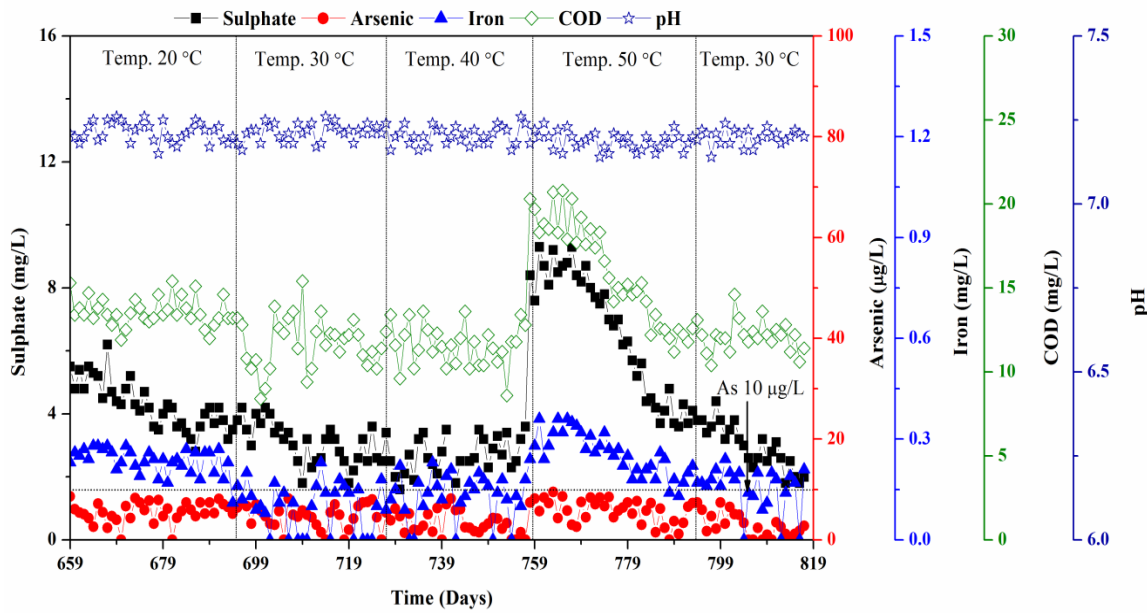


Figure 5.61 Performance evaluation of AGR-2 in phase-5 at initial arsenic = 500 µg/L, iron = 3.0 mg/L, nitrate = 50 mg/L and sulphate = 25 mg/L.

during this period. The possible reason for this increase in SO_4^{2-} and COD could be due to the time taken by microbial community to adopt in a new temperature regime. However, mixed microbial consortia showed to immediately adapt to the operating conditions of 50°C. Once the adaptation was over, the SO_4^{2-} and COD in treated water were resumed back to 3.6 mg/L and 11.2 mg/L, respectively at the end of the phase-5. Similarly, the iron and arsenic were at mean values of 0.20 ± 0.04 mg/L and 4.8 ± 2.5 µg/L respectively. The treated water pH remained between 7.15 and 7.30 throughout the phase-6 operation. The performance of AGR-2 remained stable from day 793 to day 817 when the operating temperature was reduced back to 30°C.

The occurrence, activity and quick adaptation of microbial population involved in denitrification (Braker et al., 2010), sulphate reduction (Gramp et al., 2010), and iron reduction at elevated temperatures is well documented. Interestingly, Gramp et al. (2010) showed biogenic iron sulphides precipitation with sulphate-reducing bacteria under laboratory conditions at 22, 45, and 60 °C in 16 weeks old culture. They also reported an enhanced crystallinity of the Mackinawite (FeS) and greigite (Fe_3S_4), which were the dominant iron sulphide phases, on an increase in the incubation temperature from 22 to 60°C. Also the formation and stability of amorphous orpiment is reported at 0 to 50°C

temperature range (Welch & Stollenwerk, 2007). Xia et al. (2014) also suggested 30-40°C temperature as optimum range for arsenic removal as arsenosulphides in sulphate reducing batch reactors.

5.6.7 AGR-2 Phase 6: Treatment of Real Groundwater

The AGR-2 was operated to determine its performance on removal of multipollutants from real groundwater. Characterization and treatment of contaminated groundwater in AGR-2 is discussed in details in section 5.7.

5.6.8 AGR-2 Phase 7: Performance at Lower EBCT

Figure 5.62 shows the temporal profiles of sulphate, arsenic, COD and pH at lower EBCT of 30 min. The overall performance of AGR-2 at 30 min EBCT remained stable in terms of nitrate, arsenic and iron removal. As seen during previous phases, NO_3^- in the treated water remained below detection limits and therefore, not plotted in the figure. With the decrease in EBCT from 45 min to 30 min a little drop in average SO_4^{2-} removal efficiency was seen (80% removal) but it did not negatively affect on either arsenic or iron removal in the AGR. Average iron and arsenic removal efficiencies were 94.5% and 99.2% with mean concentration in treated water were 0.16 ± 0.04 mg/L and 3.6 ± 2.1 µg/L, respectively. SO_4^{2-} and COD of only 5.0 ± 0.5 mg/L and 12.8 ± 0.7 mg/L remained in the treated water at the end of phase-7. The treated water pH remained stable between 7.19 and 7.32. The results of phase-7 suggested the presence of sufficient number of bacteria in the form of biofilms on the WAC granules over the entire length of the column, which were readily utilizing the available electron acceptors even at lower EBCT.

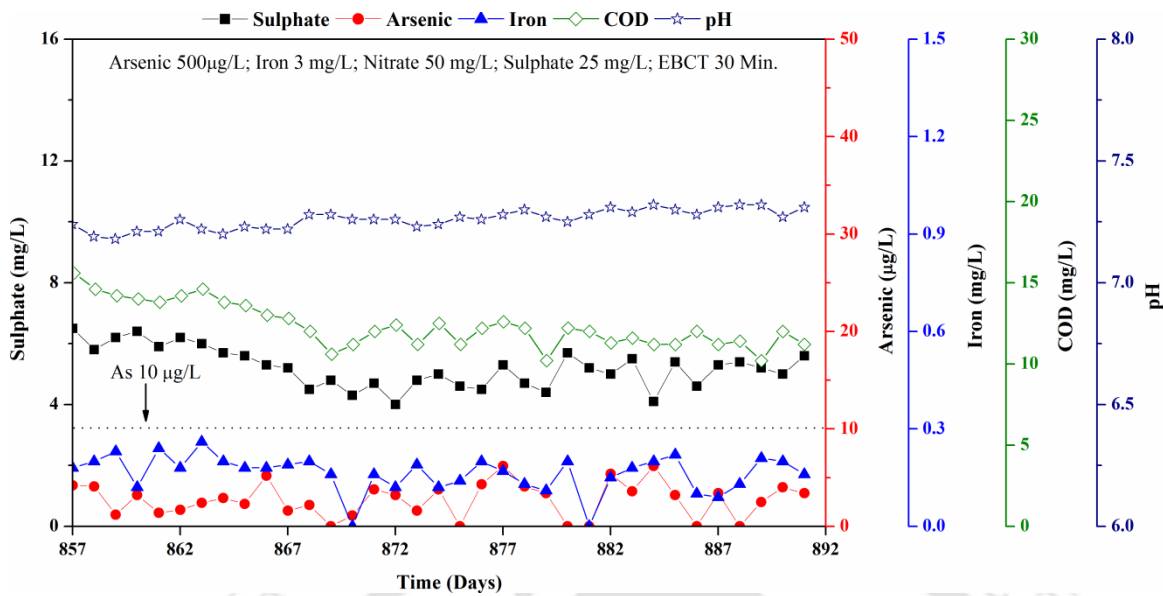


Figure 5.62 Performance evaluation of AGR-2 in phase-7 at initial arsenic = 500 µg/L, iron = 3.0 mg/L, nitrate = 50 mg/L and sulphate = 25 mg/L.

5.6.9 AGR-2 Phase 8: Performance after Shutdown

Performance of AGR-2 after 7 days shutdown period is shown in Figure 5.63. The re-adaptation period after a shutdown is an important factor in the design and performance evaluation of a bioreactor system. Like AGR-1, the NO_3^- removal was completely recovered within few hours and resumed below detection limits in the treated water after restart of AGR-2. When the AGR-2 was restarted after a one week shutdown, the removal of arsenic and iron was initially unstable immediately after the restart, but was gradually enhanced after 2-3 days. Average removal efficiency of arsenic and iron after the 1st day was 76 % and 59%, respectively, which was further enhanced with higher SO_4^{2-} reduction. More than 70% SO_4^{2-} removal efficiency was restored within 7 days of operation after shutdown and average SO_4^{2-} in the treated water was between 4.2-5.2 in last 10 days of operation (day 917 to 926). The COD removal was improved gradually with SO_4^{2-} reduction. The iron removal in the treated water was found below permissible limits after 6th day of operation in phase-8. Arsenic in the treated water was resumed to below 10 µg/L after 4 days of operation with 99% efficiency. These results indicated there was no significant inhibition on the system performance corresponding to one week-shutdown, and the reactor recovered itself fully after a few days (less than a week) of operation.

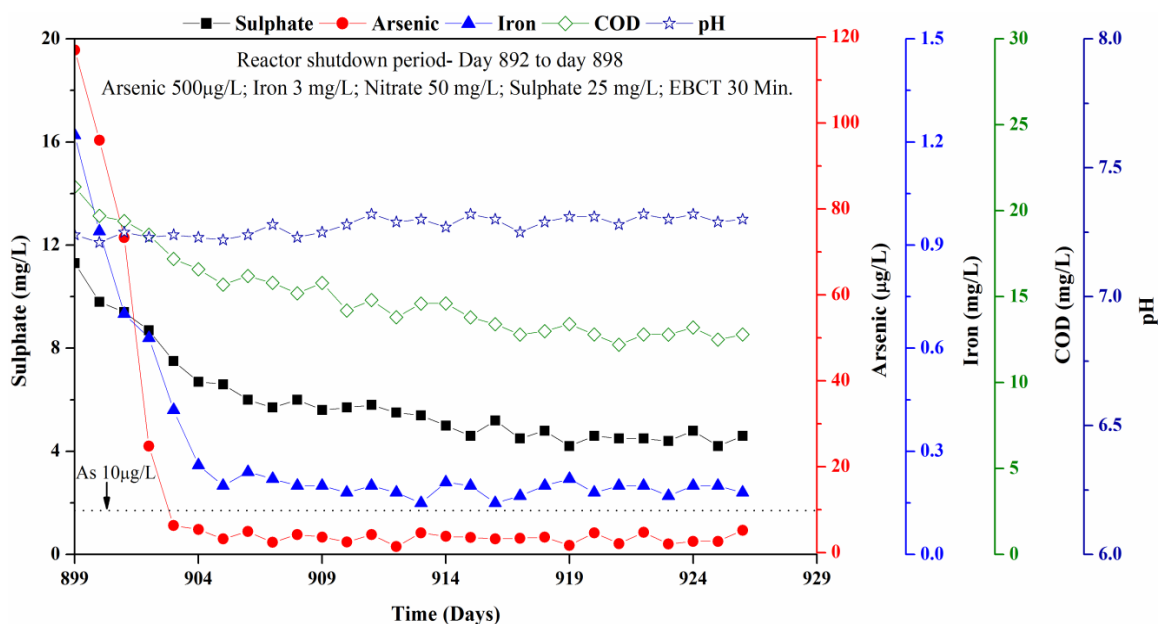


Figure 5.63 Performance evaluation of AGR-2 in phase-8 at initial arsenic = 500 µg/L, iron = 3.0 mg/L, nitrate = 50 mg/L and sulphate = 25 mg/L.

5.7 AGR-2 Operation with Real Groundwater

The performance of AGR-2 with real groundwater is shown in Figure 5.64. AGR-2 responded better to the feed change, the treated water nitrate concentration was below detection limits. From type-1 groundwater, AGR-2 reduced arsenic and iron to well below drinking water standards. From day 829 to 836, when AGR-2 was fed with type-2 groundwater the average iron concentration in the treated water rose to 3.31 mg/L. This increase in iron could be due to unavailability of sufficient sulphide for iron sulphides precipitation. The iron in treated water resumed below 0.3 mg/L when reactor was operated with enhanced amount of sulphate (100 mg/L) and longer EBCT (120 min), the arsenic in treated water was always below 2.0 µg/L in this experimental period. The average COD and SO_4^{2-} in the treated water were 11.0-14.0 mg/L and 5.5-7.5 mg/L respectively. The pH of the treated water remained between 7.28 and 7.38 during entire period of operation. The results shows that AGR-2 could remove both arsenic and iron from real groundwater provided sufficient amount of sulphate added and adequate reaction time provided in terms of EBCT.

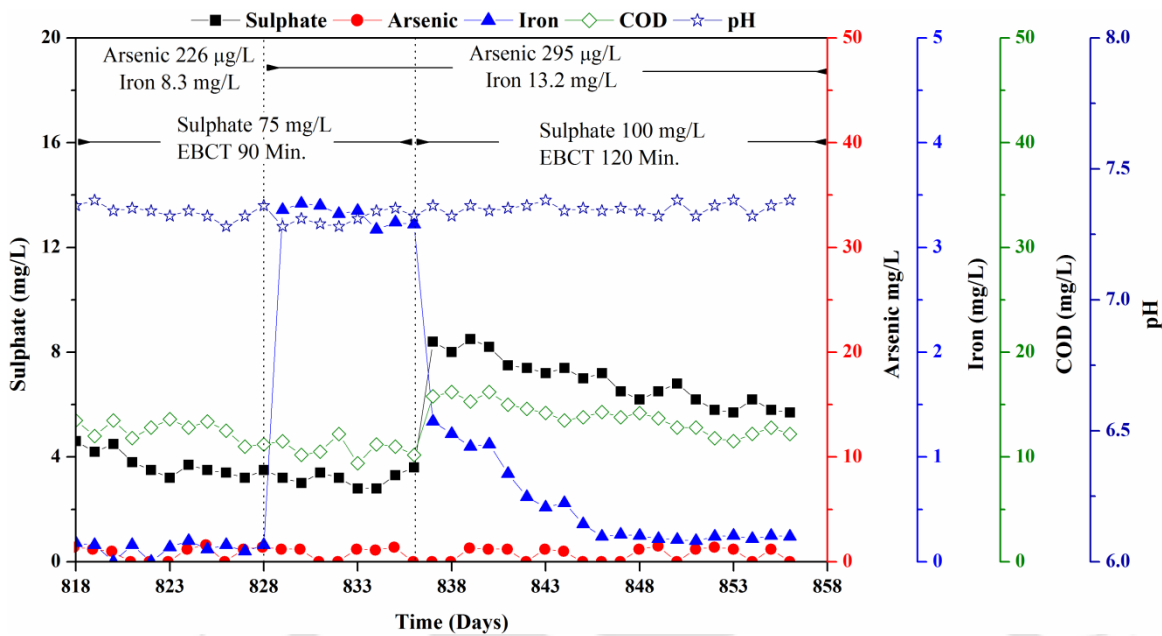


Figure 5.64 Performance of AGR-2 with real groundwater.

5.8 Characterization of Bioreactor Treated Water

5.8.1 MPN Test

The presumptive MPN test a series of nine or twelve tubes of lactose broth are inoculated with measured amounts of water to see if the water contains any lactose-fermenting bacteria that produce gas. No gas formation was seen in any of the lactose broth containing tubes, thus it was presumed that no coliforms were present in the treated water sample.

5.8.2 Whole Effluent Toxicity (WET) Test Results

There were no noticeable differences between the results of water quality parameters measured in different test vessels during the experiment (Table 5.1). The observed data of present study indicate that the test fishes, survived well during 96 h of exposure. There was no fish mortality was seen in both mode of experiments, static as well as in static renewal. The fishes have been shown complete survival in absolute as well as in diluted treated water. The changed surfacing behaviour such as fast movement and swimming as well as jumping out from the test media was observed to be increased in

first 24 h of the commencement of the toxicity experiments. Jumping out of fish and fast movement signify the avoidance reaction of fish to the treated water. With the continuation of the exposure, the fishes progressively became normal. Ahmed et al. (2013) reported acute toxicity of arsenic (96 h; LC50) in freshwater fish tilapia (*Oreochromis mossambicus*) at 28.22 ppm. The WET test result suggests the presence of very low arsenic concentration in effluents of AGR is not imposing acute toxicity as a whole.



Table 5.1 Whole Effluent Toxicity test results of AGR treated water at $30\pm 2^\circ\text{C}$.

Mode of experiment	Type of effluent water	Initial no. of test fish	Exposure Time (h)								Remarks
			24		48		72		96		
			Alive	Dead	Alive	Dead	Alive	Dead	Alive	Dead	
Static	Control	7	7	0	7	0	7	0	7	0	For first 24 h the movement of fish was high.
	50% diluted		7	0	7	0	7	0	7	0	
	Absolute		7	0	7	0	7	0	7	0	
Static renewal	Control	7	7	0	7	0	7	0	7	0	
	50% diluted		7	0	7	0	7	0	7	0	
	Absolute		7	0	7	0	7	0	7	0	

5.9 Fluoride Removal using Water Treatment Plant Residues

5.9.1 Effect of WTR Dose

The effect of WTR dose on the fluoride ions removal was studied using different mass of WTR and initial fluoride concentration of 5.0 mg/L. The amount of fluoride ions removed by 4, 8, 12, 16, 20, 24 and 28 g/L of WTRs is shown in Figure 5.65. As seen in the figure, the defluoridation was increased with an increase in WTR dose. About 90% removal efficiency was obtained within 2 h contact time at WTR dose of 28 g/L. The amount of fluoride ions adsorbed increased with increase in WTR dose this may be due to availability of more active binding sites on the surface and pore volume at higher doses (Yadav et al., 2013). Although, with the increase in dose of WTR fluoride removal efficiency was higher, the water became turbid at WTR dose greater than 16 g/L. At this dose of WTR, fluoride in the treated water was 1.4 mg/L. At lower dose up to 12 g/L of WTR, fluoride concentration in the treated water was 2.0 mg/L, which was more than the upper permissible limit in drinking water. Therefore, WTR dose of 16 g/L has been considered as the optimum dose for fluoride removal in drinking water.

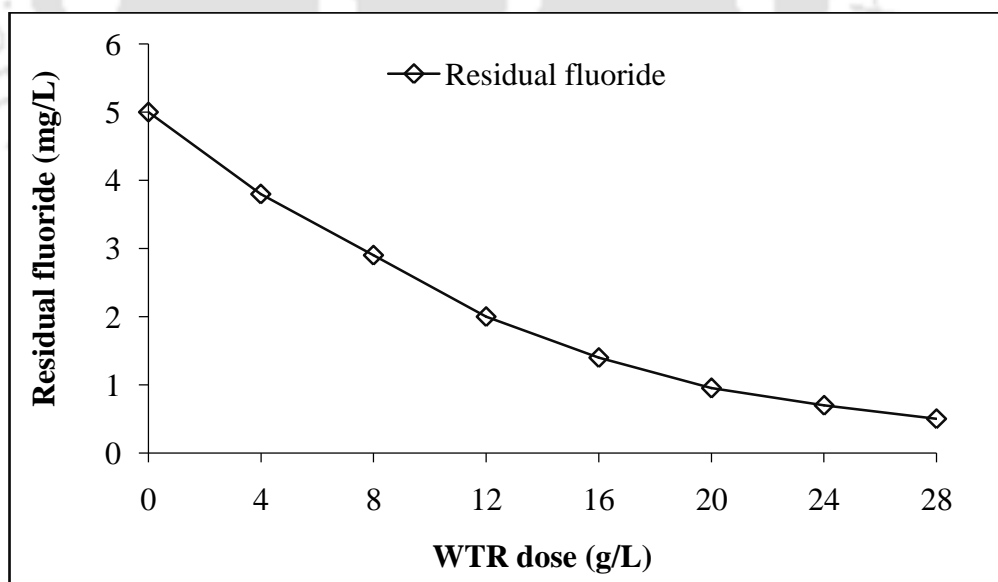


Figure 5.65 Effects of WTR dose on fluoride removal (Ini. fluoride concentration = 5.0 mg/L, contact time = 120 min., agitation speed = 100 rpm, temperature = 30°C and pH = 6.9-7.4).

5.9.2 Effect of Contact Time

The results of kinetic studies are presented in Figure 5.66. Results of the experiment showed that, fluoride ions removal increased with time up to 120 min, and thereafter removal was slowed down significantly. Fluoride in treated water was found to be 1.1 mg/L (79% removal efficiency) in 180 min. at WTR dose of 16 g/L for initial fluoride concentration of 5 mg/L. Thus, 120 min was considered as the equilibrium time for further studies.

5.9.3 Effect of Agitation Speed

The effect of agitation speed on fluoride ion adsorption was studied over the range of 50-250 rpm for 120 min. Study was carried out at an initial fluoride concentration of 5 mg/L and WTR dose of 16 g/L. As shown in Figure 5.67, fluoride removal increased with increase in agitation speed and reached the maximum at 250 rpm. At lower agitation speed of 50 rpm, the fluoride ion adsorption was the lowest and could not reduce fluoride to meet the drinking water standards. Increase in adsorption efficiency at a higher agitation speed could be explained in terms of the reduction of boundary layer thickness and/or boundary layer resistance around the adsorbent particles and increases the mobility

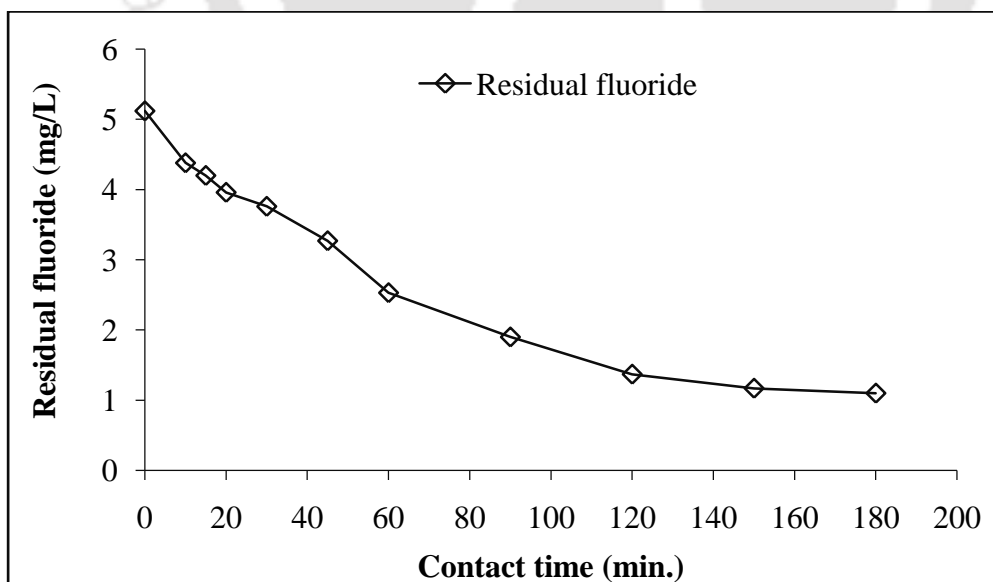


Figure 5.66 Effects of contact time on fluoride removal (Ini. fluoride concentration = 5.0 mg/L, WTR dose = 16 g/L, agitation speed = 100 rpm, temperature = 30°C and pH = 6.9-7.4).

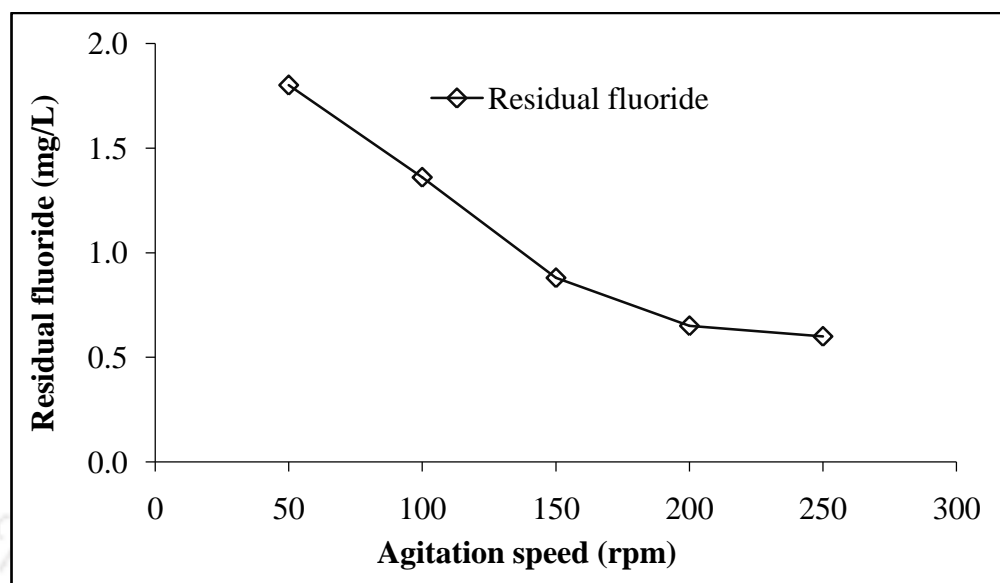


Figure 5.67 Effects of agitation speed on fluoride removal (Ini. fluoride concentration = 5.0 mg/L, WTR dose = 16 g/L, contact time = 120 min, temperature = 30°C and pH = 6.9-7.4).

of fluoride ion in the system (Geethamani et al., 2014; Hanafiah et al., 2009). Additionally, higher agitation speed also encourages better mass transfer of fluoride ions from bulk solution to the surface of the adsorbent and hence reduces the adsorption equilibrium time (Hanafiah et al., 2009). Although, fluoride removal efficiency increased with the increase in agitation speed, increase in efficiency from 200 rpm to 250 rpm was not significant. Therefore, 200 rpm was considered as optimum agitation speed for further studies.

5.9.4 Effect of Initial Fluoride Concentration

Effects of initial fluoride concentration on fluoride removal by WTR at a dose of 16 g/L are shown in Figure 5.68. When initial concentration was 8 and 9 mg/L, 1.32mg/L and 1.65 mg/L of fluoride, respectively were left out in the treated water, suggesting that the WTR (16 g/L) could reduce from up to 8 mg/L of fluoride to below the upper limit of 1.5 mg/L in drinking water.

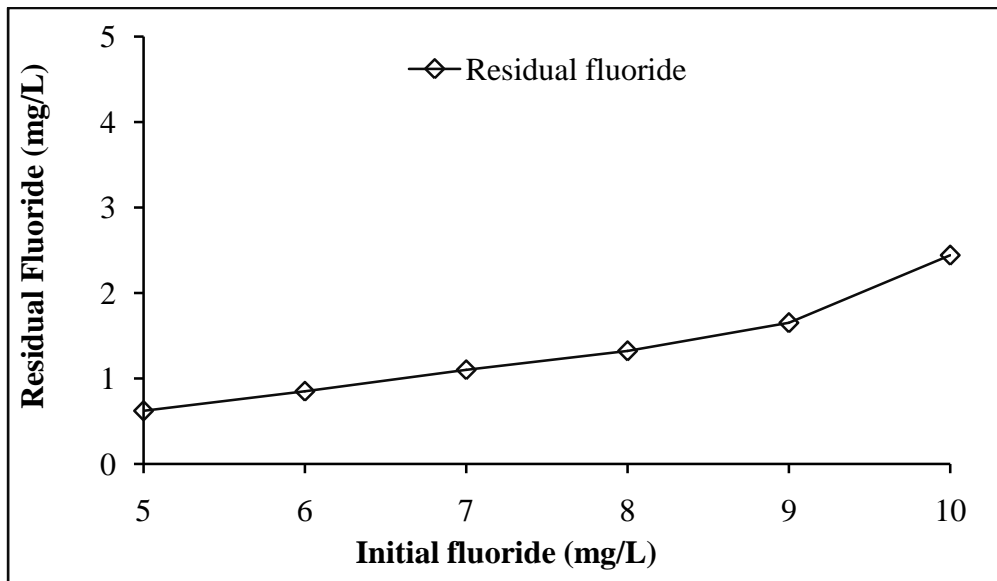


Figure 5.68 Effects of initial fluoride on fluoride removal (WTR dose = 16 g/L, contact time = 120 min, agitation speed = 200 rpm, temperature = 30°C and pH = 6.9-7.4).

5.9.5 Effect of Initial Temperature

The effect of temperature on fluoride ion adsorption was studied in solution temperature range from 15 to 55°C. As shown in Figure 5.69, residual fluoride in treated water decreased with increase in water temperature up to 45°C. However, removal efficiency remained fairly constant at temperature between 25 and 45°C. At 55°C, fluoride removal efficiency decreased and 1.32 g/L of fluoride was left out in the treated water. This decrease in removal efficiency may be due to the fact that at high temperature the thickness of the boundary layer decreases due to increased tendency of the molecules to escape from the adsorbent surface to the solution phase, which results in a decrease in the adsorption capacity at increased temperatures (Sujana & Anand, 2011). The minimum adsorption efficiency of 74% was seen at 15°C. The poor adsorption at 15°C might be due to the unavailability of adsorption sites. Based on the above results, 30°C was considered as optimum for further experiments.

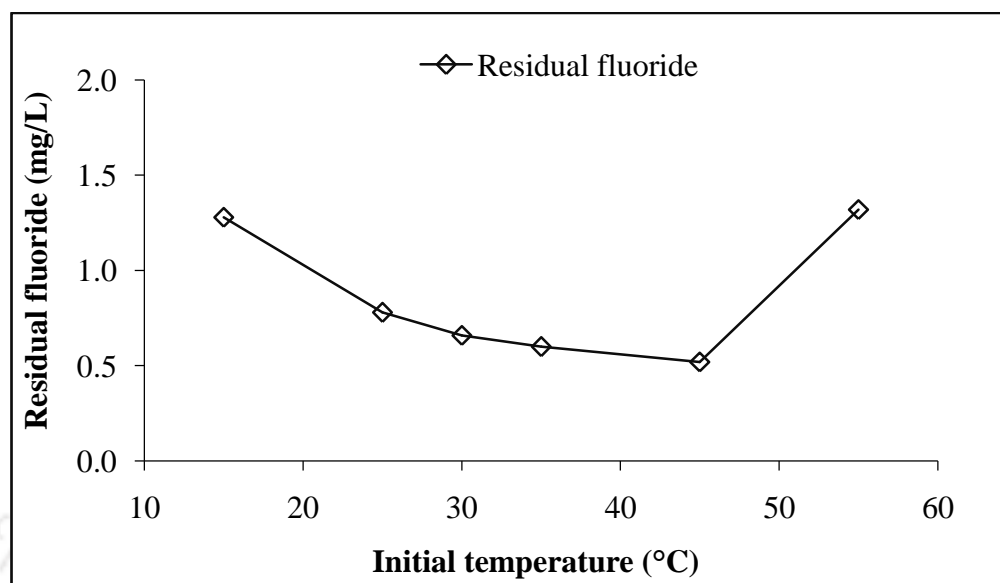


Figure 5.69 Effect of initial temperature on fluoride removal (Ini. Fluoride = 5.0 mg/L, WTR dose = 16 g/L, contact time = 120 min, agitation speed = 200 rpm, and pH = 6.9-7.4).

5.9.6 Effect of Initial pH

Figure 5.70 shows the pH profile of the solution during adsorption process. It can be seen from Figure.5.70 that the pH increases slightly during the entire adsorption process after the addition of WTR. It can be observed that the fluoride removal remained almost constant within the pH range of 5-7. Further increase in pH of the solution above 7 decreased the removal efficiency. The effective fluoride adsorption capacity by the WTR was observed in the near neutral pH range of 6-7, possibly due to presence of positively charged and neutral adsorption sites on the WTR surface. For the drinking water purposes, neutral pH is desirable for an adsorbent at which 82-88% fluoride removal was observed by WTR. Decrease in fluoride adsorption efficiency above pH 8 is possibly due to the electrostatic repulsion of fluoride ion to the negatively charged surface and the competition for active adsorption sites with fluoride ion, as increased number of hydroxyl groups decreases the number of positively charged sites (Kumar et al., 2008).

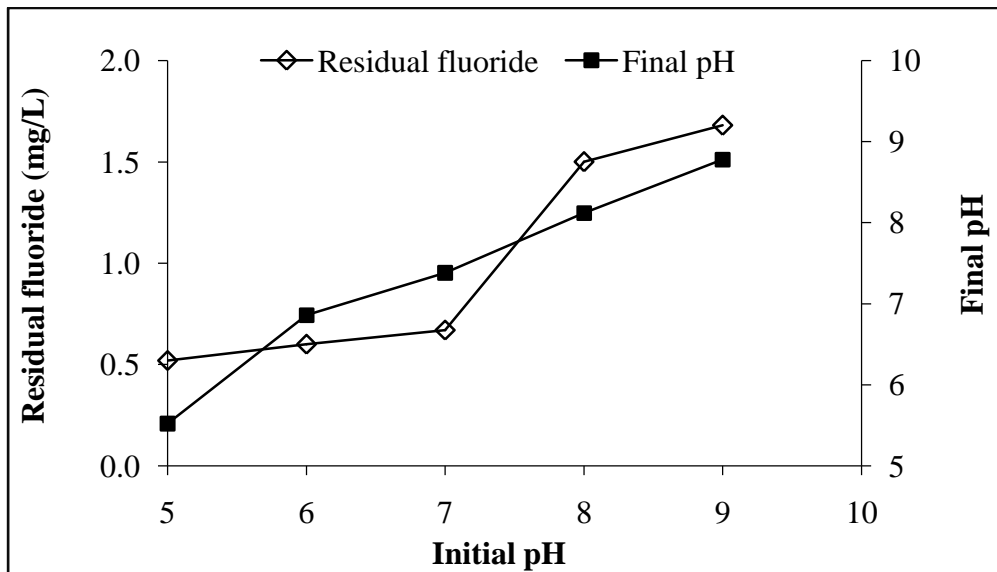


Figure 5.70 Effect of initial pH on fluoride removal (Ini. Fluoride = 5.0 mg/L, WTR dose = 16 g/L, contact time = 120 min, agitation speed = 200 rpm, and temperature = 30°C).

5.9.7 Adsorption Isotherm

The adsorption isotherm data were fitted to the linear forms Freundlich, Langmuir and Temkin isotherm models. The Langmuir, Freundlich and Temkin isotherm plot are presented in Figures 5.71, 5.72 and 5.73 respectively. The values of isotherm coefficients are given in Table 5.2. As shown in figure, a plot of C_e/q_e against C_e , yielded a straight line for WTR, which indicates the applicability of Langmuir adsorption isotherm for fluoride ions adsorption. The maximum adsorption capacity (q_m) of fluoride ion for Langmuir isotherm was found to be 0.298 mg/g. The Langmuir adsorption constant (B) is related to the affinity of binding sites and higher values of B for WTR indicate that the particle radius of adsorbent was larger toward adsorption (Bhaumik & Mondal, 2016). The R^2 value is closer to one, indicates that the Langmuir isotherm better explains the fluoride adsorption on WTR. The equilibrium parameter (R_L) value lies between 0 and 1, indicating a favourable absorption process (Nigussie et al., 2007). The data fit of Langmuir model suggests that fluoride adsorption onto WTR is monolayer chemisorption. The experimental data can also fit the Freundlich model well. Freundlich isotherm plot is shown in Figure. 5.71 and the corresponding parameters are given in Table 5.2.

Freundlich constant (K_f) shows ultimate adsorption capacity on heterogeneous sites with non-uniform distribution of energy level and adsorption intensity (n) is measure of the of fluoride ions adsorption on WTR. Since the value of $1/n$ is less than one, indicates favourable adsorption. Achak et al. (2009) also suggested favourable adsorption when 'n' value lies between 1 and 10. The poorly fit Temkin isotherm is shown in Figure 5.72 and corresponding parameters are given in Table 5.2. The equilibrium binding constant (K_T) corresponds to maximum binding energy and B_T is related to heat of adsorption. The lower values of B_T indicate weak interaction between WTR and fluoride ions. The coefficients of all the three isotherms suggest that WAC was a better adsorbent in removing fluoride ions.

Table 5.2 Isotherm parameters for the removal of fluoride by untreated adsorbent (Ini. fluoride concentration = 5.0 mg/L, equilibrium contact time = 120 min., pH 7.0 \pm 0.1, and temperature = 30 \pm 2 $^\circ$ C).

Langmuir constants	q_m (mg/g) = 0.298	B (L/mg) = 1.266; R_L = 0.1340	$R^2 = 0.984$
Freundlich constants	K_f ((mg/g)/(mg/L) $^{1/n}$) = 0.163	$1/n = 0.329$	$R^2 = 0.983$
Temkin constants	K_T (L/mg) = 15.904	$B_T = 0.06$	$R^2 = 0.975$

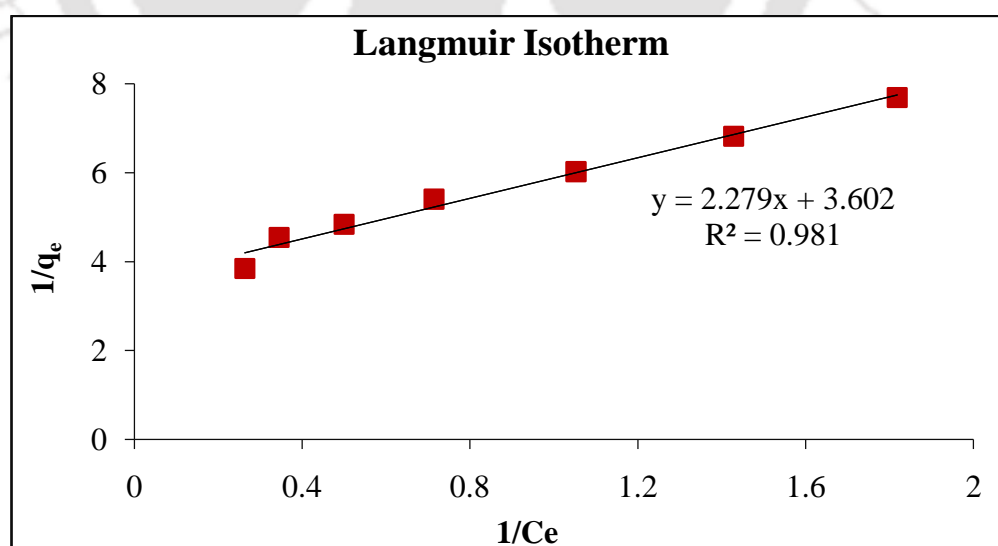


Figure 5.71 Linearized Langmuir isotherm for fluoride ion adsorption by WTR (Ini. fluoride concentration = 5.0 mg/L, equilibrium contact time = 120 min, pH 7.0, and temperature = 30 $^\circ$ C).

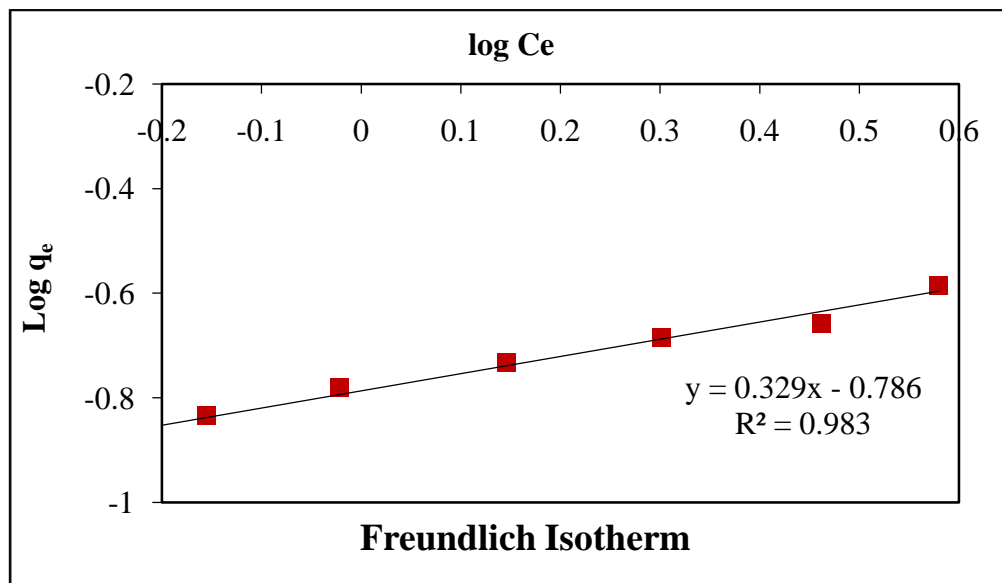


Figure 5.72 Linearized Freundlich isotherm for fluoride ion adsorption by WTR (Ini. fluoride concentration = 5.0 mg/L, equilibrium contact time = 120 min, pH 7.0, and temperature = 30 °C).

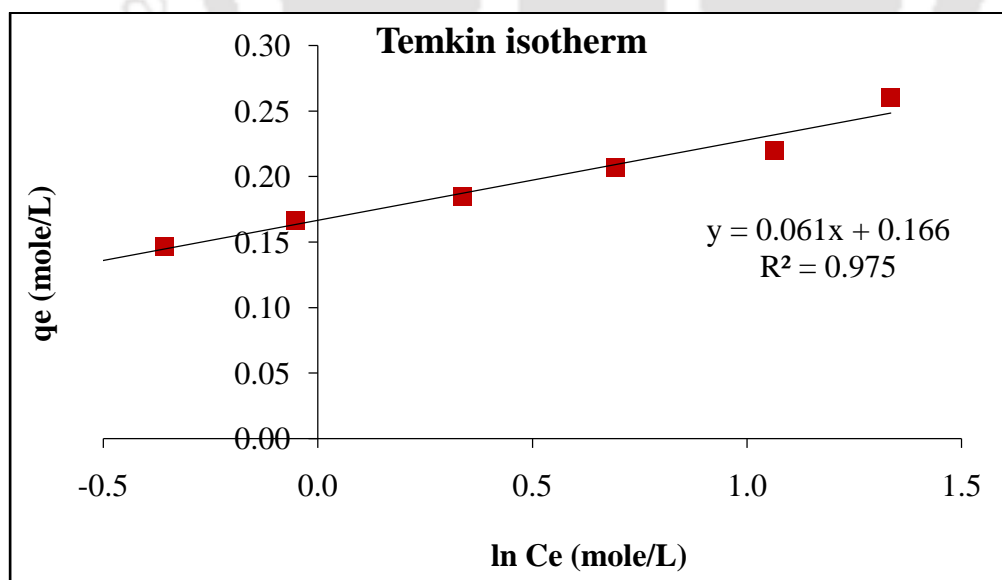


Figure 5.73 Linearized Temkin isotherm for fluoride ion adsorption by WTR (Ini. fluoride concentration = 5.0 mg/L, equilibrium contact time = 120 min, pH 7.0, and temperature = 30 °C).

5.9.8 Characterization of WTR

FESEM/EDX analysis

FESEM/EDX analysis of WTR adsorbent before fluoride adsorption is shown in Figure 5.74. FESEM image (Fig. 5.74a) revealed the surface structure of the WTR powder consisting of the fine particles of irregular shape and size.

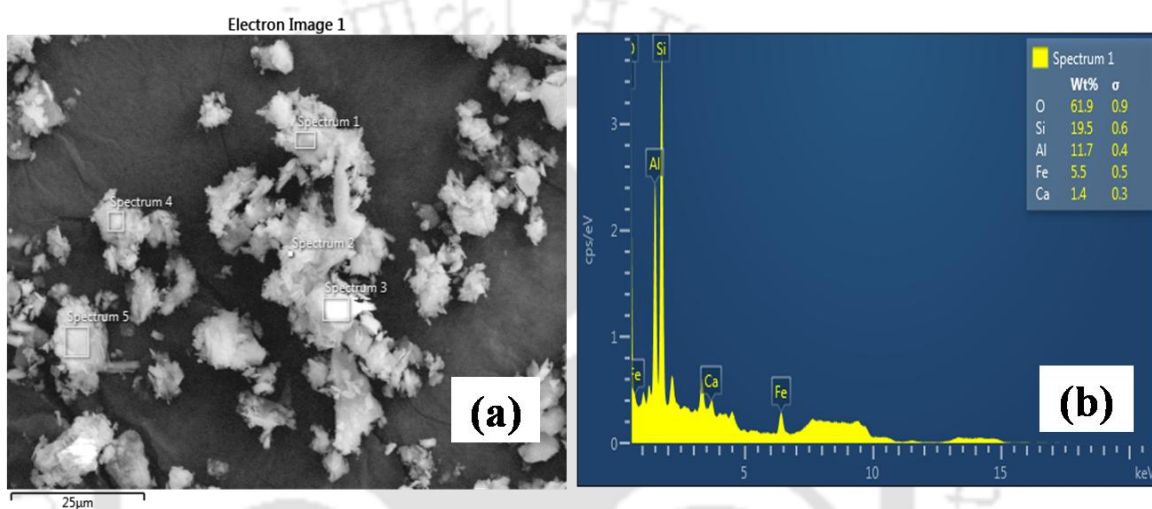


Figure 5.74 FESEM image (a) and EDX pattern (b) of WTR before fluoride adsorption.

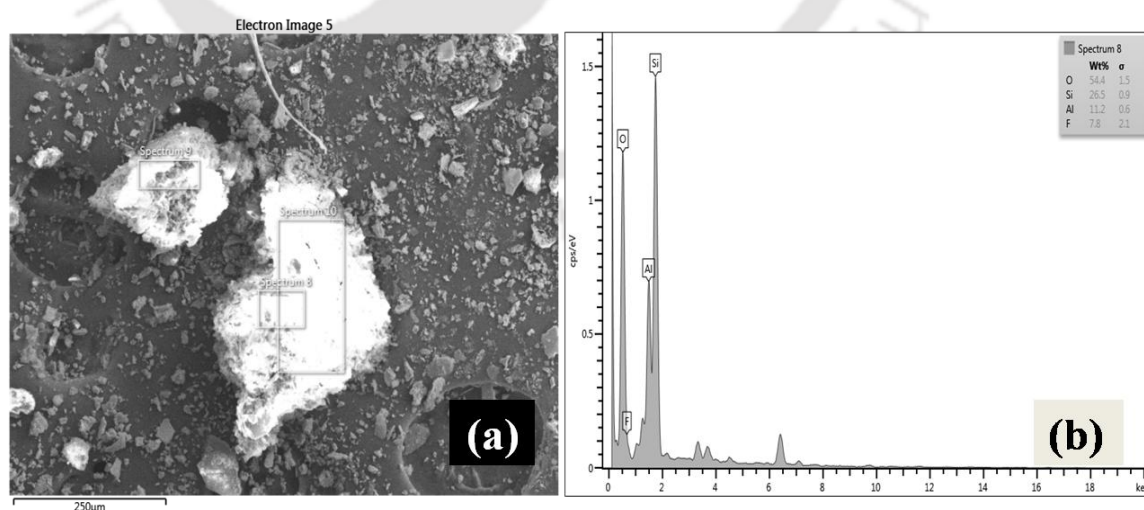


Figure 5.75 FESEM image (a) and EDX pattern (b) of WTR after fluoride adsorption.

This irregular shape of particles with their surface exhibiting a micro-rough texture, promotes the fluoride adherence on it. The EDX pattern (Fig.5.74b) of WTR shows the elemental presence of aluminium, iron, silicon, potassium, calcium, magnesium, oxygen, and carbon. The results of EDX analysis was again confirmed by FTIR and XRD patterns. FESEM/EDX pattern of WTR after adsorption given in Figure 5.75.

FT-IR analysis

The FT-IR spectra of WTR were obtained to understand the nature of the functional groups present in it. FT-IR spectra of WTR before and after adsorption are shown in Figure 5.76. FT-IR spectra (Fig. 5.76A) displayed a number of peaks, indicating the complex nature of the adsorbent. The peak positions in the FT-IR pattern indicated the composition of the tested substances, and the amplitudes reflected the relative content levels of different components. The WTR are physical mixtures of aluminium and iron oxides containing substantial amounts of silica. The broad band in the range of 1500–1875/cm is due to the oxides of aluminium and iron oxides. The structures of the WTR before and after adsorption were similar, but their contents have changed.

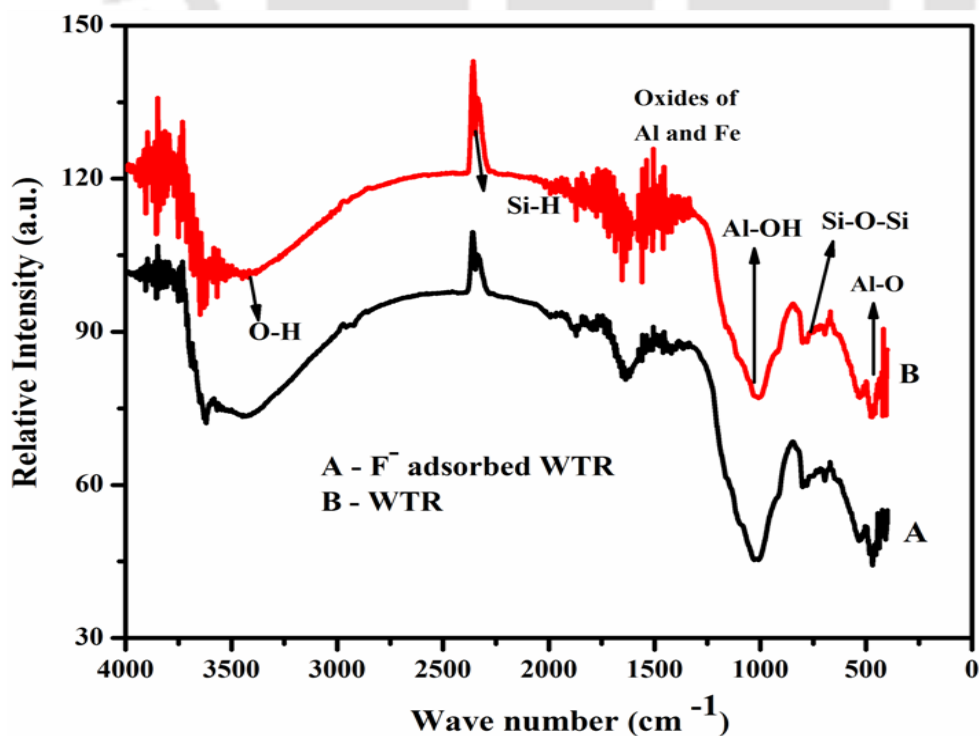


Figure 5.76 FT-IR patterns of WTR before and after adsorption.

The band at 2347/cm generally corresponds to the Si-H bending mode of water. The metal–oxygen groups are observed at 470, 800, and 1,028/cm, corresponding to Al–O, Si–O–Si, and Al–OH stretching mode, respectively (Zhang et al., 2014b). It is inferred that OH groups and metal–oxygen groups have been taking part in the adsorption procedure.

XRD analysis

The XRD pattern of the WTR confirmed the characteristic peaks of SiO_2 , Al_2O_3 , and Fe_2O_3 (Figure 5.77). The presence of oxides of silica, aluminium and iron supports the fluoride removal potential of the WTR because of their greater affinity for fluoride. Moreover, the use of above oxides as it is and their modifications is well documented for fluoride removal from drinking water (Bhatnagar et al., 2011). The possible mechanism of adsorption onto WTR were seems to be surface complexation, chemisorption and ion exchange.

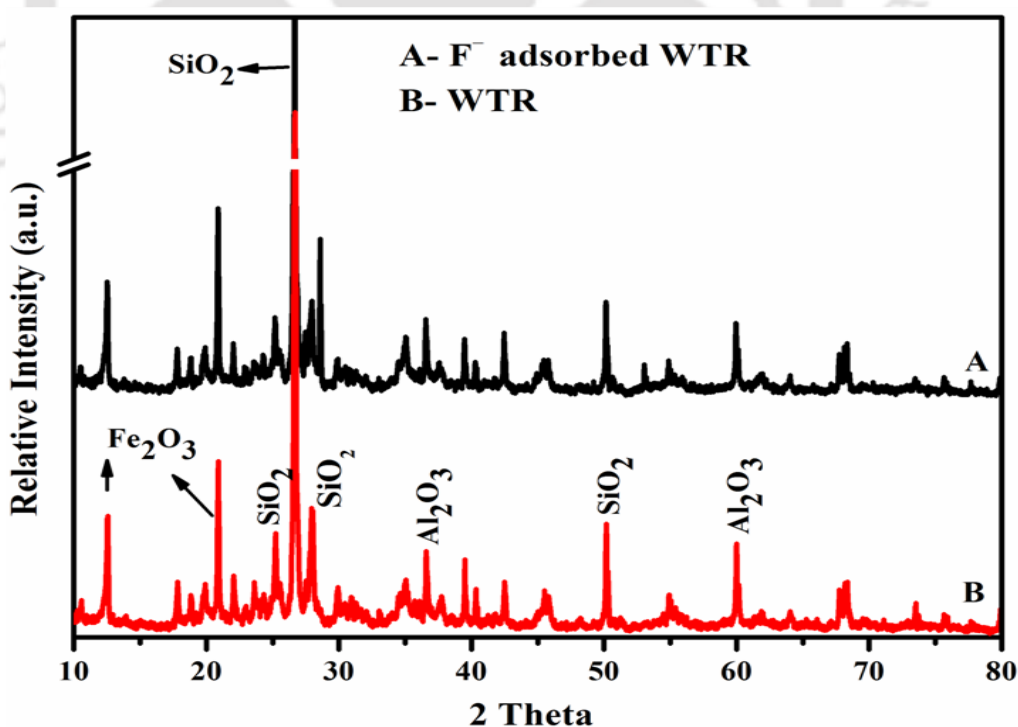


Figure 5.77 X-ray powder diffraction patterns of WTR before and after adsorption.

5.10 Microbial Population Identification and Diversity Analyses

5.10.1 Microbial Biofilm on WAC

FESEM analysis was performed on WAC granules to reveal presence of the microbial growth and biofilm formation. The virgin WAC granule was not showing any microbial growth (Figure 5.78a). The presence of small pores on the WAC is also seen, which were probably served as site for microbial growth. The presence of biofilm grown on the WAC was containing rod and cocci shaped bacteria are shown in Figure 5.78b.

5.10.2 T-RFLP Analysis

The result of a T-RFLP profiling is a graph called Electropherograms which is an intensity plot representation of an electrophoresis experiment (gel or capillary). In an electropherogram, the X-axis marks the sizes of the fragments while the Y axis marks the fluorescence intensity of each fragment. Thus, what appears on an electrophoresis gel as a band appears as a peak on the electropherogram whose integral is its total fluorescence. In a T-RFLP profile, each peak assumingly corresponds to one genetic variant in the original sample while its height or area corresponds to its relative abundance in the specific community. T-RFs having size less than 40 bases were eliminated from the analysis as they might result from primer-dimers. The data obtained from the T-RFLP analysis were

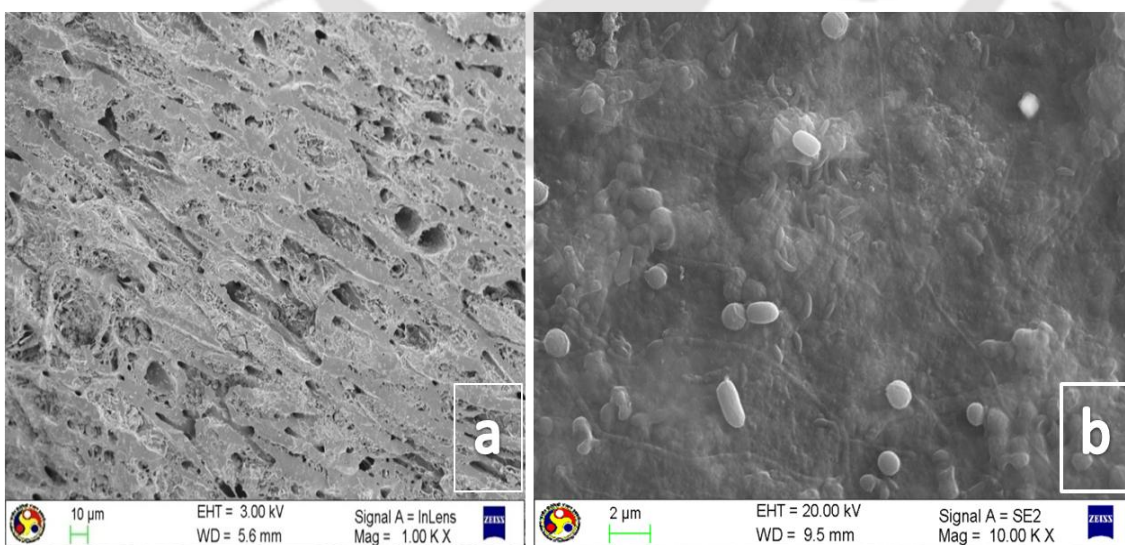


Figure 5.78 FESEM image of WAC granules from AGR-1 (a) before and (b) after biofilm growth on WAC granules.

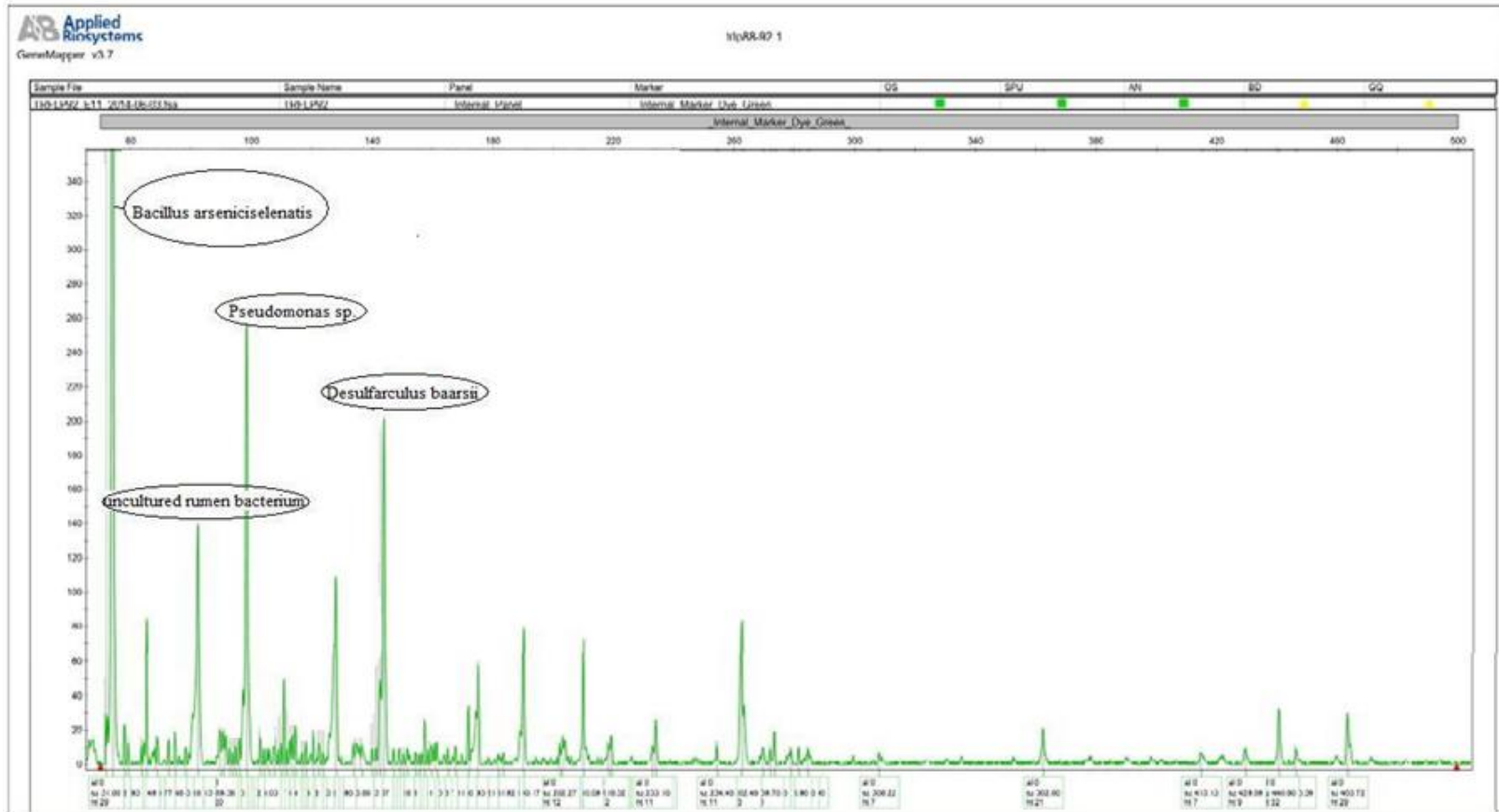


Figure 5.79 T-RFLP profile of microbial community present in AGR-1 collected after 250 days of operation.

compared with databases available at <http://mica.ibest.uidaho.edu/pat.php> to identify the probable species present. The Electropherogram revealed the presence of arsenic, nitrate and sulphate reducing microbial communities in the AGR-1, responsible for reduction of arsenic, nitrate and sulphate. The Electropherogram is given in Figure 5.79.

5.10.3 Metagenomic Analysis

The aim of the study was focused on the identification of microbial community structure involved in the reduction of electron acceptors present in the both bioreactor systems. The WAC granules harbouring biofilms collected from AGR-1 and AGR-2 were analyzed using the 16S rRNA gene and metagenomic sequencing. In addition to getting information about the microbial community, we also gained new insights into the microbial ecology of the system, specifically about how certain physiochemical changes might influence bacterioplankton communities. Here, we used Illumina MiSeq to sequence amplicons generated from the V4 region of the 16S rRNA gene to investigate the bioreactor microbiome. A total number reads were determined by pyrotag sequencing of 16S rRNA amplicons. The numbers of operational taxonomic units (OTU) that were generated for the taxonomy identification based on the fixed similarity threshold of 0.80 (80%) confidence (Table 5.2). In house-PERL program was used for read filtering and V3 consensus making whereas for V3 analysis and taxonomy studies the QIIME software-1.8.0 was used. The following illumina PCR primer sequences were used for sequencing-
Forward primer sequence- 341 Forward: 5' CCTACGGGAGGCAGCAG 3'
Reverse primer sequence- 518 Reverse: 5' ATTACCGCGGCTGCTGG 3'

Table 5.3 Total number of OTUs read in AGR-1 and AGR-2

Description	AGR-1	AGR-2
Total Reads	6,41,500	7,28,574
Total OTUs Picked	1,50,79	1,064
Total Singleton OTUs	8,026	553
Total OTUs after singleton removal	7,053	511

5.10.3.1 Overall Microbial Community Structure

Similarities in major taxonomic groups were observed for AGR-1 and AGR-2. The pie charts shown in the Figure 5.80 and 5.81 illustrate the distribution of taxonomic phylum and class for the annotations. Each slice indicates the percentage of OTUs with predicted proteins and ribosomal RNA genes annotated to the indicated taxonomic level. Only, top 10 (OTU count wise) taxonomic categories are represented as a plot in the report. The taxonomic classes other than top 10 results are categorized as “Others”. The sequences with very less similarity or no similarity or whose V3 regions do not have any alignment hits against taxonomic database are categorized as “Unknown”.

Taxonomic hits distribution at phylum level

In both the bioreactors, most of the OTUs were belongs to the Phylum *Proteobacteria* (Fig. 5.80). The mixed microbial consortia in AGR-1 & AGR-2 have 37% & 50% *Proteobacteria* as largest microbial population. The *proteobacteria* are major phylum of gram negative bacteria which includes many of the bacteria responsible for sulphate reduction and nitrogen fixation. *Actinobacteria*, *Acidobacteria*, *Bacteroidetes*, *Firmicutes*, *Spirochaetes*, and *TM6* were among other major phyla present in the AGR systems. The *Bacteroidetes* and *Firmicutes* are facultative anaerobic and obligate anaerobic group of bacteria which are widely distributed in environment. The large group of SRB falls under *Firmicutes*.

Taxonomic hits distribution at class level

Taxonomic hits distribution at class level in both reactors is shown in Figure 5.81. Most of the OTUs in AGRs were distributed in four bacterial class *Delta-*, *Beta-*, *Gamma-* and *Alphaproteobacteria* of phylum *Proteobacteria*. The Delta-subdivision was the most dominant *Proteobacteria*, followed by Beta-, Gamma-, and Alpha-subdivisions. Most of the OTUs of SRB were from taxonomic class *Deltaproteobacteria*. The DsrAB that catalyzes the energy-conserving step during dissimilatory sulphate reduction pathway that is conserved in most SRBs distributed in *Deltaproteobacteria*. *Chlorobia*, *Anaerolineae* (in AGR-1) *Clostridia* and *Actinobacteria* (in AGR-2) were the next abundant taxonomic class. The majority of denitrifying bacteria are related to *Alpha-*, *Beta-*, and *Gamma Proteobacteria* in the previous studies done with full- and pilot-scale denitrification bioreactors.

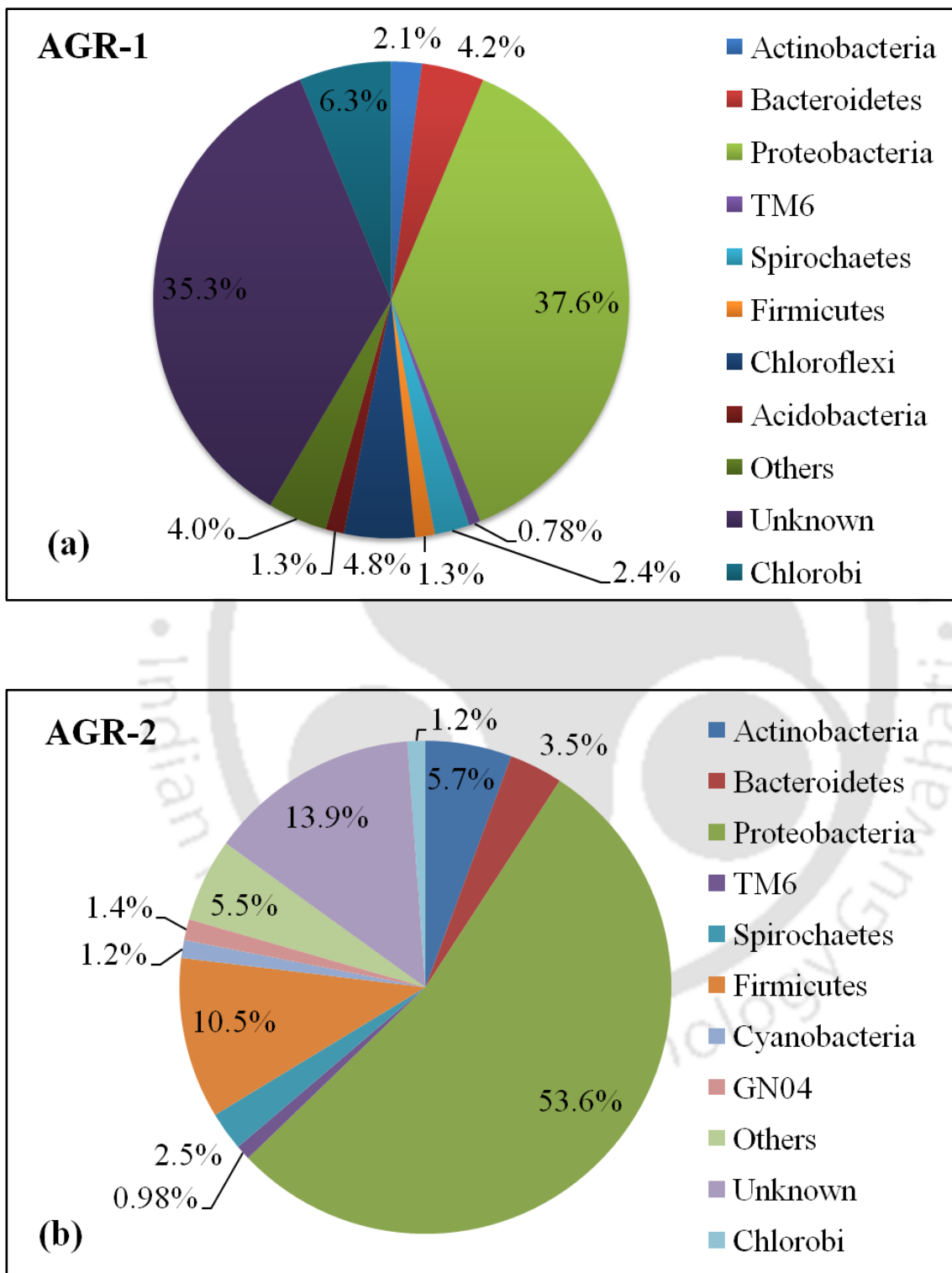


Figure 5.80 Taxonomic hits distribution at phylum level of (a) AGR-1 and (b) AGR-2.

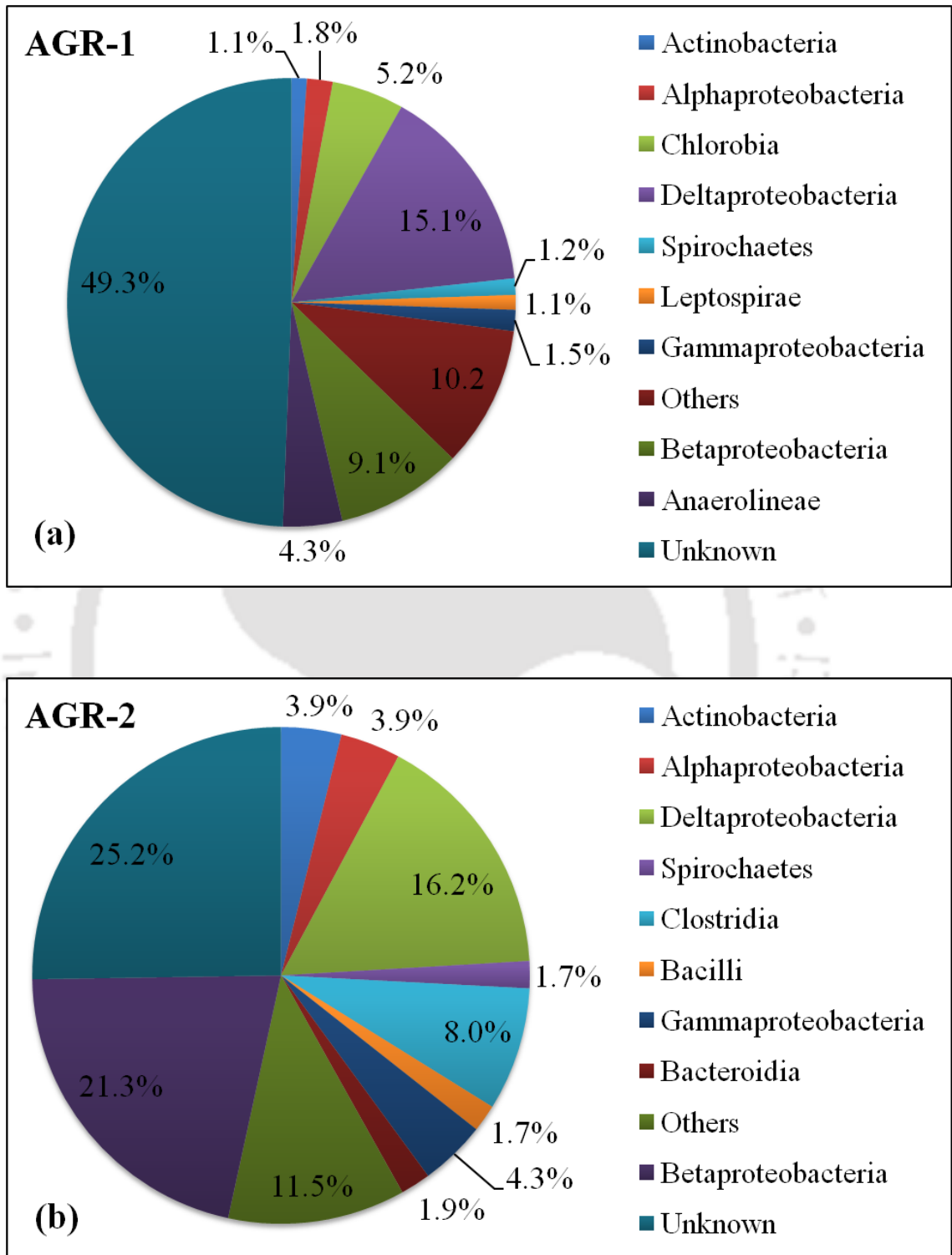


Figure 5.81 Taxonomic hits distribution at class level of (a) AGR-1 and (b) AGR-2.

5.10.3.2 Prevalence of Sulphate Reducing Microorganisms

Sulphate reducing microorganisms were the most important functional group in AGRs. Sequences affiliated to genus *Desulfosporosinus*, *Desulfovibrio*, *Desulfobacca*, *Desulfomonile*, *Desulfomicrobium*, *Desulfoglaeba*, *Desulfobulbus* and *Desulfarculus*, were detected in both AGRs. Similar microbial genera, *Desulfomicrobium* and *Desulfovibrio* (Altun et al., 2014), *Desulfosporosinus* (Battaglia-Brunet et al., 2012) were also observed in sulphidogenic arsenic removal bioreactors. Moreover, *Desulfosporosinus* related strain is reported to play major role in the As(V) respiration in sulphidogenic system. *Desulfosporosinus* strains are reported from municipal drinking water and capable of utilizing nitrate or arsenate as electron acceptors (Ramamoorthy et al., 2006). Hoelt et al. (2004) also reported MLMS-1 Strain similar to *Desulfobulbus* genera (*Delta-Proteobacteria*), from anoxic lake water. The strain was capable of reducing arsenate by using sulphide as electron donor. Based on 16S rRNA gene sequence, Sun et al. (2010a) reported that acetate oxidising genera *Desulfarculus* (*Deltaproteobacteria*) is closely related to the *Desulfovibrio*, *Syntrophobacter* and *Desulfomonile*, which are other existing SRBs in the AGRs. *Desulfovirga*, *Deltaproteobacteria* and *Syntrophobacteriales* are strictly anaerobic, having a respiratory type of metabolism. They are using C₁-C₁₂ straight-chain fatty acids, other organic acids, and alcohols as carbon sources and electron donors whereas sulphate, sulphite, thiosulphate, and sulphur serve as terminal electron acceptors and are reduced to H₂S. The electron donors are completely oxidized to CO₂. Members of the family *Syntrophobacteriaceae* are mainly found in freshwater, sewage sludge, or marine habitats. Thus high prevalence of sulphate reducers related sequences were observed in the AGRs.

5.10.3.3 Prevalence of Nitrate-Reducing Microorganisms

The most predominant denitrifiers in AGRs are of Betaproteobacteria (*Acidovorax*, *Achromobacter*, *Burkholderia*, and *Thiobacillus*), Alphaproteobacteria (*Azospirillum*, *novosphingobium* and *paracoccus*), Gammaproteobacteria (*Acinetobacter*, *Pseudomonas* and *Methylobacterium*) genera. *Flavobacterium* (Bacteroidetes), *Corynebacterium* and *Propionibacterium* (Actinobacteria) and *Geothrix* (Acidobacteria) were some of the other major nitrate reducers in AGRs. Wrighton et al. (2010) also identified denitrifiers belongs to genera Firmicutes, Chlorobia, Actinobacteria,

Bacterioidetes and Chloroflexi members along with Proteobacteria in active denitrifying biofilms generated during acetate oxidation. Similarly, denitrifiers found in water treatment plants covers more than 50 genera that belongs to Firmicutes and Bacterioidetes other than the class Protobacteria (Liu et al., 2008; Per Halkjær Nielsen, 2009). The denitrifying population detected in the AGR systems is similar to communities detected in denitrifying reactors treating high levels of nitrate, heavy metals and radionuclides. In previous studies done with full- and pilot-scale groundwater denitrification bioreactors, the most frequently detected denitrifying taxa were related to Alpha-, Beta-, Delta-, and Gamma-Proteobacteria, Bacteroidetes, Actinobacteria and Acidobacteria (Spain & Krumholz, 2011). They reviewed most commonly found denitrifying taxa in different bioremediation environments, particularly in contaminated wastewater of different geochemical conditions, of different nitrate contamination levels and pH, based on 16S rRNA genes and/or nirK and nirS genes studies. Spain and Krumholz (2011) reported the active in situ presence of *Acidovorax*, *Burkholderia* and *Thiobacillus* (Betaproteobacteria) under high concentrations of nitrate and heavy metals in 16S rRNA gene surveys. The presence of all above genera is also observed in our systems. Additionally, *Burkholderia* species is also reported to contain genes responsible for arsenic reduction, resistance and oxidation (Li et al., 2014). The capacity to utilize arsenic and iron as electron acceptor allowed the denitrifying taxonomic groups to exist in the studied system.

5.10.3.4 Prevalence of Other Metabolically Important Microorganisms

Sequences related to taxa capable of utilizing more than one electron acceptors were found. The presence of taxa such as *Acidithiobacillus*, *Acidiphillum*, *Geobacter* and *Geothrix* is also detected in AGR-1. *Acidiphilium* is capable of dissimilatory iron reduction at near neutral pH under anoxic and micro-aerophilic conditions. Bilgin et al. (2004) reported that this bacterium leads precipitation of iron and thus preventing its loss in to drainage water. Similarly, *Geothrix* an iron reducer, also grows with nitrate as electron acceptor by using acetate as electron donor in strict anaerobic medium (Coates et al., 1999). AGRs also have OTUs related to genus *Thiomonas* (Betaproteobacteria), which are ubiquitous in arsenic rich environments. They grow on media containing reduced inorganic sulphur compounds. *Thiomonas sp.* 3As is resistant to up to 50 mM As(V) and up to 6 mM As(III). The analysis of the *Thiomonas* genome revealed the presence of two copies of the *ars* operon (Freel et al., 2015). *Acidithiobacillus* (gamma-

proteobacterium) related OTUs were also observed in both AGRs. They are having anaerobic metabolism, found in many sulphur-rich environments, a major participant in biomining microorganisms including sulphur reduction and nitrogen fixation (Valdés et al., 2008).

The bioreactors used in present study contained highly diverse microbial community where *Proteobacteria*, *Chlorobi*, *Bacteroidetes*, *Firmicutes* and *Cyanobacteria* constitute the major bacterial groups. This suggests a much wider metabolic potential and occurrence of many diverse metabolic processes within the AGRs. This is likely due to AGRs inoculation with different sources, the different composition of influent waters, which may contribute to a different geochemical environment, and the aging of AGR operation. The microbial communities might have evolved somewhat during the AGRs operation. However, both abiotic and biotic factors also regulate the structure of microbial communities in a complex system. Bell et al. (2005) also suggested that a more diverse community provides a larger contribution to a system in terms of functioning and service compared with a less diverse counterpart. This is mainly because, different microbial community use slightly different resources. Therefore, communities with higher diversity are more productive because more of the overall resource is used. Secondly, communities with higher diversity are more productive because it is more probable that they contain species with a large effect on the system functioning. Our finding suggest that the present bioreactor systems selects for a particular arsenic, nitrate and sulphate reducers community, which makes it suitable for an environment rich in multicontaminants, where they can utilize a number of terminal electron acceptors present in anoxic groundwater. Moreover, presence of OTUs related to genera with the metabolic potential to use more than one electron acceptors, suggests that there is enough potential to use indigenous microbial communities in engineered systems to develop new biotechnologies for more efficient treatment.

5.11 Biosolids Characterization

5.11.1 Biosolids Characterization of Batch Shake Flasks in Absence of Iron

FESEM/EDX

Figure 5.82 shows the FESEM image of the biosolids collected from batch shake flasks. It shows aggregation of particles with no crystal forms observable. The Qualitative EDX spectrum was recorded in selected area (Fig. 5.82b), shows the biosolids confirmed the presence of arsenic and sulphur. The characteristics peaks of other elements (C, O, Ca, Na, Mg, Cl and K) were also observed, it was mainly due to the presence of these elements in feed of the batch shake flasks. Compositional mapping of the biosolids (Fig. 5.83) depicts distribution of arsenic and sulphur over the entire biosolids, which further supports the formation of arsenosulphide precipitates in batch shake flasks.

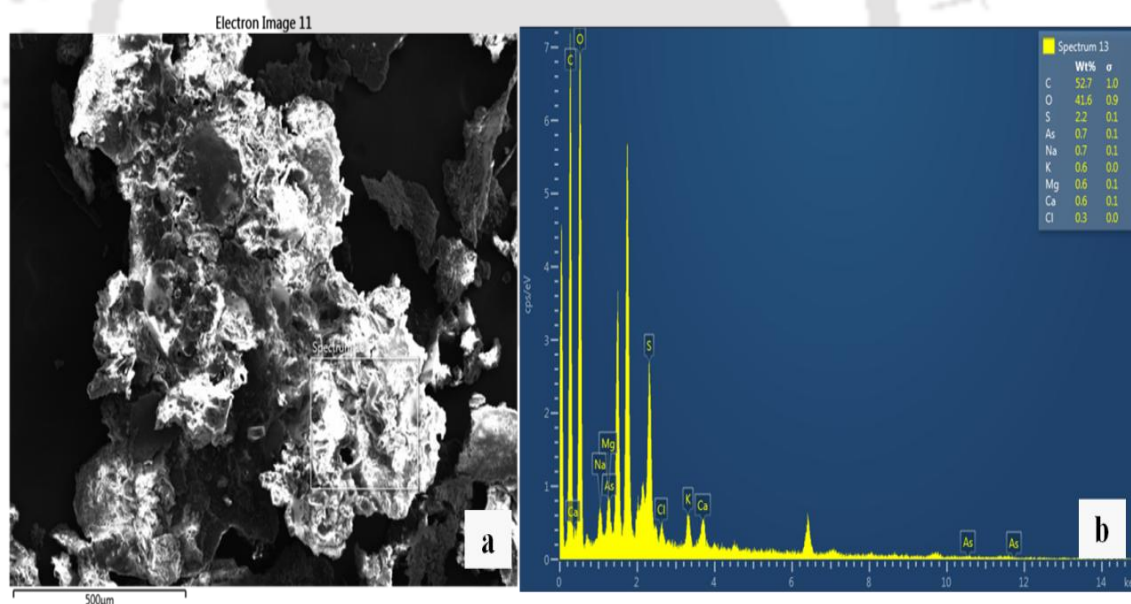


Figure 5.82 (a) FESEM micrograph and (b) EDX spectra of biosolids of batch shake flasks in absence of iron.

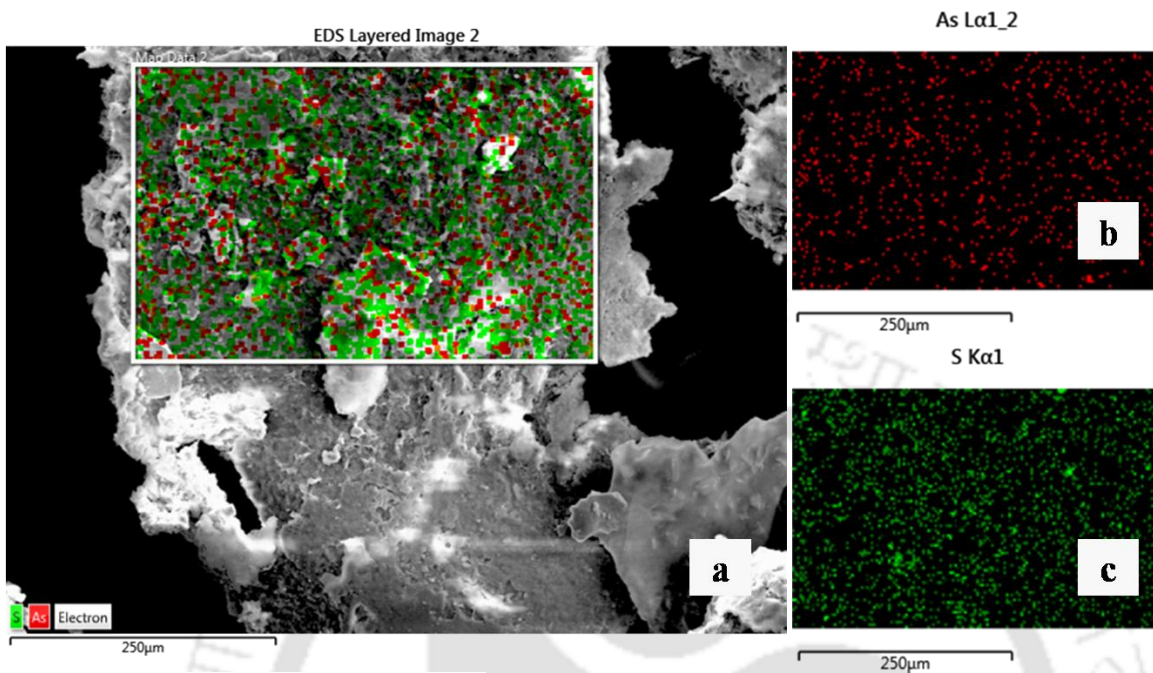


Figure 5.83 FESEM micrograph and X-ray elemental mapping of biosolids of batch shake flasks in absence of iron: (a) FESEM micrograph, (b,c) X-ray mapping of elements arsenic and sulphur.

5.11.2 Biosolids Characterization of Batch Shake Flasks in Presence of Iron

FESEM/EDX

Figure 5.84 shows the FESEM image of the biosolids collected from batch shake flasks shows aggregation of particles with no crystal forms observable. The different aggregation characteristic was observed compared with that seen in the FESEM images of the precipitates formed in absence of iron. This could be interpreted as an indication of the presence of pyrite, whose precipitates agglomerated as clumps with a smooth surface (Fig. 5.84a). Qualitative analysis by EDX conducted on selected area, confirmed the chemical composition of the precipitates. The EDX spectra confirmed the presence of arsenic, iron and sulphur in biosolids along with other elements (Fig. 5.84b). X-ray elemental mapping of biosolids is shown in Figure 5.85. X-ray elemental map is very representative of the distribution of selected elements (As, Fe, and S). Obviously, these results suggest that mixed bacterial culture induced the precipitation of arsenic and/or iron sulphides responsible for arsenic and iron removal.

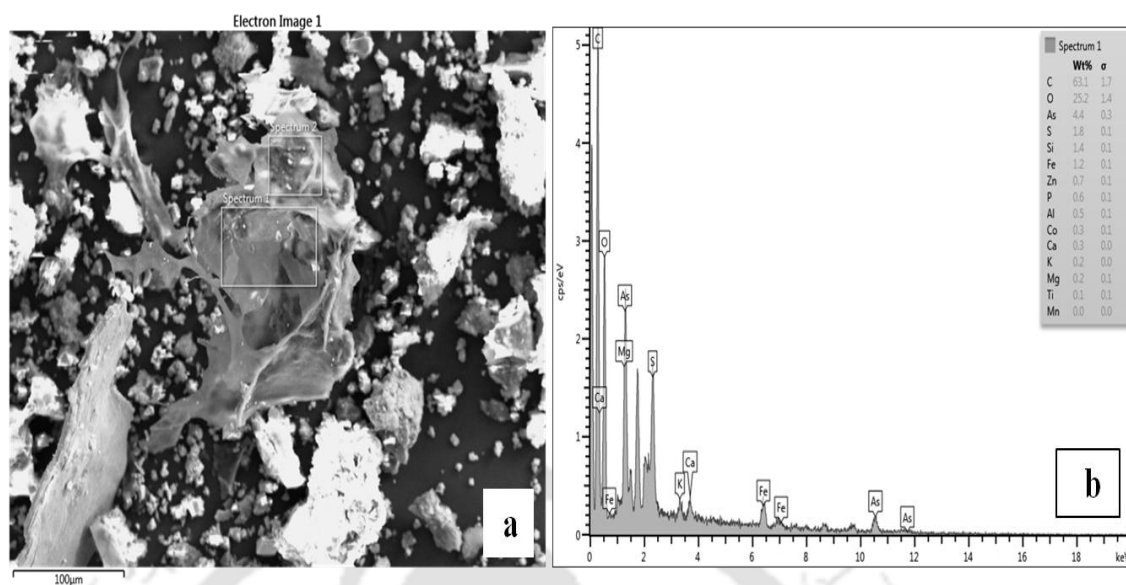


Figure 5.84 (a) FESEM micrograph and (b) EDX spectra of biosolids of batch shake flasks in presence of iron.

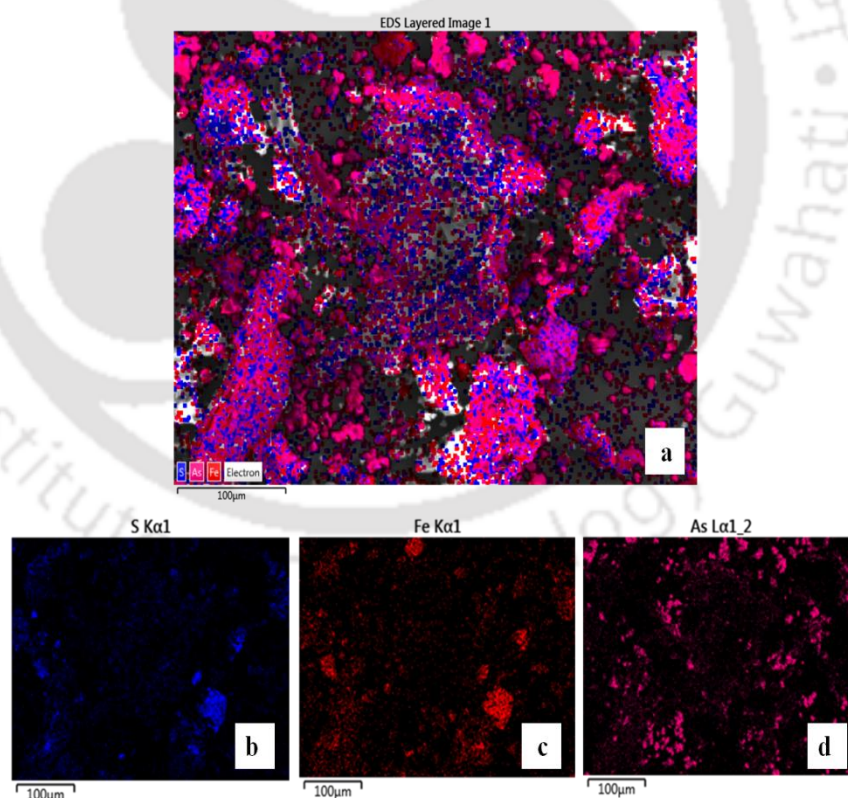


Figure 5.85 FESEM micrograph and X-ray elemental mapping of biosolids of batch shake flasks in presence of iron: (a) FESEM micrograph, (b,c,d) X-ray mapping of elements sulphur, iron and arsenic.

5.11.3 Biosolids Characterization of Semi-batch Bioreactors

5.11.3.1 SmBR-1

X-ray Fluorescence

The qualitative results of XRF and chemical composition of the biosolids of SmBR-1 is represented in Figure 5.86. The elemental presence of arsenic and sulphur was confirmed in the precipitates formed in the SmBR-1. The presence of Rh peak is due to X-ray target.

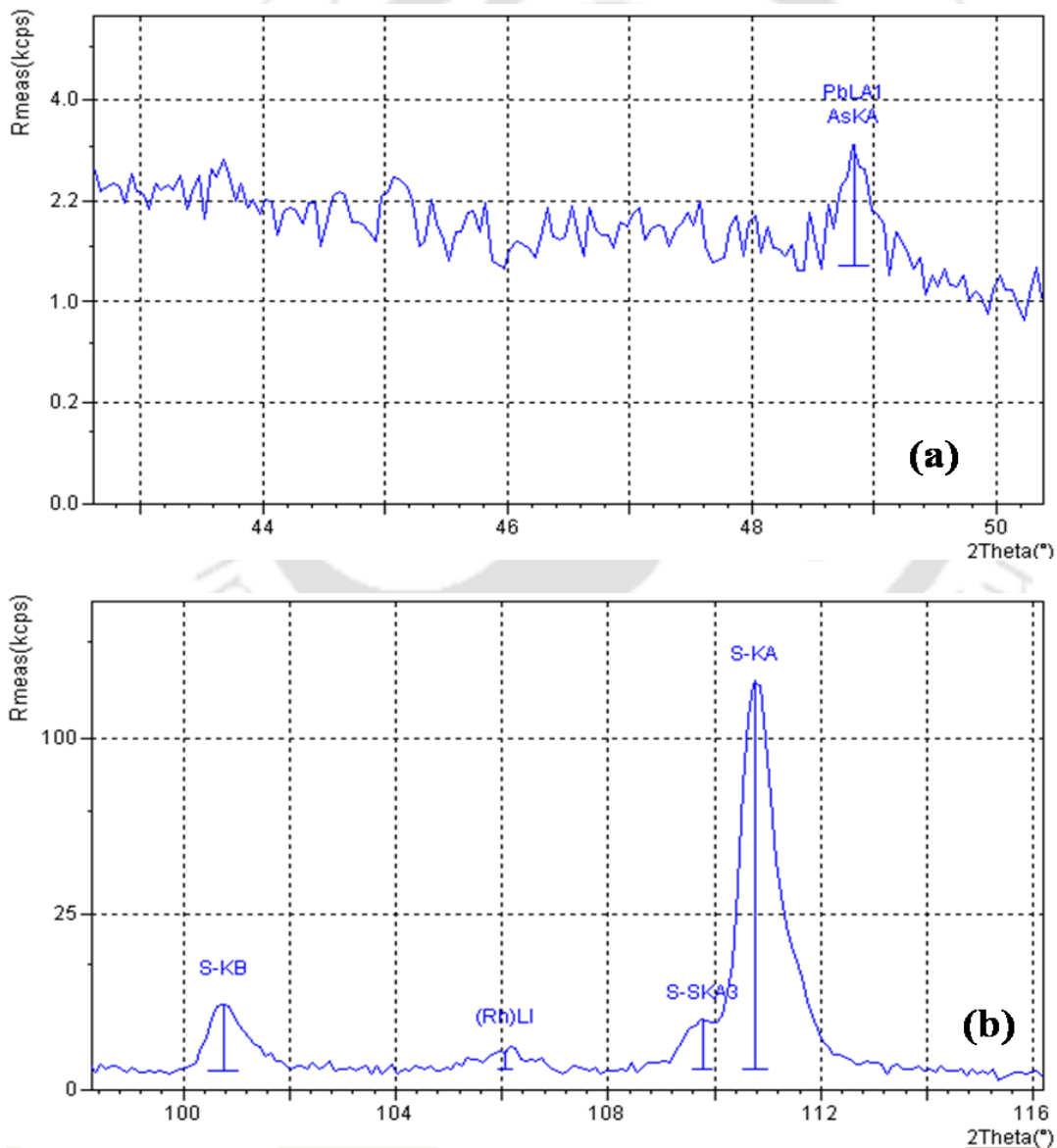


Figure 5.86 XRF spectra of biosolids of SmBR-1 showing presence of arsenic (a) and sulphur (b).

TEM/EDX

The morphology and crystallinity of the SmBR-1 biosolids were further investigated using TEM. TEM images (Fig. 5.87 a,c,e) and their representative EDX spectra (Fig. 5.87 b,d,f) of biosolids of SmBR-1 are shown in Figure. 5.87. TEM analyses demonstrate three different type of grain morphology of biosolids present in SmBR-1. The EDX spectrum shows that the grains were chemically consisted of arsenic and sulphur. The Cu peaks are due to copper TEM grid used for TEM analysis. Relatively small grains (Fig. 5.86a) is representative of small thin grains with arsenic and sulphur as major content that were confirmed in EDX analysis (Fig. 5.86b). The other grains are relatively large and exhibited a complex hexagonal shape (Fig.5.86c). These grains have well-developed morphology compared to previous small grains. The third type of grains exhibited an irregular surface with many small embayments. The grain shown in Figure 5.86c and 5.86e are representative of large granules formed in the reactor. The combination of Fig. 5.86c and e reasonably justifies that the grains were composed of arsenic and sulphur as analyzed in EDX spectra (Fig. 5.86d and f). The precipitated grains were not exhibiting crystallinity. This may be because amorphous arsenosulphides are more common than crystalline forms in terrestrial geothermal systems (Dekov et al., 2013; Ullrich et al., 2013). There are several morphologies including cell like, spiral rounded, chisel-shaped and prismatic of arsenosulphide precipitates as orpiment and realgar of varying size ranges from shallow water hydrothermal system are reported (Godelitsas et al., 2015).

5.11.3.2 SmBR-2

X-ray Fluorescence

The qualitative XRF results of the SmBR-2 biosolids are shown in Figure 5.88. The presence of arsenic, sulphur and iron were the major element components of the precipitates formed in the reactor.

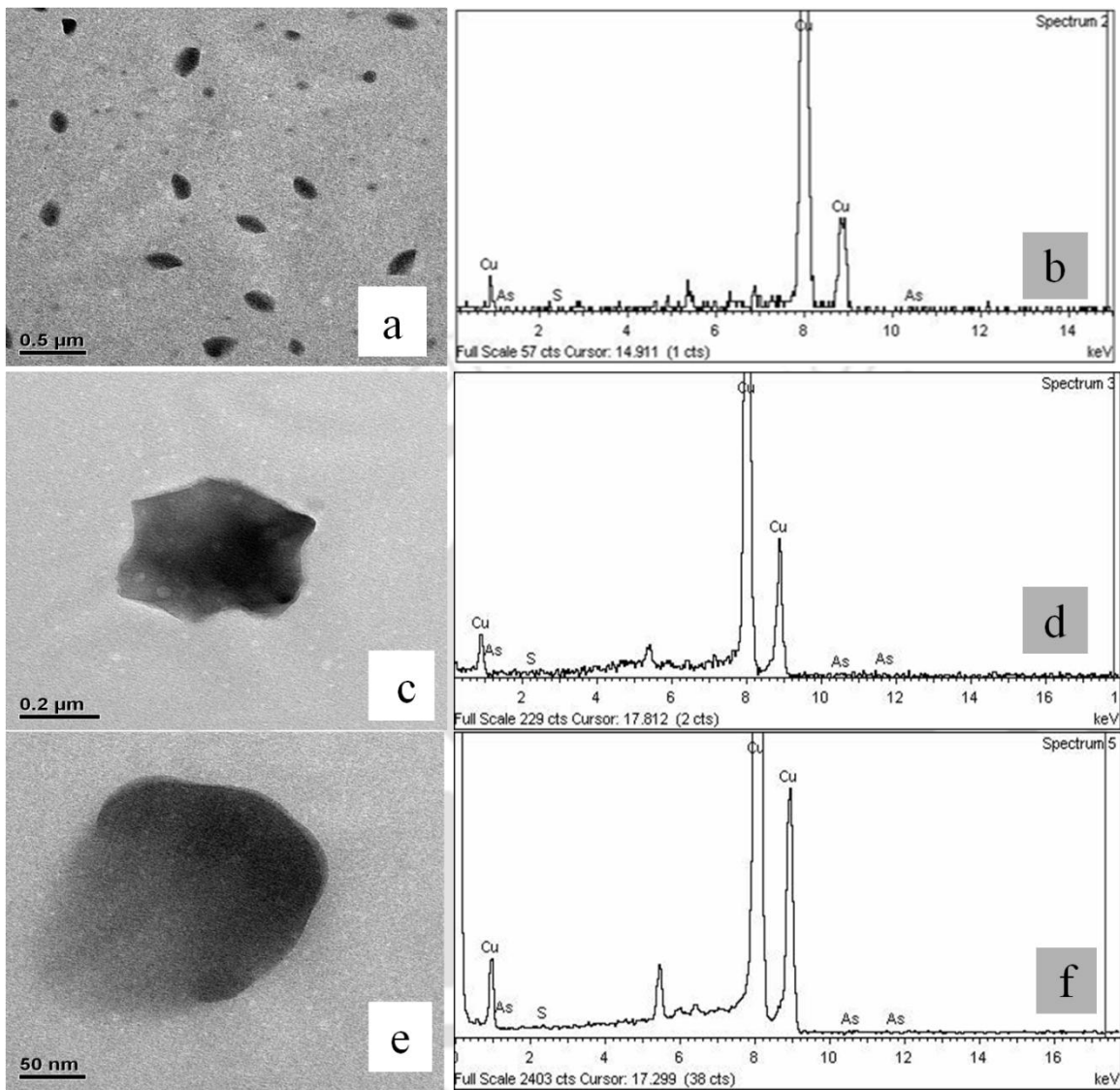


Figure 5.87 TEM images (a,c,e) and their representative EDX spectra (b,d,f) of biosolids of SmBR-1.

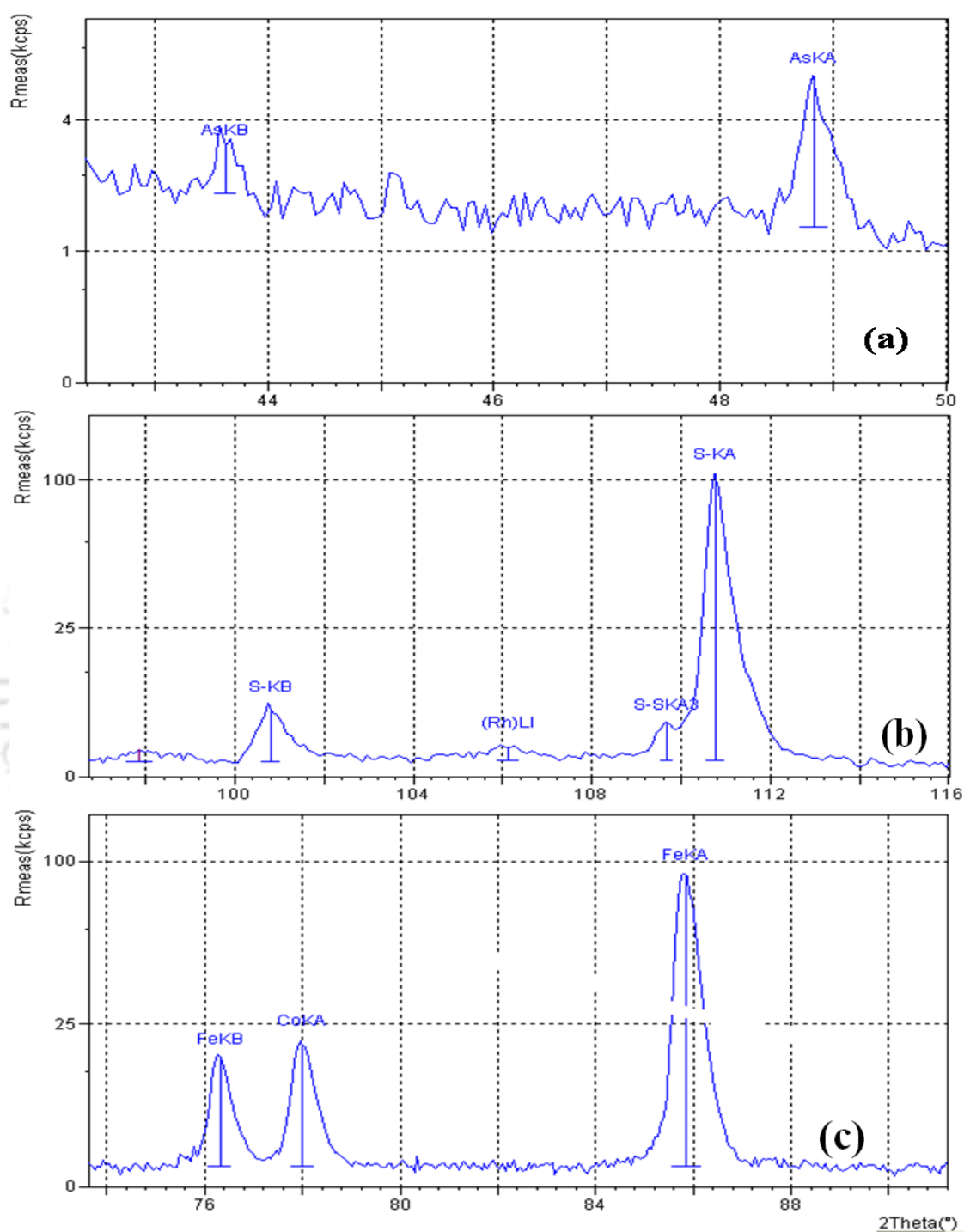


Figure 5.88 XRF spectra of biosolids of SmBR-2 showing presence of arsenic (a) sulphur (b) and iron (c).

TEM/EDX

The biosolids formed in SmBR-2 fell into two distinct morphological groups (Fig.5.89 a,b). TEM analysis exhibited pyrite grains of irregular morphology were formed in the reactor. The EDX spectra (Fig. 5.89c) of the grains suggested the presence of As, Fe and S content. The morphology and elemental analyses of these grains suggested that they were formed in the reactor as a result of microbial reduction. The presence of morphologically irregular grains of pyrite is more common with rapidly synthesized pyrite in bioreactors than natural pyrite (Kirk et al., 2010). The HRTEM image (Fig. 5.90a) shows nanodomains of sizes >10 nm embedded in crystalline matrix. The HRTEM image and SAED pattern (Fig. 5.90b) shows that the biosolids have typical crystalline morphology.

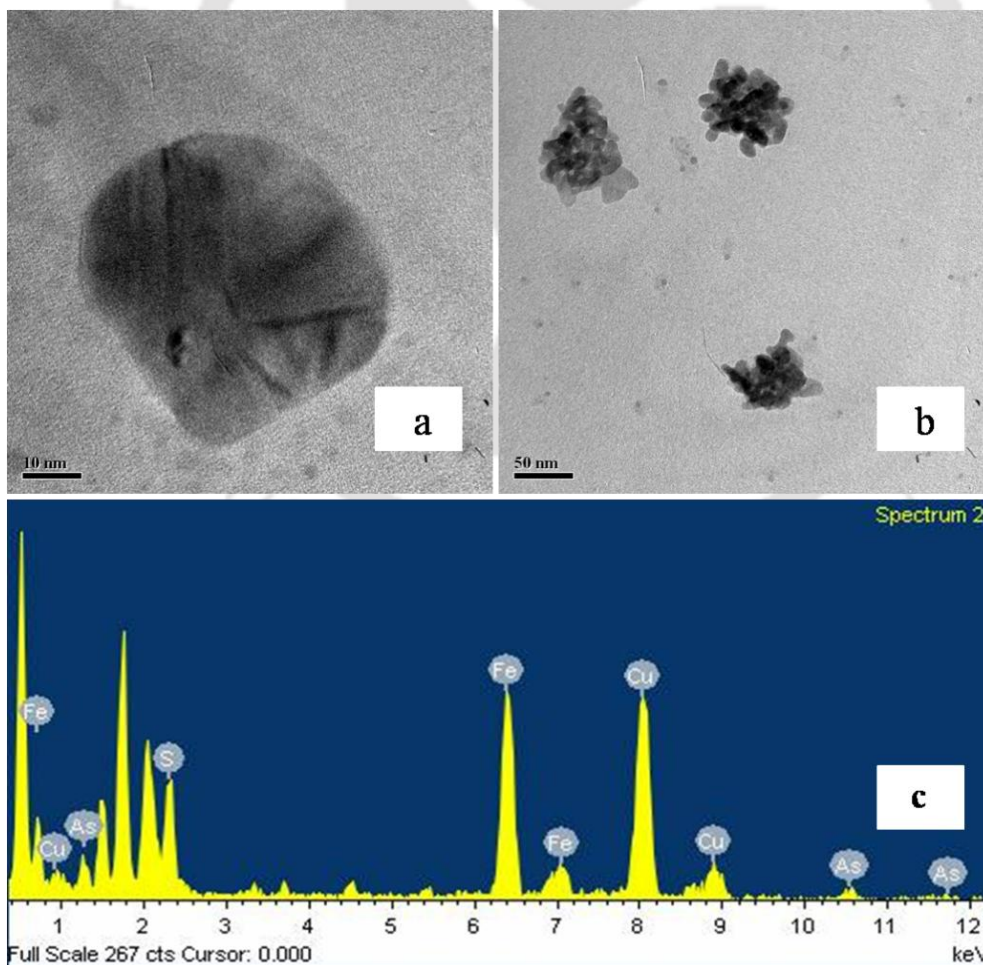


Figure 5.89 TEM images (a,b) and their representative EDX spectra (c) of biosolids of SmBR-2.

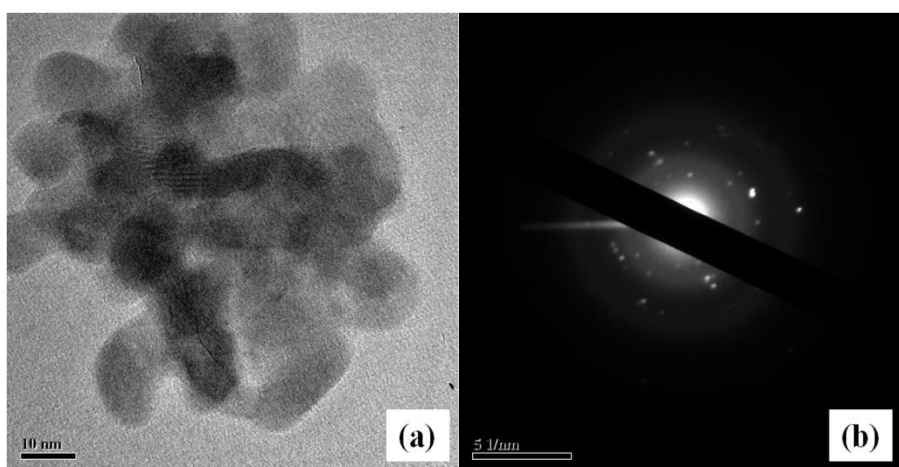


Figure 5.90 (a) HRTEM image and (b) SAED pattern of biosolids formed in SmBR-2.

5.11.4 Biosolids Characterization of Flow-through Reactors

5.11.4.1 AGR-1

FESEM and EDX

FESEM/EDX has been used as a tool for biosolids characterization and elucidation of the probable mechanism involved in arsenic removal. The cross sectional FESEM–backscattered electron (BSE) image as well as the representative EDX analyses of the precipitate of the solids collected from AGR-1 on day 183 is shown in Figure 5.91 (a,b).

The EDX spectra recorded in small area mode, preliminary EDX analysis (Fig. 5.91b) showed the presence of elements like arsenic, sulphur, carbon, oxygen, phosphorous, sodium, potassium, magnesium and calcium. The signals for tall carbon peak is due to carbon tape used for sample mounting on to stub whereas the other peaks may correspond to the proteins present on the cell wall of the biomass and/or other elements present in influent and trace mineral solution. It is most probable that arsenic precipitated mainly in the form of amorphous As_2S_3 which was further analysed by finer mineral analysis like TEM and XRD. X-ray elemental mapping of the biosolids (Fig. 5.92 a,b,c) depict a uniform distribution of arsenic and sulphur over the entire surface area which further supports the formation of arsenosulphide precipitates. The surface area of biosolids is rough and irregular with large area.

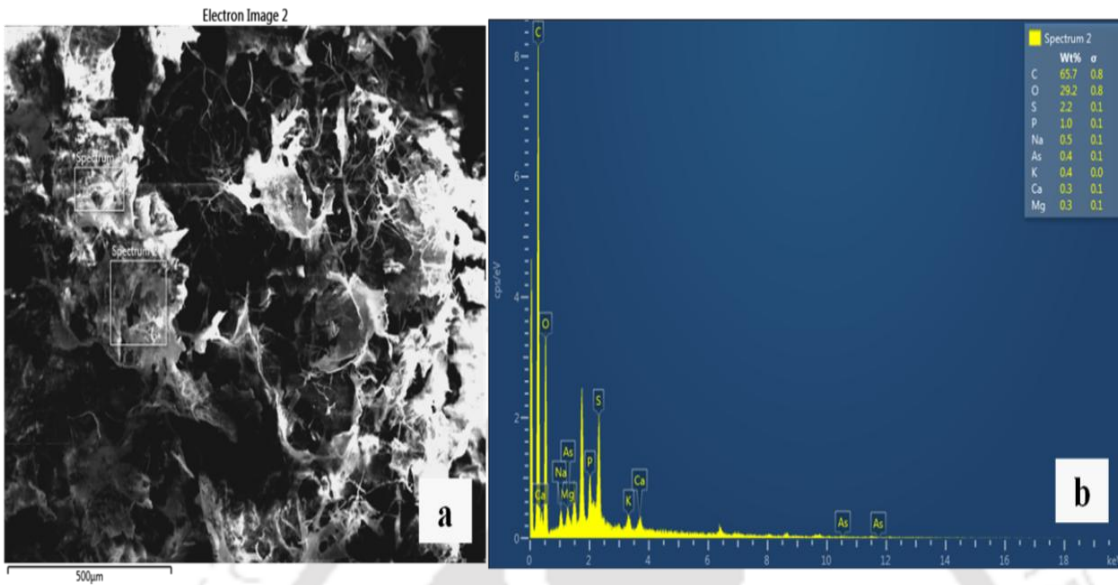


Figure 5.91 (a) FESEM micrograph and (b) EDX spectra of AGR-1 biosolids collected on day 183 of reactor run.

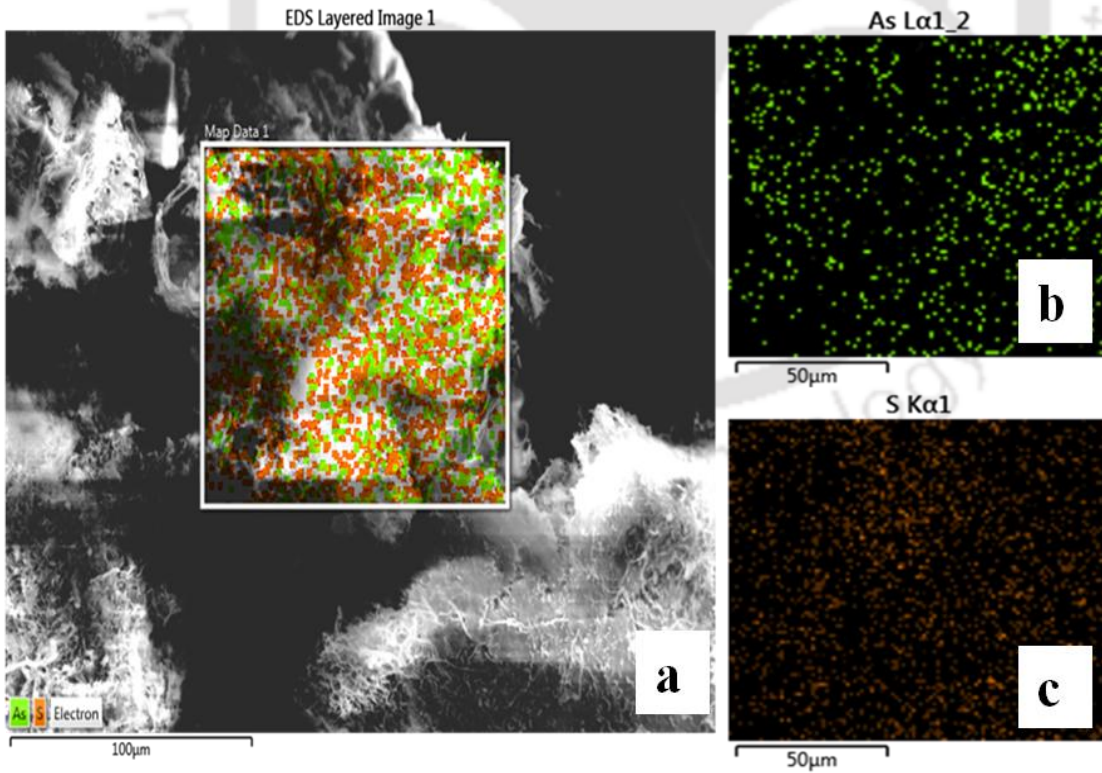


Figure 5.92 FESEM micrograph and X-ray elemental mapping of the biosolids formed in AGR-1: (a) FESEM micrograph (b) X-ray mapping of element arsenic (c) X-ray mapping of element sulphur.

X-Ray Diffraction (XRD)

The XRD pattern of the precipitates formed in AGR-1 is shown in Figure 5.93 (a, b). XRD analysis indicated the presence of orpiment (As_2S_3 ; JCPDS 00-001-0273) and realgar (AsS ; JCPDS 00-003-0113) as the solids deposited in the reactor system. The possible arsenic removal mechanism was arsenosulphides precipitation in an anaerobic reducing environment, where arsenite (As(III)) and biogenic sulphide (S(II)) react to form arsenic sulphides, such as orpiment (Newman et al., 1997) and realgar (O'Day et al., 2004). Battaglia-Brunet et al. (2012) reported arsenic sequestration from the acidic waters as arsenosulphide (orpiment) precipitation in a glycerol and H_2 -fed fixed film bioreactor. Similarly, Rodriguez-Freire et al. (2014) reported arsenosulphides precipitation (i.e., realgar and orpiment) at different pH conditions (6.1 to 7.2) in batch reactors inoculated with an anaerobic biofilm mixed culture.

TEM and EDX

Transmission electron microscopy (TEM) provides more detailed morphology of a solid while selected area electron diffraction (SAED) revealed amorphous, nanocrystalline and/or crystalline phases of the solid sample. TEM and EDX analysis were carried out on two different biosolids of AGR-1.

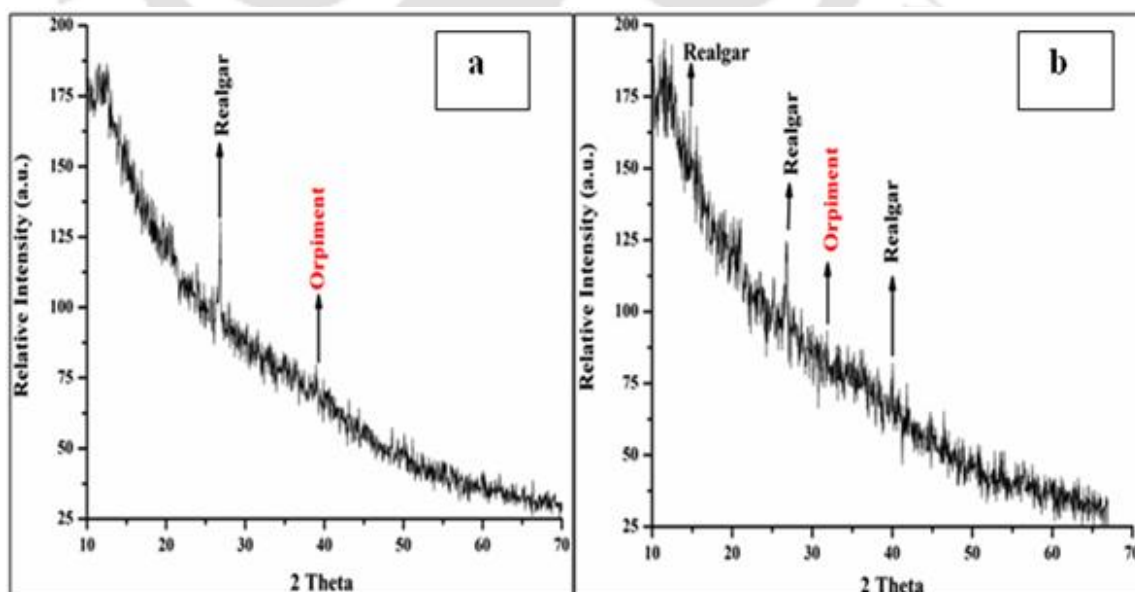


Figure 5.93 (a, b) X-ray Diffraction diagram of the precipitates formed in AGR-1 after 430 and 630 day of operation.

The first one was the sample of biosolids collected from a number of backwash suspensions when backwash frequency was 7 days or shorter. Another sample of backwash solid was collected on 757th day of AGR-1 operation, when the backwash frequency was 30 days. TEM images (a, b); SAED pattern (c) EDX spectra (d) of the biosolids collected from backwash suspension of AGR-1, when backwash frequency was 7 days of shorter is shown in Figure 5.94. The TEM images of biosolids collected on day 430 (biosolid 1) is shown in Figure 5.94 a and b. The corresponding SAED pattern (Fig. 5.94c) shows a diffused halo ring, which indicates a uniform amorphous microstructure without any crystalline feature. EDX analysis of the same confirmed the presence of arsenic and sulphur in the precipitates (Fig.5.94d), which suggests that the bio-precipitates were mainly composed of arsenosulphides. The above-mentioned biosolids were collected from backwash suspension when backwash frequency was 7 days. The duration of 7 day was found to be insufficient for crystallization. The TEM images of biosolids collected on day 757 of reactor run (biosolid 2) is shown in Figure 5.95 a,b.

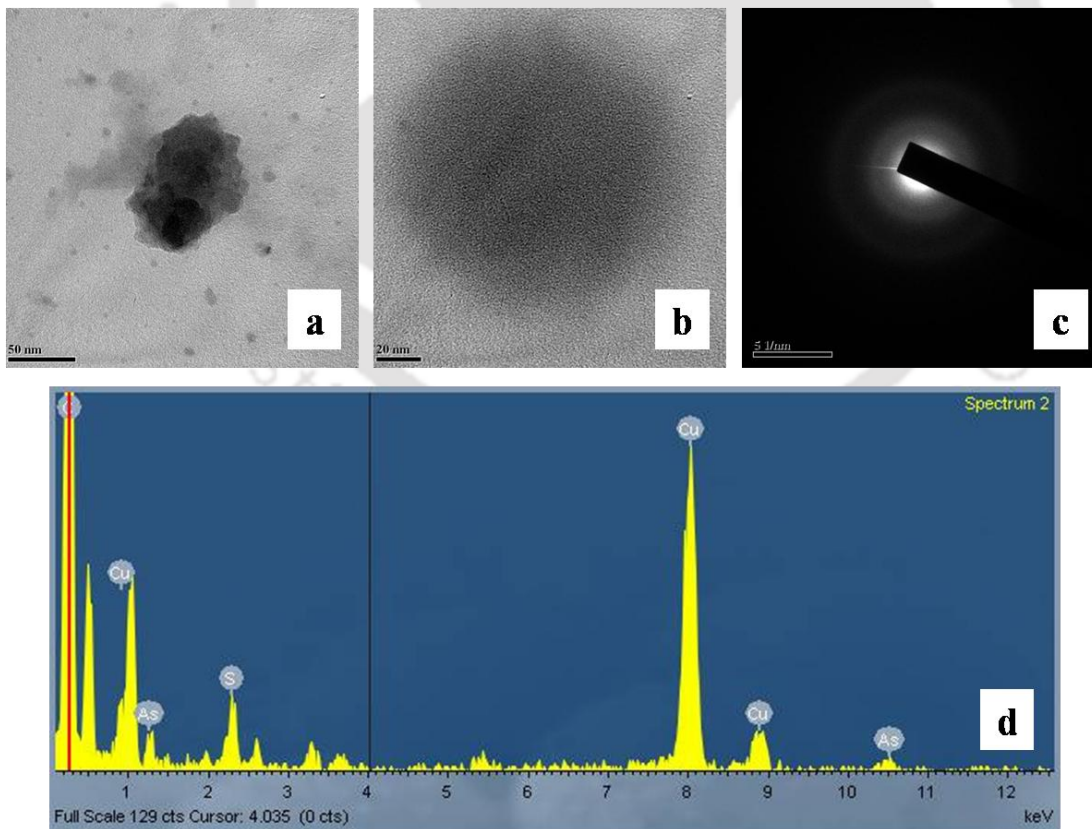


Figure 5.94 (a,b) TEM images, (c) SAED pattern, (d) EDX spectra of the biosolids collected from backwash suspension of AGR-1, when backwash frequency was 7 days or shorter.

The corresponding SAED pattern (Fig. 5.95c) indicates formation of nanocrystalline embedded amorphous structure of orpiment. TEM micrographs revealed a framboidal structure having 31.45 nm diameter (Figure 5.95b,d). The HRTEM image reveals the ultrastructure of the precipitates (Fig. 5.95d) and confirms the small amount of crystallinity.

Figure 5.95 (e) is the FFT pattern of the corresponding HRTEM image. The interplanar d-spacing values measured from IFFT analysis of high-resolution images was found to be 0.32nm (Fig. 5.95f), which corresponds to the (2 1 1) plane. The d-spacing values are in good agreement with the calculated values ($d_{211} = 3.32\text{\AA}$) which corresponds to the mineral orpiment. The SAED patterns of the solids show the presence of a continuous circular fuzzy rings either in amorphous phase (biosolid 1) or in nanocrystalline phase (biosolid 2). These results indicate that the formation of biosolids in amorphous or nanocrystalline form depends upon the incubation period. In the present study, a minimum of 30 days has been identified as the incubation period for formation of nanocrystalline form of arsenosulphide. There are many reports available on microbial precipitation of arsenic sulphide (orpiment), by pure bacterial culture and mixed bacterial culture. Newman et al. (1997) and Demergasso et al. (2007) reported orpiment precipitation in amorphous and crystalline forms respectively, in 7-14 days incubation periods by using pure bacterial strains in minimal medium having high arsenic (1 to 10 mM) and sulphate (1 to 10 mM), in the medium. There have been other reports on amorphous orpiment precipitation at higher arsenic concentrations (1 to 100 mg/L) and sulphate concentrations (1 to 1.5 g/L) at lower pH (2.7 to 7.0) in bioreactors treating acid mine waters in batch and column bioreactors respectively (Altun et al., 2014; Battaglia-Brunet et al., 2012; Rodriguez-Freire et al., 2014).

In the present study, appearance of crystalline phase orpiment could be associated with increase in incubation time of biosolids in the reactor from 7 days to 30 days. Lee et al. (2007) demonstrated an evolution in morphology of orpiment from amorphous to a polycrystalline phase with increase in incubation time from 9 day to 50 days. The TEM observations are consistent with those revealed by the XRD patterns.

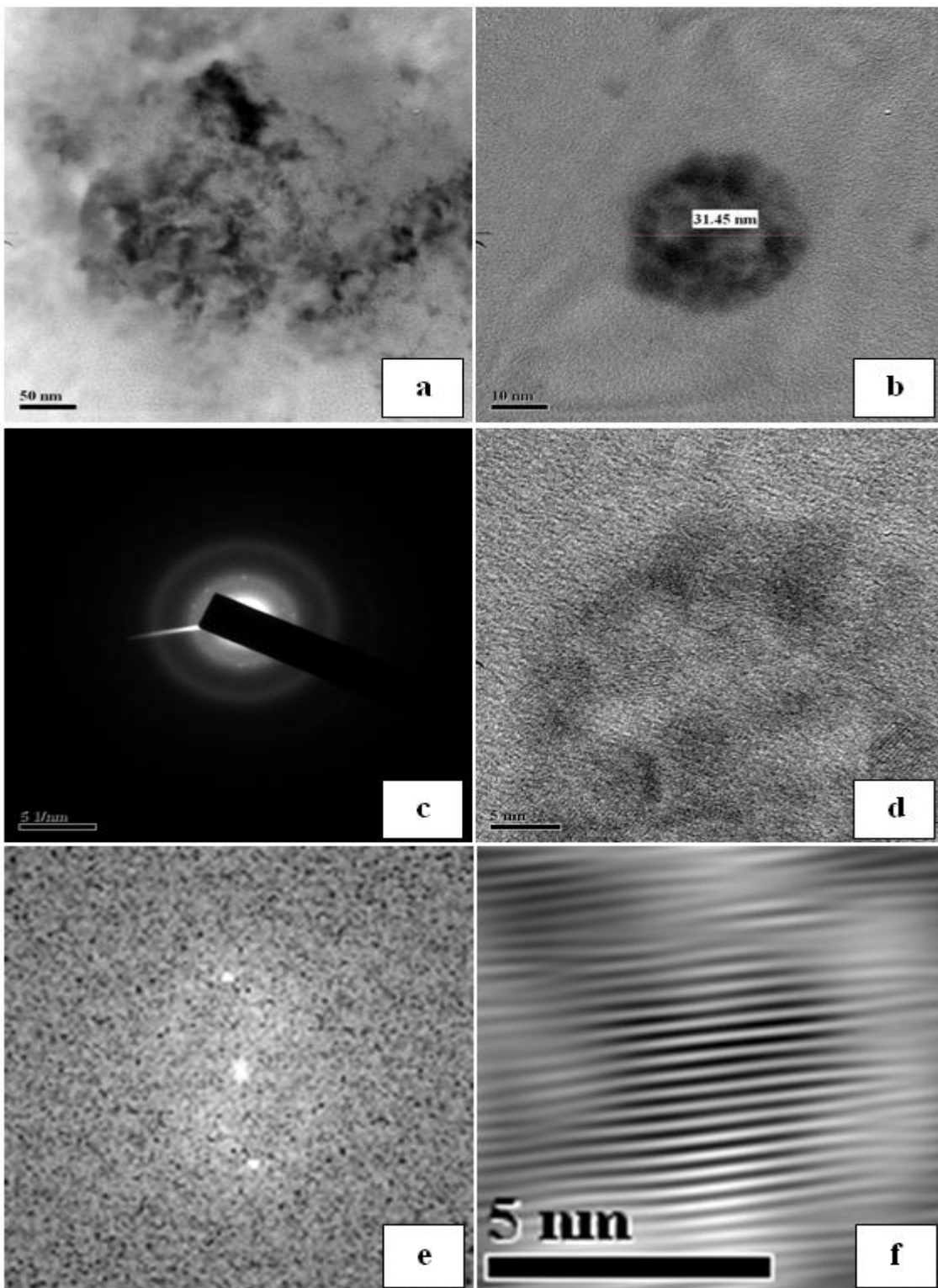


Figure 5.95 (a,b) TEM images, (c) SAED pattern, (d) HRTEM image, (e) FFT, and (f) IFFT of biosolids of AGR-1.

X-ray absorption spectroscopy (XAS)

XAS spectra were subjected to both XANES and EXAFS analyses. The oxidation state of arsenic was obtained from XANES analysis, while structural parameters such as interatomic distance (R) and coordination number (N) on the near coordination environment around arsenic were gleaned from EXAFS analysis. In XANES spectra, the absorption edges (i.e., inflection energies) of the samples are compared with those of model compounds (Fig. 5.96a). The lower absorption edge energy corresponds to a lower oxidation state while the higher one is indicative of higher oxidation state of arsenic. The absorption edge energies of dissolved As(III), dissolved As(V), and biosolids of AGR-1 were 11870.0, 11874.0, and 11870.0 eV respectively.

Figure 5.96 (b) shows normalized XANES data at As K-edge for AGR-1 sample with As³⁺ standards. The arsenic XANES spectra reveal that AGR-1 sample has As³⁺ oxidation state. Figure 5.97 shows the Fourier transform (FT) EXAFS oscillations of As K-edge for the sample. The k -range of 2.5-9 Å⁻¹ has also been used for FT of As EXAFS data. Arsenic K-edge EXAFS fitting is performed for AGR-1 using As₂S₃ (space group P 21/c where first shell As-S bond comes at 2.2701 Å distance and second next near-neighbour As-As bond comes at 3.521 Å distance. Figure 5.97 also shows the best fitted curves and best-fit values of the parameters are listed in Table 5.4. From the AGR-1 arsenic K-edge EXAFS data fitting, we have obtained variation of coordination number (CN), bond distance (R) and Debye-Waller factor (σ^2). The numbers in parentheses indicate the uncertainty in the last digit. In AGR-1, the biogenic sulphides reacted with As(III) had an absorption edge energy of 11870.0 eV, indicating that the dominant oxidation state of As in the biosolids sample was +3. The absorption energy 11870.0 eV, close to that of As(III), suggesting the formation of As₂S₃.

Table 5.4 The best fit values of the parameters for AGR-1 sample.

Sample	CN_{As-S}	$R_{As-S}(\text{Å})$	$\sigma^2_{As-S} (\text{Å}^2)$	CN_{As-As}	$R_{As-As}(\text{Å})$	$\sigma^2_{As-As} (\text{Å}^2)$
AGR-1	2.7 (2)	1.902 (3)	0.006 (2)	2.9 (3)	3.055 (3)	0.0110 (5)

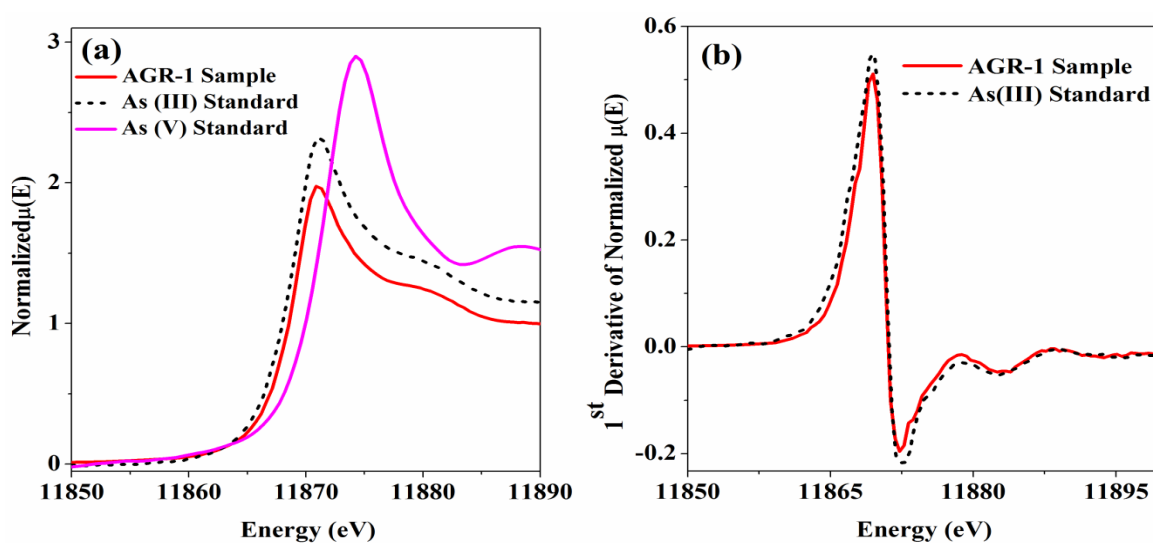


Figure 5.96 (a) Normalized XANES data at As K-edge for biosolids of AGR-1 with As^{3+} and As^{5+} standards, (b) 1st derivative data plot comparison of biosolids of AGR-1 and As^{3+} standard.

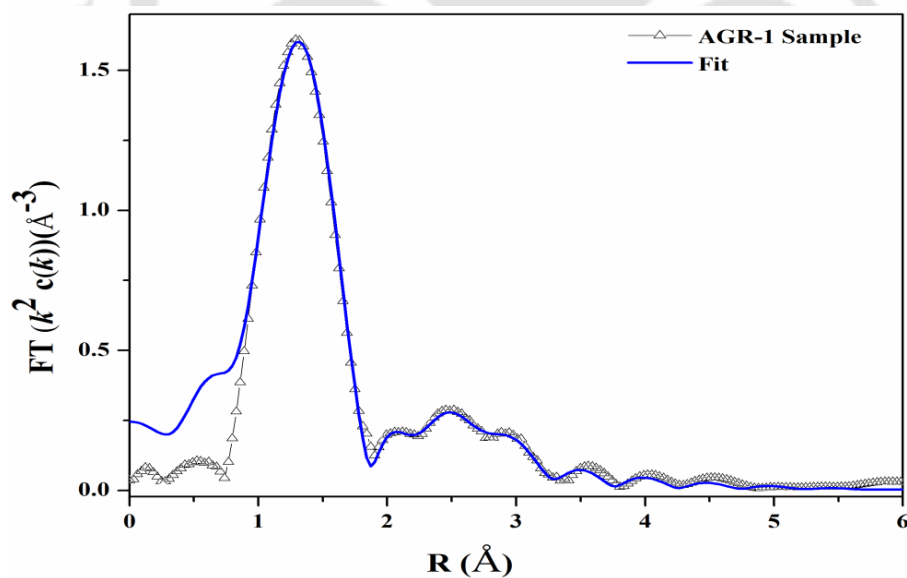


Figure 5.97 Fourier transform of k^2 -weighted of As K-edge for biosolids of AGR-1. The symbol shows experimental data and solid lines are the best fit.

5.11.4.2 AGR-2

FESEM and EDX

Figure 5.98 shows FESEM-BSE images (Fig. 5.98a, b) as well as the representative EDS analyses of the precipitates formed in AGR-2. The point EDX analyses (Figure 5.98c, d) shown the presence of substantial amounts of Fe, As and S in more or lesser percentages. The point EDX analysis of the granular structures has been shown the higher percentage of Fe (61.7-77.6%), S (17.6-34.5%) and lower contents of As (3.8-4.8%).

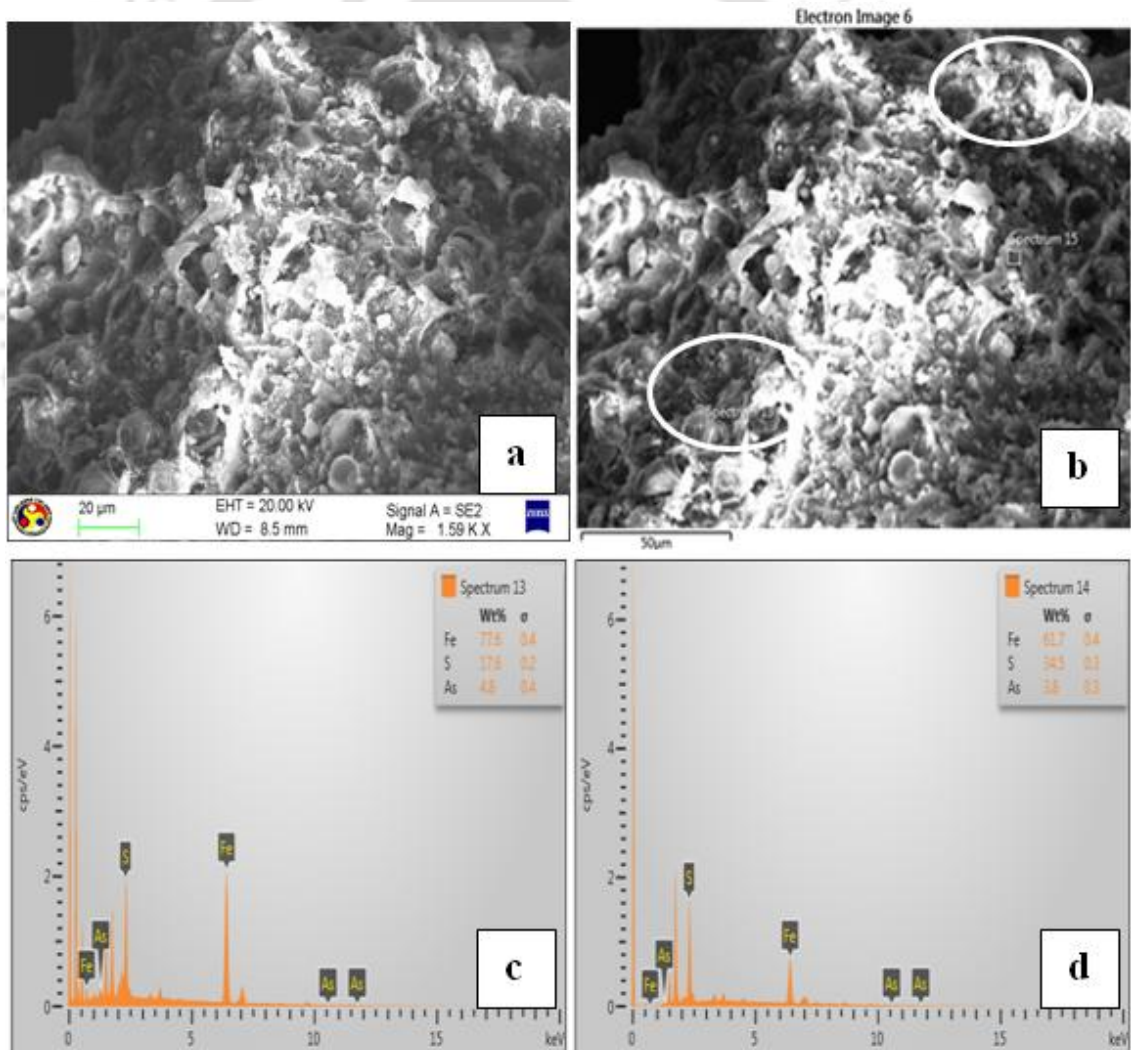


Figure 5.98 (a,b) Cross sectional FESEM-backscattered electron (BSE) images and (c,d) point EDS analyses of the biosolids precipitated in AGR-2.

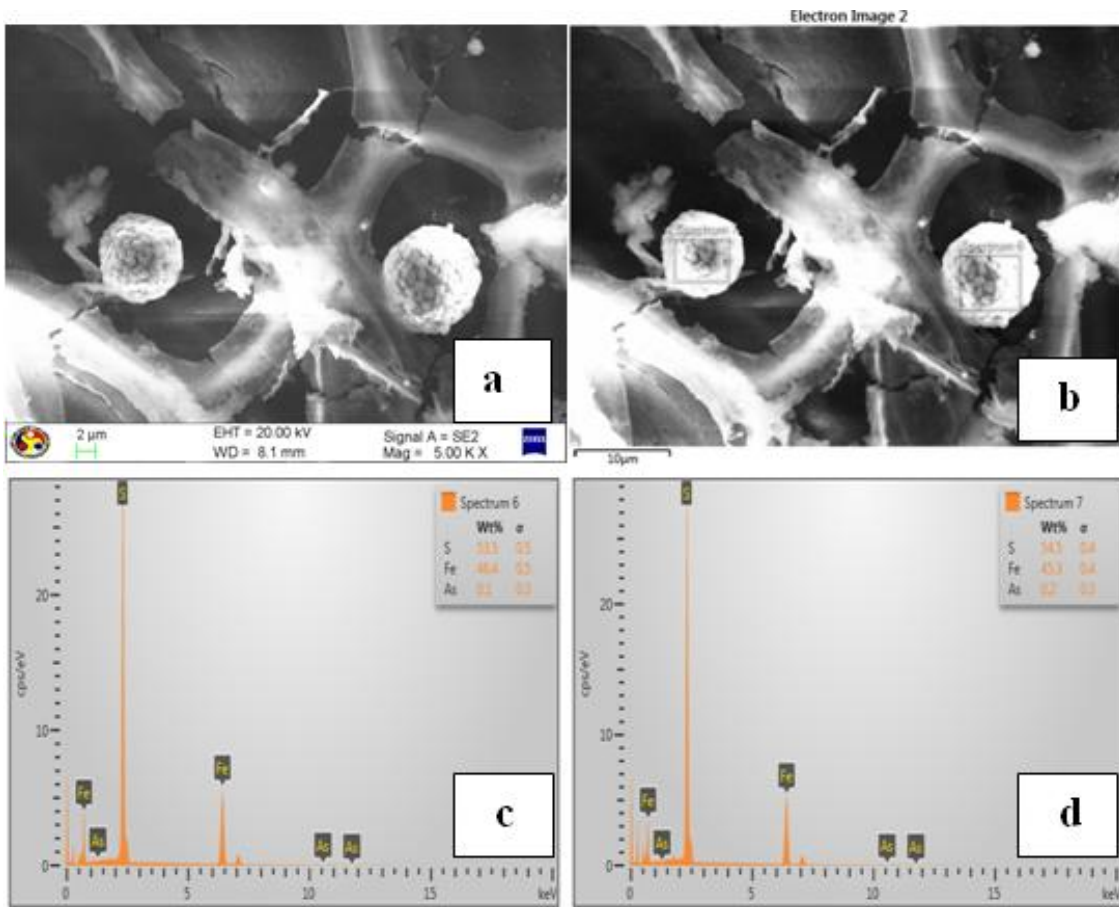


Figure 5.99 (a,b) Cross sectional FESEM-BSE images and (c,d) point EDS analyses of the precipitates formed in AGR-2.

Figure 5.99 (a,b) confirmed the presence of small granular structures in the biosolids collected on the day 182. The point EDX analysis (Fig.5.99 c,d) of the granular structures has been shown the higher percentage of S (53.5-54.5%), Fe (45.3-46.4%) and lower contents of As (0.1-0.2%). The surface morphology and EDX mapping of arsenic and iron shows good match with the morphology of iron sulphides precipitates, as shown in Figure 5.99a.b.

EDX mapping was also employed to further confirm the elemental distribution (Fig. 5.100). Figure 5.100b shows the EDX mapping of the encircled portion from Figure 5.100a. The EDX analysis in Figure 5.98 also supports the elemental mapping results. The lesser green dots in the Figure 5.100c corresponds to arsenic and this may be caused by adsorption of arsenic on to iron sulphide minerals. This is the reason for comparatively

lesser arsenic percentage (0.1 to 0.2%) of arsenic in point EDX analysis collected from precipitates as shown in Figure 5.99 a,b. The elemental mapping of iron and arsenic, together with XRD, TEM and XAS analysis, confirms the formation of iron sulphides (FeS or FeS_2) in the AGR-2. It is most probable that iron present in influent was precipitated as FeS or FeS_2 as a result of the sulphidogenic activity. It is also assumed that a part of arsenic may be also adsorbed on to these precipitates. Thus, FESEM studies indicated the precipitation of arsenic in the form of As_2S_3 and its co-precipitation with FeS , FeS_2 or FeAsS are the main arsenic removal mechanisms in the AGR systems, which is consistent with results found by other investigators (Altun et al., 2014; Xia et al., 2014).

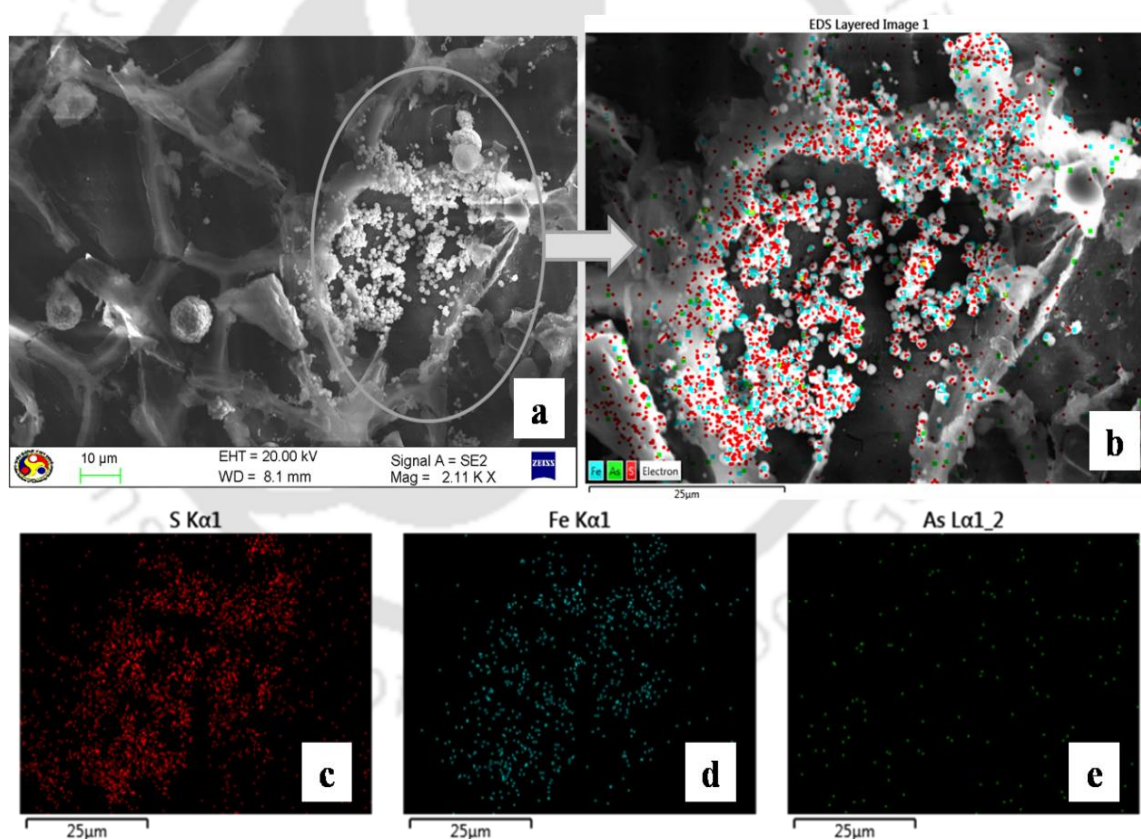


Figure 5.100 FESEM micrograph and X-ray elemental mapping of the biosolids formed in AGR-2: FESEM micrograph (a,b), X-ray mapping of element sulphur (c), X-ray mapping of element iron (d) and X-ray mapping of element arsenic (e).

X-Ray Diffraction (XRD)

XRD analysis of AGR-2 precipitates indicated (Figure 5.101a,b) the presence of pyrrhotite (FeS ; JCPDS 00-002-1241), pyrite (FeS_2 ; JCPDS 00-001-1295), realgar and orpiment (As_2S_3 ; JCPDS 00-001-0273). Altun et al. (2014) also reported bioremoval of arsenic from synthetic acidic wastewater as precipitation of arsenic in the form of orpiment (As_2S_3) and its co-precipitation with FeS , FeS_2 or FeAsS in a fixed bed column bed reactor. The arsenic removal as arsenosulphide formation, and/or surface precipitation and adsorption on iron sulphides is also observed in an acetate fed fixed-bed bioreactor treating drinking water (Upadhyaya et al., 2010). Similarly, Kirk et al. (2010) reported arsenic removal as iron sulphides precipitation in a semi-continuous bioreactor, where arsenic sulphides (i.e., realgar and orpiment) were remain undersaturated. However, due to the poor crystallinity of the precipitates, not all the species could be identified.

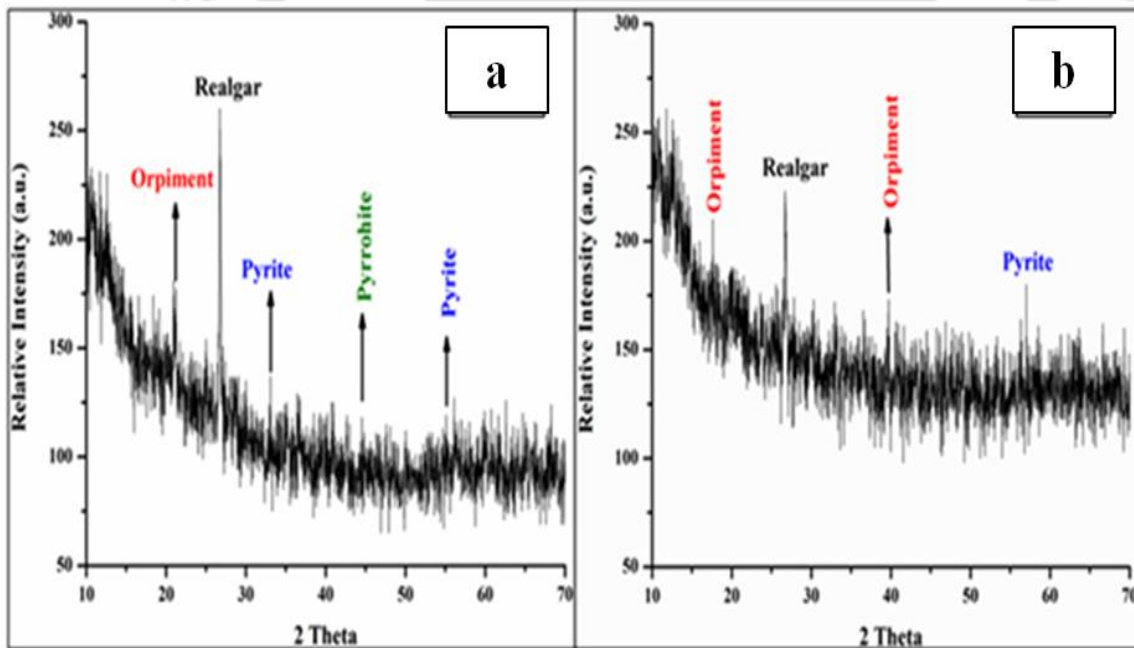


Figure 5.101 (a, b) X-ray Diffraction diagram of the precipitates formed in AGR-2 after 310 and 430 days of operation.

TEM and EDX

Figure 5.102 is showing detailed morphological structure of the precipitates formed in AGR-2. The sample of biosolids used for TEM analysis were collected from a number of backwash suspensions when backwash frequency was 7 days or shorter. TEM micrographs of the precipitates are shown in the Figure. 5.102 a and b. The SAED pattern (Fig. 5.102c) indicated the presence of diffraction patterns, which confirmed crystalline nature of the phase, which was further established by corresponding HRTEM image (Fig. 5.102d) of precipitates. The FFT pattern of the corresponding HRTEM is shown in Figure 5.102e. The IFFT pattern (Fig. 5.102f) was gleaned out from corresponding FFT pattern in order to calculate the interplanar d-spacing values. The d-spacing was measured to be 0.89 nm from IFFT pattern, which is not matching with FeS, FeS₂, As₂S₃ and AsS. Kirk et al. (2010) also reported the differences in d-spacing values measured from FFT analysis are usual and may be attributed to sample treatment or some other factors. The other possible reason for this may be due to a complex mixture of iron sulphides and arsenosulphides formed in AGR-2. Wolthers et al. (2003) also noted significant variation in d-spacing values for mackinawite. Likewise, the composition of precipitates obtained by TEM-EDX suggested the presence of arsenic, iron and sulphur.

Similar observations were also made by Kirk et al. (2010), they reported the formation of mackinawite, pyrite and greigite in a semi-batch reactor. There are many reports available on microbial as well as chemical precipitation of iron sulphide. Benning et al. (2000) reported precipitation of poorly crystalline forms of iron sulphide within 5-30 min. of reaction time. Also Gramp et al. (2010), observed precipitation of crystalline iron sulphide in 14 days reaction time, using mixed bacterial culture of sulphate reducing bacteria in modified Barr's medium containing iron and sulphate. In the present study, a minimum of 7 days has been identified as the incubation period for formation of crystalline form of iron sulphide. These results are consistent with the FESEM-EDX and XRF chemical analysis results, which also revealed the presence of same elements. The powder XRD of the same also confirmed the presence of mixture of FeS, FeS₂, As₂S₃ and AsS in AGR-2 biosolids.

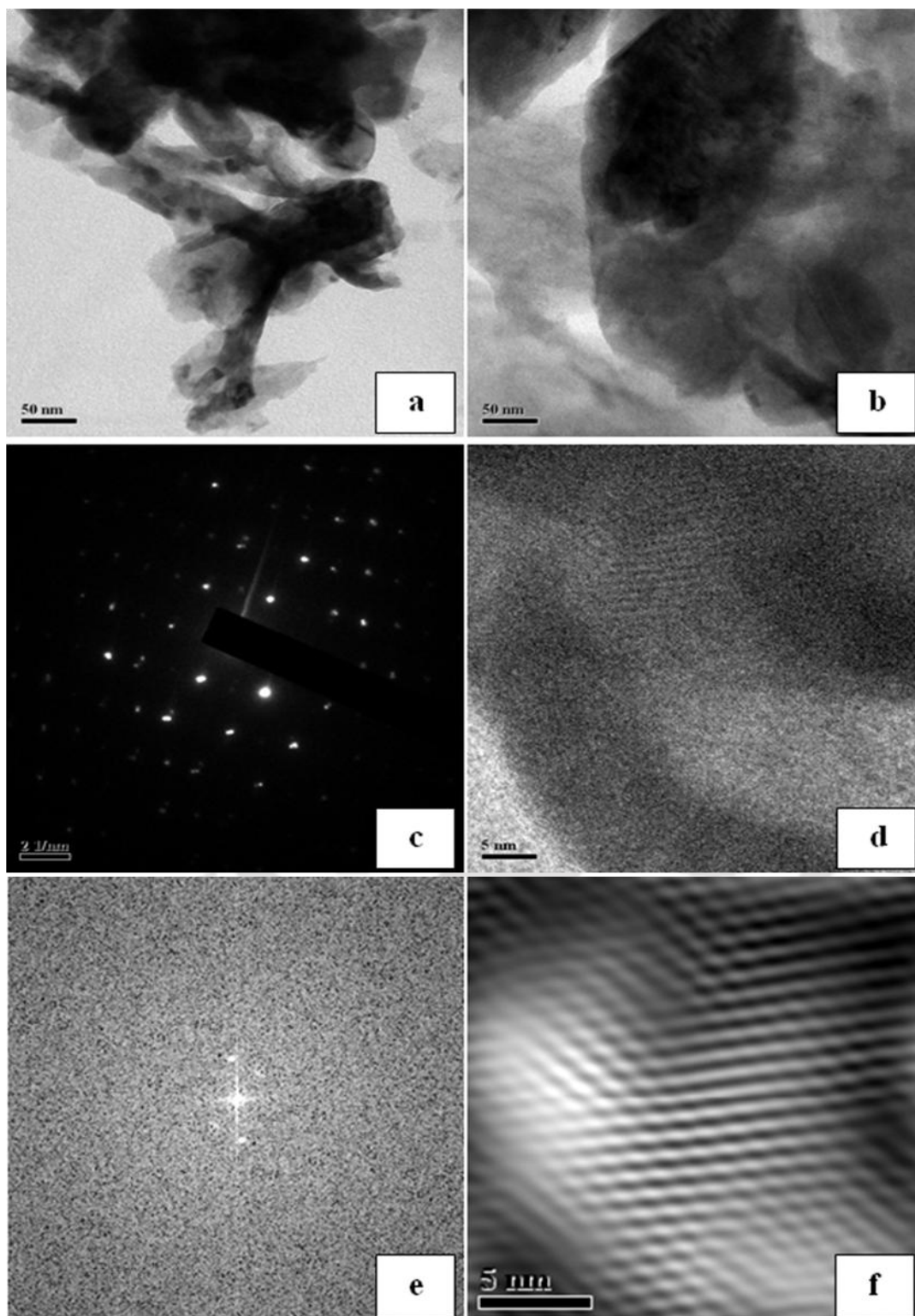


Figure 5.102 (a, b) TEM images, (c) SAED pattern, (d) HRTEM image, (e) FFT and (f) IFFT of biosolids of AGR-2.

X-ray absorption spectroscopy (XAS)

Figure 5.103. shows normalized XANES data at As K-edge for biosolids of AGR-2 with As³⁺ and As⁵⁺ standards. The XANES spectra confirmed that the oxidation state of arsenic in biosolids was +3, which indicated the precipitation of orpiment in the AGR-2. Figure 5.104 shows normalized XANES spectra at Fe K-edge for biosolids of AGR-2 with FeS (Fe²⁺) and Fe foil standards. The Fe K-edge (Fig. 5.104a,b) XANES spectra confirm that iron was in +2 oxidation state in the biosolids of AGR-2. The absorption edge energies of biosolids of AGR-2 and FeS were 7117.40 and 7117.60 eV respectively, which are very closer to each other this confirms the formation of FeS in AGR-2.

Figure 5.105 shows the Fourier transform (FT) EXAFS oscillations of Fe K-edge for biosolids of AGR-2. The k -range of 2.5–9Å⁻¹ has been used for FT of Fe EXAFS data. For AGR-2 sample, Fe K-edge has been fitted using FeS structure (space group P 4/n m) where Fe has 4 S atoms (Fe-S) at 2.255Å distance in first shell and second next near-neighbour Fe is surrounded by 4 Fe atoms (Fe-Fe) at 3.547Å distance. The fitting of EXAFS data, coordination numbers (CN) of the different shells, bond distance (R) and Debye-Waller factor (σ^2) were fitted as free parameters. Figure 5.105 also shows the best fitted curves and best fit values of the parameters are listed in Table 5.5. This data suggests the formation of iron sulphides in the AGR-2.

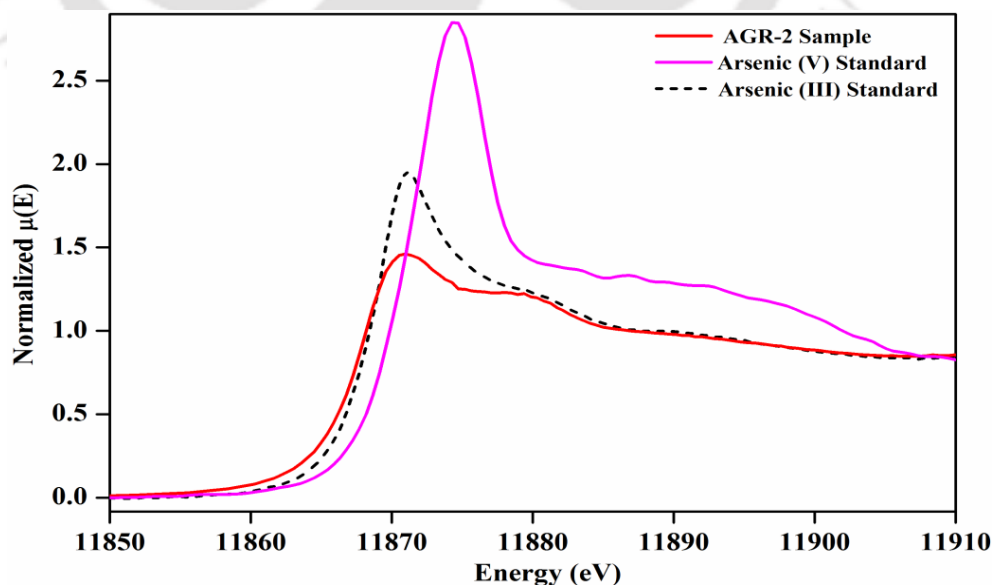


Figure 5.103 Normalized XANES data at As K-edge for biosolids of AGR-2 with As³⁺ and As⁵⁺ standards.

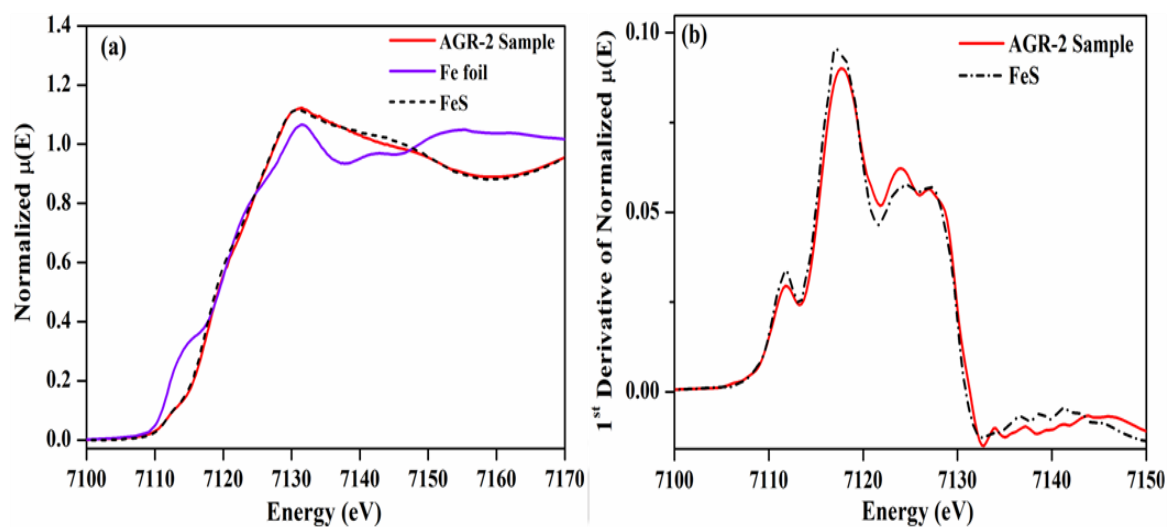


Figure 5.104 (a) Normalized XANES data at Fe K-edge for biosolids of AGR-2 with FeS (Fe^{2+}) and Fe foil, (b) 1st derivative data plot comparison of biosolids of AGR-2 and FeS standard.

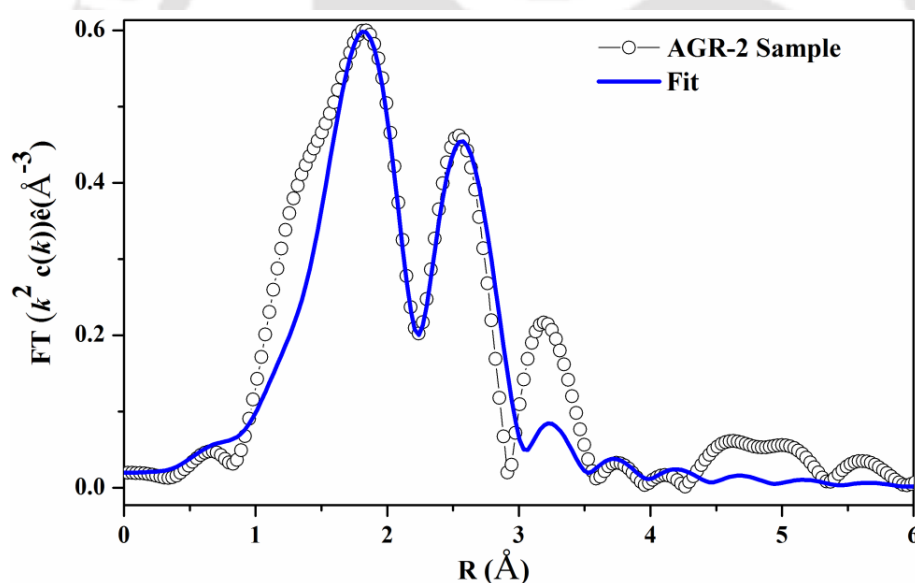


Figure 5.105 Fourier transform of k^2 -weighted of Fe K-edge for biosolids of AGR-2. The symbol shows experimental data and solid lines are the best fit.

Table 5.5 The best fit values of the parameters for biosolids of AGR-2 sample.

Sample	$CN_{\text{Fe-S}}$	$R_{\text{Fe-S}}(\text{Å})$	$\sigma_{\text{Fe-S}}^2(\text{Å}^2)$	$CN_{\text{Fe-Fe}}$	$R_{\text{Fe-Fe}}(\text{Å})$	$\sigma_{\text{Fe-Fe}}^2(\text{Å}^2)$
AGR-2-Fe	3.2 (3)	2.354 (3)	0.0159 (3)	5.1 (4)	3.227 (2)	0.0135 (3)

5.12 Stability Tests on Biosolids

5.12.1 Aging Tests Results of Biosolids of AGR-1 and AGR-2

Release of arsenic during anoxic and oxic aging of backwash solids of AGR-1 and AGR-2 are shown in Figure 5.106 and 5.107 respectively. The arsenic concentrations in the leachate have been plotted after correction by subtracting the initial concentrations of soluble arsenic in the backwash liquid from observed concentrations. Appearance of residual arsenic in backwash water at higher concentration (28-32 $\mu\text{g/L}$) than that of in treated water (1-3 $\mu\text{g/L}$) would be due to mixing up of untreated as well as partially treated water that remained in the reactor just before backwashing. Similarly, residual iron concentration of 0.28-0.33 mg/L was found in backwash water of AGR-2, whereas iron concentration in the treated water was only 0.12-0.2 mg/L.

As the ageing tests were done on backwash solids from backwash suspension collected after each backwashing of AGRs at an interval of 48 hours, knowing the operating parameters and performance of the reactor on removal of arsenic from the initial of 500 $\mu\text{g/L}$, amount of arsenic removal from aqueous phase was calculated by mass balance of arsenic. Average total amount of arsenic removal from aqueous phase during each run, thus calculated, was found to be 11.25 ± 0.014 mg. This is the amount assumed to have transferred from aqueous phase to solid phase in biosolids. Amount of iron in the biosolids of AGR-2 were also estimated by following the same procedure.

Arsenic leaching in AGR-1

As shown in the Figure 5.106, after first two days of aging, soluble arsenic concentrations were found to be 29.7 and 37.0 $\mu\text{g/L}$ in anoxic and oxic conditions respectively. With longer aging time leached arsenic increased steadily and reached the maximum of 167 and 306 $\mu\text{g/L}$ during anoxic and oxic aging periods, respectively. Multiplying the leached concentration by volume (0.25 L) corresponding amount of leached arsenic are 34.6 and 68.0 μg , respectively. This corresponds to 0.30% and 0.60% leaching of total amount of arsenic in the biosolids. pH of the liquid remained fairly constant between 7.0 and 7.20 during the entire test period.

Arsenic and iron leaching in AGR-2

As shown in Figure 5.107, after first two days of aging soluble arsenic concentrations were found to be 32.4 and 34.0 $\mu\text{g/L}$ in anoxic and oxic conditions respectively. With longer aging time leached arsenic increased steadily and reached the maximum of 123 $\mu\text{g/L}$ during anoxic aging. On the contrary, the final arsenic concentration was found to be 37 $\mu\text{g/L}$ after completion of oxic aging. Multiplying the leached concentration by volume (0.25 L) corresponding amount of leached arsenic are 23.5 and 2.5 μg , respectively. This corresponds to 0.20% and 0.02% leaching of total amount of arsenic in the biosolids in anoxic and oxic conditions respectively.

Leachate iron concentrations after first two days of aging was 0.36 mg/L and 0.62 mg/L in anoxic and oxic conditions respectively. The iron concentration increased gradually and finally reached to the maximum of 1.53 mg/L during anoxic aging periods. On the contrary, iron concentration first increased rapidly and then slowly dropped to 0.80 mg/L during oxic aging period. Multiplying the leached concentration by volume (0.25 L) corresponding amount of leached iron were 0.31 mg and 0.11 mg respectively, which corresponds to 0.48% and 0.18% leaching of total amount of iron in the biosolids during anoxic and oxic aging respectively. pH of the liquid remained fairly constant between 6.98 and 7.28 during the entire test period. It was observed that the changes in the leached arsenic and iron concentrations followed linear pattern of increase during anoxic aging. The release of arsenic and iron (in AGR-2) could be related to the dissolution of sulphide minerals formed in the reactors.

Moreover, a part of arsenic released may also be attributed to the release from the bacterial sludge which may retained some of arsenic in it. Additionally, the type of microbial population present in an environment also plays an important role in arsenic dissolution. However, the presence of both type of microbial genera those enhances (e.g., *Acidithiobacillus*) and those decrease the dissolution of arsenic (e.g. *Thiobacillus*) from arsenosulphides (Rodriguez-Freire et al., 2012), was also observed in present studied systems (Ref. section 5.10.3.4).

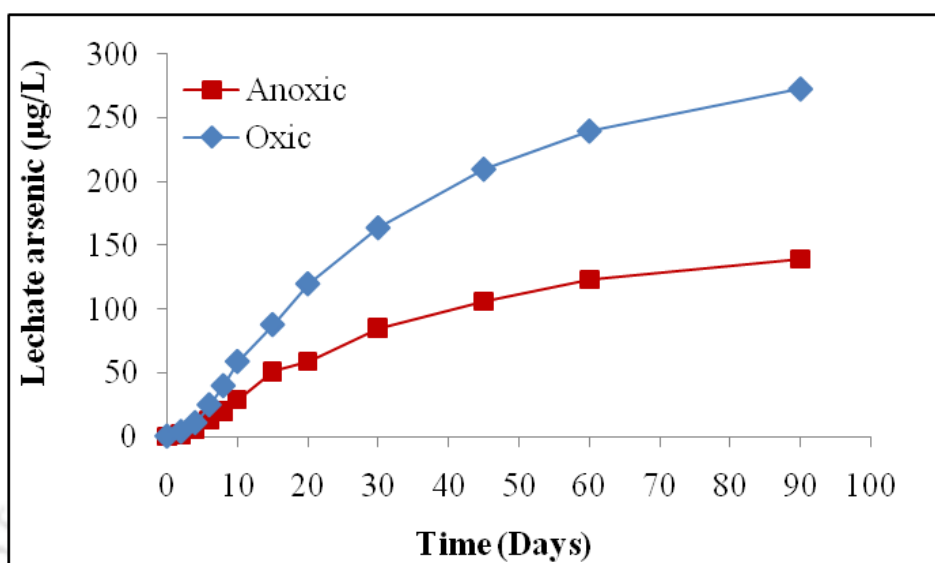


Figure 5.106 Release of arsenic during anoxic and oxic aging of backwash solids of AGR-1.

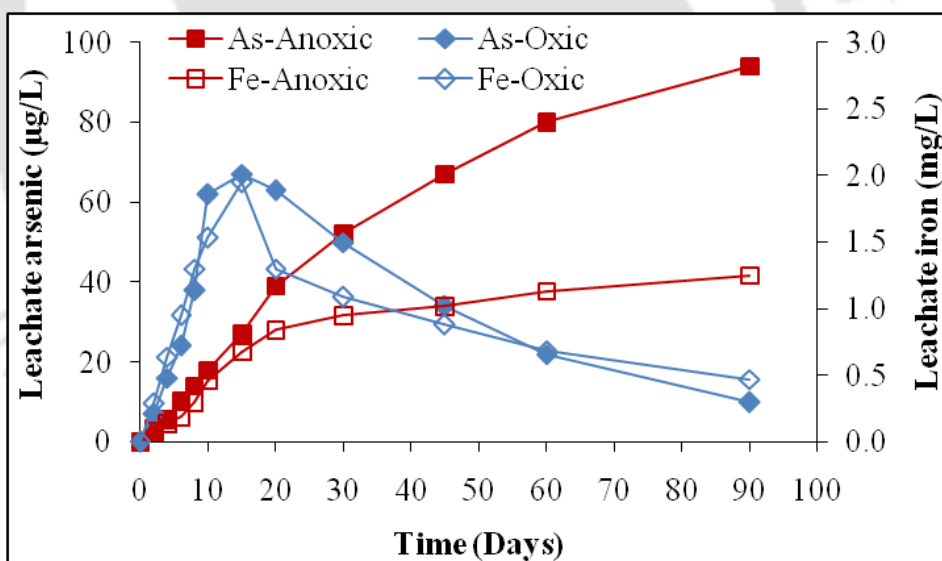


Figure 5.107 Release of arsenic and iron during anoxic and oxic aging of backwash solids AGR-2.

It should be noted that release of arsenic from the biosolids of AGR-2 was lesser than AGR-1, this might be due to the adsorption of leached arsenic possibly on to the iron hydroxides formed due to the oxidation of Fe (II) from iron sulphides in presence of the O_2 (Meng et al., 2001). The higher iron release in oxic condition is possibly due to dissolution of the iron sulphides that were formed in the suspended medium during the

course of aging. Despite of some arsenic leaching from biosolids of AGRs, the overall leaching was found to be substantially low. Engineered coprecipitation of arsenic with biogenic FeAsS, FeS or FeS₂ is reported to have long term kinetic stability even up to several hundred milligrams of arsenic (Onstott et al., 2011b; Suthan S & Fred C, 2004). The release of arsenic from biosolids of AGR-1 was mainly due to dissolution of arsenosulphide minerals. Lengke and Tempel (2001) reported 0.15% arsenic mobilization in 30 days from amorphous orpiment in pH range of 6.8-8.2 in presence of high DO concentration. Rodriguez-Freire et al. (2012) observed orpiment dissolution at the rate of $7.25 \times 10^{-5} \%$ /min in aerobic experiments conducted at 7.2 pH and 8.5 ppm DO level. These evidences, combined with the results obtained in this research, suggest that the arsenosulphides formed in the reactor systems are relatively stable in aerobic conditions over time at near neutral pH.

5.12.2 TCLP Test Results

Characteristics of backwash biosolids used for TCLP test

The total nitric-perchloric acid extractable arsenic and iron in the biosolids of AGRs along with some other physical and chemical properties are given in Table 5.6. Very high TSS/VSS values of the backwash solids suggest that the major fraction of the backwash solids was mainly composed of metal sulphides.

Table 5.6 Characteristics of AGR-1 and AGR-2 backwash solids.

Sample type	pH	TSS (mg/L)	VSS (mg/L)	As (mg/kg of dry BWS)	Fe (mg/kg of dry backwash solids)
AGR-1	6.84	3190	246	29.8	-
AGR-2	6.92	3417	288	23.3	134.8

Results of kinetic TCLP extraction tests:

Arsenic leaching profile during kinetic TCLP leaching tests on biosolids of AGR-1 is shown in Figure 5.108. As seen in the figure, rate of arsenic leaching was faster during first few hours of the test, whereas, it gradually decreased with time. However, leaching of arsenic seemed to have continued even after 24 hours. Maximum arsenic concentrations in the leachates were found to be 21 µg/L and 14 µg/L in oxic and anoxic

conditions, respectively after 24 hours. This corresponds to 0.94% and 1.44% leaching, respectively. Arsenic and iron leaching profile during kinetic TCLP leaching tests on biosolids of AGR-2 is shown in Figure 5.109. From the Figure, the arsenic and iron concentrations gradually increased to 13 µg/L and 318 µg/L respectively, in the extractions carried out in anoxic conditions. In anoxic condition, arsenic and iron release was faster during first 8 hr and thereafter it became slower during next 16 hr of extraction. On the contrary, arsenic and iron concentrations increased to 34 µg/L and 604 µg/L till 6 hr and then decreased slowly to 11 µg/L and 287 µg/L between 6 hr and 24 hr of TCLP extractions conducted in oxic environment. This decrease in iron concentration during the kinetic TCLP leaching conducted in oxic environment is attributed to the dissolution of iron sulphides present in biosolids followed by oxidation of released Fe^{2+} ions which lead to the iron(hydr)oxides precipitation. Thus any arsenic (III) that has been oxidised to arsenic (V) was get adsorbed and led to decrease in arsenic concentration due to arsenic adsorption on iron(hydr)oxides as later are also good adsorbents of arsenic. The rapid oxidation of As(III) to As(V) in aerated waters in just 2 hr reaction time in the pH range 5-9 is reported (Katsoyiannis et al. (2015). Mähler and Persson (2013) found that both As (III) and As (V) can be efficiently adsorbed on granular ferric hydroxides in than 1 to 2 minute of contact time at pH range of 5-7. Yang et al. (2014) and Katsoyiannis and Zouboulis (2004) also reported on arsenic removal during iron oxidation by iron oxidising bacteria and adsorption of As(V) onto biogenic iron hydroxide precipitates.

Microbial community analysis of the present AGR systems also revealed the presence of genera (Ref. section 5.10.3.4) such as (*Acidithiobacillus*) which are capable of arsenic removal in presence of iron at lower pH. Ahoranta et al. (2016) also observed similar microbial genera in a biological reactor removing arsenic from biogenic ferric precipitates. The lower arsenic and iron release in the extractions carried out in anoxic conditions might be associated with the stable nature of biosolids as well as slower oxidation in anoxic environments.

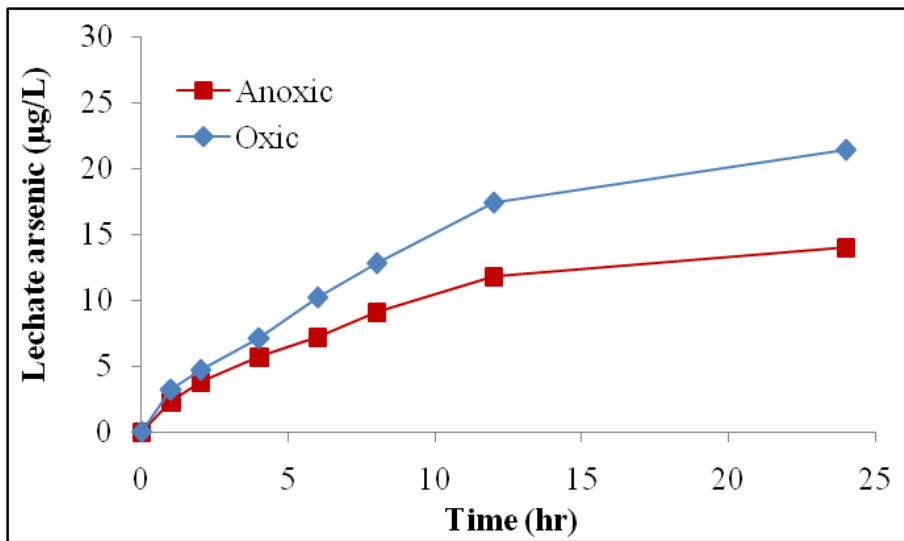


Figure 5.108 Arsenic leaching profile during kinetic TCLP leaching tests on biosolids of AGR-1.

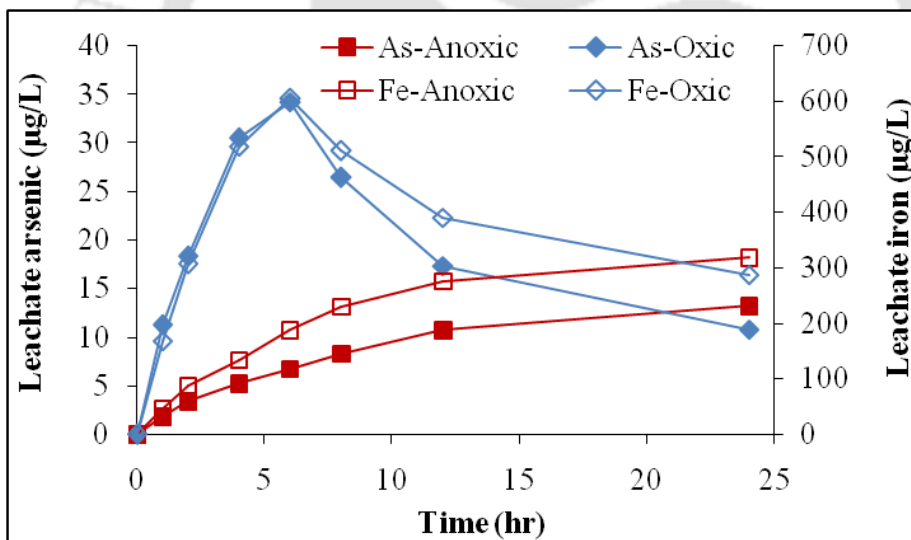


Figure 5.109 Arsenic and iron leaching profile during kinetic TCLP leaching tests on biosolids of AGR-2.

Extended TCLP extractions test results

The kinetic TCLP test results have shown gradual increase in arsenic and iron concentrations up to 24 hr, thus extended TCLP extractions (84 hr) were performed onto biosolids of AGRs to check if leaching out of more arsenic and/or iron from biosolids of AGRs. The results of extended TCLP extractions conducted on biosolids of AGR-1 and AGR-2 at constant V_g/V_L ratio of 0.5 is shown in Figure 5.110.

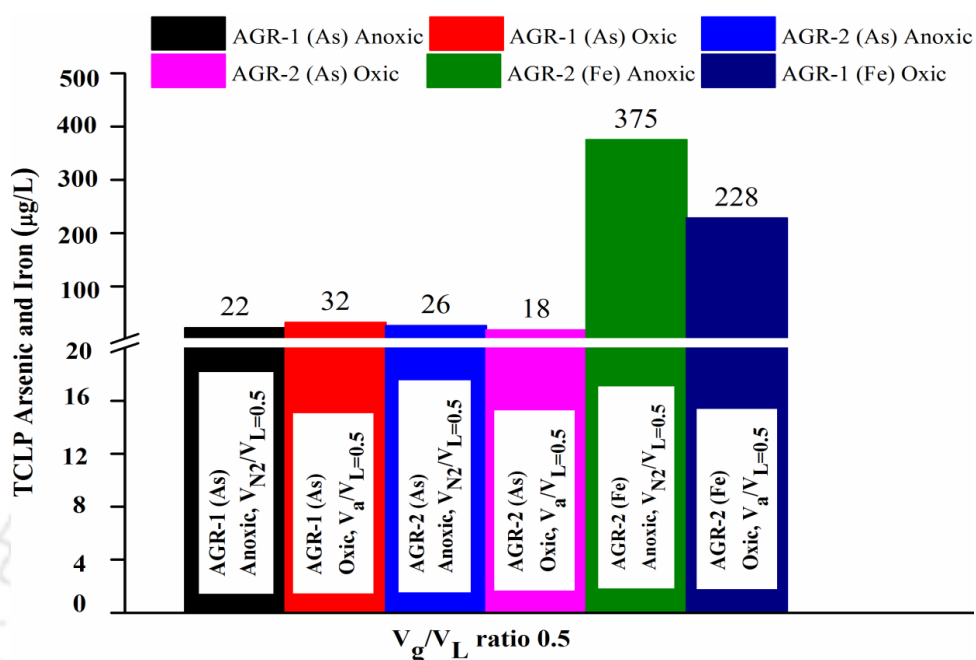


Figure 5.110 Leaching of arsenic and iron as estimated through extended TCLP test on biosolids of AGR-1 and AGR-2 at constant V_g/V_L ratio of 0.5.

It shows that when the extractions were performed on biosolids of AGR-1 in presence of air, the TCLP extracted arsenic was 32 µg/L corresponding to 2.17% leaching. On the other hand, the leachate arsenic concentration was decreased to 23 µg/L corresponding to 1.52% leaching, when the slurry was supplied with N_2 (TCLP- N_2) for 20 min, prior to the TCLP extraction.

The TCLP extracted arsenic was 18 µg/L and 26 µg/L corresponding to 1.21% and 1.74% leaching respectively, in the extractions carried out on biosolids of AGR-2 in presence of air and nitrogen. In the TCLP extractions carried out in presence of nitrogen (TCLP- N_2), the leachate arsenic concentration was 1.44 fold higher than TCLP performed in air. The total TCLP leachate iron was 228 µg/L and 375 µg/L, which corresponds to 3.38% and 5.56% leaching in the extractions carried out in presence of air and nitrogen. The leachate iron for TCLP- N_2 , was 375 µg/L which was 1.64 times more than TCLP performed in air. The leached arsenic and iron concentration in TCLP- N_2 was higher than the TCLP at V_{air}/V_L ratio 0.50. These results showed that the presence of oxygen in the extraction vessels decreased the leachability of arsenic and iron in the biosolids of AGR-

2. This may be due to underestimation of leachate arsenic and iron in anoxic solid phase-sulphide samples in the TCLP conducted in presence of oxygen. This is because in presence of air, oxidised iron in the form of iron hydroxides adsorbs leached arsenic hence provide stability to arsenic in anoxic arsenic containing wastes (Clancy et al., 2013; Jong & Parry, 2005). Thus, the results also indicates that TCLP test conducted in presence of air, is unable to predict correct leachability of arsenic for reduced arsenic bearing waste associated with iron. Both Meng et al. (2001) from anoxic sludge samples and Jong and Parry (2005) from biogenic solid phase sulphide minerals, observed similar arsenic leaching results. However, underestimated arsenic leaching from the arsenic solids associated with iron compounds under a landfill-like situation which is anoxic as well as acidic, is also documented (Ghosh et al., 2004). On the other hand, less arsenic leaching from biosolids of AGR-1 in extended TCLP-N₂ may be attributed to stability of arsenosulphides in reduced environments and partly due to the absence of iron in the samples, as presence of iron provides an additional sink for arsenic adsorption. On the basis of the extended TCLP results, it may be concluded that arsenic leaching from the backwash solids of the AGRs was very low as the leachate arsenic concentrations were well below than TCLP leachate values of 5000 and 300 µg/L, as per USEPA (USEPA, 1986) or Australian (EA, 2002) guidelines, respectively. Therefore, the sludge generated in the AGRs would not be classified as hazardous waste material under the Australian Hazardous Waste Act. 1989 or US Resource Conservation and Recovery ACT 1976, respectively.

Effects of DO on TCLP

The effect of dissolved oxygen on the TCLP leaching was further investigated by varying the $V_{\text{air}}/V_{\text{L}}$ ratio in extraction vessels. Effects of $V_{\text{air}}/V_{\text{L}}$ ratios on leachability of arsenic from the biosolids of AGR-1 during extended TCLP tests are shown in Figure 5.111. The results are summarised in Table 5.7. For biosolids of AGR-1, the leachate arsenic concentration was increased from 18 to 64 µg/L along with an increase in DO level from 0.54 to 5.16 mg/L, when the $V_{\text{air}}/V_{\text{L}}$ ratio was increased from 0.25 to 1.25.

Effects of $V_{\text{air}}/V_{\text{L}}$ ratios on leachability of arsenic and iron from the biosolids of AGR-2 during extended TCLP tests are shown in Figure 5.112 and 5.113 respectively. The results are summarised in Table 5.8. Arsenic concentration in biosolids of AGR-2

decreased from 40 to 7.9 $\mu\text{g/L}$ when the DO content in the extraction solutions was increased from 0.65 to 5.38 mg/L. The leachate iron concentration decreased from 415 to 54 $\mu\text{g/L}$ with the increase in DO level from 0.62 mg/L to 5.35 mg/L in the extraction solutions. The lower arsenic concentration at higher $V_{\text{air}}/V_{\text{L}}$ ratios may be attributed to arsenic oxidation at high DO level which lead to adsorption of arsenic(V) on to iron(hydr)oxides precipitates. Similar pattern of leaching were also observed by Meng et al. (2001) and Jong and Parry (2005).

Table 5.7 Leachability of arsenic by the TCLP at different $V_{\text{air}}/V_{\text{L}}$ ratios in AGR-1.

Method	$V_{\text{air}}/V_{\text{L}}$ ratio	As Concentration ($\mu\text{g/L}$)	Fraction of total As leached (%)	Final leachate pH	Final DO (mg/L)
TCLP	0.25	29	1.2	5.32	0.54
TCLP	0.5	46	2.0	5.38	3.16
TCLP	1.0	79	3.2	5.34	4.14
TCLP	1.25	122	4.3	5.31	5.1

Table 5.8 Leachability of arsenic and iron by the TCLP at different $V_{\text{air}}/V_{\text{L}}$ ratios in AGR-2.

Method	$V_{\text{air}}/V_{\text{L}}$ ratio	Concentration ($\mu\text{g/L}$)		Fraction of total leached (%)		Final leachate pH	Final DO (mg/L)
		As	Fe	As	Fe		
TCLP	0.25	41	567	2.7	6.2	5.16	0.68
TCLP	0.50	20	346	1.3	3.5	5.25	2.87
TCLP	1.00	13	190	0.86	1.4	5.28	3.54
TCLP	1.25	8	62	0.54	0.81	5.26	4.78

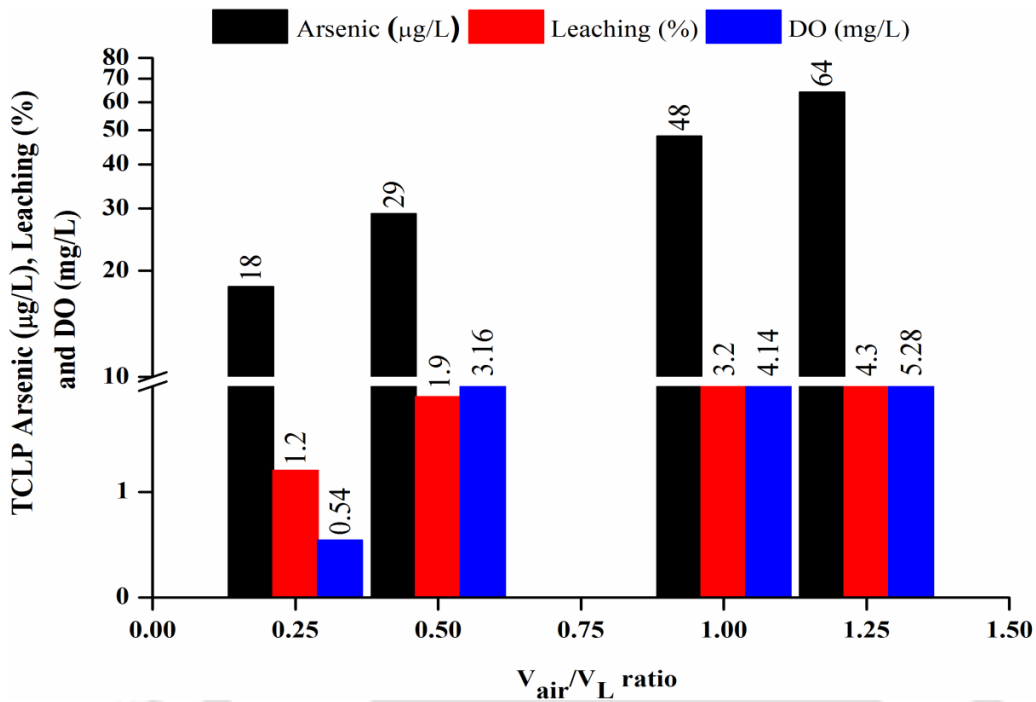


Figure 5.111 Effects of V_{air}/V_L ratios on leachability of arsenic from the biosolids of AGR-1 during extended TCLP tests.

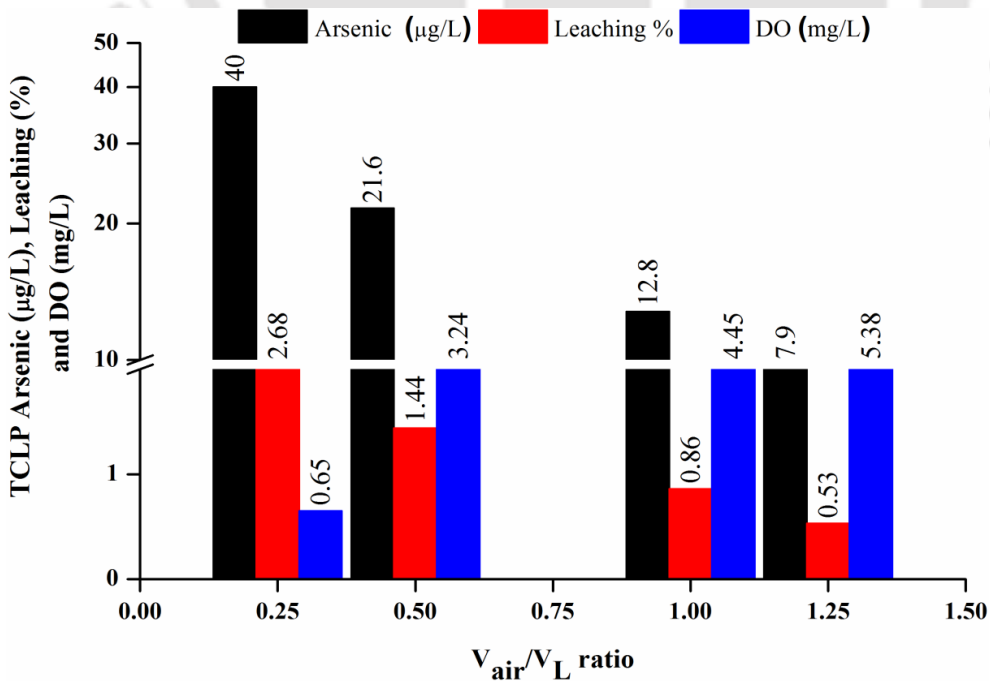


Figure 5.112 Effects of V_{air}/V_L ratios on leachability of arsenic from the biosolids of AGR-2 during extended TCLP tests.

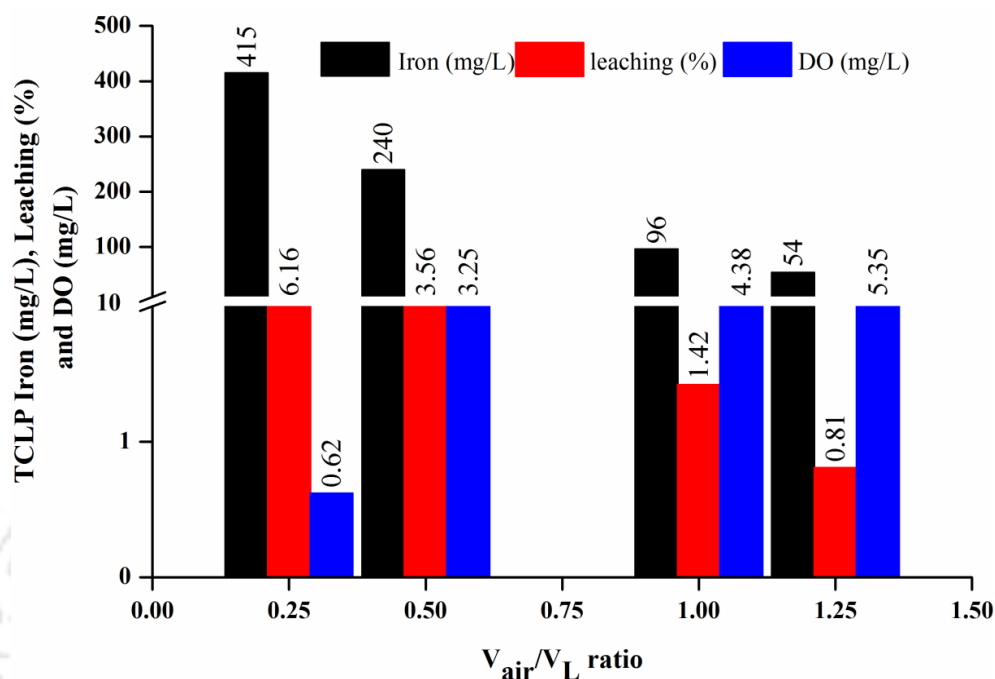


Figure 5.113 Effects of V_{air}/V_L ratios on leachability of iron from the biosolids of AGR-2 during extended TCLP tests.

5.12.3 Long-term Aerobic Leaching Tests

Arsenic leaching as observed during long-term leaching test on biosolids of AGR-1 is shown in Figure 5.114. As shown in the figure, arsenic concentration in the effluent (leachate) was gradually increased over 95 pore volumes of the AGR-1. Arsenic concentration in the leachate was seen to decrease gradually from 95 to 156 pore volume. After leaching out of DI water equivalent to 156 pore volume of the AGR-1, arsenic concentration in the effluent become below detection limit. Cumulative percentage arsenic leaching from the reactor (Fig. 5.114) was estimated to be 0.27% of total arsenic present in the reactor as biosolids. Total arsenic in the biosolids was estimated through mass balance of arsenic considering the amount of arsenic introduced in to the reactor as influent before the leaching test, percentage arsenic removal and total volume of arsenic contaminated water introduced. It is clear from the Figure 5.114 that leached arsenic concentration over 46 pore volumes is below drinking water permissible limits for arsenic then gradual increase in the effluent arsenic concentration over 95 pore volumes of leachate was seen, which was followed by slow decrease over 156 pore volumes in AGR-1.

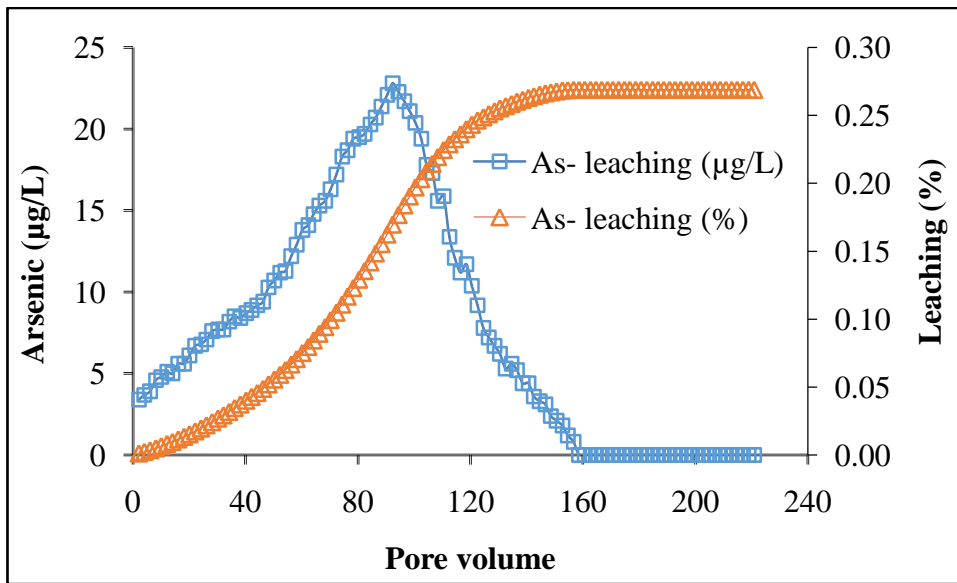


Figure 5.114 Arsenic leaching as observed during long-term leaching test on biosolids of AGR-1.

After that a steady-state was observed when leachate arsenic concentration was either very low or undetectable. A total of 0.27% arsenic was leached during the entire test duration from the precipitates formed in the AGR-1. The percent leaching calculations were based on the arsenic immobilized in the reactors during 20 days operation of the reactor.

The amount of arsenic and iron leached during long-term aerobic leaching tests conducted in AGR-2 is shown in the Figure 5.115 and 5.116, respectively. The arsenic release was seen over 34 pore volumes with linear increase, followed by a decrease up to 92 pore volume followed by steady-state of undetectable arsenic concentrations (Figure 5.114). A total of 0.07% arsenic was leached during the entire test duration from the precipitates formed in AGR-2. Similar leaching pattern was observed for iron release. The results show maximum 236 µg/L of iron leaching up to 50 pore volumes then a slow-moderate decrease up to 78 µg/L in the effluent iron concentration over 78 pore volumes of leachate, followed by a steady-state leachate containing undetectable iron concentrations. A total of 0.29% iron was released over 220 pore volumes in the AGR-2.

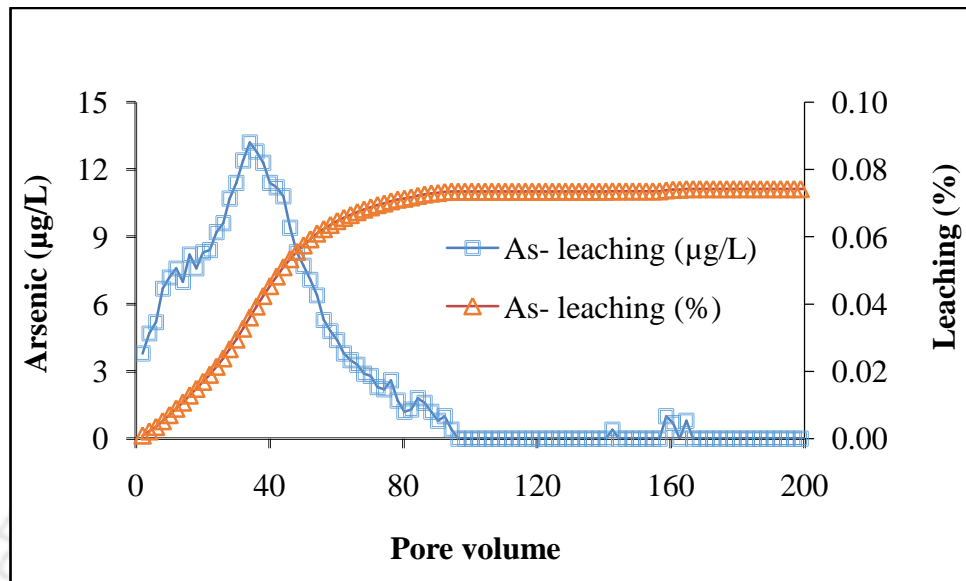


Figure 5.115 Arsenic leaching as observed during long-term leaching test on biosolids of AGR-2.

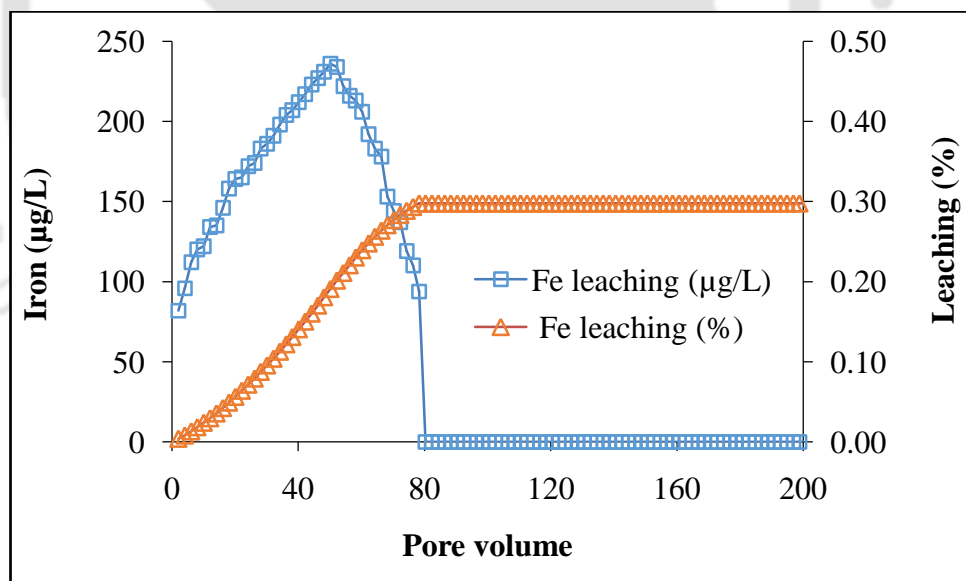


Figure 5.116 Iron leaching as observed during long-term leaching test on biosolids of AGR-2.

The principle mechanisms dealing with the re-release of arsenic in long term storage of solids generated during sulphidogenic removal are oxidation and dissolution of the sulphidogenic precipitates. The amount of arsenic leached from AGR-1 was slightly higher than AGR-2 this was probably because of formation of iron (oxy) hydroxide in

AGR-2 which rearrested the leached As. Lengke and Tempel (2005) also reported greater oxidation rates for amorphous As_2S_3 and AsS at pH 8 compared to pyrite. The increased arsenic release over 95 pore volumes in AGR-1 may be associated with cumulative effect of oxidative dissolution of arsenosulphide precipitates as well as release of adsorbed arsenic from the anaerobic biomass surface and/or release of assimilated arsenic within the bacterial cells (Chowdhury & Mulligan, 2011; Jong & Parry, 2005; Lengke & Tempel, 2005; Lengke & Tempel, 2003; Rodriguez-Freire et al., 2012). In general, interactions with bacteria enhance the oxidation rates of As-bearing sulphide minerals, but at rates lower than those measured in the laboratory under optimum conditions (Lengke et al., 2009). Some arsenic may also leached as a result of bacterial cell death due to increasing oxic conditions and the lack of organic carbon sources. The lesser arsenic release in AGR-2 can be attributed to the adsorption of arsenic on to the iron hydroxides that may form in the reactor as a result of Fe (II) oxidation as well as adsorption on to iron sulphides that remain intact in the system. The similar results for As leaching in aerobic column leaching tests were observed by (Onstott et al., 2011a), and they suggested that these precipitates are resistant to dissolution for decades even under aerobic conditions. Similar observations were also made by (Jong & Parry, 2005). The long term aerobic leaching results suggests that spent WAC and the precipitates formed in the AGR systems were not imposing any further threat to the environment in terms of potential arsenic release in subsurface environments.

XAS analysis

Long-term leaching test on biosolids of AGRs were performed by introducing aerated DI water. Therefore, it is expected to change in oxidation states of arsenic and iron in biosolids. To know the local structure and change in oxidation states of arsenic and/or iron, Fe K-edge XANES and EXAFS spectra of biosolids of AGR-2, collected after TCLP test, were recorded.

Normalized XANES data at Fe K-edge for the (biosolid) sample with FeS (Fe^{2+}), Fe_2O_3 (Fe^{3+}) standards and Fe foil, 1st derivative data plot comparison of the sample and Fe_2O_3 standard are shown in Figure 5.117. Normalized XANES data at As K-edge for the (biosolid) sample with As(III), As(V) standards and 1st derivative data plot comparison of the sample and As (V) standard are shown in Figure 5.118. The XANES spectra confirms

that the arsenic and iron present in biosolids of AGR-2 collected after TCLP has got oxidized and found to be present in +5 and +3 oxidation states respectively.

Figure 5.119 shows the Fourier transform (FT) EXAFS oscillations of Fe K-edge for AGR-2 TCLP samples. The k -range of 2.5-9 \AA^{-1} has been used for FT of Fe EXAFS data. For CR-2 TCLP Fe K edge has been fitted using FeO(OH) structure (space group P n m a) where first shell Fe-O bond is at 1.953 \AA distance and second next near-neighbour Fe-Fe bond is at 3.01 \AA distance. The fitting of EXAFS data, coordination numbers (CN) of the different shells, bond distance (R) and Debye-Waller factor (σ^2) were fitted as free parameters. Figure 5.119 also shows the best fitted curves and best fit values of the parameters are listed in Table 5.9.

Table 5.9 The best fit values of the parameters for AGR-2 sample.

Sample	$CN_{\text{Fe-O}}$	$R_{\text{Fe-O}}(\text{\AA})$	$\sigma^2_{\text{Fe-O}}(\text{\AA}^2)$	$CN_{\text{Fe-Fe}}$	$R_{\text{Fe-Fe}}(\text{\AA})$	$\sigma^2_{\text{Fe-Fe}}(\text{\AA}^2)$
AGR-2 TCLP	4.3(2)	1.919(3)	0.0036 (3)	3.2 (3)	3.114 (2)	0.0086 (3)

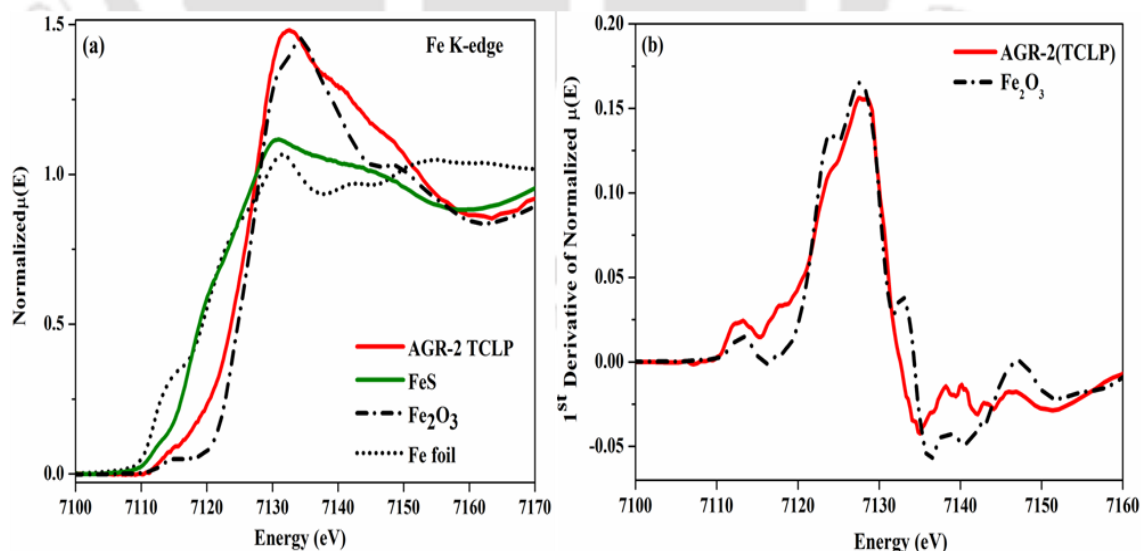


Figure 5.117 (a) Normalized XANES data at Fe K-edge for long term leaching test in AGR-2 TCLP samples with FeS (Fe^{2+}), Fe₂O₃ (Fe^{3+}) standards and Fe foil, (b) 1st derivative data plot comparison of AGR-2 TCLP sample and Fe₂O₃ standard.

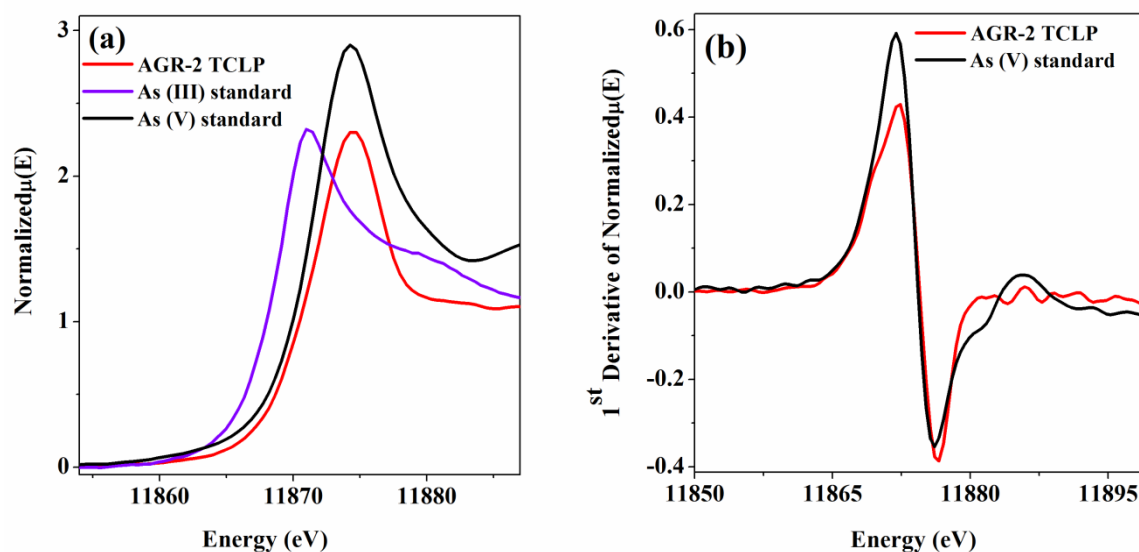


Figure 5.118 (a) Normalized XANES data at As K-edge for long term leaching test in AGR-2 TCLP samples with As(III), As (V) standards and sample, (b) 1st derivative data plot comparison of AGR-2 TCLP sample and As (V) standard.

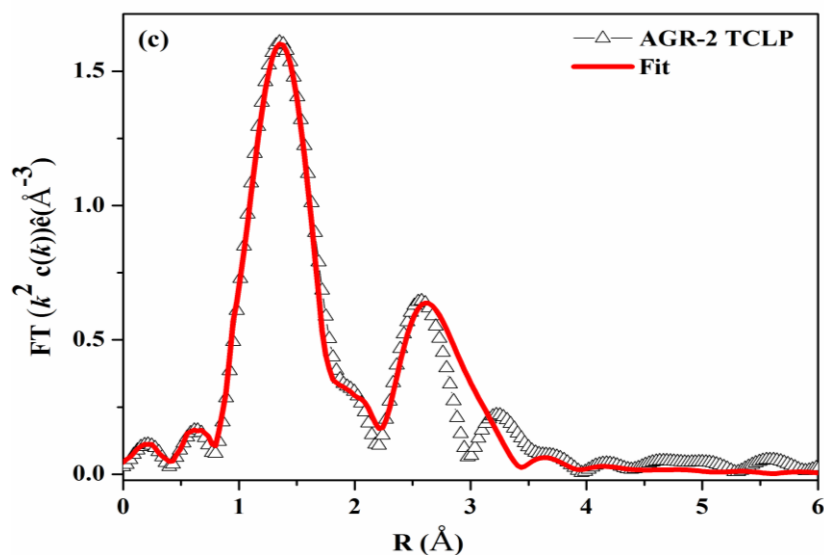


Figure 5.119 Fourier transform of k^2 -weighted of Fe K-edge for AGR-2 TCLP sample. The symbol shows experimental data and solid lines are the best fit.

CHAPTER 6

CONCLUSION AND SCOPE OF FUTURE STUDIES

Summary and Conclusions

The main objective of the present investigation was to develop a complete treatment system for simultaneous removal of mainly arsenic, nitrate, iron and fluoride from contaminated groundwater by biological process. In this study, mixed microbial culture was used to evaluate its performance on simultaneous removal of target pollutants, arsenic, nitrate, iron and fluoride as well as effects of one pollutant on the others in batch, semi-batch and flow through reactor systems. Waste activated carbon (WAC) was used as supporting material for bacterial growth in flow through reactors, AGR-1 and AGR-2. Arsenic adsorption characteristics of mixed bacterial culture as well as the WAC were evaluated before being used in bioreactors. Besides performance evaluation of mixed bacterial culture on simultaneous removal of target pollutants from groundwater, microbial population dynamics in AGRs, post treatment of AGR treated water and mechanisms of arsenic removal were also investigated through their characterization. Collection, preparation, characterization and performance evaluation of an adsorbent from water treatment plant residues (WTR) on fluoride removal from AGR treated water was performed to evaluate its potential as a post treatment unit. In addition to this, stability of the biosolids as well as the spent WAC were checked under aerobic as well as anoxic conditions through “Ageing test”, “Toxicity Characteristics Leaching Procedure (TCLP) test” and “Long Term Leaching test”.

Summary of the salient results and conclusions made out of the present investigation are given below:

1. Batch studies with WAC (@ 2g/L) showed that the removal of As(V) by adsorption was less than 10% from an initial of 250 $\mu\text{g/L}$ after 12 h of agitation at 150 rpm and 30°C. Removal of arsenic by mixed microbial culture was even low and it was about 3% from an initial of 500 $\mu\text{g/L}$.
2. In batch shake flasks, in absence of iron, mixed bacterial culture could reduce from 500 $\mu\text{g/L}$ of arsenic in simulated groundwater to below 10 $\mu\text{g/L}$ within 3-4 days of operation, in presence of 25 mg/L of sulphate and up to 150 mg/L of nitrate. In presence of iron, irrespective of initial arsenic (up to 1000 $\mu\text{g/L}$) and nitrate (up to 150 mg/L) concentration, arsenic in the treated water was reduced to below permissible limit in drinking water (10 $\mu\text{g/L}$) within 3-6 days of reaction.
3. In SmBR-1, arsenic in treated water was always remained below 10 $\mu\text{g/L}$, from up to an initial arsenic concentration of 600 $\mu\text{g/L}$ in simulated groundwater, whereas the arsenic removal was dropped to 90% and 80% at initial arsenic concentration of 700 $\mu\text{g/L}$ and 800 $\mu\text{g/L}$ respectively. In SmBR-2, arsenic removal remained stable at below 10 $\mu\text{g/L}$ for all tested initial arsenic concentration of up to 1000 $\mu\text{g/L}$. The iron was found below detection limits in all instances except first few days of SmBR-2 operation.
4. In AGR-1, high arsenic removal efficiency of 99.4% was observed from 750 $\mu\text{g/L}$ of initial arsenic concentration in simulated groundwater and the performance was found to be a function of EBCT and initial sulphate concentration. Controlling flow rate and providing adequate sulphate increased reactor performance for simultaneous removal of arsenic and nitrate up to 750 $\mu\text{g/L}$ and 200 mg/L, respectively.
5. In presence of iron, arsenic was reduced to below 10 $\mu\text{g/L}$, from an initial of up to 1500 $\mu\text{g/L}$ and iron was reduced to below 0.3 mg/L from an initial of 10 mg/L in AGR-2. Experimental results suggested that the reactor would be able to remove simultaneously even higher concentration of arsenic, nitrate and iron provided sufficient reaction time (EBCT) and sulphate was added. Removal of iron from an initial of 13.2 mg/L and arsenic from an initial of 295 $\mu\text{g/L}$ in real groundwater to below 0.3 mg/L and 10 $\mu\text{g/L}$, respectively in the AGR-2 confirmed this hypothesis.

6. Performances of the AGRs were not adversely affected at temperature between 20°C and 50°C.
7. Although dextrose was found to be the best on faster removal of pollutants, all the carbon sources used in the present investigation were found to be acceptable to be used as electron donor when assessed in terms of percentage removal of pollutants.
8. Complete nitrate removal from up to 250 mg/L in simulated groundwater was noticed in batch shake flasks, semi batch reactors and flow through reactors within 24 hours of reactor run.
9. The T-RFLP and metagenomic analysis of microbial community confirmed the presence of arsenic, nitrate and sulphate reducers in AGRs.
10. Fluoride removal in AGR-1 remained below 5% from an initial of 5 mg/L in simulated groundwater. The adsorbent prepared from WTR could remove fluoride from an initial of 5 mg/L to 0.55 mg/L.
11. FESEM/EDX analysis shown that biosolids precipitated in both AGRs were mainly composed of arsenic, sulphur and/or iron. XRD analysis confirmed the precipitation of orpiment (As_2S_3) and realgar (AsS) in AGR-1 and orpiment (As_2S_3), realgar (AsS) pyrrhotite (FeS), and pyrite (FeS_2) in AGR-2. TEM analysis revealed amorphous, nanocrystalline and crystalline phases formed in the AGR systems. XANES of the AGR biosolids confirmed that arsenic and iron was in +3 and +2 oxidation states respectively. Moreover, the EXAFS analysis established the formation of orpiment (As_2S_3) and iron sulphide (FeS) in AGR-1 and AGR-2 respectively.
12. The results suggest that precipitation of arsenosulphide is the main mechanism of arsenic removal in AGR-1, whereas, in AGR-2 precipitation as arsenosulphide and/or co-precipitation of arsenic with biogenic iron sulphides are the main arsenic removal mechanisms.
13. Maximum arsenic leaching from biosolids of either AGRs was less than or equal to 0.6%, whereas maximum iron leaching of 0.48% was noticed from AGR-2 biosolids, after 90 days of experiment in anoxic and oxic environment. TCLP and long term leaching test results show that the biosolids as well as spent WAC were non hazardous and stable that can be dumped in sanitary landfill safely.

14. In summary, the AGR systems developed in this project could remove arsenic and its co-pollutants such as nitrate and iron from simulated as well as real groundwater at wide range of temperature to meet the drinking water standards, leaving a non hazardous and stable biosolids as well as spent WAC, which can be dumped in sanitary landfill safely. However, fluoride needs to be treated separately in an additional treatment unit. A waste product, WTR, proved to be efficient for fluoride removal to meet the drinking water standards.

Scope for Future Studies

The present study was confined to assess the ability of the bioreactor system for removal of arsenic, iron and nitrate using synthetic as well as real groundwater.

In order to carry forward the research of the present investigation, following suggestions are listed:

1. Fabrication of pilot plant scale bioreactor and its performance evaluation on simultaneous removal of target contaminants on treatment of real groundwater.
2. Studies on the introduction of other co-pollutants (such as uranium, selenium and perchlorate etc.) and performance evaluation of AGRs.
3. Studies on the feasibility of other freely available industry based carbohydrate-based electron donors on performance evaluation of AGRs for multi-contaminant removal.
4. Applicability of other supporting materials that can be used for biofilm growth can be investigated.
5. Detailed study of the microbial community involved in each of the different operating conditions.

VISIBLE RESEARCH OUTPUT

International/National Conferences

1. **Shakya, A. K.,** and Ghosh, P. K. 2016. Poster presentation on “Investigation of multipollutants removal in anaerobic batch bioreactors by means of terminal electron accepting process” in **ICCB 2016 'International Conference on Current Trends in Biotechnology'** held at VIT Vellore, India, during December 8th-10th, 2016. (*Best Poster Award*)
2. **Shakya, A. K.,** and Ghosh, P. K. 2016. Oral presentation on “Stability check of biosolids generated in sulfidogenic arsenic removal from drinking water” in **RECYCLE 2016 'International Conference on Waste Management'** held at IIT Guwahati, India, during April 1st-2nd, 2016.
3. **Shakya, A. K.,** and Ghosh, P. K. 2016. Oral presentation on “Simultaneous removal of arsenic and nitrate in anaerobic batch reactors” in **ICWEES 2016 'International Conference on Water, Environment, Energy and Society'** held at AISECT University, Bhopal, India, during March 15th-18th, 2016.
4. **Shakya, A. K.,** and Ghosh, P. K. 2015. Oral presentation on “Simultaneous bioremoval of arsenic and iron in sulfidogenic suspended growth batch reactors” in the National conference **CHEMCON 2015 'Chemical Engineering: From Laboratory to Industry'**, held at IIT Guwahati, India, during December 27th-30th, 2015.
5. **Shakya, A. K.,** and Ghosh, P. K. 2015. Oral presentation on “Bioremoval of arsenic in sulfidogenic suspended growth batch reactors” National conference (**NCOCER 2015**) held at IIT Guwahati, during June 4th-6th, 2015.
6. **Shakya, A. K.,** and Ghosh, P. K. 2015. Oral presentation on “Arsenic removal as biogenic sulfides” in **TEQIP National course** held at IIT Guwahati, during March 4th-6th, 2015.



REFERENCES

- Achak, M., Hafidi, A., Ouazzani, N., Sayadi, S., Mandi, L. 2009. Low cost biosorbent “banana peel” for the removal of phenolic compounds from olive mill wastewater: Kinetic and equilibrium studies. *Journal of hazardous materials*, **166**(1), 117-125.
- Æsø, A., Ødegaard, H., Bach, K., Pujol, R., Hamon, M. 1998. Denitrification in a packed bed biofilm reactor (BIOFOR)—Experiments with different carbon sources. *Water Research*, **32**(5), 1463-1470.
- Afkar, E., Lisak, J., Saltikov, C., Basu, P., Oremland, R.S., Stolz, J.F. 2003. The respiratory arsenate reductase from *Bacillus selenitireducens* strain MLS10. *FEMS Microbiology Letters*, **226**(1), 107-112.
- Ahmed, M.K., Habibullah-Al-Mamun, M., Parvin, E., Akter, M.S., Khan, M.S. 2013. Arsenic induced toxicity and histopathological changes in gill and liver tissue of freshwater fish, tilapia (*Oreochromis mossambicus*). *Experimental and Toxicologic Pathology*, **65**(6), 903-909.
- Ahn, J.H., Kim, S., Park, H., Rahm, B., Pagilla, K., Chandran, K. 2010. N₂O emissions from activated sludge processes, 2008– 2009: results of a national monitoring survey in the United States. *Environmental science & technology*, **44**(12), 4505-4511.
- Ahoranta, S.H., Kokko, M.E., Papirio, S., Özkaya, B., Puhakka, J.A. 2016. Arsenic removal from acidic solutions with biogenic ferric precipitates. *Journal of Hazardous Materials*, **306**, 124-132.
- Aichele, S.S. 2004. *Arsenic, nitrate, and chloride in groundwater, Oakland County, Michigan*. US Department of the Interior, US Geological Survey.
- Akin, I., Arslan, G., Tor, A., Cengeloglu, Y., Ersoz, M. 2011. Removal of arsenate [As (V)] and arsenite [As (III)] from water by SWHR and BW-30 reverse osmosis. *Desalination*, **281**, 88-92.
- Ako, A., Eyong, G., Shimada, J., Koike, K., Hosono, T., Ichianagi, K., Richard, A., Tandia, B., Nkeng, G., Roger, N. 2014. Nitrate contamination of groundwater in two areas of the Cameroon Volcanic Line (Banana Plain and Mount Cameroon area). *Applied Water Science*, **4**(2), 99-113.
- Akunna, J.C., Bizeau, C., Moletta, R. 1993. Nitrate and nitrite reductions with anaerobic sludge using various carbon sources: glucose, glycerol, acetic acid, lactic acid and methanol. *Water Research*, **27**(8), 1303-1312.
- Alarcón-Herrera, M.T., Bundschuh, J., Nath, B., Nicolli, H.B., Gutierrez, M., Reyes-Gomez, V.M., Nuñez, D., Martín-Dominguez, I.R., Sracek, O. 2013. Co-occurrence of arsenic and fluoride in groundwater of semi-arid regions in Latin America: Genesis, mobility and remediation. *Journal of Hazardous Materials*, **262**(0), 960-969.
- Albretsen, J. 2006. Toxicology Brief: The toxicity of iron, an essential element.
- Altun, M., Sahinkaya, E., Durukan, I., Bektas, S., Komnitsas, K. 2014. Arsenic removal in a sulfidogenic fixed-bed column bioreactor. *Journal of Hazardous Materials*, **269**(0), 31-37.
- An, B., Fu, Z., Xiong, Z., Zhao, D., SenGupta, A.K. 2010. Synthesis and characterization of a new class of polymeric ligand exchangers for selective removal of arsenate from drinking water. *Reactive and Functional Polymers*, **70**(8), 497-507.
- Andrianisa, H.A., Ito, A., Sasaki, A., Aizawa, J., Umita, T. 2008. Biotransformation of arsenic species by activated sludge and removal of bio-oxidised arsenate from wastewater by coagulation with ferric chloride. *Water Research*, **42**(19), 4809-4817.
- Ankrah, D.A., Sjøgaard, E.G. 2009. A review of biological iron removal. *Thirteenth International Water Technology Conference Hurgada, Egypt*.

- APHA. 2005. Standard methods for the examination of water & wastewater. *American Public Health Association, Washington DC.*, **21st edition**.
- Avtar, R., Kumar, P., Surjan, A., Gupta, L., Roychowdhury, K. 2013. Geochemical processes regulating groundwater chemistry with special reference to nitrate and fluoride enrichment in Chhatarpur area, Madhya Pradesh, India. *Environmental Earth Sciences*, **70**(4), 1699-1708.
- Awual, M.R., Shenashen, M., Yaita, T., Shiwaku, H., Jyo, A. 2012. Efficient arsenic (V) removal from water by ligand exchange fibrous adsorbent. *Water Research*, **46**(17), 5541-5550.
- AWWA, A.a. 1990. Iron and manganese removal. In: *Water Treatment Plant Design.*, **Chapter 11**, (Second Edition, McGraw Hill Publishing Company), 283-320.
- Bacquart, T., Frisbie, S., Mitchell, E., Grigg, L., Cole, C., Small, C., Sarkar, B. 2015. Multiple inorganic toxic substances contaminating the groundwater of Myingyan Township, Myanmar: Arsenic, manganese, fluoride, iron, and uranium. *Science of The Total Environment*, **517**(0), 232-245.
- Baig, J.A., Kazi, T.G., Arain, M.B., Afridi, H.I., Kandhro, G.A., Sarfraz, R.A., Jamal, M.K., Shah, A.Q. 2009. Evaluation of arsenic and other physico-chemical parameters of surface and ground water of Jamshoro, Pakistan. *Journal of Hazardous Materials*, **166**(2), 662-669.
- Bajpai, S., Chaudhuri, M. 1999. Removal of arsenic from ground water by manganese dioxide-coated sand. *Journal of Environmental Engineering*, **125**(8), 782-784.
- Bakermans, C., Tollaksen, S.L., Giometti, C.S., Wilkerson, C., Tiedje, J.M., Thomashow, M.F. 2007. Proteomic analysis of *Psychrobacter cryohalolentis* K5 during growth at subzero temperatures. *Extremophiles*, **11**(2), 343-354.
- Barton, L.L., Tomei, F.A. 1995. Characteristics and activities of sulfate-reducing bacteria. in: *Sulfate-reducing bacteria*, Springer, pp. 1-32.
- Battaglia-Brunet, F., Crouzet, C., Burnol, A., Coulon, S., Morin, D., Joulain, C. 2012. Precipitation of arsenic sulphide from acidic water in a fixed-film bioreactor. *Water Research*, **46**(12), 3923-3933.
- Baumann, B., Snozzi, M., Zehnder, A., Van Der Meer, J.R. 1996. Dynamics of denitrification activity of *Paracoccus denitrificans* in continuous culture during aerobic-anaerobic changes. *Journal of bacteriology*, **178**(15), 4367-4374.
- Bedolla, L., Avilés, M., Tirado, L., Cortés, J. 1999. Remoción de arsénico del agua para consumo humano mediante coagulación-floculación a nivel domiciliario. *Instituto Mexicano de Tecnología del Agua (IMTA), México*.
- Bell, T., Newman, J.A., Silverman, B.W., Turner, S.L., Lilley, A.K. 2005. The contribution of species richness and composition to bacterial services. *Nature*, **436**(7054), 1157-1160.
- Benning, L.G., Wilkin, R.T., Barnes, H. 2000. Reaction pathways in the Fe-S system below 100 C. *Chemical Geology*, **167**(1), 25-51.
- Berg, M., Luzi, S., Trang, P.T.K., Viet, P.H., Giger, W., Stüben, D. 2006. Arsenic removal from groundwater by household sand filters: comparative field study, model calculations, and health benefits. *Environmental science & technology*, **40**(17), 5567-5573.
- Bhatnagar, A., Kumar, E., Sillanpaa, M. 2011. Fluoride removal from water by adsorption—a review. *Chemical Engineering Journal*, **171**(3), 811-840.
- Bhatnagar, A., Sillanpaa, M. 2011. A review of emerging adsorbents for nitrate removal from water. *Chemical Engineering Journal*, **168**(2), 493-504.
- Bhattacharya, S., Gupta, K., Debnath, S., Ghosh, U.C., Chattopadhyay, D., Mukhopadhyay, A. 2012. Arsenic bioaccumulation in rice and edible plants and subsequent transmission through food chain in Bengal basin: a review of the perspectives for environmental health. *Toxicological & Environmental Chemistry*, **94**(3), 429-441.

- Bhaumik, R., Mondal, N.K. 2016. Optimizing adsorption of fluoride from water by modified banana peel dust using response surface modelling approach. *Applied Water Science*, **6**(2), 115-135.
- Bibi, S., Farooqi, A., Hussain, K., Haider, N. 2015. Evaluation of industrial based adsorbents for simultaneous removal of arsenic and fluoride from drinking water. *Journal of Cleaner Production*, **87**(0), 882-896.
- Bilgin, A.A., Silverstein, J., Jenkins, J.D. 2004. Iron respiration by *Acidiphilium cryptum* at pH 5. *FEMS microbiology ecology*, **49**(1), 137-143.
- Birhane, M., Abebe, A., Alemayehu, E., Mengistie, E. 2014. Efficiency of locally available filter media on fluoride and phosphate removal for household water treatment system. *Chinese Journal of Population Resources and Environment*, **12**(2), 110-115.
- BIS:10500. 2012. Indian Standard: Drinking Water - Specification. *Bureau of Indian Standard, New Delhi, India., Second Revision.*
- Bleifuss, P.S., Hanson, G., Schoonen, M. 1998. Tracing sources of nitrate in the Long Island aquifer system, State University of New York at Stony Brook.
- Blum, J.S., Kulp, T.R., Han, S., Lanoil, B., Saltikov, C.W., Stolz, J.F., Miller, L.G., Oremland, R.S. 2012. *Desulfohalophilus alkaliarsenatis* gen. nov., sp. nov., an extremely halophilic sulfate- and arsenate-respiring bacterium from Searles Lake, California. *Extremophiles*, **16**(5), 727-742.
- Boller, M., Kobler, D., Koch, G. 1997. Particle separation, solids budgets and headloss development in different biofilters. *Water science and technology*, **36**(4), 239-247.
- Bolton, M., Beckie, R. 2011. Aqueous and mineralogical analysis of arsenic in the reduced, circumneutral groundwater and sediments of the lower Fraser River delta, British Columbia, Canada. *Applied Geochemistry*, **26**(4), 458-469.
- Borah, K.K., Bhuyan, B., Sarma, H.P. 2010. Lead, arsenic, fluoride, and iron contamination of drinking water in the tea garden belt of Darrang district, Assam, India. *Environmental Monitoring and Assessment*, **169**(1-4), 347-352.
- Bordoloi, S., Nath, S.K., Gogoi, S., Dutta, R.K. 2013. Arsenic and iron removal from groundwater by oxidation-coagulation at optimized pH: Laboratory and field studies. *Journal of Hazardous Materials*, **260**(0), 618-626.
- Bostick, B.C., Fendorf, S. 2003. Arsenite sorption on troilite (FeS) and pyrite (FeS₂). *Geochimica et Cosmochimica Acta*, **67**(5), 909-921.
- Boušková, A., Dohányos, M., Schmidt, J.E., Angelidaki, I. 2005. Strategies for changing temperature from mesophilic to thermophilic conditions in anaerobic CSTR reactors treating sewage sludge. *Water Research*, **39**(8), 1481-1488.
- Brahmacharimayum, B. 2014. Studies on Sulfate Reduction to Elemental Sulfur Under Anaerobic/Microaerobic Conditions. *Ph.D Thesis, Indian Institute of Technology, Guwahati, India.*
- Braker, G., Schwarz, J., Conrad, R. 2010. Influence of temperature on the composition and activity of denitrifying soil communities. *FEMS microbiology ecology*, **73**(1), 134-148.
- Brandhuber, P., Amy, G. 1998. Alternative methods for membrane filtration of arsenic from drinking water. *Desalination*, **117**(1), 1-10.
- Brinkel, J., Khan, M.H., Kraemer, A. 2009. A systematic review of arsenic exposure and its social and mental health effects with special reference to Bangladesh. *International journal of environmental research and public health*, **6**(5), 1609-1619.
- Brown, J.C. 2008. Biological treatments of drinking water. *National Academy of Engineering. Frontiers of Engineering: Reports on Leading-Edge Engineering from the 2007 Symposium. National Academies Press, Washington DC.*

- Brown, J.C., Snoeyink, V.L., Raskin, L., Lin, R. 2003. The sensitivity of fixed-bed biological perchlorate removal to changes in operating conditions and water quality characteristics. *Water Research*, **37**(1), 206-214.
- Buschmann, J., Berg, M., Stengel, C., Winkel, L., Sampson, M.L., Trang, P.T.K., Viet, P.H. 2008. Contamination of drinking water resources in the Mekong delta floodplains: Arsenic and other trace metals pose serious health risks to population. *Environment International*, **34**(6), 756-764.
- Cabrera, G., Pérez, R., Gomez, J., Abalos, A., Cantero, D. 2006. Toxic effects of dissolved heavy metals on *Desulfovibrio vulgaris* and *Desulfovibrio* sp. strains. *Journal of Hazardous Materials*, **135**(1), 40-46.
- Calderer, M., Gibert, O., Marti, V., Rovira, M., de Pablo, J., Jordana, S., Duro, L., Guimerà, J., Bruno, J. 2010. Denitrification in presence of acetate and glucose for bioremediation of nitrate-contaminated groundwater. *Environmental technology*, **31**(7), 799-814.
- Camacho, J., Wee, H.-Y., Kramer, T.A., Autenrieth, R. 2009. Arsenic stabilization on water treatment residuals by calcium addition. *Journal of Hazardous Materials*, **165**(1), 599-603.
- Casiot, C., Morin, G., Juillot, F., Bruneel, O., Personné, J.-C., Leblanc, M., Duquesne, K., Bonnefoy, V., Elbaz-Poulichet, F. 2003. Bacterial immobilization and oxidation of arsenic in acid mine drainage (Carnoulès creek, France). *Water Research*, **37**(12), 2929-2936.
- Cavalca, L., Corsini, A., Zaccheo, P., Andreoni, V., Muyzer, G. 2013. Microbial transformations of arsenic: perspectives for biological removal of arsenic from water. *Future microbiology*, **8**(6), 753-768.
- CEFIC. 1986. Test Methods for Activated Carbon. *European Council of Chemical Manufacturer's Federations*.
- CGWB. 2014. Concept note on geogenic contamination of groundwater in India: with a special note on nitrate. *Central Ground Water Board, Ministry of Water Resources, Govt. of India*
- CGWB. 2010. Ground water quality in shallow aquifers of India. *Central Ground Water Board, Ministry of Water Resources, Govt. of India*.
- Chakrabarty, S., Sarma, H.P. 2011. Fluoride, iron and nitrate contaminated drinking water in Kamrup district, Assam, India. *Archives of Applied Science Research*, **3**(4), 186-192.
- Challenger, F. 2006. Biological methylation. *Advances in Enzymology and Related Areas of Molecular Biology, Volume 12*, 429-491.
- Chaturvedi, R., Banerjee, S., Chattopadhyay, P., Bhattacharjee, C.R., Raul, P., Borah, K. 2014. High iron accumulation in hair and nail of people living in iron affected areas of Assam, India. *Ecotoxicology and Environmental Safety*, **110**(0), 216-220.
- Chen, C., Ren, N., Wang, A., Yu, Z., Lee, D.-J. 2008. Microbial community of granules in expanded granular sludge bed reactor for simultaneous biological removal of sulfate, nitrate and lactate. *Applied Microbiology and Biotechnology*, **79**(6), 1071-1077.
- Cheng, H., Hu, Y., Luo, J., Xu, B., Zhao, J. 2009. Geochemical processes controlling fate and transport of arsenic in acid mine drainage (AMD) and natural systems. *Journal of Hazardous Materials*, **165**(1-3), 13-26.
- Chiang, Y.W., Ghyselbrecht, K., Santos, R.M., Martens, J.A., Swennen, R., Cappuyns, V., Meesschaert, B. 2012. Adsorption of multi-heavy metals onto water treatment residuals: Sorption capacities and applications. *Chemical Engineering Journal*, **200-202**, 405-415.
- Chiu, H.-F., Tsai, S.-S., Yang, C.-Y. 2007. Nitrate in drinking water and risk of death from bladder cancer: an ecological case-control study in Taiwan. *Journal of Toxicology and Environmental Health, Part A*, **70**(12), 1000-1004.
- Choi, Y.C., Li, X., Raskin, L., Morgenroth, E. 2007. Effect of backwashing on perchlorate removal in fixed bed biofilm reactors. *Water research*, **41**(9), 1949-1959.

- Chouhan, S., Flora, S. 2010. Arsenic and fluoride: two major ground water pollutants. *Indian J Exp Biol.*, **48**(7), 666-78.
- Chowdhury, M.R.I., Mulligan, C.N. 2011. Biosorption of arsenic from contaminated water by anaerobic biomass. *Journal of Hazardous Materials*, **190**(1–3), 486-492.
- Chung, J., Li, X., Rittmann, B.E. 2006. Bio-reduction of arsenate using a hydrogen-based membrane biofilm reactor. *Chemosphere*, **65**(1), 24-34.
- Chung, J., Rittmann, B.E., Wright, W.F., Bowman, R.H. 2007. Simultaneous bio-reduction of nitrate, perchlorate, selenate, chromate, arsenate, and dibromochloropropane using a hydrogen-based membrane biofilm reactor. *Biodegradation*, **18**(2), 199-209.
- Clancy, T., Reddy, R., Tan, J., Hayes, K., Raskin, L. 2014. Linking Microbial Activity with Arsenic Fate during Cow Dung Disposal of Arsenic-Bearing Wastes. *AGU Fall Meeting Abstracts*. pp. 0923.
- Clancy, T.M., Hayes, K.F., Raskin, L. 2013. Arsenic waste management: a critical review of testing and disposal of arsenic-bearing solid wastes generated during arsenic removal from drinking water. *Environmental science & technology*, **47**(19), 10799-10812.
- Clifford, D., Liu, X. 1993. Ion exchange for nitrate removal. *Journal (American Water Works Association)*, 135-143.
- Clifford, D.A., Lin, C.-C., Horng, L.-L., Boegel, J. 1987. *Nitrate removal from drinking water in Glendale, Arizona*. US Environmental Protection Agency, Water Engineering Research Laboratory.
- Coates, J.D., Ellis, D.J., Gaw, C.V., Lovley, D.R. 1999. Geothrix fermentans gen. nov., sp. nov., a novel Fe (III)-reducing bacterium from a hydrocarbon-contaminated aquifer. *International journal of systematic and evolutionary microbiology*, **49**(4), 1615-1622.
- Coates, J.D., Phillips, E., Lonergan, D.J., Jenter, H., Lovley, D.R. 1996. Isolation of Geobacter species from diverse sedimentary environments. *Applied and environmental microbiology*, **62**(5), 1531-1536.
- Costa, V., Boopathy, R., Manning, J. 1996. Isolation and characterization of a sulfate-reducing bacterium that removed TNT (2, 4, 6-trinitrotoluene) under sulfate-and nitrate-reducing conditions. *Bioresource Technology*, **56**(2), 273-278.
- CPCB. 2007. Status of groundwater quality in India. *Central Pollution Control Board, Ministry of Environment and Forests, Govt. of India*.(GROUNDWATER QUALITY SERIES:GWQS/09/2006-2007).
- Currell, M., Cartwright, I., Raveggi, M., Han, D. 2011. Controls on elevated fluoride and arsenic concentrations in groundwater from the Yuncheng Basin, China. *Applied Geochemistry*, **26**(4), 540-552.
- D'Acunto, B., Esposito, G., Frunzo, L., Pirozzi, F. 2011. Dynamic modeling of sulfate reducing biofilms. *Computers & Mathematics with Applications*, **62**(6), 2601-2608.
- Dalsgaard, T., Bak, F. 1994. Nitrate reduction in a sulfate-reducing bacterium, *Desulfovibrio desulfuricans*, isolated from rice paddy soil: sulfide inhibition, kinetics, and regulation. *Applied and environmental microbiology*, **60**(1), 291-297.
- Das, B., Talukdar, J., Sarma, S., Gohain, B., Dutta, R.K., Das, H.B., Das, S.C. 2003. Fluoride and other inorganic constituents in groundwater of Guwahati, Assam, India. *CURRENT SCIENCE-BANGALORE-*, **85**(5), 657-660.
- Daughney, C.J., Reeves, R.R. 2005. Definition of hydrochemical facies in the New Zealand national groundwater monitoring programme. *Journal of Hydrology (New Zealand)*, **44**(2), 105.
- Daus, B., von Tümpling, W., Wennrich, R., Weiss, H. 2007. Removal of hexafluoroarsenate from waters. *Chemosphere*, **68**(2), 253-258.

- Davis, J. 1997. Removing iron and manganese from natural waters. *Plant Engineering (Chicago)*, **51**(11).
- Dekov, V.M., Bindi, L., Burgaud, G., Petersen, S., Asael, D., Rédou, V., Fouquet, Y., Pracejus, B. 2013. Inorganic and biogenic As-sulfide precipitation at seafloor hydrothermal fields. *Marine Geology*, **342**(0), 28-38.
- Demergasso, C.S., Guillermo, C.D., Lorena, E.G., Mur, J.J.P., Pedrós-Alió, C. 2007. Microbial precipitation of arsenic sulfides in Andean salt flats. *Geomicrobiology Journal*, **24**(2), 111-123.
- Demlie, M., Hingston, E., Mnisi, Z. 2014. A study of the sources, human health implications and low cost treatment options of iron rich groundwater in the northeastern coastal areas of KwaZulu-Natal, South Africa. *Journal of Geochemical Exploration*, **144**, Part C(0), 504-510.
- Denaro, R., D'auria, G., Di Marco, G., Genovese, M., Troussellier, M., Yakimov, M., Giuliano, L. 2005. Assessing terminal restriction fragment length polymorphism suitability for the description of bacterial community structure and dynamics in hydrocarbon-polluted marine environments. *Environmental microbiology*, **7**(1), 78-87.
- Deng, S., Li, Z., Huang, J., Yu, G. 2010. Preparation, characterization and application of a Ce-Ti oxide adsorbent for enhanced removal of arsenate from water. *Journal of Hazardous Materials*, **179**(1), 1014-1021.
- Devi, R., Alemayehu, E., Singh, V., Kumar, A., Mengistie, E. 2008. Removal of fluoride, arsenic and coliform bacteria by modified homemade filter media from drinking water. *Bioresource Technology*, **99**(7), 2269-2274.
- Devi, S., Premkumar, R. 2012. Physicochemical analysis of groundwater samples near industrial area, Cuddalore District, Tamilnadu, India. *Int J Chem Tech Res*, **4**(1), 29-34.
- Devinsky, J.S., Deshusses, M.A., Webster, T.S. 1998. *Biofiltration for air pollution control*. CRC press, USA.
- Dilling, W., Cypionka, H. 1990. Aerobic respiration in sulfate-reducing bacteria. *FEMS Microbiology Letters*, **71**(1-2), 123-127.
- Dombrowski, P.M., Long, W., Farley, K.J., Mahony, J.D., Capitani, J.F., Di Toro, D.M. 2005. Thermodynamic analysis of arsenic methylation. *Environmental science & technology*, **39**(7), 2169-2176.
- Donald, R., Southam, G. 1999. Low temperature anaerobic bacterial diagenesis of ferrous monosulfide to pyrite. *Geochimica et Cosmochimica Acta*, **63**(13), 2019-2023.
- Dong, D., Ohtsuka, T., Dong, D.T., Amachi, S. 2014. Arsenite oxidation by a facultative chemolithoautotrophic *Sinorhizobium* sp. KGO-5 isolated from arsenic-contaminated soil. *Bioscience, biotechnology, and biochemistry*, **78**(11), 1963-1970.
- Donia, A.M., Atia, A.A., Mabrouk, D.H. 2011. Fast kinetic and efficient removal of As (V) from aqueous solution using anion exchange resins. *Journal of Hazardous Materials*, **191**(1), 1-7.
- DPHE. 2001. DPHE-DANIDA water supply and sanitation components. Hydrogeology Summary Report, 2001.
- Drewniak, L., Stasiuk, R., Uhrynowski, W., Sklodowska, A. 2015. *Shewanella* sp. O23S as a Driving Agent of a System Utilizing Dissimilatory Arsenate-Reducing Bacteria Responsible for Self-Cleaning of Water Contaminated with Arsenic. *International journal of molecular sciences*, **16**(7), 14409-14427.
- EA. 2002. Guidance on whether wastes containing metals or metal compounds are regulated under the Hazardous Waste Act, 2nd ed, Information Paper, no. 5, Department of Environment and Heritage, Australia,. *Environment Australia (EA)*, 1-22.

- EC. 1998. European Union Council Directive 98/83/EC on the quality of water intended for human consumption.
- Edmunds, W.M., Smedley, P.L. 2013. Fluoride in natural waters. in: *Essentials of medical geology*, Springer, pp. 311-336.
- Ehrlich, H.L., Newman, D.K. 2008. *Geomicrobiology (Fifth edition)*. CRC press, U.K.
- El-Naggar, M. 2009. Development Of Low-Cost Technology For The Removal Of Iron and Manganese From Ground Water In Siwa Oasis. *Journal of Egypt Public Hrtzlth Assor*, **85**(3), 169-188.
- Ellis, D., Bouchard, C., Lantagne, G. 2000. Removal of iron and manganese from groundwater by oxidation and microfiltration. *Desalination*, **130**(3), 255-264.
- Emerson, D., Fleming, E.J., McBeth, J.M. 2010. Iron-oxidizing bacteria: an environmental and genomic perspective. *Annual review of microbiology*, **64**, 561-583.
- Engineers, C. 2008. Drinking Water Biological treatment.
- EPA. 2009. National Primary Drinking Water Standards. <http://water.epa.gov/drink/contaminant/index.cfm#list>.
- Epsztein, R., Nir, O., Lahav, O., Green, M. 2015. Selective nitrate removal from groundwater using a hybrid nanofiltration–reverse osmosis filtration scheme. *Chemical Engineering Journal*, **279**, 372-378.
- Farooqi, A., Masuda, H., Firdous, N. 2007. Toxic fluoride and arsenic contaminated groundwater in the Lahore and Kasur districts, Punjab, Pakistan and possible contaminant sources. *Environmental Pollution*, **145**(3), 839-849.
- Feller, G., Gerday, C. 2003. Psychrophilic enzymes: hot topics in cold adaptation. *Nature Reviews Microbiology*, **1**(3), 200-208.
- Finke, N., Vandieken, V., Jørgensen, B.B. 2007. Acetate, lactate, propionate, and isobutyrate as electron donors for iron and sulfate reduction in Arctic marine sediments, Svalbard. *FEMS microbiology ecology*, **59**(1), 10-22.
- Frankel, R.B., Blakemore, R.P. 1991. Iron biominerals. *Conference on Iron Biominerals (1989: University of New Hampshire)*. Plenum press.
- Frankenberger Jr, W.T. 2001. *Environmental chemistry of arsenic*. CRC Press, New York, NY.
- Freel, K.C., Krueger, M.C., Farasin, J., Brochier-Armanet, C., Barbe, V., Andrès, J., Cholley, P.-E., Dillies, M.-A., Jagla, B., Koechler, S., Leva, Y., Magdelenat, G., Plewniak, F., Proux, C., Coppée, J.-Y., Bertin, P.N., Heipieper, H.J., Arsène-Ploetze, F. 2015. Adaptation in Toxic Environments: Arsenic Genomic Islands in the Bacterial Genus Thiomonas. *PLoS ONE*, **10**(9), e0139011.
- Frunzo, L., Esposito, G., Pirozzi, F., Lens, P. 2012. Dynamic mathematical modeling of sulfate reducing gas-lift reactors. *Process Biochemistry*, **47**(12), 2172-2181.
- Fukui, M., Suwa, Y., Urushigawa, Y. 1996. High survival efficiency and ribosomal RNA decaying pattern of *Desulfobacter latus*, a highly specific acetate-utilizing organism, during starvation. *FEMS Microbiology Ecology*, **19**(1), 17-25.
- Fytianos, K., Christophoridis, C. 2004. Nitrate, arsenic and chloride pollution of drinking water in Northern Greece. Elaboration by applying GIS. *Environmental Monitoring and Assessment*, **93**(1-3), 55-67.
- Gallegos, T.J., Han, Y.-S., Hayes, K.F. 2008. Model predictions of realgar precipitation by reaction of As (III) with synthetic mackinawite under anoxic conditions. *Environmental science & technology*, **42**(24), 9338-9343.
- Gallegos, T.J., Hyun, S.P., Hayes, K.F. 2007. Spectroscopic investigation of the uptake of arsenite from solution by synthetic mackinawite. *Environmental science & technology*, **41**(22), 7781-7786.

- Gates, J., Nicot, J., Scanlon, B., Reedy, R. 2011. Arsenic enrichment in unconfined sections of the southern Gulf Coast aquifer system, Texas. *Applied Geochemistry*, **26**(4), 421-431.
- Gayle, B., Boardman, G., Sherrard, J., Benoit, R. 1989. Biological denitrification of water. *Journal of Environmental Engineering*, **115**(5), 930-943.
- Geethamani, C., Ramesh, S., Gandhimathi, R., Nidheesh, P. 2014. Alkali-treated fly ash for the removal of fluoride from aqueous solutions. *Desalination and Water Treatment*, **52**(19-21), 3466-3476.
- Geucke, T., Deowan, S., Hoinkis, J., Pätzold, C. 2009. Performance of a small-scale RO desalinator for arsenic removal. *Desalination*, **239**(1), 198-206.
- Ghafari, S., Hasan, M., Aroua, M.K. 2008. Bio-electrochemical removal of nitrate from water and wastewater—a review. *Bioresource Technology*, **99**(10), 3965-3974.
- Ghosh, A. 2013. Studies on Microbial Reduction of Perchlorate in Batch and Continuous System. *Ph.D Thesis, Indian Institute of Technology, Guwahati, India.*
- Ghosh, A., Mukiibi, M., Ela, W. 2004. TCLP underestimates leaching of arsenic from solid residuals under landfill conditions. *Environmental science & technology*, **38**(17), 4677-4682.
- Ghosh, D., Sarkar, S., Sengupta, A.K., Gupta, A. 2014. Investigation on the long-term storage and fate of arsenic obtained as a treatment residual: A case study. *Journal of Hazardous Materials*, **271**, 302-310.
- Ghurye, G., Clifford, D. 2004. As (III) oxidation using chemical and solid-phase oxidants. *Journal (American Water Works Association)*, 84-96.
- Ghurye, G., Clifford, D., Tripp, A. 2004. Iron coagulation and direct microfiltration to remove arsenic from groundwater. *Journal (American Water Works Association)*, 143-152.
- Gihring, T.M., Banfield, J.F. 2001. Arsenite oxidation and arsenate respiration by a new *Thermus* isolate. *FEMS Microbiology Letters*, **204**(2), 335-340.
- Gihring, T.M., Druschel, G.K., McCleskey, R.B., Hamers, R.J., Banfield, J.F. 2001. Rapid arsenite oxidation by *Thermus aquaticus* and *Thermus thermophilus*: field and laboratory investigations. *Environmental science & technology*, **35**(19), 3857-3862.
- Giloteaux, L., Holmes, D.E., Williams, K.H., Wrighton, K.C., Wilkins, M.J., Montgomery, A.P., Smith, J.A., Orellana, R., Thompson, C.A., Roper, T.J. 2013. Characterization and transcription of arsenic respiration and resistance genes during in situ uranium bioremediation. *The ISME journal*, **7**(2), 370-383.
- Giménez, M.C., Blanes, P.S., Buchhamer, E.E., Osicka, R.M., Morisio, Y., Farías, S.S. 2013. Assessment of heavy metals concentration in arsenic contaminated groundwater of the Chaco Plain, Argentina. *ISRN Environmental Chemistry*, **2013**.
- Glass, C., Silverstein, J. 1998. Denitrification kinetics of high nitrate concentration water: pH effect on inhibition and nitrite accumulation. *Water Research*, **32**(3), 831-839.
- Glass, C., Silverstein, J. 1999. Denitrification of high-nitrate, high-salinity wastewater. *Water Research*, **33**(1), 223-229.
- Godelitsas, A., Price, R., Pichler, T., Amend, J., Gamaletsos, P., Göttlicher, J. 2015. Amorphous As-sulfide precipitates from the shallow-water hydrothermal vents off Milos Island (Greece). *Marine Chemistry*, **177**, 687-696.
- Gramp, J.P., Bigham, J.M., Jones, F.S., Tuovinen, O.H. 2010. Formation of Fe-sulfides in cultures of sulfate-reducing bacteria. *Journal of Hazardous Materials*, **175**(1-3), 1062-1067.
- Greben, H., Maree, J., Eloff, E., Murray, K. 2007. Improved sulphate removal rates at increased sulphide concentration in the sulphidogenic bioreactor. *Water SA*, **31**(3), 351-358.
- Greenwood, N.N., Earnshaw, A. 1984. Chemistry of the Elements, 2nd Edition, U.K.

- Gruyer, N., Dorais, M., Alsanjus, B.W., Zagury, G.J. 2013. Simultaneous Removal of Nitrate and Sulfate from Greenhouse Wastewater by Constructed Wetlands. *Journal of environmental quality*, **42**(4), 1256-1266.
- Guha, S., Raymahashay, B., Banerjee, A., Acharyya, S., Gupta, A. 2005. Collection of depth-specific groundwater samples from an arsenic contaminated aquifer in West Bengal, India. *Environmental engineering science*, **22**(6), 870-881.
- Guo, H., Zhang, Y., Xing, L., Jia, Y. 2012. Spatial variation in arsenic and fluoride concentrations of shallow groundwater from the town of Shagai in the Hetao basin, Inner Mongolia. *Applied Geochemistry*, **27**(11), 2187-2196.
- Gupta, B.S., Chatterjee, S., Rott, U., Kauffman, H., Bandopadhyay, A., DeGroot, W., Nag, N., Carbonell-Barrachina, A., Mukherjee, S. 2009. A simple chemical free arsenic removal method for community water supply—A case study from West Bengal, India. *Environmental Pollution*, **157**(12), 3351-3353.
- Guter, G.A. 1982. *Removal of nitrate from contaminated water supplies for public use: Final report*. US Environmental Protection Agency, Municipal Environmental Research Laboratory.
- Gutierrez, O., Park, D., Sharma, K.R., Yuan, Z. 2009. Effects of long-term pH elevation on the sulfate-reducing and methanogenic activities of anaerobic sewer biofilms. *Water Research*, **43**(9), 2549-2557.
- Hanafiah, M., Zakaria, H., Ngah, W.W. 2009. Preparation, characterization, and adsorption behavior of Cu (II) ions onto alkali-treated weed (*Imperata cylindrica*) leaf powder. *Water, air, and soil pollution*, **201**(1-4), 43-53.
- Hao, O. 2000. Metal effects on sulfur cycle bacteria and metal removal by sulfate reducing bacteria. *Environmental technologies to treat sulfur pollution. Principles and engineering/PN L. Lens, PL Hulshoff eds. London: IWA publishing*, 393-414.
- Hao, O.J., Chen, J.M., Huang, L., Buglass, R.L. 1996. Sulfate-reducing bacteria. *Critical Reviews in Environmental Science and Technology*, **26**(2), 155-187.
- Hassan, A., Abdel-Mohsen, A., Elhadidy, H. 2014. Adsorption of arsenic by activated carbon, calcium alginate and their composite beads. *International journal of biological macromolecules*, **68**, 125-130.
- Hatva, T. 1989. *Iron and manganese in groundwater in Finland: Occurrence in glacial fluvial aquifers and removal by biofiltration*. National Board of Waters and the Environment. Vesi-ja ympäristöhallitus.
- Hayes, K.F., Adriaens, P., Demond, A.H., Olson, T., Abriola, L.M. 2009. Reduced Iron Sulfide Systems for Removal of Heavy Metal Ions from Groundwater. Michigan Univ. Ann Arbor Dept. Of Civil and Environmental Engineering.
- Hayes, K.F., Bi, Y., Carpenter, J., Hyng, S.P., Rittmann, B.E., Zhou, C., Vannela, R., Davis, J.A. 2014. Assessing the Role of Iron Sulfides in the Long Term Sequestration of Uranium by Sulfate-Reducing Bacteria. University of Michigan, Ann Arbor, MI.
- Hem, J.D. 1985. *Study and interpretation of the chemical characteristics of natural water*. Department of the Interior, US Geological Survey.
- Henke, K. 2009. *Arsenic: environmental chemistry, health threats and waste treatment*, Ltd, Chichester, UK. doi: 10.1002/9780470741122.ch2. John Wiley & Sons.
- Hering, J.G., Chen, P.-Y., Wilkie, J.A., Elimelech, M. 1997. Arsenic removal from drinking water during coagulation. *Journal of Environmental Engineering*, **123**(8), 800-807.
- Hijnen, W., Jong, R., Van der Kooij, D. 1999. Bromate removal in a denitrifying bioreactor used in water treatment. *Water Research*, **33**(4), 1049-1053.

- Ho, L.N., Ishihara, T., Ueshima, S., Nishiguchi, H., Takita, Y. 2004. Removal of fluoride from water through ion exchange by mesoporous Ti oxhydroxide. *Journal of colloid and interface science*, **272**(2), 399-403.
- Hocaoglu, S.M., Insel, G., Cokgor, E.U., Orhon, D. 2011. Effect of low dissolved oxygen on simultaneous nitrification and denitrification in a membrane bioreactor treating black water. *Bioresource Technology*, **102**(6), 4333-4340.
- Hoefl, S.E., Kulp, T.R., Stolz, J.F., Hollibaugh, J.T., Oremland, R.S. 2004. Dissimilatory arsenate reduction with sulfide as electron donor: experiments with mono lake water and isolation of strain MLMS-1, a chemoautotrophic arsenate respirer. *Applied and environmental microbiology*, **70**(5), 2741-2747.
- Höll, W.H. 2010. Mechanisms of arsenic removal from water. *Environmental geochemistry and health*, **32**(4), 287-290.
- Hollocher, T.C., Kristjánsson, J.K. 1992. Thermophilic denitrifying bacteria: a survey of hot springs in Southwestern Iceland. *FEMS Microbiology Letters*, **101**(2), 113-119.
- Holloway, J., Dahlgren, R., Hansen, B., Casey, W. 1998. Contribution of bedrock nitrogen to high nitrate concentrations in stream water. *Nature*, **395**(6704), 785-788.
- Hooper, K., Iskander, M., Sivia, G., Hussein, F., Hsu, J., DeGuzman, M., Odion, Z., Ileyay, Z., Sy, F., Petreas, M. 1998. Toxicity characteristic leaching procedure fails to extract oxoanion-forming elements that are extracted by municipal solid waste leachates. *Environmental science & technology*, **32**(23), 3825-3830.
- Horing, H., Chapman, D. 2004. Nitrates and nitrites in drinking water: World Health Organization Drinking Water Series, IWA Publishing, London.
- Hristovski, K., Westerhoff, P., Möller, T., Sylvester, P., Condit, W., Mash, H. 2008. Simultaneous removal of perchlorate and arsenate by ion-exchange media modified with nanostructured iron (hydr) oxide. *Journal of Hazardous Materials*, **152**(1), 397-406.
- Hu, C., Liu, H., Chen, G., Qu, J. 2012. Effect of aluminum speciation on arsenic removal during coagulation process. *Separation and Purification Technology*, **86**, 35-40.
- Hu, K., Dickson, J.M. 2006. Nanofiltration membrane performance on fluoride removal from water. *Journal of membrane science*, **279**(1), 529-538.
- Hug, S.J., Canonica, L., Wegelin, M., Gechter, D., von Gunten, U. 2001. Solar oxidation and removal of arsenic at circumneutral pH in iron containing waters. *Environmental science & technology*, **35**(10), 2114-2121.
- IARC. 2004. IARC Monographs on the Evaluation of Carcinogenic Risks to Humans. *International Agency for Cancer Research (IARC)* **84**.
- Ibrahim, M., A.R.M., Sumalatha, M., Prabhakar, P. 2011. EFFECTS OF FLUORIDE CONTENTS IN GROUND WATER: A REVIEW. *International Journal of Pharmaceutical Applications*, **2**(2), 128-134.
- Ingallinella, A.M., Pacini, V.A., Fernández, R.G., Vidoni, R.M., Sanguinetti, G. 2011. Simultaneous removal of arsenic and fluoride from groundwater by coagulation-adsorption with polyaluminum chloride. *Journal of Environmental Science and Health, Part A*, **46**(11), 1288-1296.
- Ippolito, J., Barbarick, K., Elliott, H. 2011. Drinking water treatment residuals: A review of recent uses. *Journal of environmental quality*, **40**(1), 1-12.
- Irtle, C.H. 2001. Properties of waste resulting from arsenic removal processes in drinking water treatment, Virginia Polytechnic Institute and State University.
- Ito, A., Miura, J.-i., Ishikawa, N., Umita, T. 2012. Biological oxidation of arsenite in synthetic groundwater using immobilised bacteria. *Water Research*, **46**(15), 4825-4831.
- Jagtap, S., Yenkie, M.K., Labhsetwar, N., Rayalu, S. 2012. Fluoride in drinking water and defluoridation of water. *Chemical reviews*, **112**(4), 2454-2466.

- Jain, C., Ali, I. 2000. Arsenic: occurrence, toxicity and speciation techniques. *Water Research*, **34**(17), 4304-4312.
- Jain, C., Singh, R. 2012. Technological options for the removal of arsenic with special reference to South East Asia. *Journal of Environmental Management*, **107**, 1-18.
- Jensen, V., Darby, J., Seidel, C., Gorman, C. 2012. Drinking water treatment for nitrate. *Book Drinking Water Treatment for Nitrate vol. Technical Report*, **6**.
- Jha, D., Bose, P. 2005. Use of pyrite for pH control during hydrogenotrophic denitrification using metallic iron as the ultimate electron donor. *Chemosphere*, **61**(7), 1020-1031.
- Jing, C., Cui, J., Huang, Y., Li, A. 2012. Fabrication, characterization, and application of a composite adsorbent for simultaneous removal of arsenic and fluoride. *ACS applied materials & interfaces*, **4**(2), 714-720.
- Jing, C., Liu, S., Patel, M., Meng, X. 2005. Arsenic leachability in water treatment adsorbents. *Environmental science & technology*, **39**(14), 5481-5487.
- Jong, T., Parry, D.L. 2005. Evaluation of the stability of arsenic immobilized by microbial sulfate reduction using TCLP extractions and long-term leaching techniques. *Chemosphere*, **60**(2), 254-265.
- Jong, T., Parry, D.L. 2003. Removal of sulfate and heavy metals by sulfate reducing bacteria in short-term bench scale upflow anaerobic packed bed reactor runs. *Water Research*, **37**(14), 3379-3389.
- Jordana, S., Piera, E.B. 2004. Natural groundwater quality and health. *Geologica Acta*, **2**(2), 175.
- Jusoh, H., Sapari, N., Azie, R.R. 2011. Removal of Iron from Groundwater by Sulfide Precipitation. *Assessment*, **232**, 1457.
- Kakar, Y.P. 1981. Nitrate Pollution of Ground Water in Southern and South-Western Haryana, India. in: *Studies in Environmental Science*, (Eds.) P.G. W. van Duijvenbooden, H.v. Lelyveld, Vol. Volume 17, Elsevier, pp. 125-129.
- Kalyuzhnyi, S., Fedorovich, V. 1998. Mathematical modelling of competition between sulphate reduction and methanogenesis in anaerobic reactors. *Bioresource Technology*, **65**(3), 227-242.
- Kampschreur, M.J., Tan, N.C., Kleerebezem, R., Picioreanu, C., Jetten, M.S., Loosdrecht, M.C.v. 2007. Effect of dynamic process conditions on nitrogen oxides emission from a nitrifying culture. *Environmental science & technology*, **42**(2), 429-435.
- Kapoor, A., Viraraghavan, T. 1997. Nitrate Removal From Drinking Water—Review. *Journal of Environmental Engineering*, **123**(4), 371-380.
- Karanasios, K., Vasiliadou, I., Pavlou, S., Vayenas, D. 2010. Hydrogenotrophic denitrification of potable water: a review. *Journal of Hazardous Materials*, **180**(1), 20-37.
- Katsoyiannis, I.A., Voegelin, A., Zouboulis, A.I., Hug, S.J. 2015. Enhanced As(III) oxidation and removal by combined use of zero valent iron and hydrogen peroxide in aerated waters at neutral pH values. *Journal of Hazardous Materials*, **297**, 1-7.
- Katsoyiannis, I.A., Zikoudi, A., Hug, S.J. 2008. Arsenic removal from groundwaters containing iron, ammonium, manganese and phosphate: A case study from a treatment unit in northern Greece. *Desalination*, **224**(1), 330-339.
- Katsoyiannis, I.A., Zouboulis, A.I. 2004. Application of biological processes for the removal of arsenic from groundwaters. *Water Research*, **38**(1), 17-26.
- Katsoyiannis, I.A., Zouboulis, A.I. 2006. Use of Iron- and Manganese-Oxidizing Bacteria for the Combined Removal of Iron, Manganese and Arsenic from Contaminated Groundwater. *Water quality research journal of Canada*, **41**(2), 117-129.
- Katsoyiannis, I.A., Zouboulis, A.I., Jekel, M. 2004. Kinetics of bacterial As (III) oxidation and subsequent As (V) removal by sorption onto biogenic manganese oxides during groundwater treatment. *Industrial & engineering chemistry research*, **43**(2), 486-493.

- Kaur, S., Kamli, M.R., Ali, A. 2009. Diversity of arsenate reductase genes (arsC genes) from arsenic-resistant environmental isolates of *E. coli*. *Current microbiology*, **59**(3), 288-294.
- Kawaichi, S., Ito, N., Kamikawa, R., Sugawara, T., Yoshida, T., Sako, Y. 2013. *Ardenticatena maritima* gen. nov., sp. nov., a ferric iron-and nitrate-reducing bacterium of the phylum 'Chloroflexi' isolated from an iron-rich coastal hydrothermal field, and description of *Ardenticatena classis* nov. *International journal of systematic and evolutionary microbiology*, **63**(Pt 8), 2992-3002.
- Kay, P. 2011. Arsenic pollution: a global synthesis—By Peter Ravenscroft, Hugh Brammer and Keith Richards. *Area*, **43**(1), 118-119.
- Keimowitz, A., Mailloux, B., Cole, P., Stute, M., Simpson, H., Chillrud, S. 2007. Laboratory investigations of enhanced sulfate reduction as a groundwater arsenic remediation strategy. *Environmental science & technology*, **41**(19), 6718-6724.
- Kemper, J.M., Westerhoff, P., Dotson, A., Mitch, W.A. 2008. Nitrosamine, dimethylnitramine, and chloropicrin formation during strong base anion-exchange treatment. *Environmental science & technology*, **43**(2), 466-472.
- Kesserú, P., Kiss, I., Bihari, Z., Polyak, B. 2002. Investigation of the denitrification activity of immobilized *Pseudomonas butanovora* cells in the presence of different organic substrates. *Water Research*, **36**(6), 1565-1571.
- Khardenavis, A.A., Kapley, A., Purohit, H.J. 2007. Simultaneous nitrification and denitrification by diverse *Diaphorobacter* sp. *Applied Microbiology and Biotechnology*, **77**(2), 403-409.
- Khatiwada, N., Takizawa, S., Tran, T., Inoue, M. 2002. Groundwater contamination assessment for sustainable water supply in Kathmandu Valley, Nepal. *Water Science & Technology*, **46**(9), 147-154.
- Khurshid, S. 2013. Geochemistry of Groundwater: An Overview of Sporadic Fluoride and Nitrate Contamination in Parts of Yamuna River Basin, India *Int. j. econ. environ. geol.*, **4**(1), 36-40.
- Kim, J., Benjamin, M.M. 2004. Modeling a novel ion exchange process for arsenic and nitrate removal. *Water Research*, **38**(8), 2053-2062.
- Kim, J., Benjamin, M.M., Kwan, P., Chang, Y. 2003. A novel ion exchange process for As removal. *Journal (American Water Works Association)*, 77-85.
- Kim, S.-H., Harzman, C., Davis, J.K., Hutcheson, R., Broderick, J.B., Marsh, T.L., Tiedje, J.M. 2012a. Genome sequence of *Desulfitobacterium hafniense* DCB-2, a Gram-positive anaerobe capable of dehalogenation and metal reduction. *BMC microbiology*, **12**(1), 21.
- Kim, S.-H., Kim, K., Ko, K.-S., Kim, Y., Lee, K.-S. 2012b. Co-contamination of arsenic and fluoride in the groundwater of unconsolidated aquifers under reducing environments. *Chemosphere*, **87**(8), 851-856.
- Kimura, S., Hallberg, K.B., Johnson, D.B. 2006. Sulfidogenesis in low pH (3.8–4.2) media by a mixed population of acidophilic bacteria. *Biodegradation*, **17**(2), 57-65.
- Kirk, M.F., Holm, T.R., Park, J., Jin, Q., Sanford, R.A., Fouke, B.W., Bethke, C.M. 2004. Bacterial sulfate reduction limits natural arsenic contamination in groundwater. *Geology*, **32**(11), 953-956.
- Kirk, M.F., Roden, E.E., Crossey, L.J., Brealey, A.J., Spilde, M.N. 2010. Experimental analysis of arsenic precipitation during microbial sulfate and iron reduction in model aquifer sediment reactors. *Geochimica et Cosmochimica Acta*, **74**(9), 2538-2555.
- Knocke, W.R., Association, A.W.W. 1990. *Alternative oxidants for the removal of soluble iron and manganese*. AWWA Research Foundation and American Water Works Association.
- Kosolapov, D., Kuschik, P., Vainshtein, M., Vatsourina, A., Wiessner, A., Kästner, M., Müller, R. 2004. Microbial Processes of Heavy Metal Removal from Carbon-Deficient Effluents in Constructed Wetlands. *Engineering in Life Sciences*, **4**(5), 403-411.

- Krafft, T., Macy, J.M. 1998. Purification and characterization of the respiratory arsenate reductase of *Chrysiogenes arsenatis*. *European Journal of Biochemistry*, **255**(3), 647-653.
- Kretzmann, H. 2014. http://www.biologicaldiversity.org/news/press_releases/2014/fracking-10-06-2014.html as on 17/7/2015).
- Kumar, S., Gupta, A., Yadav, J. 2008. Removal of fluoride by thermally activated carbon prepared from neem (*Azadirachta indica*) and kikar (*Acacia arabica*) leaves. *Journal of Environmental Biology*, **29**(2), 227.
- Kumar, V., Talreja, N., Deva, D., Sankararamakrishnan, N., Sharma, A., Verma, N. 2011. Development of bi-metal doped micro-and nano multi-functional polymeric adsorbents for the removal of fluoride and arsenic (V) from wastewater. *Desalination*, **282**, 27-38.
- Kundu, M.C., Mandal, B., Hazra, G.C. 2009. Nitrate and fluoride contamination in groundwater of an intensively managed agroecosystem: A functional relationship. *Science of The Total Environment*, **407**(8), 2771-2782.
- Kuzelka, R.D., Ennenga, W. 2013. *Nitrate contamination: exposure, consequence, and control*. Springer Science & Business Media.
- Lacasa, E., Canizares, P., Sáez, C., Fernández, F.J., Rodrigo, M.A. 2011. Removal of arsenic by iron and aluminium electrochemically assisted coagulation. *Separation and Purification Technology*, **79**(1), 15-19.
- Lakshmanan, D., Clifford, D.A., Samanta, G. 2010. Comparative study of arsenic removal by iron using electrocoagulation and chemical coagulation. *Water Research*, **44**(19), 5641-5652.
- Law, Y., Ye, L., Pan, Y., Yuan, Z. 2012. Nitrous oxide emissions from wastewater treatment processes. *Philosophical Transactions of the Royal Society B: Biological Sciences*, **367**(1593), 1265-1277.
- Lee, J.-H., Kim, M.-G., Yoo, B., Myung, N.V., Maeng, J., Lee, T., Dohnalkova, A.C., Fredrickson, J.K., Sadowsky, M.J., Hur, H.-G. 2007. Biogenic formation of photoactive arsenic-sulfide nanotubes by *Shewanella* sp. strain HN-41. *Proceedings of the National Academy of Sciences*, **104**(51), 20410-20415.
- Lee, K.-C., Rittmann, B.E. 2003. Effects of pH and precipitation on autohydrogenotrophic denitrification using the hollow-fiber membrane-biofilm reactor. *Water Research*, **37**(7), 1551-1556.
- Leist, M., Casey, R., Caridi, D. 2003. The fixation and leaching of cement stabilized arsenic. *Waste Management*, **23**(4), 353-359.
- Lengke, M.F., Sanpawanitchakit, C., Tempel, R.N. 2009. The oxidation and dissolution of arsenic-bearing sulfides. *The Canadian Mineralogist*, **47**(3), 593-613.
- Lengke, M.F., Tempel, R.N. 2005. Geochemical modeling of arsenic sulfide oxidation kinetics in a mining environment. *Geochimica et Cosmochimica Acta*, **69**(2), 341-356.
- Lengke, M.F., Tempel, R.N. 2001. Kinetic rates of amorphous As₂S₃ oxidation at 25 to 40°C and initial pH of 7.3 to 9.4. *Geochimica et Cosmochimica Acta*, **65**(14), 2241-2255.
- Lengke, M.F., Tempel, R.N. 2003. Natural realgar and amorphous AsS oxidation kinetics. *Geochimica et Cosmochimica Acta*, **67**(5), 859-871.
- Lenntech. 2015. Sources of Ground water pollution *Lenntech : water treatment and air purification*. Available at <http://www.lenntech.com/groundwater/pollution-sources.htm>.
- Lens, P., Vallerol, M., Esposito, G., Zandvoort, M. 2002. Perspectives of sulfate reducing bioreactors in environmental biotechnology. *Reviews in Environmental Science and Biotechnology*, **1**(4), 311-325.
- Leupin, O.X., Hug, S.J. 2005. Oxidation and removal of arsenic (III) from aerated groundwater by filtration through sand and zero-valent iron. *Water Research*, **39**(9), 1729-1740.
- Li, X., Zhang, L., Wang, G. 2014. Genomic evidence reveals the extreme diversity and wide distribution of the arsenic-related genes in Burkholderiales. *PLoS ONE*, **9**(3), e92236.

- Liamleam, W., Annachhatre, A.P. 2007. Electron donors for biological sulfate reduction. *Biotechnology Advances*, **25**(5), 452-463.
- Lièvremon, D., Bertin, P.N., Lett, M.-C. 2009. Arsenic in contaminated waters: Biogeochemical cycle, microbial metabolism and biotreatment processes. *Biochimie*, **91**(10), 1229-1237.
- Lim, M.-S., Yeo, I., Roh, Y., Lee, K.-K., Jung, M. 2008. Arsenic reduction and precipitation by shewanella sp.: Batch and column tests. *Geosciences Journal*, **12**(2), 151-157.
- Liu, A., Garcia-Dominguez, E., Rhine, E., Young, L. 2004. A novel arsenate respiring isolate that can utilize aromatic substrates. *FEMS microbiology ecology*, **48**(3), 323-332.
- Liu, R., Gong, W., Lan, H., Yang, T., Liu, H., Qu, J. 2012. Simultaneous removal of arsenate and fluoride by iron and aluminum binary oxide: Competitive adsorption effects. *Separation and Purification Technology*, **92**(0), 100-105.
- Liu, X., Gao, C., Zhang, A., Jin, P., Wang, L., Feng, L. 2008. The nos gene cluster from gram-positive bacterium *Geobacillus thermodenitrificans* NG80-2 and functional characterization of the recombinant NosZ. *FEMS Microbiology Letters*, **289**(1), 46-52.
- Loganathan, P., Vigneswaran, S., Kandasamy, J. 2013a. Enhanced removal of nitrate from water using surface modification of adsorbents—A review. *Journal of Environmental Management*, **131**, 363-374.
- Loganathan, P., Vigneswaran, S., Kandasamy, J., Naidu, R. 2013b. Defluoridation of drinking water using adsorption processes. *Journal of Hazardous Materials*, **248–249**(0), 1-19.
- Lovley, D.R., Baedeker, M.J., Lonergan, D.J., Cozzarelli, I.M., Phillips, E.J., Siegel, D.I. 1989. Oxidation of aromatic contaminants coupled to microbial iron reduction. *Nature*, **339**(6222), 297-300.
- Lovley, D.R., Chapelle, F.H. 1995. Deep subsurface microbial processes. *Reviews of Geophysics*, **33**(3), 365-381.
- Lovley, D.R., Holmes, D.E., Nevin, K.P. 2004. Dissimilatory Fe (iii) and Mn (iv) reduction. *Advances in microbial physiology*, **49**, 219-286.
- Lovley, D.R., Phillips, E.J., Gorby, Y.A., Landa, E.R. 1991. Microbial reduction of uranium. *Nature*, **350**(6317), 413-416.
- Luef, B., Fakra, S.C., Csencsits, R., Wrighton, K.C., Williams, K.H., Wilkins, M.J., Downing, K.H., Long, P.E., Comolli, L.R., Banfield, J.F. 2013. Iron-reducing bacteria accumulate ferric oxyhydroxide nanoparticle aggregates that may support planktonic growth. *ISME J*, **7**(2), 338-350.
- Luján, C. 1999. Desarsenicación del agua utilizando hidrogel activado de hidróxido de aluminio. *Rev. med. Tucumán*, **5**(4), 181-90.
- Luo, Q., Tsukamoto, T., Zamzow, K., Miller, G. 2008. Arsenic, selenium, and sulfate removal using an ethanol-enhanced sulfate-reducing bioreactor. *Mine Water and the Environment*, **27**(2), 100-108.
- Macedonio, F., Drioli, E. 2008. Pressure-driven membrane operations and membrane distillation technology integration for water purification. *Desalination*, **223**(1), 396-409.
- Macur, R.E., Wheeler, J.T., McDermott, T.R., Inskeep, W.P. 2001. Microbial populations associated with the reduction and enhanced mobilization of arsenic in mine tailings. *Environmental science & technology*, **35**(18), 3676-3682.
- Macy, J.M., Nunan, K., Hagen, K.D., Dixon, D.R., Harbour, P.J., Cahill, M., Sly, L.I. 1996. *Chrysiogenes arsenatis* gen. nov., sp. nov., a new arsenate-respiring bacterium isolated from gold mine wastewater. *International journal of systematic bacteriology*, **46**(4), 1153-1157.
- Macy, J.M., Santini, J.M., Pauling, B.V., O'Neill, A.H., Sly, L.I. 2000. Two new arsenate/sulfate-reducing bacteria: mechanisms of arsenate reduction. *Archives of Microbiology*, **173**(1), 49-57.

- Madigan, M.T., Martinko, J.M., Parker, J., Brock, T.D. 1997. *Biology of microorganisms*. prentice hall Upper Saddle River, NJ.
- Mähler, J., Persson, I. 2013. Rapid adsorption of arsenic from aqueous solution by ferrihydrite-coated sand and granular ferric hydroxide. *Applied Geochemistry*, **37**, 179-189.
- Maiti, A., Thakur, B.K., Basu, J.K., De, S. 2013. Comparison of treated laterite as arsenic adsorbent from different locations and performance of best filter under field conditions. *Journal of Hazardous Materials*, **262**, 1176-1186.
- Majumdar, D., Gupta, N. 2000. *Nitrate pollution of groundwater and associated human health disorders*. National Environmental Engineering Research Institute, Nagpur, India.
- Mallick, S., Banerji, S. 1981. Nitrate Pollution of Ground Water as Result of Agricultural Development in Indo-Ganga Plain, India. in: *Studies in Environmental Science*, (Eds.) P.G. W. van Duijvenbooden, H.v. Lelyveld, Vol. Volume 17, Elsevier, pp. 155-162.
- Manna, A.K., Sen, M., Martin, A.R., Pal, P. 2010. Removal of arsenic from contaminated groundwater by solar-driven membrane distillation. *Environmental Pollution*, **158**(3), 805-811.
- Margane, A., Tatong, T. 1999. Aspects of the hydrogeology of the Chiang Mai-Lamphun basin, Thailand, that are important for groundwater management. *ZEITSCHRIFT FUR ANGEWANDTE GEOLOGIE*, **45**(4), 188-197.
- Marietou, A., Griffiths, L., Cole, J. 2009. Preferential reduction of the thermodynamically less favorable electron acceptor, sulfate, by a nitrate-reducing strain of the sulfate-reducing bacterium *Desulfovibrio desulfuricans* 27774. *Journal of bacteriology*, **191**(3), 882-889.
- Marshall, R. 2016. Whole Effluent Toxicity Testing Guidance and Test Review Criteria. *Water quality program, Washington state, Department of Ecology, Olympia, Washington*. (WQ-R-95-80).
- Massol-Deya, A.A., Whallon, J., Hickey, R.F., Tiedje, J.M. 1995. Channel structures in aerobic biofilms of fixed-film reactors treating contaminated groundwater. *Applied and environmental microbiology*, **61**(2), 769-777.
- Mateju, V., Cizinska, S., Krejci, J., Janoch, T. 1992. Biological water denitrification—a review. *Enzyme and Microbial Technology*, **14**(3), 170-183.
- Matos, C.T., Velizarov, S., Crespo, J.G., Reis, M.A. 2006. Simultaneous removal of perchlorate and nitrate from drinking water using the ion exchange membrane bioreactor concept. *Water Research*, **40**(2), 231-240.
- Mayorga, P., Moyano, A., Anawar, H.M., García-Sánchez, A. 2013. Temporal variation of arsenic and nitrate content in groundwater of the Duero River Basin (Spain). *Physics and Chemistry of the Earth, Parts A/B/C*, **58-60**(0), 22-27.
- Mazumder, D.N.G., Ghosh, A., Majumdar, K.K., Ghosh, N., Saha, C., Mazumder, R.N.G. 2010. Arsenic contamination of ground water and its health impact on population of district of Nadia, West Bengal, India. *Indian journal of community medicine: official publication of Indian Association of Preventive & Social Medicine*, **35**(2), 331.
- McMahon, P., Chapelle, F. 2008. Redox processes and water quality of selected principal aquifer systems. *Groundwater*, **46**(2), 259-271.
- Meenakshi, Maheshwari, R.C. 2006. Fluoride in drinking water and its removal. *Journal of Hazardous Materials*, **137**(1), 456-463.
- Meenakshi, S., Viswanathan, N. 2007. Identification of selective ion-exchange resin for fluoride sorption. *Journal of colloid and interface science*, **308**(2), 438-450.
- Mekonen, A., Kumar, P., Kumar, A. 2001. Integrated biological and physiochemical treatment process for nitrate and fluoride removal. *Water Research*, **35**(13), 3127-3136.

- Meng, X., Korfiatis, G.P., Jing, C., Christodoulatos, C. 2001. Redox transformations of arsenic and iron in water treatment sludge during aging and TCLP extraction. *Environmental science & technology*, **35**(17), 3476-3481.
- Mizuno, O., Li, Y., Noike, T. 1994. Effects of sulfate concentration and sludge retention time on the interaction between methane production and sulfate reduction for butyrate. *Water science and technology*, **30**(8), 45-54.
- Mogensen, G.L., Kjeldsen, K.U., Ingvorsen, K. 2005. *Desulfovibrio aerotolerans* sp. nov., an oxygen tolerant sulphate-reducing bacterium isolated from activated sludge. *Anaerobe*, **11**(6), 339-349.
- Mohan, D., Pittman Jr, C.U. 2007. Arsenic removal from water/wastewater using adsorbents—A critical review. *Journal of Hazardous Materials*, **142**(1–2), 1-53.
- Mohapatra, D., Mishra, D., Chaudhury, G.R., Das, R.P. 2008. Removal of arsenic from arsenic rich sludge by volatilization using anaerobic microorganisms treated with cow dung. *Soil & Sediment Contamination*, **17**(3), 301-311.
- Mohapatra, M., Anand, S., Mishra, B., Giles, D.E., Singh, P. 2009. Review of fluoride removal from drinking water. *Journal of Environmental Management*, **91**(1), 67-77.
- Mohseni-Bandpi, A., Elliott, D. 1998. Groundwater denitrification with alternative carbon sources. *Water science and technology*, **38**(6), 237-243.
- Mohseni-Bandpi, A., Elliott, D.J., Zazouli, M.A. 2013. Biological nitrate removal processes from drinking water supply—a review. *Journal of Environmental Health Science and Engineering*, **11**, 35-35.
- Mokashi, S., Paknikar, K. 2002. Arsenic (III) oxidizing Microbacterium lacticum and its use in the treatment of arsenic contaminated groundwater. *Letters in applied microbiology*, **34**(4), 258-262.
- Mondal, P., Bhowmick, S., Chatterjee, D., Figoli, A., Van der Bruggen, B. 2013. Remediation of inorganic arsenic in groundwater for safe water supply: A critical assessment of technological solutions. *Chemosphere*, **92**(2), 157-170.
- Mondal, P., Majumder, C.B., Mohanty, B. 2008. Treatment of arsenic contaminated water in a batch reactor by using *Ralstonia eutropha* MTCC 2487 and granular activated carbon. *Journal of Hazardous Materials*, **153**(1–2), 588-599.
- Moore, J.N., Ficklin, W.H., Johns, C. 1988. Partitioning of arsenic and metals in reducing sulfidic sediments. *Environmental science & technology*, **22**(4), 432-437.
- Motzer, W. 2006. Nitrate forensics. *Hydro. Visions*, **15**(3), 116-17.
- Mouchet, P. 1992. From Conventional to Biological Removal of Iron and Manganese in France (PDF). *Journal-American Water Works Association*, **84**(4), 158-167.
- Mukhopadhyay, R., Rosen, B.P. 2002. Arsenate reductases in prokaryotes and eukaryotes. *Environmental health perspectives*, **110**(Suppl 5), 745.
- Muller, D., Médigue, C., Koechler, S., Barbe, V., Barakat, M., Talla, E., Bonnefoy, V., Krin, E., Arsène-Ploetze, F., Carapito, C. 2007. A tale of two oxidation states: bacterial colonization of arsenic-rich environments. *PLoS Genet*, **3**(4), e53.
- Munir, A., Rasul, S., Habibuddowla, M., Alauddin, M., Hussam, A., Khan, A. 2001. Evaluation of performance of Sono 3-Kolshi filter for arsenic removal from groundwater using zero valent iron through laboratory and field studies. *Proceedings International Workshop on Technology for Arsenic Removal from Drinking Water, Bangladesh University of Engineering and Technology and United Nations University, Japan*. pp. 171-189.
- Murillo, F.M., Gugliuzza, T., Senko, J., Basu, P., Stolz, J.F. 1999. A heme-C-containing enzyme complex that exhibits nitrate and nitrite reductase activity from the dissimilatory iron-reducing bacterium *Geobacter metallireducens*. *Archives of Microbiology*, **172**(5), 313-320.

- Myrold, D.D. 1998. Transformations of nitrogen. *Principles and applications of soil microbiology*, **12**, 259-294.
- Narasingarao, P., Haggblom, M.M. 2007. Identification of anaerobic selenate-respiring bacteria from aquatic sediments. *Applied and environmental microbiology*, **73**(11), 3519-3527.
- Nath, S.K., Bhattacharyya, K.G. 2015. Adsorption of Arsenite and Fluoride on Untreated and Treated Bamboo Dust. in: *Management of Natural Resources in a Changing Environment*, Springer, pp. 167-180.
- Nerenberg, R., Rittmann, B. 2002. Perchlorate as a secondary substrate in a denitrifying, hollow-fiber membrane biofilm reactor. *Water Supply*, **2**(2), 259-265.
- Newman, D.K., Kennedy, E.K., Coates, J.D., Ahmann, D., Ellis, D.J., Lovley, D.R., Morel, F.M. 1997. Dissimilatory arsenate and sulfate reduction in *Desulfotomaculum auripigmentum* sp. nov. *Archives of Microbiology*, **168**(5), 380-388.
- Ngai, T.K., Shrestha, R.R., Dangol, B., Maharjan, M., Murcott, S.E. 2007. Design for sustainable development—household drinking water filter for arsenic and pathogen treatment in Nepal. *Journal of Environmental Science and Health Part A*, **42**(12), 1879-1888.
- Niggemyer, A., Spring, S., Stackebrandt, E., Rosenzweig, R.F. 2001. Isolation and characterization of a novel As (V)-reducing bacterium: implications for arsenic mobilization and the genus *Desulfitobacterium*. *Applied and environmental microbiology*, **67**(12), 5568-5580.
- Nigussie, W., Zewge, F., Chandravanshi, B. 2007. Removal of excess fluoride from water using waste residue from alum manufacturing process. *Journal of Hazardous Materials*, **147**(3), 954-963.
- NovaScotia. 2008. Iron and manganese. Available at: http://www.gov.ns.ca/nse/water/docs/droponwaterFAQ_IronManganese.pdf Accessed on: Jul 16 2015.
- O'Day, P.A., Vlassopoulos, D., Root, R., Rivera, N. 2004. The influence of sulfur and iron on dissolved arsenic concentrations in the shallow subsurface under changing redox conditions. *Proceedings of the National Academy of Sciences of the United States of America*, **101**(38), 13703-13708.
- O'Flaherty, V., Mahony, T., O'Kennedy, R., Colleran, E. 1998. Effect of pH on growth kinetics and sulphide toxicity thresholds of a range of methanogenic, syntrophic and sulphate-reducing bacteria. *Process Biochemistry*, **33**(5), 555-569.
- Ocheri, M.I. 2010. Distribution of Iron in Rural Groundwater of Benue State, Nigeria. *Journal of Research in Forestry, Wildlife and Environment*, **2**(2), 164-170.
- Omeregic, E.O., Couture, R.-M., Van Cappellen, P., Corkhill, C.L., Charnock, J.M., Polya, D.A., Vaughan, D., Vanbroekhoven, K., Lloyd, J.R. 2013. Arsenic bioremediation by biogenic iron oxides and sulfides. *Applied and environmental microbiology*, **79**(14), 4325-4335.
- Onstott, T., Chan, E., Polizzotto, M., Lanzon, J., DeFlaun, M. 2011a. Precipitation of arsenic under sulfate reducing conditions and subsequent leaching under aerobic conditions. *Applied Geochemistry*, **26**(3), 269-285.
- Onstott, T.C., Chan, E., Polizzotto, M.L., Lanzon, J., DeFlaun, M.F. 2011b. Precipitation of arsenic under sulfate reducing conditions and subsequent leaching under aerobic conditions. *Applied Geochemistry*, **26**(3), 269-285.
- Oremland, R.S., Hoef, S.E., Santini, J.M., Bano, N., Hollibaugh, R.A., Hollibaugh, J.T. 2002. Anaerobic oxidation of arsenite in Mono Lake water and by a facultative, arsenite-oxidizing chemoautotroph, strain MLHE-1. *Applied and environmental microbiology*, **68**(10), 4795-4802.
- Oremland, R.S., Stolz, J.F. 2003. The ecology of arsenic. *Science*, **300**(5621), 939-944.
- Ozsvath, D.L. 2009. Fluoride and environmental health: a review. *Reviews in Environmental Science and Bio/Technology*, **8**(1), 59-79.

- Padilla, A.P., Saitua, H. 2010. Performance of simultaneous arsenic, fluoride and alkalinity (bicarbonate) rejection by pilot-scale nanofiltration. *Desalination*, **257**(1), 16-21.
- Páez-Espino, D., Tamames, J., de Lorenzo, V., Cánovas, D. 2009. Microbial responses to environmental arsenic. *Biometals*, **22**(1), 117-130.
- Pallier, V., Feuillade-Cathalifaud, G., Serpaud, B., Bollinger, J.-C. 2010. Effect of organic matter on arsenic removal during coagulation/flocculation treatment. *Journal of colloid and interface science*, **342**(1), 26-32.
- Park, J.Y., Yoo, Y.J. 2009. Biological nitrate removal in industrial wastewater treatment: which electron donor we can choose. *Applied Microbiology and Biotechnology*, **82**(3), 415-429.
- Per Halkjær Nielsen, H.D., Hilde Lemmer. 2009. FISH Handbook for Biological Wastewater Treatment.
- Petrie, L., North, N.N., Dollhopf, S.L., Balkwill, D.L., Kostka, J.E. 2003. Enumeration and characterization of iron (III)-reducing microbial communities from acidic subsurface sediments contaminated with uranium (VI). *Applied and environmental microbiology*, **69**(12), 7467-7479.
- Petrusevski, B., Sharma, S., vander Meer, W., Kruis, F., Khan, M., Barua, M., Schippers, J. 2008. Four years of development and field-testing of IHE arsenic removal family filter in rural Bangladesh. *Water science and technology*, **58**(1), 53.
- Pokhrel, D., Viraraghavan, T. 2009. Biological filtration for removal of arsenic from drinking water. *Journal of Environmental Management*, **90**(5), 1956-1961.
- Pontie, M., Dach, H., Lhassani, A., Diawara, C.K. 2013. Water defluoridation using nanofiltration vs. reverse osmosis: the first world unit, Thiadiaye (Senegal). *Desalination and Water Treatment*, **51**(1-3), 164-168.
- Postma, D., Jakobsen, R. 1996. Redox zonation: equilibrium constraints on the Fe (III)/SO 4-reduction interface. *Geochimica et Cosmochimica Acta*, **60**(17), 3169-3175.
- Pourmoghaddas, A., Sanei, H., Garakyaraghi, M., Esteki-Ghashghaei, F., Gharaati, M. 2014. The relation between body iron store and ferritin, and coronary artery disease. *ARYA atherosclerosis*, **10**(1), 32.
- Qin, J., Rosen, B.P., Zhang, Y., Wang, G., Franke, S., Rensing, C. 2006. Arsenic detoxification and evolution of trimethylarsine gas by a microbial arsenite S-adenosylmethionine methyltransferase. *Proceedings of the National Academy of Sciences of the United States of America*, **103**(7), 2075-2080.
- Ra, J.S., Kim, H.K., Chang, N.I., Kim, S.D. 2007. Whole effluent toxicity (WET) tests on wastewater treatment plants with *Daphnia magna* and *Selenastrum capricornutum*. *Environmental monitoring and assessment*, **129**(1-3), 107-113.
- Rabus, R., Hansen, T.A., Widdel, F. 2013. Dissimilatory sulfate- and sulfur-reducing prokaryotes. in: *The Prokaryotes*, Springer, pp. 309-404.
- Raghav, M., Shan, J., Sáez, A.E., Ela, W.P. 2013. Scoping candidate minerals for stabilization of arsenic-bearing solid residuals. *Journal of Hazardous Materials*, **263**, 525-532.
- Raju, N.J., Ram, P., Dey, S. 2009. Groundwater quality in the lower Varuna river basin, Varanasi district, Uttar Pradesh. *Journal of the Geological Society of India*, **73**(2), 178-192.
- Ramamoorthy, S., Piotrowski, J.S., Langner, H.W., Holben, W.E., Morra, M.J., Rosenzweig, R.F. 2009. Ecology of sulfate-reducing bacteria in an iron-dominated, mining-impacted freshwater sediment. *Journal of environmental quality*, **38**(2), 675-684.
- Ramamoorthy, S., Sass, H., Langner, H., Schumann, P., Kroppenstedt, R., Spring, S., Overmann, J., Rosenzweig, R. 2006. *Desulfosporosinus lacus* sp. nov., a sulfate-reducing bacterium isolated from pristine freshwater lake sediments. *International journal of systematic and evolutionary microbiology*, **56**(12), 2729-2736.

- Rao, N.M., Bhaskaran, C. 1988. Studies on defluoridation of water. *Journal of Fluorine Chemistry*, **41**(1), 17-24.
- Rao, P., Puttanna, K. 2000. Nitrates, agriculture and environment. *Current Science*, **79**(9), 1163-1169.
- Ravel, B., Newville, M. 2005. ATHENA, ARTEMIS, HEPHAESTUS: data analysis for X-ray absorption spectroscopy using IFEFFIT. *Journal of synchrotron radiation*, **12**(4), 537-541.
- Ravenscroft, P., Brammer, H., Richards, K. 2009. *Arsenic pollution: a global synthesis*. John Wiley & Sons.
- Ravishankara, A., Daniel, J.S., Portmann, R.W. 2009. Nitrous oxide (N₂O): the dominant ozone-depleting substance emitted in the 21st century. *Science*, **326**(5949), 123-125.
- Reardon, E.J., Wang, Y. 2000. A limestone reactor for fluoride removal from wastewaters. *Environmental science & technology*, **34**(15), 3247-3253.
- Reddy, A. 2014. Geochemical evaluation of nitrate and fluoride contamination in varied hydrogeological environs of Prakasam district, southern India. *Environmental Earth Sciences*, **71**(10), 4473-4495.
- Remoundaki, E., Kousi, P., Jouliau, C., Battaglia-Brunet, F., Hatzikioseyan, A., Tsezos, M. 2008. Characterization, morphology and composition of biofilm and precipitates from a sulphate-reducing fixed-bed reactor. *Journal of Hazardous Materials*, **153**(1), 514-524.
- Ren, Z., Zhang, G., Chen, J.P. 2011. Adsorptive removal of arsenic from water by an iron-zirconium binary oxide adsorbent. *Journal of colloid and interface science*, **358**(1), 230-237.
- Rezaie-Boroon, M.H., Chaney, J., Bowers, B. 2014. The Source of Arsenic and Nitrate in Borrego Valley Groundwater Aquifer. *Journal of Water Resource and Protection*, **6**(17), 1589.
- Rhine, E.D., Phelps, C.D., Young, L. 2006. Anaerobic arsenite oxidation by novel denitrifying isolates. *Environmental microbiology*, **8**(5), 899-908.
- Rich, J.J., Myrold, D.D. 2004. Community composition and activities of denitrifying bacteria from adjacent agricultural soil, riparian soil, and creek sediment in Oregon, USA. *Soil Biology and Biochemistry*, **36**(9), 1431-1441.
- Richard, D. 1969. The microbiological formation of iron sulphides. *Stockholm Contrib. Geol*, **20**, 49-66.
- Richey, C., Chovanec, P., Hoeft, S.E., Oremland, R.S., Basu, P., Stolz, J.F. 2009. Respiratory arsenate reductase as a bidirectional enzyme. *Biochemical and biophysical research communications*, **382**(2), 298-302.
- Rickard, D. 1995. Kinetics of FeS precipitation: Part 1. Competing reaction mechanisms. *Geochimica et Cosmochimica Acta*, **59**(21), 4367-4379.
- Rittmann, B.E., Snoeyink, V.L. 1984. Achieving Biologically Stable Drinking Water (PDF). *Journal-American Water Works Association*, **76**(10), 106-114.
- Rocha-Amador, D., Navarro, M.E., Carrizales, L., Morales, R., Calderón, J. 2007. Decreased intelligence in children and exposure to fluoride and arsenic in drinking water. *Cadernos de Saúde Pública*, **23**, S579-S587.
- Rodriguez-Freire, L., Field, D.J.A., Sierra-Alvarez, D.R. 2012. Arsenic biomineralization: The role of the sulfur cycle in preventing arsenic groundwater contamination.
- Rodriguez-Freire, L., Sierra-Alvarez, R., Root, R., Chorover, J., Field, J.A. 2014. Biomineralization of arsenate to arsenic sulfides is greatly enhanced at mildly acidic conditions. *Water Research*, **66**(0), 242-253.
- Ronald, H. 2013. Iron: Deficiency and toxicity. *Hoffman Center Staff*, Accessed on: Jul 16 2016.
- Rosen, B.P. 2002. Biochemistry of arsenic detoxification. *Febs Letters*, **529**(1), 86-92.

- Rosen, M.R., Reeves, R.R., Green, S., Clothier, B., Ironside, N. 2004. Prediction of groundwater nitrate contamination after closure of an unlined sheep feedlot. *Vadose Zone Journal*, **3**(3), 990-1006.
- Rusch, A., Islam, S., Savalia, P., Amend, J.P. 2015. Burkholderia insulsa sp. nov., a facultatively chemolithotrophic bacterium isolated from an arsenic-rich shallow marine hydrothermal system. *International journal of systematic and evolutionary microbiology*, **65**(Pt 1), 189-194.
- Rust, C.M., Aelion, C.M., Flora, J.R. 2000. Control of pH during denitrification in subsurface sediment microcosms using encapsulated phosphate buffer. *Water Research*, **34**(5), 1447-1454.
- Ryan, P.C., Kim, J., Wall, A.J., Moen, J.C., Corenthal, L.G., Chow, D.R., Sullivan, C.M., Bright, K.S. 2011. Ultramafic-derived arsenic in a fractured bedrock aquifer. *Applied Geochemistry*, **26**(4), 444-457.
- Saha, D., Sinha, U., Dwivedi, S. 2011. Characterization of recharge processes in shallow and deeper aquifers using isotopic signatures and geochemical behavior of groundwater in an arsenic-enriched part of the Ganga Plain. *Applied Geochemistry*, **26**(4), 432-443.
- Salgado-Bustamante, M., Ortiz-Pérez, M.D., Calderón-Aranda, E., Estrada-Capetillo, L., Niño-Moreno, P., González-Amaro, R., Portales-Pérez, D. 2010. Pattern of expression of apoptosis and inflammatory genes in humans exposed to arsenic and/or fluoride. *Science of The Total Environment*, **408**(4), 760-767.
- Saltikov, C.W., Cifuentes, A., Venkateswaran, K., Newman, D.K. 2003. The ars detoxification system is advantageous but not required for As (V) respiration by the genetically tractable *Shewanella* species strain ANA-3. *Applied and environmental microbiology*, **69**(5), 2800-2809.
- Samatya, S., Kabay, N., Yüksel, Ü., Arda, M., Yüksel, M. 2006. Removal of nitrate from aqueous solution by nitrate selective ion exchange resins. *Reactive and Functional Polymers*, **66**(11), 1206-1214.
- Sangole, S., Deshmukh, B., Panaskar, D. 2012. Comparative Study of Basaltic and Granitic Aquifers of Dharmabad Taluka of Nanded District, Maharashtra from Groundwater Quality Perspective.
- Sani, R.K., Peyton, B.M., Jandhyala, M. 2003. Toxicity of lead in aqueous medium to *Desulfovibrio desulfuricans* G20. *Environmental toxicology and chemistry*, **22**(2), 252-260.
- Santini, J.M., Sly, L.I., Schnagl, R.D., Macy, J.M. 2000. A new chemolithoautotrophic arsenite-oxidizing bacterium isolated from a gold mine: phylogenetic, physiological, and preliminary biochemical studies. *Applied and environmental microbiology*, **66**(1), 92-97.
- Santini, J.M., Stolz, J.F., Macy, J.M. 2002. Isolation of a New Arsenate-Respiring Bacterium--Physiological and Phylogenetic Studies. *Geomicrobiology Journal*, **19**(1), 41-52.
- Saunders, J., Lee, M.-K., Shamsudduha, M., Dhakal, P., Uddin, A., Chowdury, M., Ahmed, K. 2008. Geochemistry and mineralogy of arsenic in (natural) anaerobic groundwaters. *Applied Geochemistry*, **23**(11), 3205-3214.
- Say, R., Yilmaz, N., Denizli, A. 2003. Biosorption of cadmium, lead, mercury, and arsenic ions by the fungus *Penicillium purpurogenum*. *Separation Science and Technology*, **38**(9), 2039-2053.
- Schütte, U.M., Abdo, Z., Bent, S.J., Shyu, C., Williams, C.J., Pierson, J.D., Forney, L.J. 2008. Advances in the use of terminal restriction fragment length polymorphism (T-RFLP) analysis of 16S rRNA genes to characterize microbial communities. *Applied Microbiology and Biotechnology*, **80**(3), 365-380.

- Seidel, A., Waypa, J.J., Elimelech, M. 2001. Role of charge (Donnan) exclusion in removal of arsenic from water by a negatively charged porous nanofiltration membrane. *Environmental engineering science*, **18**(2), 105-113.
- Seki, H., Suzuki, A., Maruyama, H. 2005. Biosorption of chromium (VI) and arsenic (V) onto methylated yeast biomass. *Journal of Colloid and Interface Science*, **281**(2), 261-266.
- Sen, M., Manna, A., Pal, P. 2010. Removal of arsenic from contaminated groundwater by membrane-integrated hybrid treatment system. *Journal of membrane science*, **354**(1), 108-113.
- Shafiquzzaman, M., Azam, M.S., Nakajima, J., Bari, Q.H. 2010. Arsenic leaching characteristics of the sludges from iron based removal process. *Desalination*, **261**(1-2), 41-45.
- Shankar, B.S., Balasubramanya, N., Maruthesha Reddy, M.T. 2008. Impact of industrialization on groundwater quality – a case study of Peenya industrial area, Bangalore, India. *Environmental Monitoring and Assessment*, **142**(1-3), 263-268.
- Sharma, A.K., Tjell, J.C., Sloth, J.J., Holm, P.E. 2014a. Review of arsenic contamination, exposure through water and food and low cost mitigation options for rural areas. *Applied Geochemistry*, **41**, 11-33.
- Sharma, C., Mahajan, A., Kumar Garg, U. 2014b. Fluoride and nitrate in groundwater of south-western Punjab, India—occurrence, distribution and statistical analysis. *Desalination and Water Treatment*(ahead-of-print), 1-12.
- Sharma, S., Petrusovski, B., Schippers, J. 2005. Biological iron removal from groundwater: a review. *Aqua*, **54**, 239-247.
- Sharma, S.K. 2001. *Adsorptive iron removal from groundwater*. CRC Press, USA.
- Sharma, S.K., Solti, R.C. 2012. Nitrate removal from ground water: a review. *Journal of Chemistry*, **9**(4), 1667-1675.
- Shen, J., Schäfer, A. 2014. Removal of fluoride and uranium by nanofiltration and reverse osmosis: A review. *Chemosphere*, **117**, 679-691.
- Silva, E., Rajapakse, N., Kortenkamp, A. 2002. Something from “nothing”-eight weak estrogenic chemicals combined at concentrations below NOECs produce significant mixture effects. *Environmental science & technology*, **36**(8), 1751-1756.
- Silver, S., Phung, L.T. 2005. Genes and enzymes involved in bacterial oxidation and reduction of inorganic arsenic. *Applied and environmental microbiology*, **71**(2), 599-608.
- Silverstein, J. 1997. Demonstration of Biological Denitrification of Drinking Water for Rural Communities. *Final Report-Phase*, **1**.
- Sima, J., Cao, X., Zhao, L., Luo, Q. 2015. Toxicity characteristic leaching procedure over-or under-estimates leachability of lead in phosphate-amended contaminated soils. *Chemosphere*, **138**, 744-750.
- Singh, A., Bhagowati, S., Das, T., Yubbe, D., Rahman, B., Nath, M., Obing, P., Singh, W., Renthlei, C., Pachau, L. 2008. Assessment of arsenic, fluoride, iron, nitrate and heavy metals in drinking water of northeastern India. *Envis Bull Himal Ecol*, **16**(1), 6-12.
- Singh, J., Singh, P., Singh, A. 2016. Fluoride ions vs removal technologies: A study. *Arabian Journal of Chemistry*(0).
- Singh, K., Lataye, D.H., Wasewar, K.L., Yoo, C.K. 2013. Removal of fluoride from aqueous solution: status and techniques. *Desalination and Water Treatment*, **51**(16-18), 3233-3247.
- Singh, R., Singh, S., Parihar, P., Singh, V.P., Prasad, S.M. 2015. Arsenic contamination, consequences and remediation techniques: a review. *Ecotoxicology and Environmental Safety*, **112**, 247-270.
- Slavik, I., Jehmlich, A., Uhl, W. 2013. Impact of backwashing procedures on deep bed filtration productivity in drinking water treatment. *Water research*, **47**(16), 6348-6357.

- Slobodkin, A.I., Jeanthon, C., L'haridon, S., Nazina, T., Miroshnichenko, M., Bonch-Osmolovskaya, E. 1999. Dissimilatory reduction of Fe (III) by thermophilic bacteria and archaea in deep subsurface petroleum reservoirs of Western Siberia. *Current microbiology*, **39**(2), 99-102.
- Smedley, P., Kinniburgh, D. 2002. A review of the source, behaviour and distribution of arsenic in natural waters. *Applied Geochemistry*, **17**(5), 517-568.
- Smedley, P., Nicolli, H., Macdonald, D., Kinniburgh, D. 2008. Arsenic in groundwater and sediments from La Pampa province, Argentina. *Natural arsenic in groundwater of Latin America—occurrence, health impact and remediation*, 35-45.
- Smedley, P., Zhang, M., Zhang, G., Luo, Z. 2003. Mobilisation of arsenic and other trace elements in fluvio-lacustrine aquifers of the Huhhot Basin, Inner Mongolia. *Applied Geochemistry*, **18**(9), 1453-1477.
- Soares, M. 2000. Biological denitrification of groundwater. in: *Environmental Challenges*, Springer, pp. 183-193.
- Sorokin, D., Tourova, T., Muyzer, G. 2013. Isolation and characterization of two novel alkalitolerant sulfidogens from a Thiopaq bioreactor, *Desulfonatronum alkalitolerans* sp. nov., and *Sulfurospirillum alkalitolerans* sp. nov. *Extremophiles*, **17**(3), 535-543.
- Spain, A.M., Krumholz, L.R. 2011. Nitrate-reducing bacteria at the nitrate and radionuclide contaminated Oak Ridge Integrated Field Research Challenge site: A review. *Geomicrobiology Journal*, **28**(5-6), 418-429.
- Sprent, J.I. 1987. *The ecology of the nitrogen cycle*. Cambridge University Press.
- Stolz, J.F., Basu, P., Oremland, R.S. 2010. Microbial arsenic metabolism: new twists on an old poison. *Issues*.
- Stolz, J.F., Oremland, R.S. 1999. Bacterial respiration of arsenic and selenium. *FEMS Microbiology Reviews*, **23**(5), 615-627.
- Sujana, M., Anand, S. 2011. Fluoride removal studies from contaminated ground water by using bauxite. *Desalination*, **267**(2), 222-227.
- Sujana, M., Soma, G., Vasumathi, N., Anand, S. 2009. Studies on fluoride adsorption capacities of amorphous Fe/Al mixed hydroxides from aqueous solutions. *Journal of Fluorine Chemistry*, **130**(8), 749-754.
- Sullivan, C., Tyrer, M., Cheeseman, C.R., Graham, N.J.D. 2010. Disposal of water treatment wastes containing arsenic — A review. *Science of The Total Environment*, **408**(8), 1770-1778.
- Sun, H., Spring, S., Lapidus, A., Davenport, K., Del Rio, T.G., Tice, H., Nolan, M., Copeland, A., Cheng, J.-F., Lucas, S., Tapia, R., Goodwin, L., Pitluck, S., Ivanova, N., Pagani, I., Mavromatis, K., Ovchinnikova, G., Pati, A., Chen, A., Palaniappan, K., Hauser, L., Chang, Y.-J., Jeffries, C.D., Detter, J.C., Han, C., Rohde, M., Brambilla, E., Göker, M., Woyke, T., Bristow, J., Eisen, J.A., Markowitz, V., Hugenholtz, P., Kyrpides, N.C., Klenk, H.-P., Land, M. 2010a. Complete genome sequence of *Desulfarculus baarsii* type strain (2st14(T)). *Standards in genomic sciences*, **3**(3), 276-284.
- Sun, W., Sierra-Alvarez, R., Milner, L., Oremland, R., Field, J.A. 2009. Arsenite and ferrous iron oxidation linked to chemolithotrophic denitrification for the immobilization of arsenic in anoxic environments. *Environmental science & technology*, **43**(17), 6585-6591.
- Sun, W., Sierra-Alvarez, R., Field, J.A. 2010b. The role of denitrification on arsenite oxidation and arsenic mobility in an anoxic sediment column model with activated alumina. *Biotechnology and bioengineering*, **107**(5), 786-794.
- Sun, W., Sierra-Alvarez, R., Hsu, I., Rowlette, P., Field, J.A. 2010c. Anoxic oxidation of arsenite linked to chemolithotrophic denitrification in continuous bioreactors. *Biotechnology and bioengineering*, **105**(5), 909-917.

- Sun, Y., Polishchuk, E.A., Radoja, U., Cullen, W.R. 2004. Identification and quantification of arsC genes in environmental samples by using real-time PCR. *Journal of microbiological methods*, **58**(3), 335-349.
- Suthan S, S., Fred C, P. 2004. In Situ Remediation Engineering. *CRC Press, USA*, 532.
- Suthar, S. 2011. Contaminated drinking water and rural health perspectives in Rajasthan, India: an overview of recent case studies. *Environmental Monitoring and Assessment*, **173**(1-4), 837-849.
- Tebo, B.M., Obratsova, A.Y. 1998. Sulfate-reducing bacterium grows with Cr (VI), U (VI), Mn (IV), and Fe (III) as electron acceptors. *FEMS Microbiology Letters*, **162**(1), 193-199.
- Teclu, D., Tivchev, G., Laing, M., Wallis, M. 2008. Bioremoval of arsenic species from contaminated waters by sulphate-reducing bacteria. *Water Research*, **42**(19), 4885-4893.
- Tekerlekopoulou, A., Vayenas, D. 2007. Ammonia, iron and manganese removal from potable water using trickling filters. *Desalination*, **210**(1), 225-235.
- Tellez, R.T., Chacon, P.M., Abarca, C.R., Blount, B.C., Landingham, C.B.V., Crump, K.S., Gibbs, J.P. 2005. Long-term environmental exposure to perchlorate through drinking water and thyroid function during pregnancy and the neonatal period. *Thyroid*, **15**(9), 963-975.
- Tonkes, M., De Graaf, P.J., Graansma, J. 1999. Assessment of complex industrial effluents in the Netherlands using a whole effluent toxicity (or WET) approach. *Water Science and Technology*, **39**(10-11), 55-61.
- Türk, T., Alp, İ., Devenci, H. 2009. Adsorption of As (V) from water using nanomagnetite. *Journal of Environmental Engineering*, **136**(4), 399-404.
- Twort, A.C., Ratnayaka, D.D., Brandt, M.J. 2000. *Water supply. 5th edition. ed.* Butterworth-Heinemann, London.
- Tyrrel, S., Gardner, S., Howsam, P., Carter, R. 1998. Biological removal of iron from well-handpump water supplies. *Waterlines*, **16**(4), 29-31.
- Uddin, A., Shamsudduha, M., Saunders, J., Lee, M.-K., Ahmed, K., Chowdhury, M. 2011. Mineralogical profiling of alluvial sediments from arsenic-affected Ganges–Brahmaputra floodplain in central Bangladesh. *Applied Geochemistry*, **26**(4), 470-483.
- Ullrich, M.K., Pope, J.G., Seward, T.M., Wilson, N., Planer-Friedrich, B. 2013. Sulfur redox chemistry governs diurnal antimony and arsenic cycles at Champagne Pool, Waiotapu, New Zealand. *Journal of Volcanology and Geothermal Research*, **262**, 164-177.
- Upadhyaya, G., Jackson, J., Clancy, T.M., Hyun, S.P., Brown, J., Hayes, K.F., Raskin, L. 2010. Simultaneous removal of nitrate and arsenic from drinking water sources utilizing a fixed-bed bioreactor system. *Water Research*, **44**(17), 4958-4969.
- USEPA. 1986. Hazardous waste management system; land disposal restriction, Appendix I to Part 268: Toxicity Characteristics Leaching Procedure (TCLP),. 40643–40654.
- USEPA. 2002. Methods for Measuring the Acute Toxicity of Effluents and Receiving Waters to Freshwater and Marine Organisms. (Fifth edition).
- USEPA. 2004. SW-846 Test Method 9045D: Soil and Waste pH. (November, 2004).
- USEPA. 1997. Test methods for evaluating solid waste, physical chemical methods. *SW 846*.
- USEPA. 1992. Test Methods for Evaluating Solid Waste, Physical/Chemical Methods. (3rd edition).
- Vaaramaa, K., Lehto, J. 2003. Removal of metals and anions from drinking water by ion exchange. *Desalination*, **155**(2), 157-170.
- Valdés, J., Pedroso, I., Quatrini, R., Dodson, R.J., Tettelin, H., Blake, R., Eisen, J.A., Holmes, D.S. 2008. *Acidithiobacillus ferrooxidans* metabolism: from genome sequence to industrial applications. *BMC genomics*, **9**(1), 597.

- Van Halem, D., Bakker, S., Amy, G., Van Dijk, J. 2009. Arsenic in drinking water: a worldwide water quality concern for water supply companies. *Drinking Water Engineering and Science*, **2**, 2009.
- Van Halem, D., Olivero, S., de Vet, W., Verberk, J., Amy, G., van Dijk, J. 2010. Subsurface iron and arsenic removal for shallow tube well drinking water supply in rural Bangladesh. *Water Research*, **44**(19), 5761-5769.
- Vanden Hoven, R.N., Santini, J.M. 2004. Arsenite oxidation by the heterotroph *Hydrogenophaga* sp. str. NT-14: the arsenite oxidase and its physiological electron acceptor. *Biochimica et Biophysica Acta (BBA)-Bioenergetics*, **1656**(2), 148-155.
- Vaxevanidou, K., Christou, C., Kremmydas, G., Georgakopoulos, D., Papassiopi, N. 2015. Role of indigenous arsenate and iron (III) Respiring microorganisms in controlling the mobilization of arsenic in a Contaminated soil Sample. *Bulletin of environmental contamination and toxicology*, **94**(3), 282-288.
- Velizarov, S., Crespo, J.G., Reis, M.A. 2004. Removal of inorganic anions from drinking water supplies by membrane bio/processes. *Reviews in Environmental Science and Bio/Technology*, **3**(4), 361-380.
- Velizarov, S., Matos, C., Reis, M., Crespo, J. 2005. Removal of inorganic charged micropollutants in an ion-exchange membrane bioreactor. *Desalination*, **178**(1), 203-210.
- Venkataraman, K., Uddameri, V. 2012. Modeling simultaneous exceedance of drinking-water standards of arsenic and nitrate in the Southern Ogallala aquifer using multinomial logistic regression. *Journal of Hydrology*, **458-459**(0), 16-27.
- Villegas-Torres, M.F., Bedoya-Reina, O.C., Salazar, C., Vives-Florez, M.J., Dussan, J. 2011. Horizontal arsC gene transfer among microorganisms isolated from arsenic polluted soil. *International Biodeterioration & Biodegradation*, **65**(1), 147-152.
- Visser, A., Beeksmas, I., Van der Zee, F., Stams, A., Lettinga, G. 1993a. Anaerobic degradation of volatile fatty acids at different sulphate concentrations. *Applied Microbiology and Biotechnology*, **40**(4), 549-556.
- Visser, A., Gao, Y., Lettinga, G. 1993b. Effects of short-term temperature increases on the mesophilic anaerobic breakdown of sulfate containing synthetic wastewater. *Water Research*, **27**(4), 541-550.
- Visser, A., Pol, L.H., Lettinga, G. 1996. Competition of methanogenic and sulfidogenic bacteria. *Water science and technology*, **33**(3), 99-110.
- Wakida, F.T., Lerner, D.N. 2005. Non-agricultural sources of groundwater nitrate: a review and case study. *Water Research*, **39**(1), 3-16.
- Walker, M., Seiler, R.L., Meinert, M. 2008. Effectiveness of household reverse-osmosis systems in a Western US region with high arsenic in groundwater. *Science of The Total Environment*, **389**(2), 245-252.
- Wall, J.D., Rapp-Giles, B.J., Brown, M.F., White, J.A. 1990. Response of *Desulfovibrio desulfuricans* colonies to oxygen stress. *Canadian Journal of Microbiology*, **36**(6), 400-408.
- Wang, P.-P., Sun, G.-X., Zhu, Y.-G. 2014a. Identification and characterization of arsenite methyltransferase from an archaeon, *Methanosarcina acetivorans* C2A. *Environmental science & technology*, **48**(21), 12706-12713.
- Wang, P., Sun, G., Jia, Y., Meharg, A.A., Zhu, Y. 2014b. A review on completing arsenic biogeochemical cycle: Microbial volatilization of arsines in environment. *Journal of Environmental Sciences*, **26**(2), 371-381.
- Wang, S.-X., Wang, Z.-H., Cheng, X.-T., Li, J., Sang, Z.-P., Zhang, X.-D., Han, L.-L., Qiao, X.-Y., Wu, Z.-M., Wang, Z.-Q. 2007. Arsenic and fluoride exposure in drinking water: children's IQ

- and growth in Shanyin county, Shanxi province, China. *Environmental health perspectives*, 643-647.
- Wang, S., Mulligan, C.N. 2006. Occurrence of arsenic contamination in Canada: Sources, behavior and distribution. *Science of The Total Environment*, **366**(2–3), 701-721.
- Wang, S., Zhao, X. 2009. On the potential of biological treatment for arsenic contaminated soils and groundwater. *Journal of Environmental Management*, **90**(8), 2367-2376.
- Wang, Y., Qian, P.-Y. 2009. Conservative Fragments in Bacterial 16S rRNA Genes and Primer Design for 16S Ribosomal DNA Amplicons in Metagenomic Studies. *PLoS ONE*, **4**(10), e7401.
- Wang, Y., Shvartsev, S.L., Su, C. 2009. Genesis of arsenic/fluoride-enriched soda water: a case study at Datong, northern China. *Applied Geochemistry*, **24**(4), 641-649.
- Ward, M.H., DeKok, T.M., Levallois, P., Brender, J., Gulis, G., Nolan, B.T., VanDerslice, J. 2005. Workgroup report: Drinking-water nitrate and health-recent findings and research needs. *Environmental health perspectives*, 1607-1614.
- Waypa, J.J., Elimelech, M., Hering, J.G. 1997. Arsenic removal by RO and NF membranes. *Journal-American Water Works Association*, **89**(10), 102-114.
- Welch, A.H., Stollenwerk, K.G. 2007. *Arsenic in ground water*. Springer Science & Business Media.
- WHO. 2011. Guidelines for Drinking-Water Quality *World Health Organisation, Geneva*, **4**, 315-318.
- WHO. 2006. Guidelines for Drinking-Water Quality [Electronic Resource]: Incorporating First Addendum,. 375-377.
- WHO. 1996. Guidelines for Drinking Water Quality. Health Criteria and Other Supporting Information. *World Health Organisation, Geneva.*, **2nd edition** ((2)).
- WHO. 2004a. Rolling Revision of the WHO Guidelines for Drinking-Water Quality.
- WHO. 2004b. *World Health Organization, Guidelines for drinking-water quality: recommendations*. World Health Organization.
- Wickramasinghe, S., Han, B., Zimbron, J., Shen, Z., Karim, M. 2004. Arsenic removal by coagulation and filtration: comparison of groundwaters from the United States and Bangladesh. *Desalination*, **169**(3), 231-244.
- Wielinga, B., Mizuba, M.M., Hansel, C.M., Fendorf, S. 2001. Iron promoted reduction of chromate by dissimilatory iron-reducing bacteria. *Environmental science & technology*, **35**(3), 522-527.
- Willow, M.A., Cohen, R.R. 2003. pH, dissolved oxygen, and adsorption effects on metal removal in anaerobic bioreactors. *Journal of environmental quality*, **32**(4), 1212-1221.
- Wilson, A., Parrott, K., Ross, B. Household water quality: Water hardness: Virginia Cooperative Extension. Publication No. 356-490,(1999).
- Wolthers, M., Charlet, L., van Der Weijden, C.H., Van der Linde, P.R., Rickard, D. 2005. Arsenic mobility in the ambient sulfidic environment: Sorption of arsenic (V) and arsenic (III) onto disordered mackinawite. *Geochimica et Cosmochimica Acta*, **69**(14), 3483-3492.
- Wolthers, M., Van der Gaast, S.J., Rickard, D. 2003. The structure of disordered mackinawite. *American Mineralogist*, **88**(11-12), 2007-2015.
- Wrighton, K.C., Virdis, B., Clauwaert, P., Read, S.T., Daly, R.A., Boon, N., Piceno, Y., Andersen, G.L., Coates, J.D., Rabaey, K. 2010. Bacterial community structure corresponds to performance during cathodic nitrate reduction. *The ISME journal*, **4**(11), 1443-1455.
- Xia, S., Shen, S., Xu, X., Liang, J., Zhou, L. 2014. Arsenic removal from groundwater by acclimated sludge under autohydrogenotrophic conditions. *Journal of Environmental Sciences*, **26**(2), 248-255.
- Xin, W., JiYun, L., QingGang, K. 2009. Drinking water quality investigation in rural areas of Yunnan Province. *Journal of Environment and Health*, **26**(1), 26-27.

- Xu, L., Zhao, Z., Wang, S., Pan, R., Jia, Y. 2011a. Transformation of arsenic in offshore sediment under the impact of anaerobic microbial activities. *Water Research*, **45**(20), 6781-6788.
- Xu, Y., Qiu, T.-L., Han, M.-L., Li, J., Wang, X.-M. 2011b. Heterotrophic Denitrification of Nitrate-Contaminated Water Using Different Solid Carbon Sources. *Procedia Environmental Sciences*, **10, Part A**, 72-77.
- Yadav, A.K., Abbassi, R., Gupta, A., Dadashzadeh, M. 2013. Removal of fluoride from aqueous solution and groundwater by wheat straw, sawdust and activated bagasse carbon of sugarcane. *Ecological engineering*, **52**, 211-218.
- Yamamura, S., Amachi, S. 2014. Microbiology of inorganic arsenic: from metabolism to bioremediation. *Journal of bioscience and bioengineering*, **118**(1), 1-9.
- Yan, X.-P., Kerrich, R., Hendry, M.J. 2000. Distribution of arsenic (III), arsenic (V) and total inorganic arsenic in porewaters from a thick till and clay-rich aquitard sequence, Saskatchewan, Canada. *Geochimica et Cosmochimica Acta*, **64**(15), 2637-2648.
- Yang, L., Li, X., Chu, Z., Ren, Y., Zhang, J. 2014. Distribution and genetic diversity of the microorganisms in the biofilter for the simultaneous removal of arsenic, iron and manganese from simulated groundwater. *Bioresource Technology*, **156**, 384-388.
- Yang, X., Wang, S., Zhou, L. 2012. Effect of carbon source, C/N ratio, nitrate and dissolved oxygen concentration on nitrite and ammonium production from denitrification process by *Pseudomonas stutzeri* D6. *Bioresource Technology*, **104**, 65-72.
- Yarlagadda, S., Gude, V.G., Camacho, L.M., Pinappu, S., Deng, S. 2011. Potable water recovery from As, U, and F contaminated ground waters by direct contact membrane distillation process. *Journal of Hazardous Materials*, **192**(3), 1388-1394.
- Yu, Y., Yu, L., Paul Chen, J. 2015. Adsorption of fluoride by Fe–Mg–La triple-metal composite: Adsorbent preparation, illustration of performance and study of mechanisms. *Chemical Engineering Journal*, **262**, 839-846.
- Yuan, T., Luo, Q.-F., Hu, J.-Y., Ong, S.-L., Ng, W.-J. 2003. A study on arsenic removal from household drinking water. *Journal of Environmental Science and Health, Part A*, **38**(9), 1731-1744.
- Zabinsky, S., Rehr, J., Ankudinov, A., Albers, R., Eller, M. 1995. Multiple-scattering calculations of X-ray-absorption spectra. *Physical Review B*, **52**(4), 2995.
- Zhang, C., Liu, S., Phelps, T.J., Cole, D.R., Horita, J., Fortier, S.M., Elles, M., Valley, J.W. 1997. Physiochemical, mineralogical, and isotopic characterization of magnetite-rich iron oxides formed by thermophilic iron-reducing bacteria. *Geochimica et Cosmochimica Acta*, **61**(21), 4621-4632.
- Zhang, R., Thiyagarajan, V., Qian, P.-Y. 2008. Evaluation of terminal-restriction fragment length polymorphism analysis in contrasting marine environments. *FEMS microbiology ecology*, **65**(1), 169-178.
- Zhang, X., Mi, Z., Wang, Y., Liu, S., Niu, Z., Lu, P., Wang, J., Gu, J., Chen, C. 2014a. A red water occurrence in drinking water distribution systems caused by changes in water source in Beijing, China: mechanism analysis and control measures. *Frontiers of Environmental Science & Engineering*, **8**(3), 417-426.
- Zhang, Y.-C., Slomp, C.P., Broers, H.P., Bostick, B., Passier, H.F., Böttcher, M.E., Omoregie, E.O., Lloyd, J.R., Polya, D.A., Van Cappellen, P. 2012. Isotopic and microbiological signatures of pyrite-driven denitrification in a sandy aquifer. *Chemical Geology*, **300**, 123-132.
- Zhang, Y., Dou, X., Zhao, B., Yang, M., Takayama, T., Kato, S. 2010. Removal of arsenic by a granular Fe–Ce oxide adsorbent: fabrication conditions and performance. *Chemical Engineering Journal*, **162**(1), 164-170.

- Zhang, Y., Yang, L., Wang, D., Zhang, T. 2014b. Resource utilization of water treatment residual sludge (WTRS): effective defluoridation from aqueous solution. *Desalination and Water Treatment*(ahead-of-print), 1-15.
- Zhou, C., Vannela, R., Hayes, K.F., Rittmann, B.E. 2014. Effect of growth conditions on microbial activity and iron-sulfide production by *Desulfovibrio vulgaris*. *Journal of Hazardous Materials*, **272**, 28-35.
- Zouboulis, A., Katsoyiannis, I. 2002a. Removal of arsenates from contaminated water by coagulation–direct filtration. *Separation Science and Technology*, **37**(12), 2859-2873.
- Zouboulis, A.I., Katsoyiannis, I.A. 2002b. Arsenic removal using iron oxide loaded alginate beads. *Industrial & engineering chemistry research*, **41**(24), 6149-6155.
- Zumft, W.G. 1997. Cell biology and molecular basis of denitrification. *Microbiology and molecular biology reviews*, **61**(4), 533-616.



APPENDIX

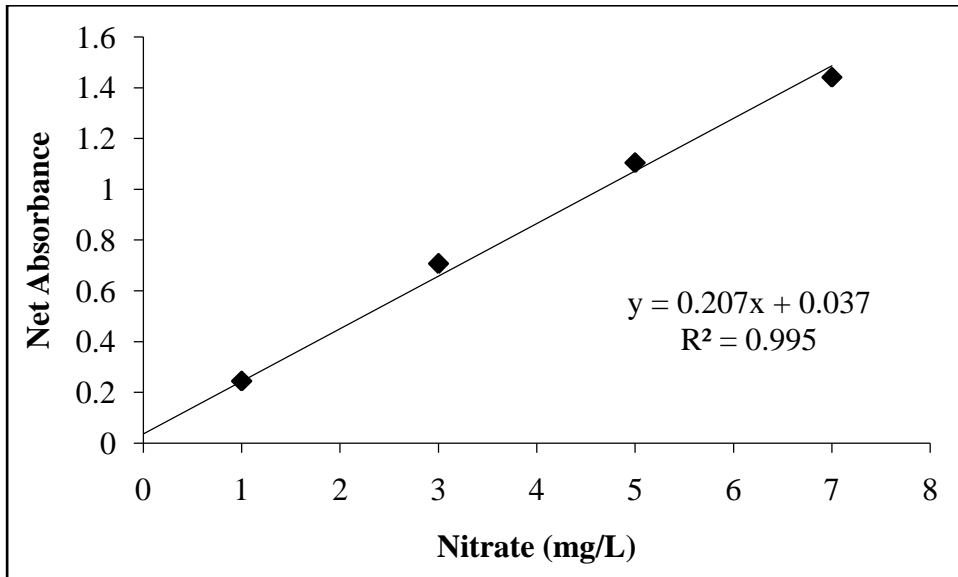


Figure A1 Calibration curve for nitrate determination.

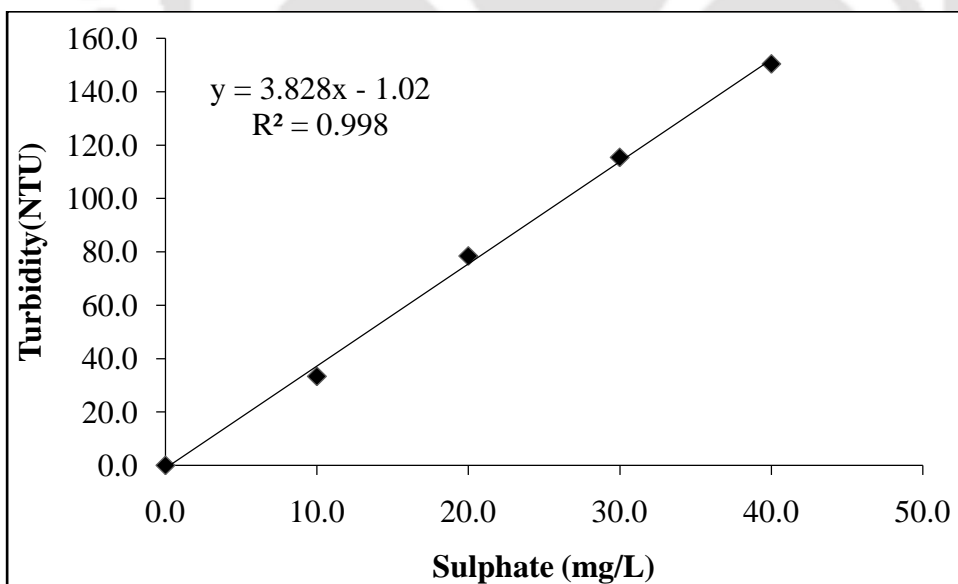


Figure A2 Calibration curve for sulphate determination.

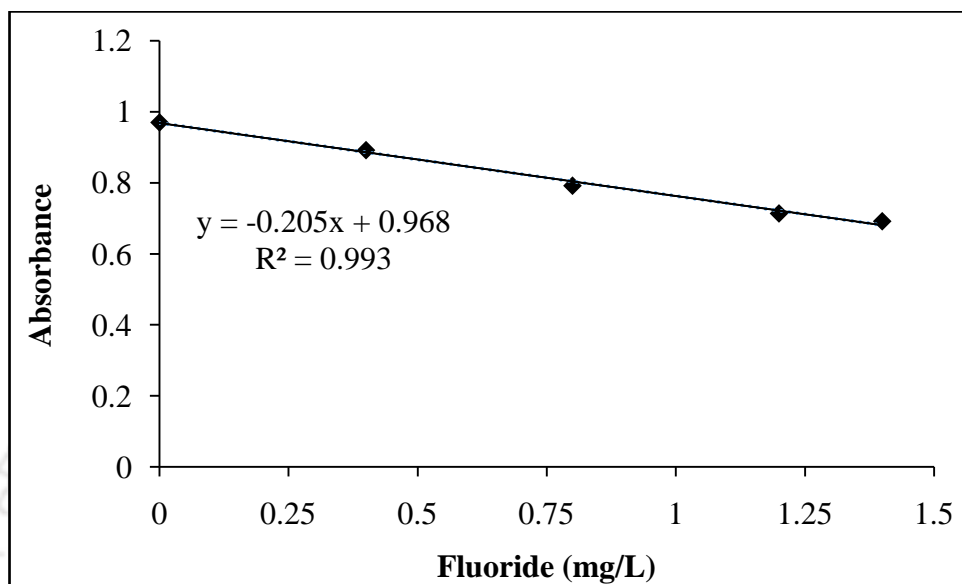


Figure A3 Calibration curve for fluoride determination.

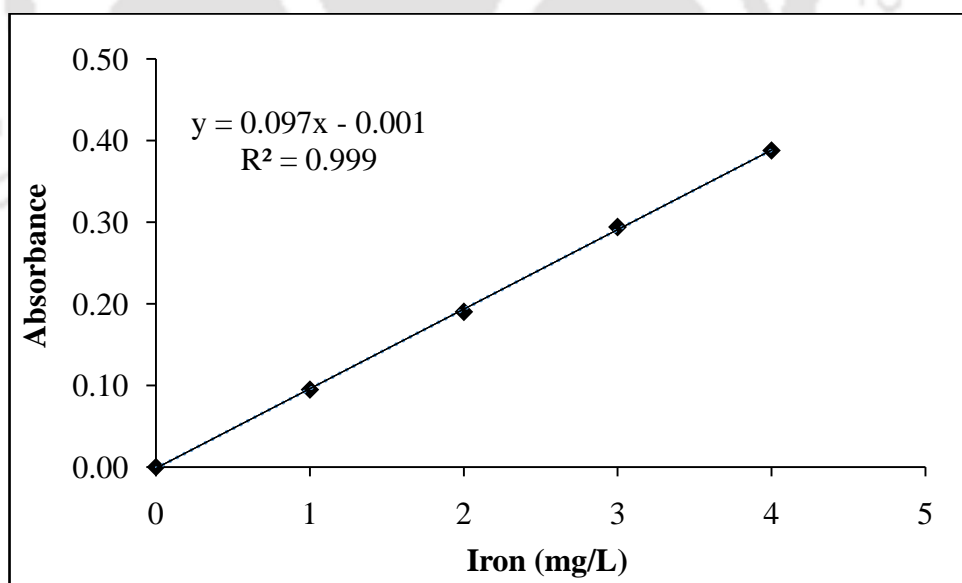


Figure A4 Calibration curve for iron determination.



Figure A5 Collection of sewage sludge from IIT Guwahati sewage treatment plant.

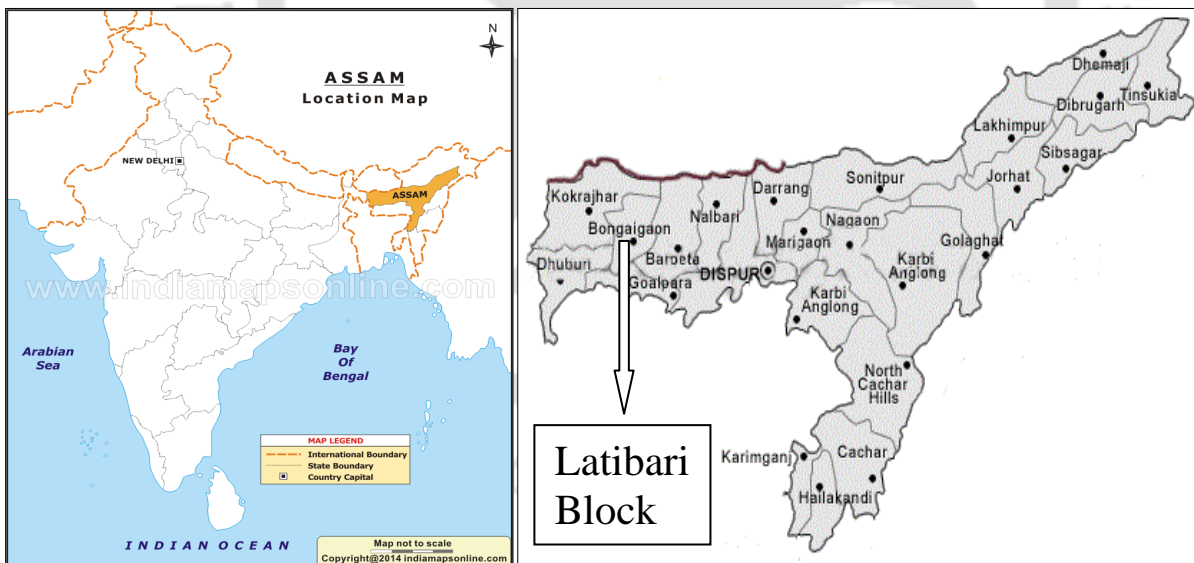


Figure A6 Location of Bongaigaon district in India.



Figure A7 Location map of real groundwater sampling site.



Figure A8 (a) Collection of real ground water (b) onsite determination of water quality parameters and arsenic.